Universidad Autónoma de Madrid

Facultad de Ciencias

Departamento de Biología Molecular

*Interacción funcional entre HLA-B*27 y las aminopeptidasas del retículo endoplásmico ERAP1 y 2: Implicaciones patogénicas en la Espondilitis Anquilosante*

Memoria para optar al grado de Doctor por la

Universidad Autónoma de Madrid

Adrián Martín Esteban

Director: Dr José Antonio López de Castro Álvarez

Profesor de investigación CSIC

Centro de Biología Molecular Severo Ochoa (CSIC-UAM)

Tutor: Dr Miguel Ángel Iñiguez Peña

Profesor Titular UAM

Centro de Biología Molecular Severo Ochoa (CSIC-UAM)

Enero

2017

Summary

The final steps of the antigen processing pathway of Major Histocompatibility Complex Class I (MHC-I) molecules take place in the endoplasmic reticulum (ER). The peptides reaching this compartment are often longer than those optimal for MHC-I binding. In humans, the final cut of MHC-I ligands is carried out by two related aminopeptidases, ERAP1 and ERAP2, differing in trimming specificity and substrate handling. ERAP1 cleaves virtually all N-terminal residues, except Pro, with preference for hydrophobic ones. ERAP2 preferently cleaves basic residues. Moreover, ERAP1 is almost unable to digest peptides shorter than nonamers, whereas, ERAP2 optimally cleaves peptides of 7-8 residues, quickly becoming less efficient with longer substrates. Yet, the precise role of ERAP2 in shaping MHC-I peptidomes is unknown. Due to the association of ERAP1 and ERAP2 with ankylosing spondylitis (AS). The influence of both enzymes on the HLA-B*27-bound peptidome has relevance to explain the molecular mechanism underlying the strong association of HLA-B*27 with this disease.

The aim of this thesis was to characterize the alterations induced by AS-associated haplotypes of ERAP1, and the presence of ERAP2, on the HLA-B*27 peptidome. The comparison of HLA-B*27- bound peptidomes from cells expressing different ERAP1 /2 combinations revealed that ERAP1 altered the length and N-terminal residue usage of many peptides while ERAP2 induced a moderate peptide length optimization and a significantly reduced abundance of peptides with N-terminal basic residues, independently of the ERAP1 context

The results suggest that ERAP1 and ERAP2 largely act as separate entities *in vivo* and have significant and distinct effects on the HLA-B*27 peptidome. They also support a central role of peptides in AS pathogenesis. The magnitude of the effects suggests that they could affect not only specific antigen presentation, but also the pro-inflammatory and autoimmune potential of HLA-B*27.

Abreviaturas

aa: aminoácidos

β2m: β2 microglobulina

DRiP: Defective Ribosomal Products

EA: Espondilitis Anquilosante

ERAP: Endoplasmatic reticulum Aminopeptidase

HC: Heavy Chain

HLA: Human Leucocyte Antigen

IL: Interleucina

IR: Intensity Ratio

MHC: Mayor Histocompatibility Complex

RE: Retículo Endoplásmico

TAP: Transportador Asociado al Procesamiento antigénico

TCR: T Cell Receptor

TOP: Oligopeptidasa Thimet

TPPII Tripeptidil Peptidasa II

UPR: Unfolding Protein Response

SNP: Single Nucleotide Polymorphism

ÍNDICE

INTRODUCCIÓN

Introducción

El sistema inmune es el conjunto de estructuras y procesos biológicos en el interior de los organismos que permite mantener la homeostasis frente a agresiones externas de carácter biológico (virus y bacterias), físico-químico (contaminantes o radiaciones), e internas, como el cáncer. La respuesta inmunológica puede ser de dos tipos: temprana o innata y tardía o adaptativa.

La inmunidad innata está presente prácticamente en todos los seres vivos y consiste en una respuesta rápida, inespecífica y de amplio espectro. En los organismos superiores está compuesta por barreras físicas como los epitelios, células fagocíticas, como los macrófagos y neutrófilos, células citolíticas, como los linfocitos NK y por diferentes proteínas sanguíneas como el complemento.

La respuesta inmunitaria adaptativa es más lenta y específica, ya que requiere el reconocimiento de antígenos que no son propios mediante un proceso llamado *presentación antigénica*. Se lleva a cabo principalmente por los linfocitos B y T. Los linfocitos B son los encargados de generar anticuerpos específicos contra el antígeno, mientras que los linfocitos T son los encargados de la destrucción de células infectadas (linfocitos T citotóxicos) o de regular la respuesta inmune (linfocitos T reguladores).

La presentación antigénica es crucial en la activación específica de linfocitos T contra un antígeno. Implica el reconocimiento de moléculas del sistema MHC (Major Histocompatibility Complex), que portan el péptido antigénico, por el receptor específico de los linfocitos T (T Cell Receptor : TCR). La ausencia de respuesta ante un antígeno propio se llama tolerancia inmunológica. La ruptura de esta tolerancia es conocida como respuesta autoinmune y lleva al sistema inmune a atacar al propio organismo.

1. Moléculas del complejo mayor de histocompatibilidad MHC de clase I.

Estas glicoproteínas están codificadas por una familia de genes altamente polimórficos, dentro de la región de clase I del MHC (MHC-I), en el brazo corto del cromosoma 6. Los antígenos del MHC-I clásicos están codificados en humanos en los loci HLA-A, HLA-B y HLA-C. Las proteínas correspondientes están formadas por tres entidades unidas de forma no covalente: Una cadena pesada (HC) de 44 KDa, una cadena ligera o

β2microglobulina (β2m) de 12 KDa., y un péptido antigénico de una longitud variable de entre 8-14 aa. **Figura I1**.

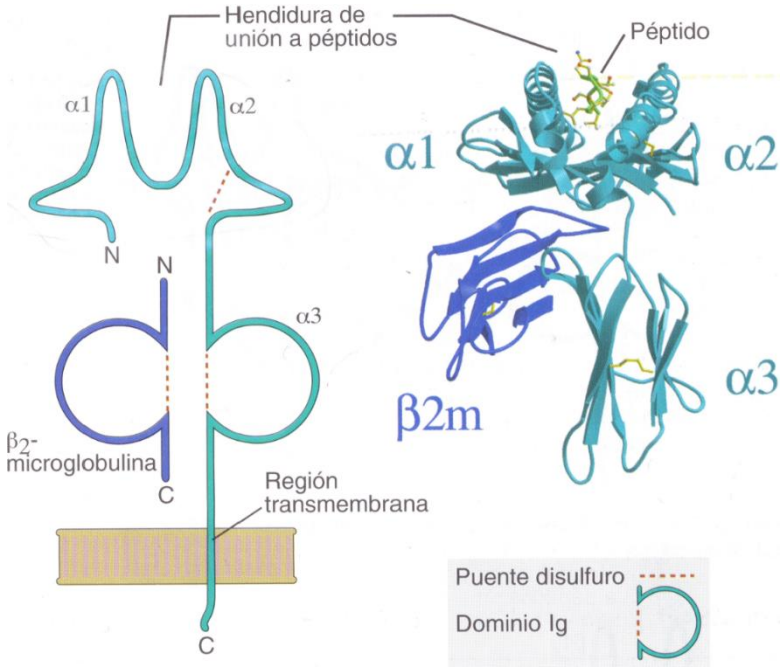

Figura I1. Estructura de una molécula de MHC de clase I: La imagen de la izquierda muestra un diagrama esquemático que representa las diferentes regiones de la molécula. La imagen de la derecha muestra la estructura de la porción extracelular de la molécula con un péptido unido. (Abbas et al. 2007)

La proteína completa consta de una región extracelular, una segmento transmembrana y una región intracitoplasmática. La porción extracelular consta de cuatro dominios: tres de ellos pertenecen a la HC (α1, α2 y α3) y uno a la β2m (Orr et al. 1979). Los dominios α1y α2 interactúan para formar una lámina de ocho bandas β antiparalelas sobre las que se disponen dos hélices α, formando el sitio de unión a péptidos. Los dominios α3 y β2m se pliegan de forma similar a los dominios constantes de las inmunoglobulinas, aunque interaccionan entre sí de forma diferente (Bjorkman et al. 1987, Bjorkman et al. 1987, Garrett et al. 1989, Saper et al. 1991, Madden et al. 1992, Madden 1995). El dominio α3 contiene un bucle que interacciona con la molécula CD8 del linfocito T (Gao et al. 1997). Los dominios α1y α2 son altamente polimórficos, lo que confiere a las moléculas de MHC-I la función de unir conjuntos de péptidos diferentes. La unión del péptido se realiza mediante interacciones no covalentes que involucran al esqueleto peptídico y a las cadenas laterales de varios residuos, denominados de anclaje. Los péptidos se unen en una serie de subcavidades designadas de la A a la F, que interaccionan con diferentes

residuos peptídicos. Estas interacciones determinan la especificidad de unión de cada alotipo. Las subcavidades A y F son las encargadas de unir los residuos N y C-terminales respectivamente. La subcavidad B une el residuo en posición P2, que suele ser un residuo de anclaje principal (Garrett et al. 1989, Saper et al. 1991, Bouvier et al. 1994). **Figura I2**

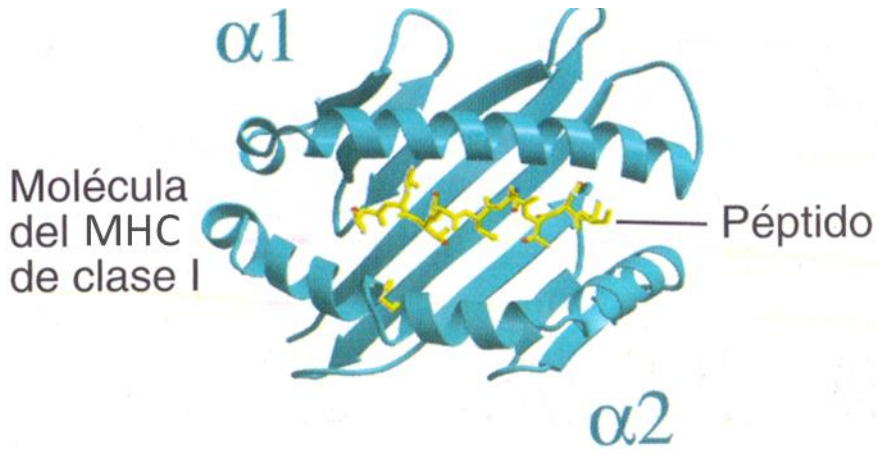

Figura I2. Unión del péptido a la molécula de MHC-I. Esta imagen muestra como interaccionan los péptidos (en amarillo) con el sitio de unión al péptido y como están accesibles para su reconocimiento por el TCR. (Abbas et al. 2007)

2. Procesamiento y presentación antigénica por MHC-I.

Los ligandos naturales de las moléculas de MHC-I proceden principalmente de proteínas autólogas que al final de su vida útil son degradadas por el proteosoma y de productos defectivos de la síntesis de proteínas (DRiPS) (Yewdell et al. 1996, Reits et al. 2000, Bourdetsky et al. 2014). Los antígenos procedentes de proteínas víricas sintetizadas endógenamente se incorporan al MHC-I a través de la misma ruta. El proteosoma es un complejo multienzimático responsable de la degradación de la mayoría de las proteínas intracelulares, localizado tanto en el núcleo como en el citosol. Está compuesto por una subunidad principal denominada 20S y dos subunidades reguladoras denominadas 19 S que, junto a la subunidad 20S, forman el proteosoma 26S. Cada complejo 19S está compuesto por casi 20 subunidades diferentes formando dos subestructuras, la tapa y la base. La tapa está constituida por 8 subunidades no ATPasas, situadas hacia el exterior, que son necesarias para eliminar la ubiquitina de las proteínas poliubiquitanadas. La

ubiquitina es una pequeña molécula que sirve de señal para que el proteosoma identifique las proteínas que tienen que ser degradadas. La principal función de la base es la de desnaturalizar los sustratos y permitir su acceso a la subunidad 20S. Ésta se compone de 4 anillos apilados formando una estructura cilíndrica. Cada uno de los dos anillos externos está formado por siete subunidades α diferentes, que permiten la entrada de los sustratos e interaccionan con complejos reguladores. Los dos anillos centrales están formados por siete subunidades β diferentes, encargadas de llevar a cabo la degradación de los sustratos. De las siete subunidades β solo tres presentan actividad catalítica β1, β2 y β5 y poseen especificidades diferentes: caspasa, caracterizada por cortar tras residuos ácidos, tríptica, tras residuos básicos y quimiotríptica, tras residuos hidrofóbicos (Arendt et al. 1997, Groll et al. 1997, Heinemeyer et al. 1997). La función del proteosoma no solo es producir los fragmentos proteicos, sino también generar la inmensa mayoría de los extremos C-terminales de los péptidos que se van a unir a MHC-I (Eggers et al. 1995, Howard 1995, Craiu et al. 1997, Alvarez et al. 2001, Cascio 2014), siendo su selectividad en los extremos N-terminales mucho menor (Rock et al. 1999)

El IFN-γ induce la expresión de tres subunidades β alternativas que conforman el inmunoproteosoma (Groettrup et al. 1996, Griffin et al. 1998, Chapiro et al. 2006). Estas nuevas subunidades dan al inmunoproteasoma una especificidad de corte parcialmente distinta a la del proteosoma 20S. Otras peptidasas citosólicas contribuyen a la ulterior destrucción de la mayoría de los productos de degradación proteosomica. Entre éstas se encuentra la oligopeptidasa thimet (TOP), que corta péptidos de 9-17 aa (Saric et al. 2001); la nardilisina, una metaloproteasa que corta sustratos con residuos N-terminales dibásicos (Saric et al. 2004), o la tripeptidil peptidasa II (TPPII), una serin proteasa que recorta tripéptidos del extremo N-terminal de péptidos largos, (York et al. 2006). Aproximadamente el 1/1000 de los péptidos generados por el proteosoma sobreviven a la degradación citosólica (Princiotta et al. 2003) y son transportados al lumen del RE a través del Transportador Asociado al Procesamiento Antigénico (TAP). Éste es un heterodimero formado por dos subunidades homólogas llamadas TAP1 y TAP2 cuya función es transportar péptidos con una longitud variable de entre 9-16 aa (Koopmann et al. 1996). Aunque TAP tiene un selectividad baja, de manera óptima transporta péptidos con residuos C-terminales básicos o hidrofóbicos, residuos P2 cargadas o hidrofóbicos y residuos P3 hidrofóbicos. No transporta péptidos con Pro en posición P1 o P2 y lo hace

con ineficacia con los que poseen residuos ácidos o aromáticos en P1 (van Endert et al. 1994).

Una vez dentro del RE, los péptidos son hidrolizados hasta alcanzar un tamaño de unos 8-10 aa, óptimo para la unión a la molécula de MHC-I. Este último corte lo realizan las aminopeptidasas del Retículo Endoplasmático (ERAP) 1 y 2. Éstas comparten el 50 % de identidad, presentan diferencias de especificidad y parecen actuar de manera concertada en la digestión de los péptidos (Saveanu et al. 2005, Birtley et al. 2012, Lorente et al. 2013, Evnouchidou et al. 2014). Por su importancia en esta tesis se describen en detalle más adelante.

Los péptidos de longitud adecuada se incorporan al complejo de carga peptídica durante la biosíntesis de la molécula de MHC-I. La unión del péptido hace que ésta pueda plegarse y estabilizarse adecuadamente. Al principio la HC está asociada a calnexina. Al unirse la β2m la calnexina es sustituida por calreticulina, (Sadasivan et al. 1996). La ERp57 cataliza la formación de puentes disulfuro intercatenarios que favorecen la unión del péptido a la molécula de MHC-I. ERp57 está unida covalentemente a la tapasina, una chaperona específica, que selecciona los péptidos en función de su afinidad por la molécula de MHC-I (Blum et al. 2013). Una vez que la molécula de MHC-I unida al péptido consigue una estabilidad suficiente, se disocia del complejo de carga y sale del RE a través de una ruta exocítica hasta la superficie celular, donde puede ser reconocida por receptores de antígeno y NK **Figura I3.**

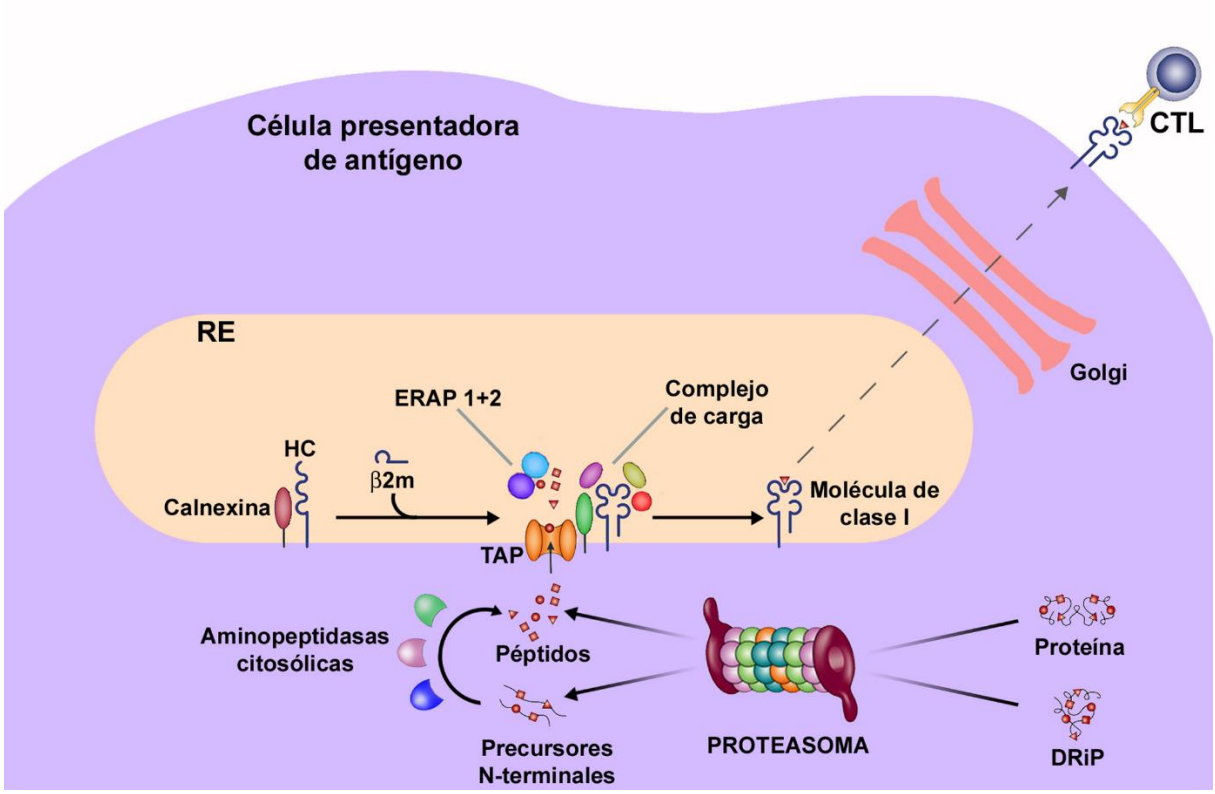

Figura I3. Ruta de procesamiento y presentación antigénica de MHC-I. Los péptidos se generan principalmente en el citosol por la acción del proteosoma, aunque también intervienen otras peptidasas citosólicas. A continuación son transportados al interior del retículo endoplasmático a través de TAP. En el lumen del RE sufren un procesamiento N-terminal por las aminopeptidasas ERAP1 y ERAP2. Los péptidos procesados se cargan en la correspondiente molécula de MHC-I uniéndose previamente al complejo de carga formado por TAP, tapasina, calreticulina y ERp57. La unión de un péptido de alta afinidad al MHC-I induce su disociación del complejo de carga y el transporte del complejo HC/β2m péptido a la superficie celular.

3. Asociación de MHC-I a enfermedades inflamatorias.

Existen múltiples enfermedades inflamatorias que se encuentran asociadas fuertemente a la presencia de algunos alotipos de MHC-I (Lopez de Castro et al. 2016). La razón de estas asociaciones se desconoce. En principio, los mecanismos patogénicos podrían ser dependientes de la presentación de antígenos específicos o de un potencial proinflamatorio intrínseco de la molécula de MHC dependiente de sus características de estabilidad o plegamiento.

Las enfermedades asociadas a MHC-I más importantes son las siguientes: la retinopatía en perdigonada (BSCR), una enfermedad inflamatoria de la retina y el coroide (Shah et

al. 2005), que está asociada con HLA-A*29:02, la espondilitis anquilosante (EA), una enfermedad autoinflamatoria crónica del esqueleto axial asociada a HLA-B*27 (Brewerton et al. 1973), la enfermedad de Behçet (BD), una vasculitis sistémica que provoca lesiones oculares, de piel y de mucosas que está asociada a HLA-B*51 (Sakane et al. 1999) y la psoriasis, una enfermedad que provoca hiperproliferación de la epidermis e inflamación de la piel asociada a HLA-C*06:02 (Henseler et al. 1985, Gudjonsson et al. 2006). **Tabla 1**

Tiene gran importancia potencial, para entender la patogenia de estas enfermedades, el hecho de que todas ellas están asociadas a ERAP1 y/o ERAP2. Además, la asociación de ERAP1 con EA, BD y Psoriasis está en epistasis con el alelo de MHC-I de susceptibilidad, lo que, muy probablemente, involucra a los ligandos de MHC-I en el mecanismo patogénico de estas enfermedades.

Enfermedad	Alelo de MHC-I	Enzimas
BSCR	**A*29:02**	**ERAP1/ERAP2**
EA	**B*27**	**ERAP1/ERAP2**
Behçet	**B*51:01**	**ERAP1**
Psoriasis	**C*06:02**	**ERAP1/ERAP2**

Tabla 1: Principales enfermedades asociadas a MHC-I: Se incluyen las enzimas del retículo endoplásmico y los principales alotipos MHC-I asociados a cada enfermedad: BSCR: Retinopatía en perdigonada EA: Espondilitis Anquilosante

4. HLA-B*27 y espondilitis anquilosante.

4.1. Características y asociación de subtipos de HLA-B*27 con EA

EA es una enfermedad inflamatoria crónica que afecta principalmente al esqueleto axial, pero con frecuentes afecciones periféricas, caracterizada por entesitis y neoformación ósea. La asociación entre la espondilitis anquilosante y HLA-B*27 es una de las más fuertes entre un alotipo de MHC y enfermedad. Hay descritos numerosos subtipos de esta molécula. Entre los más frecuentes distinguimos algunos asociados (HLA-B*27:02, 04,

05 y 07) y otros no asociados (HLA-B*27:06 y 09) a EA (D'Amato et al. 1995, Lopez-Larrea et al. 1995). Los subtipos de HLA-B*27 presentan diferencias en su plegamiento, estabilidad y en sus peptidomas constitutivos (Galocha et al. 2008, Galocha et al. 2010, Garcia-Medel et al. 2014, Schittenhelm et al. 2015). Aunque todos estos subtipos presentan una estructura idéntica en las subcavidades A y B, lo que les confiere similares características de unión de los extremos N-terminales, presentan al menos una diferencia en un residuo de la cavidad F, que modula el motivo peptídico C-terminal. La mayoría de los subtipos asociados a EA presentan Asp en la posición 116, lo que hace que unan péptidos con residuos C-terminales más masivos y químicamente diversos, mientras que los subtipos que no presentan Asp116 unen mayoritariamente residuos C-terminales apolares y de menor tamaño (Garcia-Medel et al. 2014).

La presencia o ausencia de Asp116 también se correlaciona con la termoestabilidad y el plegamiento, siendo los subtipos con Asp116 de alta termoestabilidad y plegamiento lento y los que poseen otros residuos en esta posición (Tyr116, His116) de baja termoestabilidad y plegamiento rápido **Tabla 2.**

Subtipo	Asociación a EA	Posición 116	Plegamiento	Termoestabilidad	Residuos C-terminales
B27:02	Si	Asp	Lento	Alta	Apolares, Tyr
B27:04	Si	Asp	Lento	Alta	Apolares, Tyr
B27:05	Si	Asp	Lento	Alta	Apolares, Tyr, básicos
B27:06	No	Tyr	Rápido	Baja	Apolares
B27:07	Si	Tyr	Rápido	Baja	Apolares
B27:09	No	His	Rápido	Baja	Apolares

Tabla 2: Asociación a EA y características bioquímicas de los subtipos de HLA-B*27

4.2 Mecanismos de asociación de HLA-B*27 con EA.

Hay tres hipótesis principales que intentan explicar la asociación de HLA-B*27 con EA **Figura I4**. La primera invoca la presentación de un péptido específico que provocaría una respuesta autoinmune a través del mimetismo molecular con un péptido de un patógeno (Benjamin et al. 1990). La mayor objeción que existe contra esta hipótesis es que los linfocitos $CD8^+$ no están implicados en la patogenia de la artritis asociada a HLA-B*27 en ratas transgénicas que desarrollan una enfermedad análoga a la EA en humanos (Breban et al. 1996, May et al. 2003). Una variante reciente de esta hipótesis propone que HLA-B*27 podría ser deficiente en la presentación de algún antígeno necesario para el control de la homeostasis inmune en el intestino, favoreciendo el desarrollo de disbiosis e inflamación intestinal (Kenna 2013, Costello et al. 2014).

La segunda hipótesis es que un mal plegamiento de la cadena pesada de HLA-B27, induciría estrés del retículo endoplásmico y respuesta de proteína mal plegada (UPR), induciendo la sobrexpresión de IL-23 (Colbert et al. 2014). Hay datos convincentes en ratas que apoyan esta hipótesis (Turner et al. 2005, Turner et al. 2007) pero en humanos es difícilmente demostrable. Aunque el mal plegamiento de HLA-B*27 se detecta en el intestino de pacientes, parece ser la autofagia y no la UPR la que induce la sobrexpresión de IL-23 (Ciccia et al. 2014).

Una tercera hipótesis es la formación de homodimeros de cadena pesada de HLA-B*27 en la superficie celular, que serían reconocidos por los receptores KIR3DL2 y estimularían la formación de una población de linfocitos Th17 que portan este receptor (Allen et al. 2001, Bird et al. 2003, Bowness et al. 2011, Shaw et al. 2014). Las dos últimas hipótesis implican que la molécula de HLA-B27 actuaría directamente estimulando el eje IL-23/IL17.

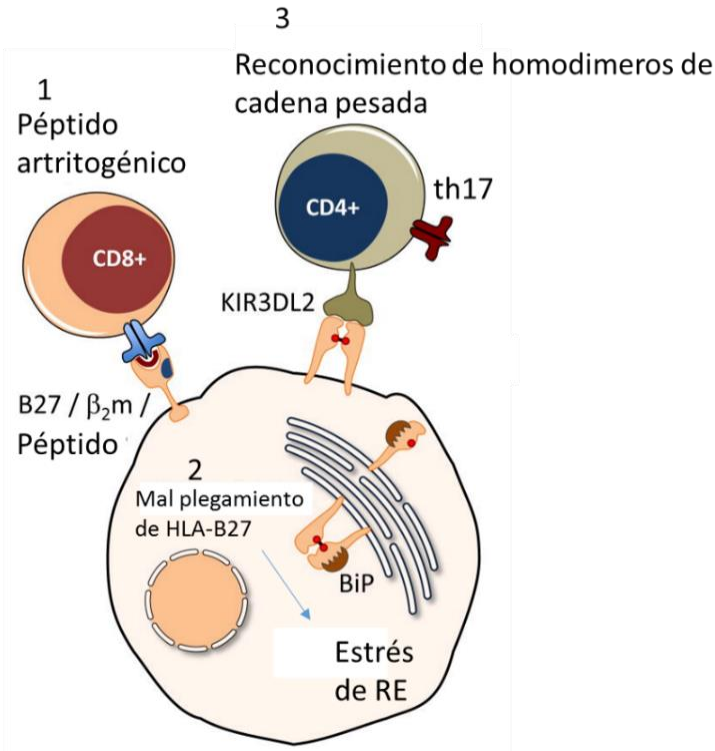

Figura I4: Resumen de las tres hipótesis principales sobre el papel patogénico de HLA-B27 en EA: 1 Hipótesis del péptido artritogénico, 2 Hipótesis del mal plegamiento de HLA-B27 y 3 Hipótesis de los homodimeros de cadena pesada en superficie. Modificado de (Colbert et al. 2014)

5. Aminopeptidasas del retículo endoplasmico implicadas en el procesamiento antigénico de MHC-I.

Una gran parte de los péptidos generados por el proteosoma que alcanzan el RE posee un tamaño superior al óptimo para su unión al MHC-I. El corte de estos péptidos al tamaño apropiado se realiza por ERAP1 y ERAP2. Estas aminopeptidasas, pertenecen a la subfamilia M1 de zinc metalopeptidasas, poseen una identidad de secuencia del 50% y comparten los motivos consenso GAMEN y $HEXXH(X)_{18,}$ pero su especificidad es diferente (Hooper 1994).

5.1. ERAP1.

La principal función de ERAP1 es hidrolizar los extremos N-terminales peptídicos hasta que éstos alcancen una longitud de 9-10 aa. (Serwold et al. 1999, Serwold et al. 2001, Saric et al. 2002, Serwold et al. 2002, York et al. 2002). Su influencia en la generación del peptidoma de MHC-I quedó demostrada cuando se silenció la expresión de esta

proteína y se vio una disminución de ligandos presentados por MHC-I en torno a un 20% y una disminución de su estabilidad en superficie (Hammer, Gonzalez et al. 2007). ERAP1 muestra una cinética de inhibición por sustrato (Evnouchidou et al. 2011) y su actividad se regula por un mecanismo llamado de regla molecular **(Figura I5)**, que consiste en que la hidrólisis enzimática cesa cuando el sustrato alcanza una longitud de 8 a 9 aa. Esta propiedad, aparentemente única entre las aminopeptidasas, se basa en que existe una separación física entre el sitio regulador, al que se une el sustrato, y el sitio catalítico. Por lo tanto, la longitud del péptido tiene que ser suficientemente larga para que, una vez unido al sitio regulador por el extremo C-terminal, el residuo N-terminal alcance el sitio catalítico. La unión del sustrato promueve un cambio conformacional que activa a la enzima. De ahí que ERAP1 es más eficaz cortando péptidos de 9-14 aa y muy poco eficaz cortando péptidos de tamaño inferior (Chang et al. 2005).

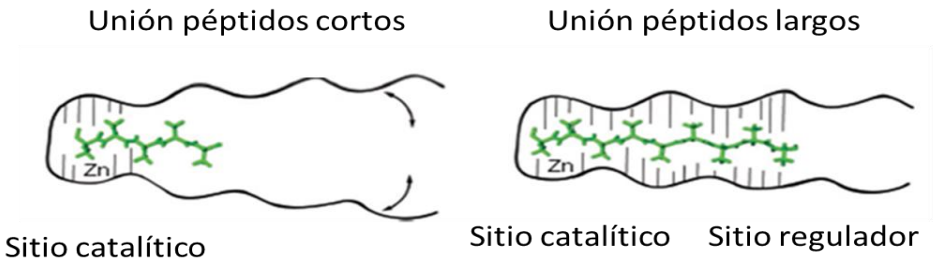

Figura I5: Esquema del mecanismo de regla molecular: El péptido, para poder ser cortado por ERAP1, tiene que tener una longitud suficiente para que una vez unido al sitio regulador llegue al sitio catalítico. Modificado de (Tina T Nguyen et al (2011))

Por tanto, ERAP1 presenta dos conformaciones: una abierta inactiva y otra cerrada activa, que se adopta tras la unión del sustrato (Kochan et al. 2011, Nguyen et al. 2011). Esta enzima consta de cuatro dominios designados I-IV, que comprenden los residuos 1-254, 255-527/529, 528/530-613/614 y 614/615-941 **Figura I6**. La transición entre ambas conformaciones consiste en una rotación del interdominio II-III, haciendo que el dominio IV se cierre sobre el dominio I. El sitio de unión al péptido se encuentra en los dominios II y IV. El péptido se une a ERAP1 por su extremo C-terminal y el extremo N-terminal alcanza el sitio catalítico en el dominio II donde se realiza la hidrólisis.

La especificidad de la molécula por diferentes residuos N-terminales fue definida inicialmente con sustratos fluorogénicos (Saveanu et al. 2005, Evnouchidou et al. 2008,

Goto et al. 2008, Evnouchidou et al. 2009, Zervoudi et al. 2011) y posteriormente con péptidos (Hearn et al. 2009). Estos estudios determinaron la preferencia de esta enzima por residuos hidrofóbicos y su baja eficacia con residuos polares y cargados (ácidos y básicos), asi como su incapacidad de hidrolizar enlaces en los que interviene Prolina.

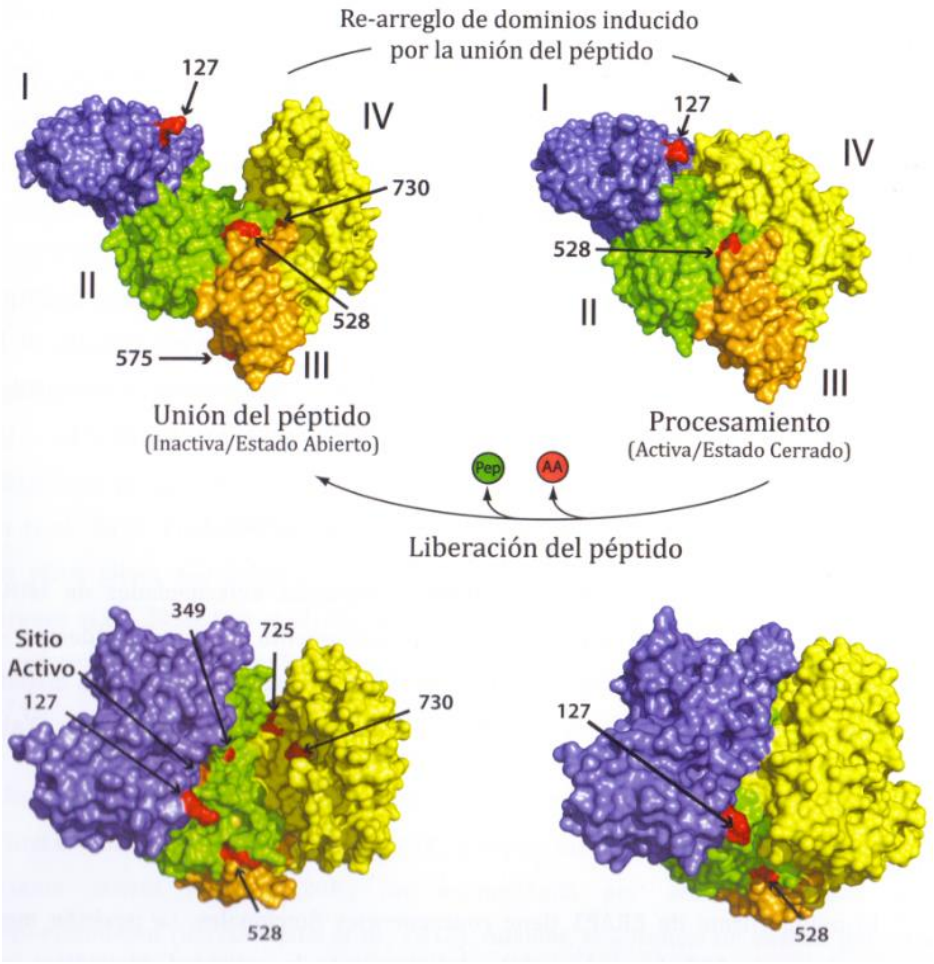

Figura I6 : Estructura de ERAP1, posible mecanismo y topología de los polimorfismos asociados a EA. La sección superior muestra una vista lateral de ERAP1. Los dominios de la proteína estan indicados (I-IV). Modificado de (Alvarez-Navarro et al. 2014)

ERAP 1 es una proteína muy polimórfica y las variantes naturales de esta enzima son alotipos complejos que difieren entre si en varios residuos, codificados por otros tantos cambios no sinónimos de nucleótidos (SNPs) y designados como haplotipos. Los polimorfismos de ERAP1, al menos los de las posiciones 528, 575, 725, y 730 afectan a su actividad enzimática, probablemente induciendo alteraciones en la dinámica de la transición conformacional (residuos 528 y 575) o en la unión al sustrato (residuos 725 y

730). (Goto et al. 2006, Evans et al. 2011, Evnouchidou et al. 2011, Kochan et al. 2011, Martin-Esteban et al. 2014, Sanz-Bravo et al. 2015, Stamogiannos et al. 2015) **Figura I6 y Tabla 3**. La actividad catalítica no solo es dependiente de los polimorfismos aislados, sino sobre todo del conjunto de los polimorfismos presentes en la proteína, ya que, como se demuestra en esta Tesis y en otros estudios, el efecto de una mutación depende de su contexto estructural concreto (Martin-Esteban et al. 2014, Reeves et al. 2014). Existe un gran número de variantes funcionales o haplotipos en la población humana (Ombrello et al. 2015) **Tabla 4**

SNP	MUTACION	DOMINIO	EFECTO EN LA ACTIVIDAD
rs27895	G346D	II	N.D
rs26618	I276M	II	Sin efecto
rs26653	R127P	II	Sin efecto
rs2287987	M349V	II	Sin efecto
rs30187	K528R	II-III	Disminución
rs10050860	D575N	III	Incrementado in vitro
rs17482078	R725Q	IV	Disminución
rs27044	Q730E	IV	Disminución(1)

(1) El efecto de la mutación Q730E es variable dependiente de la longitud del sustrato (Stamogiannos et al. 2015). Con sustratos mayores de 9 residuos E730 muestra menor actividad

Tabla 3: Situación y descripción de los efectos de los polimorfismos asociados a EA: La tabla muestra el efecto de los diferentes polimorfismos en la actividad enzimática descritos hasta el momento. En color rojo están las mutaciones de riesgo para la espondilitis anquilosante y en color verde las mutaciones de protección.

Posición	56	127	276	346	349	528	575	725	730
Hap1	E	P	I	G	M	K	D	R	Q
Hap2	E	R	I	G	M	K	D	R	Q
Hap3	E	R	I	G	M	K	D	R	E
Hap4	E	R	I	G	M	R	D	R	E
Hap5	E	R	I	D	M	R	D	R	E
Hap6	E	P	I	G	M	R	D	R	E
Hap7	K	P	I	G	M	R	D	R	E
Hap8	E	P	M	G	M	R	D	R	E
Hap9	E	P	M	G	M	R	N	R	E
Hap10	E	P	I	G	V	R	N	Q	E

Tabla 4: Haplotipos de ERAP1 más comunes (Ombrello et al., 2015).

5.2 ERAP 2.

En humanos una segunda aminopeptidasa del RE, no presente en ratón, ERAP2, esta implicada en el procesamiento antigénico de MHC-I. (Hattori et al. 1999, Tanioka et al. 2003). Esta enzima se diferencia de ERAP1 en su especificidad enzimática y mecanismo de acción. No sigue el mecanismo de regla molecular, lo que la hace eficiente para cortar octámeros y péptidos menores. Al contrario que ERAP1, su actividad decrece según aumenta la longitud del sustrato (Birtley et al. 2012, Mpakali et al. 2015). También a diferencia de ERAP1, ERAP2 digiere preferentemente residuos básicos (Lys y Arg), sobre todo Arg (Saveanu et al. 2005, Zervoudi et al. 2011, Evnouchidou et al. 2012). Aunque es capaz de hidrolizar algunos otros residuos (Lopez de Castro et al. 2016), es poco eficiencte con los residuos que son mejor cortados por ERAP1.

ERAP2 presenta un grado de polimorfismo bajo y su actividad está modulada por un solo cambio en la posición 392: Lys392Asn (Evnouchidou et al. 2012). La variante Asn392, aunque confiere un aumento de actividad a la enzima, casi nunca se expresa debido a un alto desequilibrio de ligamiento con otro polimorfismo en el intron 11, que impide la expresión de la proteína (Andres et al. 2010). Una excepción a este hecho se ha descrito en la población chilena (Vanhille et al. 2013). Debido a la alta frecuencia y expresión codominante de ambos alelos, aproximadamente el 75% de los individuos en la mayoria de las poblaciones estudiadas expresan ERAP2 y el 25% no lo expresa.

ERAP1 y ERAP2, parecen actuar de manera concertada debido a que complementan sus actividades catalíticas (Saveanu et al. 2005, Lorente et al. 2013). Ambas enzimas pueden formar heterodimeros, aunque estos constituyen únicamente un 10-30 % del pool en el RE (Saveanu et al. 2005). *In vitro*, estos heterodimeros activan alostéricamente ERAP1, digiriendo péptidos más rápida y eficientemente, e incluso diferentes sustratos unidos a MHC-I (Evnouchidou et al. 2014, Chen et al. 2016). Sin embargo, su papel *in vivo* se desconoce.

5.3 Asociación de ERAP1 con espondilitis anquilosante.

ERAP1 está asociada con EA en epistasis con HLA-B*27 (Evans et al. 2011), lo que significa que dicha asociación se da solo en individuos HLA-B*27 positivos. Recientemente se ha descrito que ERAP1 está igualmente en epistasis con HLA-B*40, un alotipo que también se asocia a la EA, aunque mucho menos que HLA-B*27 (Cortes et al. 2015).

La asociación de ERAP1 con EA fue demostrada inicialmente con estudios genéticos que se centraron en cinco SNPs no sinónimos **Tabla 3** (Wellcome Trust Case Control et al. 2007, Brown 2008). En estos estudios se vio que algunos cambios de aminoácidos en determinadas posiciones estaban asociados con susceptibilidad o con protección a la enfermedad. Después se descubrieron nuevas asociaciones y se confirmaron en otras poblaciones y grupos étnicos (Harvey et al. 2009, Pimentel-Santos et al. 2009, Choi et al. 2010, Reveille et al. 2010, Li et al. 2011).

El patrón de asosiación de ERAP1 con EA se ajusta a un modelo de dos mutaciones. Un efecto principal de rs30187 y uno secundario de rs10050860/rs17482078 **Tabla3**. Traducidos a aminoacidos, Arg528 y Asn575/Gln725 confieren protección (Evans et al. 2011). Varios estudios, revisados por (Ombrello et al., 2015), analizaron la asociación de los haplotipos de ERAP1 con EA. Dichos estudios sugieren que de los diez haplotipos naturales de ERAP1 más frecuentes **(Tabla 4)**, tres de ellos predisponen a EA (HAP1 a HAP3) y uno de ellos es protector (HAP10). Las variantes de ERAP1 que se asocian con protección frente a EA son generalmente aquellas que determinan una disminución de la actividad enzimática.

5.4. Asociación de ERAP2 con la espondilitis anquilosante.

La asociación de ERAP2 con EA no se encuentra en epistasis con HLA-B*27. Dicha asociación fue inicialmente descrita en enfermos HLA-B*27 negativos (International Genetics of Ankylosing Spondylitis et al. 2013), ya que el desequilibrio de ligamiento entre ERAP1 y ERAP2 dificulta el análisis en individuos HLA-B*27 positivos.

La asociacion de ERAP2 con EA en individuos HLA-B*27 positivos fue demostrada posteriormente (Robinson et al. 2015). El alotipo de protección es la variante Asn392.

No obstante, como se ha dicho, esta variante no se expresa casi nunca. Por tanto es la expresión de ERAP2 (alotipo Lys392) la que determina riesgo y la variante que no se expresa es la que determina protección. Este patrón es análogo a la acción protectora de las variantes de ERAP1 de baja actividad. Sin embargo los patrones genéticos de asociacion de ERAP1 y ERAP2 con EA son diferentes, sobre todo en los que se refiere a la epistasis con MHC-I y a la naturaleza y diversidad de las variantes alélicas de ambas enzimas.

INTRODUCCIÓN A LOS ARTÍCULOS APORTADOS PARA LA TESIS Y CONTRIBUCIÓN DEL DOCTORANDO

IA 1: Artículos aportados a la tesis doctoral.

Artículo I: García-Medel N, Sanz-Bravo A, Van Nguyen D, Galocha B, Gómez-Molina P, **Martín-Esteban A**, Alvarez-Navarro C, de Lopez deCastro JA (2012). **Functional interaction of the ankylosing spondylitis-associated endoplasmic reticulum aminopeptidase 1 polymorphism and HLA-B27 in vivo.** Mol Cell Proteomics. 2012 Nov;11(11):1416-29. doi: 10.1074/mcp.M112.019588

Artículo II: Martín-Esteban A, Gómez-Molina P, Sanz-Bravo A, López de Castro JA (2014). **Combined effects of ankylosing spondylitis-associated ERAP1 polymorphisms outside the catalytic and peptide-binding sites on the processing of natural HLA-B27 ligands.** J Biol Chem. 2014 Feb 14;289(7):3978-90. doi: 10.1074/jbc.M113.529610

Artículo III: Martín-Esteban A, Guasp P, Barnea E, Admon A, López de Castro JA (2016)**. Functional interaction of the ankylosing spondylitis-associated endoplasmic reticulum aminopeptidase 2 with the HLA-B*27 peptidome in human cells.** Arthritis Rheumatol. 2016 Oct;68(10):2466-75. doi: 10.1002/art.39734.

Artículo IV: Martín-Esteban A, Sanz-Bravo A, Guasp P, Barnea E, Admon A, López de Castro JA. **Separate effects of the ankylosing spondylitis associated ERAP1 and ERAP2 aminopeptidases determine the influence of their combined phenotype on the HLA-B*27 peptidome** (submitted)

IA 2: Breve introdución de los artículos incluidos y su aportación en el campo.

La aminopeptidasa del Retículo Endoplasmático ERAP1 esta asociada a la espondilitis anquilosante en epistasis con la molecula de HLA-B*27 (Evans et al., 2012). Varios polimorfismos de esta molécula estan asociados a riesgo o a protección frente a esta enfermedad (WWTCC Consortium 2007; Brown et al., 2008; Harvey et al., 2009). El principal efecto es debido al polimorfismo de la posicion 528 (K528R) y un efecto secundario a los cambios en las posiciones 575/725. El efecto de mutaciones en posiciones individuales se estableció en varios estudios *in vitro* (Goto et al ., 2006; Evnouchidou et al ., 2011; The TASK and WTCCC 2 2011). El articulo I adjuntado en esta Tesis fue el primer estudio donde se describió el efecto de diferentes polimorfismos de ERAP1, asociados a la Espondilitis Anquilosante, sobre el peptidoma presentado por

la molécula de HLA-B*27 en células vivas. Se vio que polimorfismos asociados a la enfermedad, que determinan mayor actividad enzimática, optimizan la longitud del peptidoma para su unión con HLA-B*27 confiriendo una mayor termoestabilidad a la molécula. Dichos polimorfismos alteraban no solo la longitud de los epitopos presentados sino también su naturaleza química. Estos efectos sugieren un papel central de los péptidos en la patogenia de las enfermedades asociadas a HLA-B*27.

Una vez determinado el efecto global que tienen en el peptidoma de HLA-B*27 las variantes de ERAP1, de riesgo o protectoras para la EA, decidimos investigar las bases moleculares de dicho efecto (Articulo II). Diseñamos mutantes de esta enzima con varias combinaciones de polimorfismos asociados a la enfermedad y realizamos digestiones *in vitro* de péptidos precursores de ligandos naturales de HLA-B*27:05. En este estudio se vio que el efecto del polimorfismo en una determinada posición está influenciado por el polimorfismo en otras posiciones. El procesamiento de ligandos de HLA-B*27 por ERAP1 es dependiente de la variante enzimática y de la estructura del sustrato peptídico. Llegamos a la conclusión de que el mecanismo de interacción ERAP1/HLA-B*27 es el balance entre la generación y la destrucción de los diferentes epítopos, el cual está determinado por la diferencia de susceptibilidad de los residuos flanqueantes y N-terminales a ser cortados por ERAP1. Para cada péptido, dicho balance es diferente con las distintas variantes de esta enzima.

En humanos existe una segunda aminopeptidasa en el RE, implicada en el procesamiento antigénico, ERAP2 (Hattori et al., 1999; Tanioka et al., 2003). El estudio del papel de ERAP2 ha estado dificultado por la ausencia de esta enzima en ratón. Además, debido a su especificidad restringida, se le supuso un papel simplemente complementario a ERAP1 en humanos. En los últimos años se ha renovado el interés en ERAP2 debido a su asociación con EA y a otras enfermedades asociadas a MHC-I (Cortes et al ., 2013; Robinson et al., 2015; Lopez de Castro et al., 2016). En esta Tesis se incluye la primera demostración de cuál es su efecto en el peptidoma de una molecula MHC-I, en concreto HLA-B*27, en células vivas (Articulo III). Para ello se comparó el peptidoma de tres líneas celulares con variantes similares de ERAP1, dos de estas líneas sin ERAP2 y una que expresaba dicha enzima. Nuestro estudio demostró que ERAP2 está implicado en la optimización del peptidoma hacia péptidos del tamaño más adecuado para HLA-B*27. Esta observación se explicaría mejor por una acción indirecta sobre ERAP1. Sin embargo

el efecto más importante fue la disminución de la abundancia de péptidos con residuos básicos en P1, presumiblemente debido a una acción directa de ERAP2. Esta disminución de residuos básicos está muy relacionada con la disminución de la afinidad del peptidoma por HLA-B*27, debido principalmente a que la Arg en P1 confiere mayor afinidad. Al igual que en el artículo I, este efecto subraya un papel central de los péptidos en la patogenia de las enfermedades asociadas a HLA-B*27.

Una vez analizados los efectos de ERAP1 y ERAP2 sobre el peptidoma de HLA-B*27, se decidió estudiar el efecto de la presencia y la ausencia de ERAP2 en el contexto de diferentes variantes de ERAP1 (Articulo IV, enviado). Para ello se estudió el peptidoma de varias líneas celulares en distintos contextos ERAP1/ERAP2. Este artículo demostró que los efectos de ERAP2 sobre el peptidoma de HLA-B*27, relativos a la expresión de esta enzima, son esencialmente independientes de la actividad de ERAP1. Nuestros resultados permiten por primera vez diferenciar los efectos de ambas enzimas en la configuración del peptidoma de HLA-B*27 y sugieren que ERAP1 y ERAP2 actuan fundamentalmente como entidades separadas *in vivo*.

IA 3 Resumen de la contribucion del doctorado en estos trabajos.

Articulo I: Análisis y cuantificación de la expresión de ERAP1 y ERAP2 en las diferentes líneas celulares. Ayuda en el análisis e interpretación de los resultados y en la creación de los varemos de susceptibilidad relativa de los diferentes aminoácidos a ERAP1

Articulo II: Creación de mutantes de ERAP1 con los cambios en los principales polimorfismos naturales asociados a la EA y obtención de las correspondientes proteínas recombinantes. Realizacion de ensayos de actividad mediante sustratos fluorogénicos. Digestion de diversos precursores peptídicos de ligandos naturales de HLA-B*27 con las diferentes variantes de ERAP1. Experimentos de inhibición enzimática de las variantes de ERAP1. Análisis e interpretación de los resultados obtenidos.

Articulos III y IV: Crecimiento y aislamientos del peptidoma de HLA-B*27 en multiples líneas celulares. Filtrado y procesamiento de los datos de espectrometria de masas de los diferentes peptidomas. Comparación de éstos entre sí y análisis e interpretación de los resultados. Cuantificación del nivel de expresión de ERAP1 y ERAP2 en las diferentes

líneas celulares. Ensayos de digestión *in vitro* de diferentes ligandos de HLA-B*27 con diferentes variantes de ERAP1 en presencia y ausencia de ERAP2.

OBJETIVOS

El objetivo general de esta Tesis es determinar la interaccion funcional entre la molecula de HLA-B*27 y las aminopeptidasas del reticulo endoplásmico ERAP1 y ERAP2.

Los objetivos especificos son los siguientes:

1: Determinar el efecto de diferentes polimorfismos de ERAP1 asociados a espondilitis anquilosante sobre el peptidoma de HLA-B*27 en células vivas y sobre precursores peptidicos de ligandos individuales.

2: Analizar el procesamiento *in vitro* de precursos de ligandos naturales de HLA-B27 con diferentes variantes naturales de ERAP1 en ausencia y presencia de ERAP2 para determinar la interdependencia de ambas enzimas en este proceso.

3: Determinar el efecto de la presencia de ERAP2 sobre el peptidoma de HLA-B27 en células vivas en un mismo contexto de ERAP1.

4: Determinar el efecto conjunto de ERAP1 y ERAP2 analizando el peptidoma de HLA-B27 en el contexto de diferentes variantes de ERAP1 en presencia y ausencia de ERAP2.

ARTÍCULOS

Functional Interaction of the Ankylosing Spondylitis-associated Endoplasmic Reticulum Aminopeptidase 1 Polymorphism and HLA-B27 *in Vivo**

Noel García-Medel‡§, Alejandro Sanz-Bravo‡§, Dung Van Nguyen‡, Begoña Galocha‡¶, Patricia Gómez-Molina‡, Adrián Martín-Esteban‡, Carlos Alvarez-Navarro‡, and José A. López de Castro‡‖

The association of ERAP1 with ankylosing spondylitis (AS)[1] among HLA-B27-positive individuals suggests that ERAP1 polymorphism may affect pathogenesis by altering peptide-dependent features of the HLA-B27 molecule. Comparisons of HLA-B*27:04-bound peptidomes from cells expressing different natural variants of ERAP1 revealed significant differences in the size, length, and amount of many ligands, as well as in HLA-B27 stability. Peptide analyses suggested that the mechanism of ERAP1/HLA-B27 interaction is a variant-dependent alteration in the balance between epitope generation and destruction determined by the susceptibility of N-terminal flanking and P1 residues to trimming. ERAP1 polymorphism associated with AS susceptibility ensured efficient peptide trimming and high HLA-B27 stability. Protective polymorphism resulted in diminished ERAP1 activity, less efficient trimming, suboptimal HLA-B27 peptidomes, and decreased molecular stability. This study demonstrates that natural ERAP1 polymorphism affects HLA-B27 antigen presentation and stability *in vivo* and proposes a mechanism for the interaction between these molecules in AS. ***Molecular & Cellular Proteomics 11: 10.1074/mcp.M112.019588, 1416–1429, 2012.***

The mechanism underlying the strong association of HLA-B27 with ankylosing spondylitis (AS) remains unknown. Three main possibilities, each one based on a different molecular feature of HLA-B27, are currently being investigated. The *arthritogenic peptide* hypothesis (1), based on the canonic antigen-presenting properties of Major Histocompatibility Complex class I (MHC-I) molecules, assumes that a peptide epitope of external origin would activate HLA-B27-restricted T-cells, whose cross-reactivity with a self-derived HLA-B27 ligand would result in autoimmune damage. The *misfolding* hypothesis (2) is based on the slow folding and tendency to misfold of HLA-B27 (3, 4). An accumulation of misfolded heavy chains (HCs) in the endoplasmic reticulum (ER) would elicit an unfolded protein response and activate pro-inflammatory pathways. The *surface homodimer* hypothesis (5, 6) is based on the expression of HLA-B27 HC homodimers at the cell surface and their recognition by leukocyte receptors (7), which leads to immunomodulation of inflammatory responses. Because the constitutive binding of endogenous peptides by MHC-I molecules determines not only their antigen-presenting specificity, but also their folding and stability, it was proposed that the HLA-B27 peptidome, through its global influence on the biological behavior of the molecule, is critical to its pathogenetic role (8). This idea found strong support with the discovery of the association of ER aminopeptidase (ERAP) 1 with AS (9) in HLA-B27-positive, but not B27-negative, disease (10). With an estimated population attributable risk of 26%, ERAP1 is the non-MHC gene most strongly associated with AS. Given that ERAP1 is involved in the N-terminal trimming of peptides to their optimal size for MHC-I binding (11–13), its association with AS suggests a pathogenetic mechanism of functional interaction with HLA-B27 that influences peptide binding and antigen presentation. ERAP1 trimming is limited by peptide size, becoming highly inefficient for 8-mers and shorter peptides (13, 14). This is a seemingly unique feature of ERAP1 that is not even shared by its analog ERAP2 (14, 15). The only putative exception, which has not been entirely ruled out, might be insulin-regulated amino peptidase (IRAP), an endosomal analog of ERAP1 involved in cross-presentation, but probably not in processing of constitutive MHC-I ligands (16, 17). IRAP degrades peptides to smaller products than ERAP1 *in vitro* (18). The three-dimensional structure of ERAP1 reveals a substrate binding

From the ‡Centro de Biología Molecular Severo Ochoa, CSIC-UAM, 28049 Madrid, Spain

Received April 11, 2012, and in revised form, July 23, 2012
Published, MCP Papers in Press, August 23, 2012, DOI 10.1074/mcp.M112.019588

[1] The abbreviations used are: AS, ankylosing spondylitis; ER, endoplasmic reticulum; ERAP, endoplasmic reticulum aminopeptidase; HC, heavy chain; IR, intensity ratio; IRAP, insulin-regulated amino peptidase; LCL, lymphoblastoid cell line; mAb, monoclonal antibody; MHC-I, Major Histocompatibility Complex class I; Mw, molecular mass; SNP, single nucleotide polymorphism; WE-I, WEWAK I.

cavity close to the catalytic site, as well as four domains; the conformational rearrangement between an open and a closed conformation, presumably induced upon substrate binding, regulates its enzymatic activity (19, 20). The polymorphic residues found among natural ERAP1 variants (21), and often co-occurring in complex allotypes, are located in various topological regions, including some in close proximity to the catalytic site, the substrate binding cavity, or domain junctions. Therefore, they might alter ERAP1 activity by directly affecting catalysis, altering substrate binding, or modulating domain rearrangements. The association of ERAP1 with AS does not by itself reveal the specific feature(s) determining the pathogenetic role of HLA-B27. Indeed, ERAP1 might influence the generation of specific pathogenetic epitopes; have a general effect on the HLA-B27 peptidome, altering the stability or other features of the molecule; or both. This study investigated general effects of ERAP1 polymorphism on the HLA-B27 peptidome by comparing the size distribution, molecular features, and N-terminal flanking sequences of peptides from human cells expressing the AS-associated B*27:04 subtype and different natural variants of ERAP1.

EXPERIMENTAL PROCEDURES

Cell Lines and Antibodies—The following B*27:04-positive cell lines were used: JSL (HLA-A*11; B*27:04, *48; C*02), WEWAK I (WE-I: HLA-A*11, *24; B*27:04, *62; C*02, *04), and KNE (HLA-A*01, *02:04; B*27:04, *08) are lymphoblastoid cell lines (LCLs). C1R04 is a transfectant of the lymphoid HLA class I-defective Hmy2.C1R cell line (22) expressing B*27:04 (23). The cells were cultured in RPMI 1640 medium supplemented with 2 mM L-glutamine and 10% FBS (Invitrogen, Paisley, UK). ME1 (IgG1), an anti-HLA-B7/B27/B22 monoclonal antibody (mAb) that recognizes HC/β_2m/peptide complexes (24), was used for immunopurification of HLA-B27.

Typing of Nonsynonymous SNPs in the ERAP1 and ERAP2 Genes—DNA purification was performed using the High Pure PCR Template Preparation system (Roche Diagnostics, Barcelona, Spain) following the instructions of the manufacturer. Aliquots of 10 ng were added onto 384-well plates in duplicate, dried, and amplified using specific oligonucleotides for eight non-synonymous SNPs located in the coding sequence of the ERAP1 gene: rs26653, rs26618, rs27895, rs27044, rs30187, rs10050860, rs17482078, and rs2287987 (Table I). Samples were run in an HT7900 Fast Real-Time PCR System and genotyped using SDS2.2 software (both from Applied Biosystems, Invitrogen, Carlsbad, CA) for allelic discrimination. The nonsynonymous SNP rs2549782 (G/T), encoding for the K392N change in ERAP2, was typed by same procedure.

Sequencing of ERAP1 Variants—Exons 2–20, encompassing the coding region of ERAP1, were separately amplified via PCR and cloned into M13 for sequencing. PCR products were generated using AmpliTaq Gold PCR Master Mix (Applied Biosystems) following standard procedures, purified using ExoSap (USB Corp., Cleveland, OH), and sequenced in a 3730XL instrument (Applied Biosystems). Sequencing primers were either M13-complementary oligonucleotides, for amplicons that included this extension along the ERAP1 sequence, or the specific primers themselves when the amplicons lacked M13-derived sequences. Both strands of amplicons were routinely sequenced.

Quantitative RT-PCR—Total cellular RNA was extracted using the RNeasy Mini Kit (Qiagen, Madrid, Spain), and this was followed by digestion with DNase I (Invitrogen, Karlsruhe, Germany). Complementary DNA was synthesized from 250 ng of total RNA using the High Capacity cDNA reverse transcription kit (Invitrogen) according to the manufacturer's instructions. The primers used for the amplification were purchased from Applied Biosystems. Comparative quantification of gene expression was performed via quantitative RT-PCR with an AB7900HT instrument (Applied Biosystems) using TaqMan probes and Gene Expression Master Mix (Applied Biosystems). Amplifications were carried out with an initial hold at 50 °C for 2 min followed by denaturation at 95 °C for 10 min, 40 cycles of denaturation at 95 °C for 15 s, and annealing and extension at 60 °C for 60 s. The results were expressed as relative mRNA expression quantified with the RQ Manager software and normalized to glyceraldehyde-3-phospahate dehydrogenase transcript levels.

Western Blot—About 2×10^5 cells were lysed in 0.5% Igepal CA-630 (Sigma-Aldrich, St Louis, MO), 50 mM Tris HCl, 5 mM $MgCl_2$, pH 7.4, containing protease inhibitors (Complete Mini) (Roche, Mannheim, Germany). After SDS-PAGE (10% slab gels) of whole lysates under reducing conditions, the separated components were electroblotted onto a nitrocellulose membrane (Amersham Biosciences Hybond-ECL) (GE Healthcare, Buckinghamshire, UK) at 20 V overnight using 30% methanol in 50 mM Tris/Gly buffer, pH 8.8, 0.04% SDS. ERAP1, ERAP2, and γ-tubulin, used as an internal standard, were revealed with the 6H9 mAb (a kind gift from Peter van Endert, INSERM, Paris, France), 3F5 (R&D Systems, Minneapolis, MN), or GTU88 (Sigma-Aldrich), respectively, using peroxidase-conjugated goat anti-mouse Ig polyclonal antibody (DakoCytomation, Glostrup, Denmark). The scanned autoradiograms were quantified using TINA 2.09e image analyzer software (Raystest Isotopenmessgeräte, Straubenhardt, Germany).

Isolation of HLA-B27-bound Peptides—This was carried out as described elsewhere (25). Briefly, cells were lysed in 1% Igepal CA-630 with a mixture of protease inhibitors (Roche). The soluble fraction was subjected to affinity chromatography using the ME1 mAb. HLA-B27-bound peptides were eluted with 0.1% aqueous TFA at room temperature, filtered through Centricon 3 (Amicon, Beverly, MA) or Vivaspin 2 Hydrosart (VS02H11, Sartorious Stedim Biotech, Gottingen, Germany), concentrated, and subjected to HPLC fractionation in a Waters Alliance system (Waters, Milford, MA) using a Vydac 218TP52-C18 column (Vydac, Hesperia, CA) at a flow rate of 100 μl/min, as described elsewhere (26). Fractions of 50 μl were collected and stored at −20 °C.

Mass Spectrometry—Individual HPLC fractions were analyzed via MALDI-TOF MS using a 4800 Proteomics Analyzer (Applied Biosystems), as described elsewhere (27). The mass spectra were acquired in reflector positive mode at 25 kV in the *m/z* range of 800–2000, using a signal-to-noise ratio (s/n) cutoff of 3, and processed using Data Explorer software, version 4.9 (Applied Biosystems). Sample handling and acquisition parameters were tightly controlled to minimize differences in the experimental conditions among samples to be compared in each experiment.

Peptide sequencing was carried out with MALDI-TOF/TOF MS/MS, as described elsewhere (27). Interpretation of the MS/MS spectra was assisted by various tools. Manual inspection of the spectrum usually allowed us to derive a tentative sequence. This was used to screen the human proteome in the human protein entries of the Uniprot/Swiss-prot database (Release 57.6, June 28, 2009, with 20,331 entries), using a window of 0.5 *m/z* units for both precursor and fragment ions, for a possible match using the Mascot server 2.2 software. For those sequences showing the highest scores in this preliminary search, the MS-product tool (version 5.9.4) (University of California, San Francisco, CA) was used to match the candidate sequences to our MS/MS spectra.

Trimming Susceptibility of N-terminal Flanking and P1 Residues—The susceptibility of flanking (P-2, P-1) and P1 residues to ERAP1

TABLE I
*ERAP1 polymorphism in B*27:04 positive cell lines*[a]

SNP	Nucl./AA Position N.	Odds ratio (Ref.)	Consensus	JSL	C1R	KNE[b]	WE-I
rs26653	380/127	1.3 (21)	g/R	g/R	**c/P**	g, **c**/R, **P**	**c/P**
rs26618	828/276	0.99 (21)	a/I	a/I	**g/M**	a, **g**/I, **M**	a/I
rs27895	1037/346	1.07 (21)	g/G	g/G	g/G	g, **a**/G, **D**	g/G
rs2287987	1045/349	0.71 (56)	a/M	a/M	a/M	a/M	**g/V**
rs30187	1583/528	1.4 (56)	a/K	a/K	**g/R**	**g/R**	**g/R**
rs10050860	1723/575	0.71 (56)	g/D	g/D	g/D	g/D	**a/N**
rs17482078	2174/725	0.7 (56)	g/R	g/R	g/R	g/R	**a/Q**
rs27044	2188/730	1.4 (56)	c/Q	c/Q	**g/E**	**g/E**	**g/E**

[a] Only nonsynonymous changes in the coding strands of ERAP1 are shown. Nucleotide and amino acid residue numbering and consensus sequence are from Human ERAP1 Isoform 2 (Accession No.: Q9NZ08-2). Deviations from the consensus sequence are in boldface. Polymorphisms associated with increased risk for AS are underlined. All polymorphic positions were determined via SNP typing and confirmed by genomic sequencing.

[b] KNE was heterozygous for rs26653, rs26618, and rs27895, and this was confirmed by genomic sequencing.

trimming was estimated by assigning a score to each amino acid ranging from 0 to 100, based on a previously reported assay that measured the presentation of the SIINFEKL peptide from ER-targeted precursors (28). The score assigned to each residue (supplemental Table S1) corresponded to the mean percent of SIINFEKL expressed at the cell surface from XX- SIINFEKL precursors, relative to the most susceptible residue in this assay (Y: score 100). Proline and any residue immediately preceding it were assigned a score of 0.

Contribution of Internal Peptide Residues to ERAP1-mediated Trimming—This was estimated based on a previous study (29) in which a 9-mer library was used to assess the influence of different residues at each peptide position on the trimming of P1 by ERAP1 *in vitro*. Each residue at a given position, from P3 to P9, was assigned a score corresponding to the percentage of depleted substrate in that experiment (supplemental Table S1). Residues not directly tested in that study were not scored.

Thermostability Assay—This was performed as described elsewhere (30). Briefly, the cell lines were pulse-labeled for 15 min and chased at various times. At each time point, the cell lysates were incubated for 1 h at various temperatures, immunoprecipitated with ME1, and analyzed via SDS-PAGE. The amount of heterodimer precipitated at each temperature at any given time was expressed as a percentage of the amount precipitated at 4 °C and plotted as a function of the temperature.

RESULTS

*ERAP1 and ERAP2 Polymorphism and Expression in HLA-B*27:04-positive Cell Lines*—Four B*27:04-positive cell lines, including 3 LCL and C1R transfectants, were selected on the basis of their expression of eight SNPs encoding nonsynonymous substitutions in ERAP1, including 6 AS-associated ones (9, 21). Sequencing of all the exons of this gene in the four cell lines confirmed these polymorphisms (Table I). Whereas the coding sequence of ERAP1 from JSL was identical to the consensus and carried all six polymorphisms associated with increased susceptibility to AS, that from WE-I showed six nonsynonymous changes, including all those associated with protection from AS. ERAP1 from C1R04 showed four nonsynonymous changes relative to the consensus. KNE was heterozygous for rs26653, rs26618, and rs27895. This variability allowed us to examine the effect of various combinations of amino acid changes in natural ERAP1 variants on the HLA-B27-bound peptidome. Genotyping of the four cell lines for the nonsynonymous rs2549782 SNP of ERAP2, coding for the K392N change, revealed that WE1, C1R04, and KNE were heterozygous, whereas JSL was homozygous (T/T), expressing only the N392 allotype.

Western blot analyses of WE-I, C1R04, and KNE (Figs. 1*A* and 1*B*) revealed that these cell lines expressed fairly similar ERAP1 protein levels: the WE-I/C1R04 ratio was 1:1.2, and the C1R04/KNE ratio was 1:1.4 (Fig. 1*B*), in agreement with previous studies on LCL (31). Although protein levels could not be assessed for JSL because of the loss of this cell line in the course of this study, the relative mRNA expression of ERAP1 was determined for all four cell lines (Fig. 1*C*). This reflected closely ERAP1 protein levels in C1R04 and WE-I (WE-I/C1R04 ratio, 1:1.3). mRNA expression for KNE was similar to that for WE-I and somewhat lower than that for C1R (C1R:KNE ratio, 1:0.75). JSL showed the lowest mRNa levels (about 0.6:1 and 0.8:1 relative to C1R04 and to WE1 or KNE, respectively). ERAP2 protein expression was similar in C1R04 and KNE and about 2-fold higher in WE-I (supplemental Fig. S1).

Automated Comparison of HLA-B27-bound Peptide Repertoires—B*27:04-bound peptide pools were fractionated via HPLC, and each fraction was analyzed using MALDI-TOF MS. Three pairwise comparisons—WE-I/JSL, WE-I/C1R04, and C1R04/KNE—were carried out, following a strategy previously used for HLA-B27 subtype-bound peptidomes (32–34). In order to assess the inherent experimental error in these comparisons, the B*27:04-bound peptides from two independent batches of C1R04 cells, C1R04-I and -II, were separately processed and compared in the same way. For each cell line pair, the MS spectra of correlative HPLC fractions from consecutive chromatographic runs performed under identical conditions were automatically compared using a newly developed software, MShandler (Fig. 2). All the ion peaks in the *m/z* range of 800–2000 and s/n $>$ 3 were collected from the MS spectra of all HPLC fractions from each

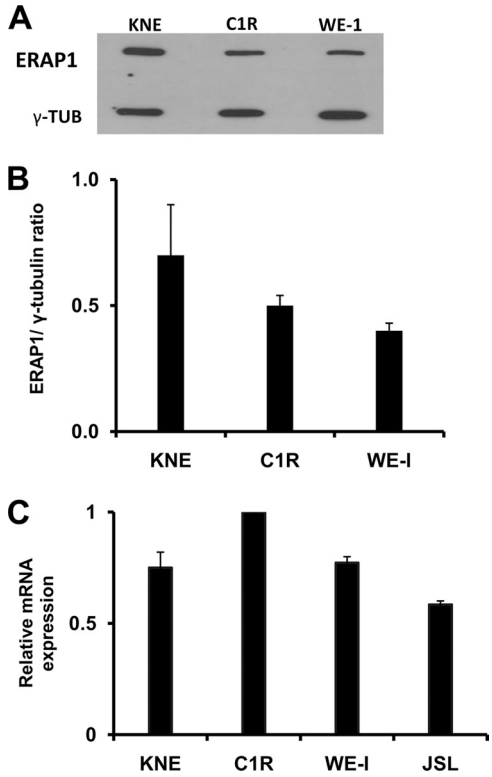

FIG. 1. **ERAP1 expression among cell lines.** *A*, Western blots were performed for the indicated cell lines using the anti-ERAP1 6H9 mAb and the anti-γ-tubulin GTU88 mAb as an internal control. A representative experiment is shown. *B*, ERAP1 protein expression in the indicated cell lines, as established by Western blot. Data are expressed as the ERAP1/γ-tubulin ratio and are means ± S.D. of five experiments. *C*, quantitative RT-PCR showing the expression of ERAP1 mRNA in the indicated cell lines relative to C1R04. Data are expressed as relative quantity values and are means ± S.D. of three experiments.

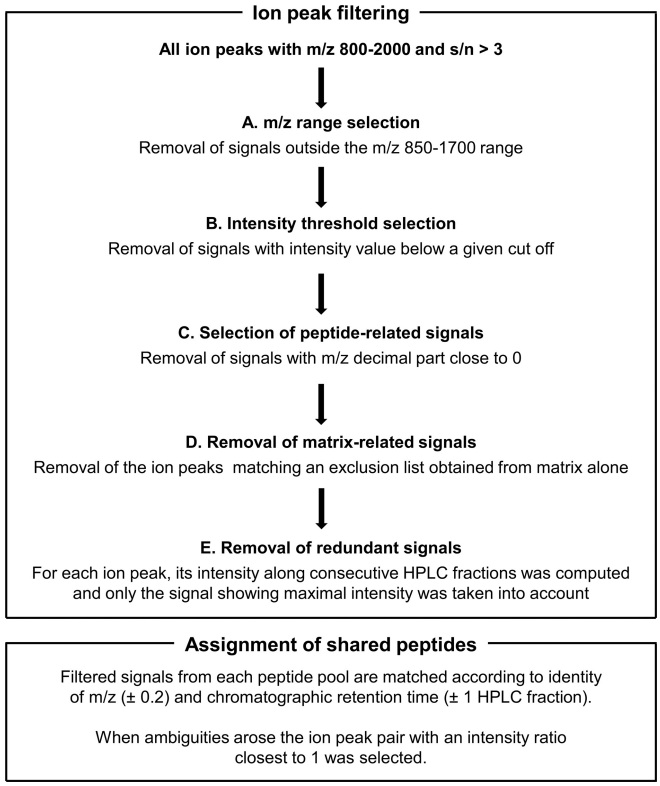

FIG. 2. **Flow chart for the automatic pairwise comparison of B*27:04-bound peptidomes.** The upper scheme shows the filtering of ion peaks from the MALDI-TOF MS spectra of HPLC fractions from each peptide pool. The following filters were applied. A: Signals with $m/z \leq 850$ and > 1700 are usually abundant in matrix-related and other MHC-I unrelated ion peaks. B: Signals with low intensity, as many of them are too close to background. The intensity cutoff was adopted depending on the total number and overall intensity of the ion peaks in each experiment. It was set at 200 for WE-I/JSL and WE-I/C1R04 and at 300 for KNE/C1R04. C: Ion peaks with decimal part of the m/z ($M + H^+$) value ranging from 0.0 to 0.2 and from 0.9 to 0.0 were removed based on the extremely low frequency (1 of 1268) of HLA-B27 ligands in these ranges (55). D: Matrix-related ion peaks were identified from MS spectra of matrix without peptide. E: The program computed identical ion peaks (±0.2 Da) along consecutive HPLC fractions and selected only the one with the maximal intensity. The lower scheme shows the criteria used for the assignment of shared peptides.

peptide pool and identified by their *m/z* and HPLC fraction numbers. Prior to each comparison, a series of filters were applied to remove irrelevant signals and maximize the selection of B27-related ion peaks. The filtered ion peak sets from the two cell lines in each experiment were compared: ion peaks with identical (±0.2) *m/z* in the correlative ±1 HPLC fraction of the other cell line were considered as shared peptides in the two cell lines and subjected to further analysis. All other peaks were disregarded (supplemental Table S2).

*Relative Expression of B*27:04 Ligands in Distinct ERAP1 Contexts*—We reasoned that if there were not a general influence of ERAP1 polymorphism on the HLA-B27 peptidome, or in the context of similar ERAP1 molecules, the size distribution of shared peptides in two cell lines would be essentially identical independent of their relative abundance in each cell line. Conversely, if ERAP1 polymorphism has a general influence on peptide trimming, the size distribution of shared B27 ligands will be shifted toward higher molecular mass (Mw) values in the cell line with the less efficient ERAP1 variant, to an extent that would depend on the relative abundance of the peptides compared. Thus, we calculated the intensity ratio (IR) between shared ion peaks in the WE-I/JSL, WE-I/C1R04, C1R04/KNE, and C1R04-I/II comparisons as an estimation of relative peptide abundance. The peptides showing IR > 1 were classified in three subsets: those showing >3-fold, >1.5- to 3-fold, and >1- to 1.5-fold intensity in one relative to the other cell line (supplemental Table S3). We next compared the mean Mw (Fig. 3) and the Mw distribution (Fig. 4) within equivalent subsets in both cell lines. The results are described below.

WE-I/JSL—The shared ion peaks showed a Gaussian size distribution with a mean *m/z* of 1162.0 (Fig. 4*A*). For peptides with IR > 1 in each cell line there was a shift of the Gaussian curve from WE-I, relative to JSL, toward higher Mw values

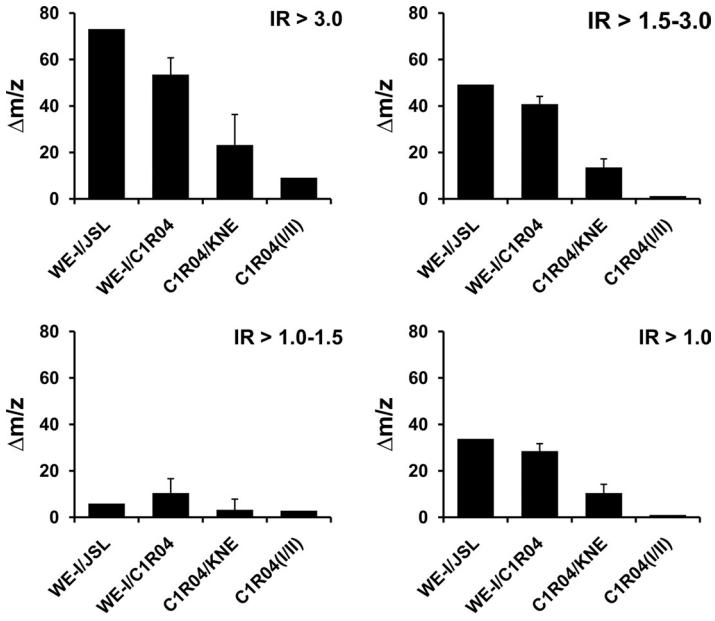

FIG. 3. **Relative expression and mean Mw of shared B*27:04 ligands in various ERAP1 contexts.** For each of the four indicated pairwise comparisons, the shared ion peaks were classified on the basis of their intensity ratio (IR) between both cell lines as indicated. The "IR > 1" set in each cell line includes the three other indicated subsets The mean *m/z* value, which in MALDI-TOF MS is equivalent to the mean Mw ($M + H^+$), of the ion peaks in each peptide subset was calculated, and the difference ($\Delta m/z$) between equivalent subsets from the two cell lines compared was represented for the four comparisons. Data for WE-I/JSL and C1R04 (I/II) are from a single experiment; those for WE-I/C1R04 and C1R04/KNE are the mean ± S.D. of two and three experiments, respectively.

($\Delta m/z = 33.8$). When the different IR subsets were compared, the magnitude of the shift was found to be highest between the IR > 3 subsets ($\Delta m/z = 73.1$), somewhat smaller between those with IR > 1.5 to 3 ($\Delta m/z = 49.2$), and virtually overlapping ($\Delta m/z = 5.9$) in the >1- to 1.5-fold subsets. This comparison was carried out only once because of the loss of JSL in the course of this study.

WE-I/C1R04—The shared ion peaks in these two cell lines showed a Gaussian size distribution with mean *m/z* values of 1154.3 and 1157.2 in two independent comparisons (supplemental Table S3) (Fig. 4*B*). The curve of the peptides with IR > 1 in WE-I was shifted toward higher Mw, relative to C1R04, similarly as for JSL ($\Delta m/z = 28.5 \pm 3.2$). When IR subsets were compared, a curve shift similar to that of WE-I/JSL was observed for the IR > 3 and >1.5 to 3 subsets, although the mean Mw differences were somewhat smaller ($\Delta m/z = 53.5 \pm 7.2$ and 40.8 ± 3.3, respectively) (Fig. 3) (supplemental Table S3). These results indicate that B27 ligands with high Mw tend to be more abundant in WE-I than in JSL or C1R04, and the opposite is true for ligands with low Mw, but differences are smaller with C1R04 than with JSL.

C1R04/KNE—The ERAP1 molecules in these two cell lines were identical except at positions 127, 276, and 346, where KNE, but not C1R, showed heterozygosis (Table I) (Fig. 4*C*). This comparison was carried out three times using three independent batches of C1R04 cells and two batches of KNE. The size distribution and average Mw of shared B27 ligands showed significantly smaller differences between both cell lines than in the previous comparisons (Figs. 3 and 4), indicating little effect of the ERAP1 or other cellular background differences between C1R04 and KNE on these features.

C1R04 I/II—The intensity of individual ion peaks corresponding to B*27:04 ligands showed variability in the two preparations that allowed their classification into IR subsets similar to those observed between different cell lines (supplemental Table S3). To some extent, this might be due to the fact that C1R04-I and -II were grown and processed as independent batches, but it also suggests that, on an individual basis, the ion peak intensity in MALDI-TOF MS might not be a reliable indicator of peptide abundance. Yet, in contrast to previous comparisons, the average Mw of B27 ligands was very similar in both peptide preparations for all IR subsets (Fig. 3), and the corresponding size and length distributions were virtually overlapping in all cases (supplemental Fig. S2), indicating that the size distribution differences observed in other comparisons are not due to the nonquantitative character of ion peak intensity as an indicator of peptide abundance. The value of $\Delta m/z = 9.1$ Da observed only between the IR > 3 subsets (Fig. 3) reflects the level of experimental error in this type of comparison when applied globally to large peptide sets.

The results indicate that allelic ERAP1 polymorphism has a global influence on the B*27:04 peptidome, affecting the relative expression of many B*27:04 ligands as a function of peptide size. The observed effects are consistent with the following ERAP1 activity ranking: JSL > C1R04/KNE > WE-I.

*Relationship between Size and Length Distribution of B*27:04 Ligands*—Because of the wide Mw range among peptides of the same length, translating the observed peptide size into length differences that best reflect the relative activity among ERAP1 variants was not straightforward. Thus, the amino acid sequence of 372 B*27:04 ligands showing various degrees of differential expression among cell lines was determined (supplemental Table S4), and the percentage of peptides of any given length within each Mw range was calculated (Table II). As these sequences were obtained due only to the high intensity of the corresponding ion peaks in the MS spectra and were not preselected otherwise, they were

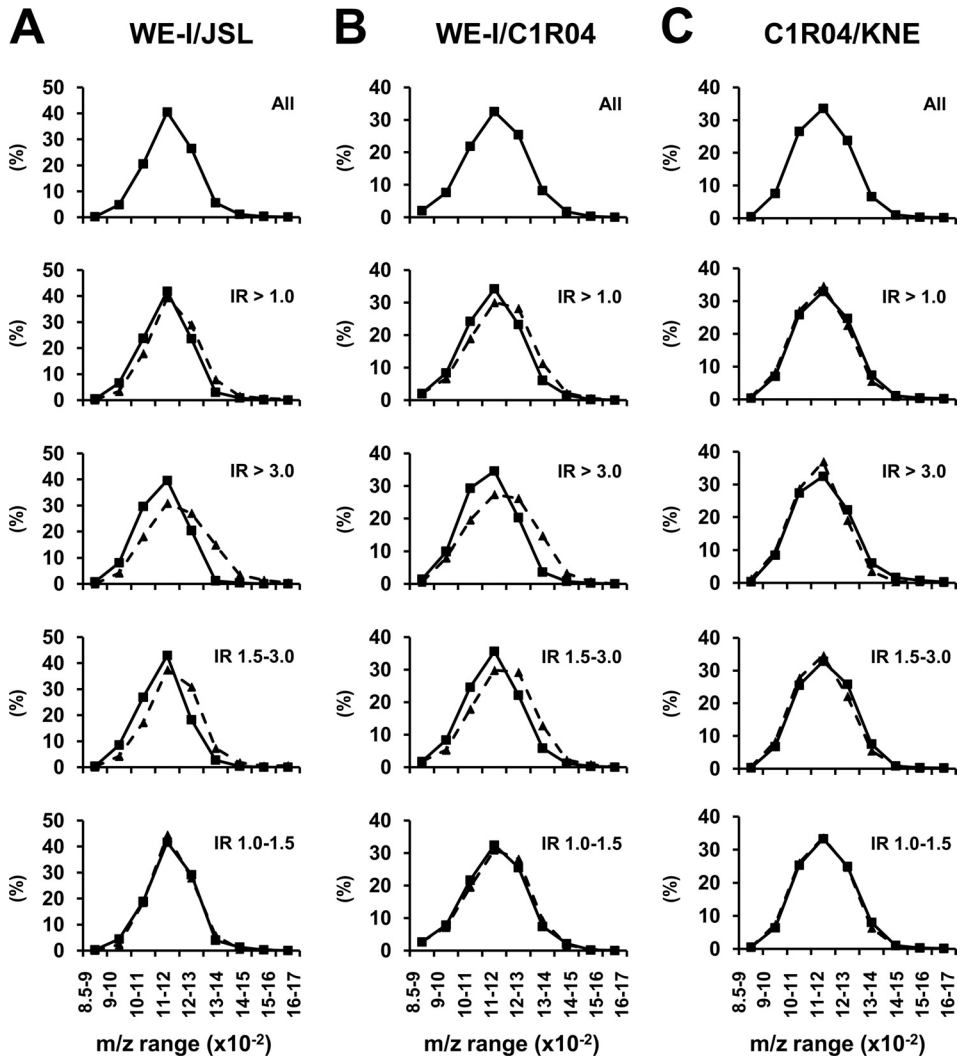

FIG. 4. **Size distribution of B*27:04 ligands as a function of their relative abundance in various ERAP1 contexts.** *A*, WE-I/JSL. The upper histogram shows the Mw distribution of 3222 shared ligands between both cell lines. The other four histograms compare the Mw distribution of the peptide sets predominant (IR > 1.0) in WE-I (*dotted line*) or JSL (*solid line*), as well the corresponding subsets showing IR > 3.0, IR > 1.5 to 3.0, and IR > 1.0 to 1.5 in each cell line. *B*, WE-I/C1R04. The upper histogram shows the Mw distribution of the shared ligands between both cell lines. The other four histograms compare the Mw distribution of the peptide sets predominant in WE-I (*dotted line*) or C1R04 (*solid line*), following the same conventions as in panel *A*. The data are means of two experiments (supplemental Table S3). *C*, C1R04/KNE. The upper histogram shows the Mw distribution of the shared ligands between both cell lines. The other four histograms compare the Mw distribution of the peptide sets predominant (IR > 1.0) in C1R04 (*solid line*) or KNE (*dotted line*), following the same conventions as in panel *A*. The data are means of three experiments (supplemental Table S3).

assumed to represent a fair sampling of the B27 peptidome. Thus, the relationship between Mw and residue length among these peptides was used to translate the Mw differences described in the preceding paragraph into peptide length differences (Fig. 5).

WE-I/JSL—The shared B*27:04 ligands between these cell lines were estimated to include 2.5% 8-mers or smaller peptides, 70.7% 9-mers, 21.1% 10-mers, and 5.8% longer peptides (Fig. 5*A*). Peptides with IR > 1 showed a skewing against short peptides (9-mers and shorter) and toward long ones (10-mers and longer) in WE-I; the magnitude of the skewing depended on the expression relative to JSL and was highest for the IR > 3 subsets, intermediate for IR > 1.5 to 3 subsets, and low among peptides with IR > 1 to 1.5

WE-I/C1R04—As in the preceding comparison, peptides with IR > 1 showed a moderate skewing against short peptides and toward long ones in WE-I (Fig. 5*B*). Length skewing again was more prominent between the IR > 3 subsets, decreased in the IR > 1.5 to 3 subsets, and was marginal in the IR > 1 to 1.5 subsets. The pattern was similar to that in WE-I/JSL, but the differences were smaller.

C1R04/KNE—Length differences among the B*27:04 ligands of these cell lines were noticeable only among the peptide subsets with IR > 3 (C1R04/KNE ratio 0.8 ± 0.0 and

TABLE II
*Relationship between Mw and length among 372 B*27:04 ligands*[a]

Mw	Peptide length							
	<9-mers[b]		9-mers		10-mers		>10-mers[c]	
	N	%	N	%	N	%	N	%
850–900	3	100	0	0	0	0	0	0
900–1000	8	21.1	30	79.0	0	0	0	0
1000–1100	7	5.9	102	86.4	8	6.8	1	0.9
1100–1200	0	0	127	85.8	20	13.5	1	0.7
1200–1300	0	0	24	52.2	19	41.3	3	6.5
1300–1400	0	0	1	8.3	7	58.3	4	33.3
1400–1500	0	0	0	0	0	0	4	100
1500–1600	0	0	0	0	0	0	2	100
1600–1700	0	0	0	0	0	0	1	100
Total	**18**	**4.8**	**284**	**76.3**	**54**	**14.5**	**16**	**4.3**

[a] Percent values are relative to each Mw range, except in the "Total" line, where the values are relative to the total number of peptide sequences.
[b] All these peptides were 8-mers, except one 7-mer.
[c] 11-mers: 10; 12-mers: 4; 13-mers: 1; 15-mers: 1.

1.7 ± 0.2 for peptides <9-mers and >10-mers, respectively) (Fig. 5*C*).

Thus, in WE-I, long B*27:04 ligands are more abundant and short ones are less abundant than in JSL and, to a lesser extent, C1R04. The results indicate that ERAP1 polymorphism in WE-I leads to decreased trimming and affects the expression level of a substantial percentage of the B27 peptidome. The idea that the observed differences are due mainly to ERAP1, rather than to unrelated factors, is strongly supported by the similarity between C1R04 and KNE.

*The N-terminal Flanking and P1 Residues Determine the ERAP1-dependent Expression of B*27:04 Ligands*—Amino acid residues differ widely in their susceptibility to ERAP1 trimming. Susceptible residues in the N-terminal flanking sequences favor the generation of B*27:04 ligands, whereas susceptible P1 residues might favor their destruction. Thus, the N-terminal flanking residues of numerous B*27:04 ligands showing distinct relative expression among cell lines were assigned from the sequence of their parental proteins (supplemental Table S4). The sequenced peptides in each pairwise comparison were classified in those with IR > 3 and those with IR > 1 to 3 in one cell line relative to the other. The flanking (P-2 and P-1) and P1 residues of each peptide were assigned a trimming susceptibility score (supplemental Table S1) based on a previously reported assay (28). For each peptide subset, a mean score was determined for P-2, P-1, P-2 + P-1, and P1. The ratio between the mean scores of equivalent peptide subsets in the cell lines compared was used as a global estimation of their relative susceptibility to trimming. The following observations emerged from this analysis (Table III).

WE-I/JSL—Both the flanking and P1 residues of the peptides in the IR > 3 subsets were more susceptible to trimming in WE-I than in JSL (added P-2 + P-1 score ratio = 1.4; P1 score ratio = 2.5), but those in the IR < 3 subsets showed smaller differences. These results strongly suggest that the predominance of B*27:04 ligands in these cell lines is determined by higher or lower susceptibility of the flanking and P1 residues to trimming in the context of the less (WE-I) or more (JSL) active ERAP1 variant, respectively.

WE-I/C1R04—The flanking residues of the peptides in the IR > 3 subsets were more susceptible to trimming in WE-I than in C1R04 (added P-2 + P-1 score ratio of 1.4). In contrast, the average susceptibility of P1 residues to trimming was very similar in both cell lines for all peptide subsets, regardless of their relative expression (Table III). Thus, again, the predominance of B*27:04 ligands in these cell lines is correlated with higher susceptibility of the flanking residues to trimming in the context of the less active variant (WE-I). The similar P1 susceptibility suggests that differential epitope destruction contributes less to peptide predominance between these two cell lines. Yet, similarly susceptible P1 residues should be more efficiently trimmed by the most active ERAP1 variant.

C1R04/KNE—This analysis revealed smaller differences in the trimming susceptibility of the flanking and P1 residues between the peptides predominant in either cell line than in the previous comparisons (Table III). Score ratios for any given position or peptide subset were no higher than 1.3, and their magnitude did not correlate with IR. Thus, peptide expression differences between C1R04 and KNE seem largely unrelated to ERAP1, in agreement with the similar activity of this enzyme in both cell lines suggested by the size and length distribution of their HLA-B27 peptidomes.

*The Internal Sequence Features of B*27:04 Ligands Do Not Determine Their Differential ERAP1-dependent Expression*—We investigated whether peptide residues other than P1 might account for the prevalence of some B*27:04 ligands in a given ERAP1 context. This analysis was carried out only for nonamers and was based on the reported role of residues downstream of P1 in modulating trimming by ERAP1 (29). Each residue at positions P3 to P9 (as P2 is nearly invariant among B*27:04 ligands) was assigned a score related to its

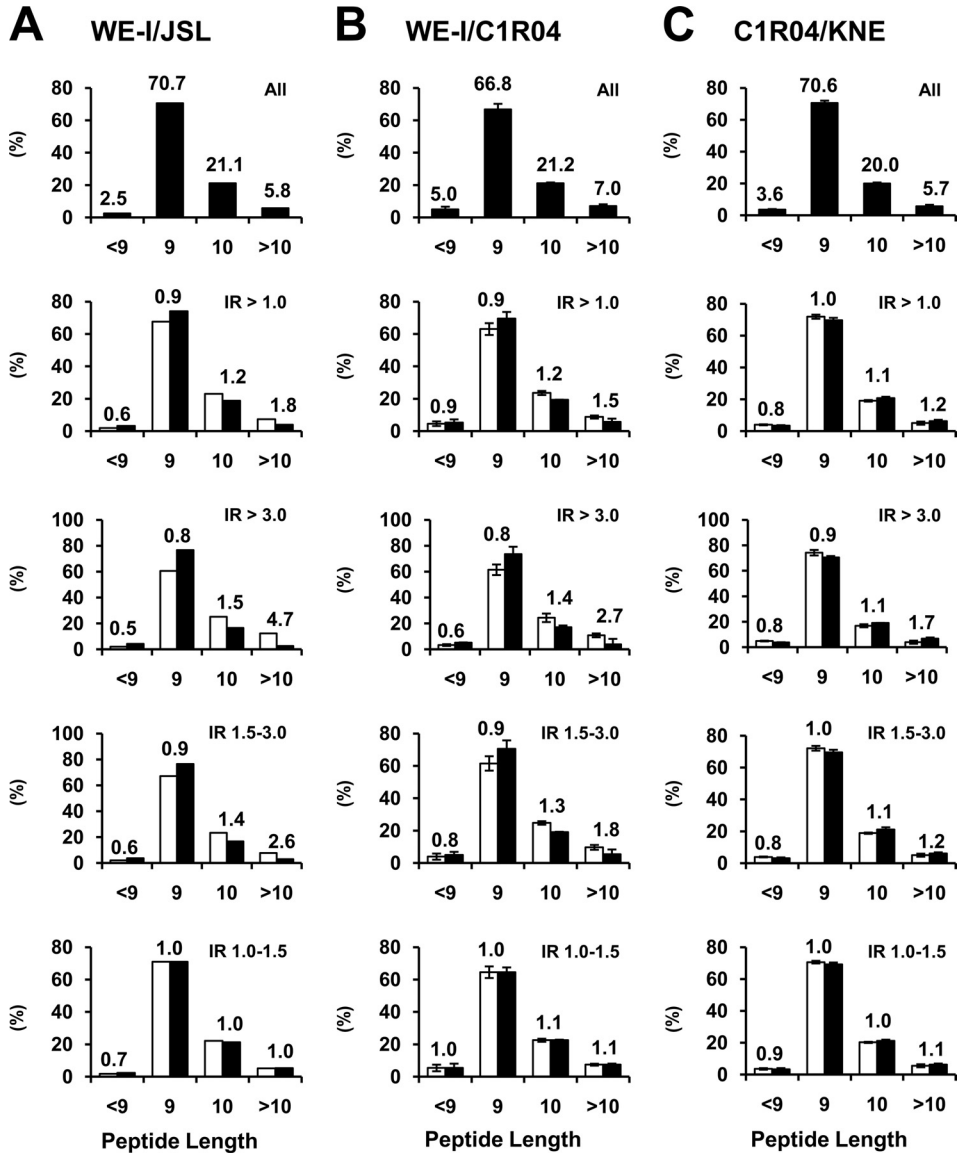

FIG. 5. **Length distribution of B*27:04 ligands as a function of their relative abundance in various ERAP1 contexts.** *A*, WE-I/JSL. The upper histogram shows the length distribution of 3222 shared ligands between both cell lines. The percent of peptides with <9, 9, 10, or >10 residues is indicated. The other four histograms compare the length distribution of the peptide sets predominant (IR > 1.0) in WE-I (*white bars*) or JSL (*black bars*) and those of the corresponding subsets showing IR > 3.0, IR > 1.5 to 3.0, and IR > 1.0 to 1.5 in each cell line. The ratio between the percentages of peptides of the same length in both cell lines (WE-I/JSL ratio) is indicated over the corresponding bars. *B*, WE-I/C1R04. The upper histogram shows the length distribution of the shared ligands between both cell lines. The other four histograms compare the length distribution of the peptide sets predominant in WE-I (*white bars*) or C1R04 (*black bars*), following the same conventions as in panel *A*, and showing the WE-I/C1R04 ratios. The data are means of two experiments. *C*, C1R04/KNE. The upper histogram shows the length distribution of the shared ligands between both cell lines. The other four histograms compare the length distribution of the peptide sets predominant (IR > 1.0) in C1R04 (*black bars*) or KNE (*white bars*), following the same conventions as in panel *A*, and showing the C1R04/KNE ratios. The data are means of three experiments.

effect on ERAP1-mediated trimming (supplemental Table S1). For each peptide subset, the mean score of each position and the means of the P3–P9 scores were calculated. Although position-dependent differences were observed (supplemental Table S5), the joint contribution of P3–P9 to trimming was virtually identical in all cases, independent of the relative abundance of the peptide subsets compared (Table IV). These results strongly suggest that, globally, the internal peptide positions do not have a significant influence on the differential expression of B*27:04 ligands in distinct ERAP1 contexts.

ERAP1 Polymorphism Influences HLA-B27 Stability—The molecular stability of B*27:04 expressed in various ERAP1 contexts was analyzed by measuring the thermostability of

TABLE III
*Influence of N-terminal flanking and P1 residues of B*27:04 ligands on ERAP1-mediated trimming*[a]

Subset[b]	Mean score			
WE-I/JSL				
IR > 3	**P-2**	**P-1**	**P-1 + P-2**	**P1**
WE-I	34.2	38.4	72.6	29.9
JSL	14.4	37.9	52.3	12.0
Ratio	**2.4**	**1.0**	**1.4**	**2.5**
IR > 1 to 3				
WE- I	34.8	44.5	79.2	17.1
JSL	23.3	48.5	71.8	20.4
Ratio	**1.5**	**0.9**	**1.1**	**0.8**
WE-I/C1R04				
IR > 3	**P-2**	**P-1**	**P-1 + P-2**	**P1**
WE-I	38.5	46.3	84.7	23.4
C1R04	26.5	36.1	62.6	22.6
Ratio	**1.5**	**1.3**	**1.4**	**1.0**
IR > 1 to 3				
WE- I	30.3	41.7	72.0	20.6
C1R04	33.8	43.6	77.5	19.5
Ratio	**0.9**	**1.0**	**0.9**	**1.1**
KNE/C1R04				
IR > 3	**P-2**	**P-1**	**P-1 + P-2**	**P1**
KNE	33.6	42.9	75.9	19.4
C1R04	30.7	36.1	66.4	23.2
Ratio	**1.1**	**1.2**	**1.1**	**0.8**
IR >1 to 3				
KNE	27.3	46.3	73.6	20.7
C1R04	25.9	36.8	62.8	21.7
Ratio	**1.1**	**1.3**	**1.2**	**1.0**

[a] The P-2, P-1, and P1 residues of each peptide were assigned a score (supplemental Table S1) related to their susceptibility to ERAP1 trimming in vivo (28). The mean score for each individual position, or for P-1 + P-2, is shown for each peptide subset. The flanking sequences are shown in supplemental Table S4.
[b] Peptide subsets whose ion peaks show the indicated intensity ratio (IR) relative to the other cell line.

TABLE IV
*The internal sequence features of B*2704-bound nonamers do not determine their ERAP1-dependent expression*[a]

Peptide subset[b]	Mean P3–P9 score		
WE-I/JSL	**WE-I**	**JSL**	**Ratio**
IR > 3	2.3	2.4	1.0
IR > 1 to 3	2.3	2.4	1.0
WE-I/C1R04	**WE-I**	**C1R04**	
IR > 3	2.7	2.4	1.1
IR > 1 to 3	2.6	2.6	1.0
KNE/C1R04	**KNE**	**C1R04**	
IR > 3	2.2	2.1	1.0
IR > 1 to 3	2.5	2.5	1.0

[a] Each residue at a given position was assigned a score (supplemental Table S1) related to its effect on ERAP1-mediated trimming (29). The mean added score of positions P3 to P9 for each peptide subset, as well as the corresponding ratios, are given (see supplemental Table S5 for full details).
[b] Peptide subsets whose ion peaks show the indicated intensity ratio (IR) relative to the other cell line.

HLA-B27 isolated from the four cell lines in this study (Fig. 6). We previously reported that B*27:04 expressed on C1R cells shows very high thermostability, a feature that was shared with two other AS-associated subtypes (B*27:02 and B*27:05) but not with the non-AS-associated B*27:06 and B*27:09 (35). An equally high thermostability of B*27:04 was observed in JSL, and it was nearly as high in KNE, but WE-I showed lower thermostability even at the 4 h chase time, which best reflects the steady state of mature HLA-B27. This result strongly suggests that the B*27:04-bound peptidome in WE-I is less optimized than in the other cell lines analyzed.

DISCUSSION

The role of natural ERAP1 polymorphism in shaping the HLA-B27 peptidome was addressed in this study. We determined quantitative effects on the expression of B27 ligands, assuming that differential processing among ERAP1 variants may affect many peptides. We did not look for specific ligands whose presence might depend on a particular ERAP1 context, because the absence of a peptide cannot be formally established, and there are no likely candidates for AS-specific epitopes.

Our experimental approach, which was a powerful one for detecting general effects on the peptidome, deserves some comments. The intensity of an ion peak in MALDI-TOF MS is influenced by many factors, including instrument settings, sample handling, the presence of other components, etc. For this reason, although the acquisition parameters and sample preparation were strictly controlled, the IR of a given ion peak from two peptide pools is not a quantitative measurement; it is only an estimation of relative amounts. Yet, when this method is applied to many ion peaks, collective tendencies can be revealed. Thus, our data should be interpreted as general patterns within large peptide sets, and not on an individual peptide basis. MALDI-TOF MS was used in earlier studies to estimate expression differences of HLA-B27 ligands in the absence or presence of tapasin (36) or among HLA-B27 subtypes (32). A second issue concerns the scores used. We based our score system for flanking and P1 residues on an assay that analyzed antigen presentation as a function of ERAP1 processing in the ER (28), rather than *in vitro* trimming of synthetic substrates, which might not accurately reflect trimming *in vivo*. To our knowledge, only one systematic study (29) analyzed the effect of internal peptide residues on ERAP1 trimming. It allowed us to examine the sequence of B27 ligands for their influence on ERAP1-dependent peptide expression. That study used nonamer libraries and did not include all residues at each position, which precluded an exhaustive scoring and restricted our analysis to nonamers. Again, although not fully accurate for individual

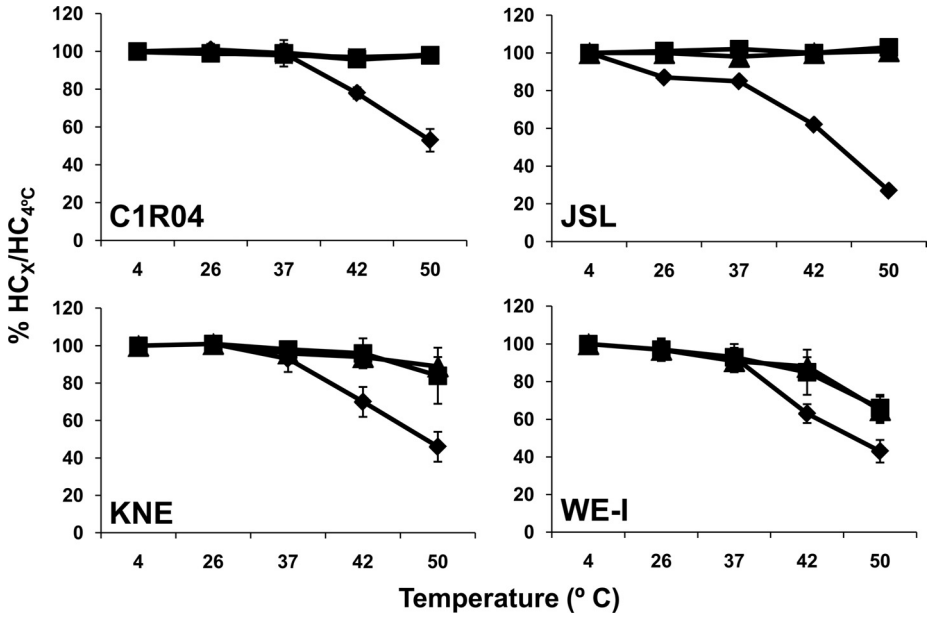

FIG. 6. **Thermostability of HLA-B*27:04 in various ERAP1 contexts.** The indicated cell lines were labeled for 15 min and chased at 0, 2, and 4 h. Equal aliquots of the lysates were kept at 4 °C or heated at the indicated temperatures for 1 h prior to immunoprecipitation with ME1 (a mAb that recognizes undissociated HLA-B27/peptide complexes but not unfolded HC), separated via SDS-PAGE, and analyzed using fluorography. The percentage of ME1-reactive HLA/peptide complexes recovered at 0 h (♦), 2 h (■), or 4 h (▲) chase after heating was plotted as the intensity of the class I HC at any given temperature (HC_X) relative to that at 4 °C ($HC_{4\,°C}$). The data are means ± S.D. of four (C1R04), five (KNE), and eight (WE-I) experiments. Only one experiment could be performed with JSL. The data concerning C1R04, except for one additional experiment included here, were reported previously (35) and are shown here only for comparison.

ligands, this was suitable for globally assessing extensive peptide sets.

Many ERAP1-independent factors, including other peptidases, can influence the relative expression of MHC-I ligands among cell lines. However, most of these factors should not imply cell-specific effects on peptide size, because no other amino peptidases, except perhaps IRAP (18), are regulated by substrate length, and this enzyme is most likely not involved in the shaping of endogenous MHC-I peptidomes (17). Thus, cells expressing similar ERAP1 molecules might be expected to generate B*27:04 peptidomes with a similar size distribution. That this was the case between C1R04 and KNE strongly suggests that the significant size differences observed in the context of more distinct variants were mostly due to ERAP1 polymorphism. Indeed, the ERAP1 activity ranking deduced from the effects on the size and length of B27 ligands, JSL > C1R04/KNE > WE-I, correlated with the number of amino acid differences among the ERAP1 molecules in these cell lines.

Differences in ERAP1 expression levels among cell lines are very unlikely to account for the observed differences among the HLA-B27 peptidomes, given that WE-I and C1R04, which expressed very similar ERAP1 amounts, showed significantly larger size differences in their B27-bound peptidomes than C1R04 and KNE, with larger ERAP1 protein expression differences. Furthermore, JSL showed the lowest expression of ERAP1 mRNA among the four cell lines, but it had the most efficient ERAP1 trimming on the B27 peptidome.

What is the mechanism by which ERAP1 polymorphism modulates the expression level of B*27:04 ligands? What peptides are more likely to be affected? ERAP1 can remove almost any N-terminal residue of peptides longer than a minimum length, albeit with different efficiencies (28). Therefore, ERAP1 variants with different enzymatic activity might show differences in the generation of MHC-I ligands as a function of their N-terminal flanking extensions. A previous study (37) showed that although residue P-3 and those more distant can probably be removed by a variety of peptidases *in vivo*, P-2 and P-1 are predominantly removed in the ER. Moreover, activity differences among ERAP1 variants will affect epitope destruction, because the P1 residue will be more efficiently cleaved by the most active variant. We have directly observed this effect with synthetic peptides *in vitro* (our observations remain unpublished). The higher susceptibility to trimming of flanking and P1 residues in the peptide subset most predominant in WE-I, relative to its equivalent in JSL, implies that these positions would be trimmed more efficiently by the more active ERAP1 variant in JSL, so that the corresponding ligands would be not only generated more efficiently but also destroyed to a greater extent in the latter cell line. The abundance of these peptides in WE-I would be explained by the presence in this cell line of a less active ERAP1 capable of removing susceptible flanking residues without extensively destroying the epitope. Many peptides predominant in JSL would be generated less efficiently in WE-I because of the lower susceptibility of their flanking residues to trimming.

The same mechanism would explain the observed differences between WE-I and C1R04, but here the similar susceptibility of P1 residues to trimming in the predominant peptide subsets from both cell lines means that the more active ERAP1 in C1R04 would still destroy B27 ligands more extensively than in WE-I, but less than in JSL. This might explain why the size differences between the B27 peptidomes from WE-I/C1R04 are smaller than in WE-I/JSL.

In conclusion, natural ERAP1 polymorphism has a significant influence on the length and abundance of many HLA-B27 ligands. The less active variant generated higher numbers of long peptides and less short ones, and it also increased the

expression of peptides of any length with susceptible flanking and/or P1 residues. Thus, the variant-dependent alteration in the balance between epitope generation and destruction, as a function of these residues, is a basic mechanism determining ERAP1-dependent differences among HLA-B27 peptidomes. Although the internal sequence features of B*27:04 ligands did not globally affect relative peptide expression in distinct ERAP1 contexts, our results do not exclude an influence of individual sequences on ERAP1 trimming, as reported *in vitro* (29). The general character of the effects observed among the four cell lines in our study should be established by extending these analyses to additional cell lines showing similar ERAP1 variants, as well as distinct ones.

Several studies have analyzed the effect of natural polymorphisms on the enzymatic activity of ERAP1. The K528R and R725Q mutations, both of which are protective with regard to AS, decreased ERAP1 activity, whereas R127P, I276M, D575N, and Q730E had a smaller or no effect (10, 20, 38). These studies were performed with single mutants *in vitro*, and the mutual influence of co-existing mutations or their effects *in vivo* were not addressed. In a recent study (39), the kinetics of ERAP1 activity was consistent with a substrate-inhibition model that was both substrate and allele specific, and it might differentially affect antigen processing *in vivo* by ERAP1 variants. In that study the Q730E mutation, which is also protective against AS, decreased the presentation of a specific B27 epitope *in vivo* even more effectively than K528R, in contrast with the relative activity of these mutants *in vitro*. The three-dimensional structure of ERAP1 (19, 20) shows that among the polymorphic positions in the cell lines used in our study, M349V is located in the active site; G346D, R725Q, and Q730E are in the substrate binding cavity; R127P, I276M, and K528R are located at or near domain junctions; and D575N is located at the surface of domain III. Thus, these polymorphisms could affect ERAP1 function by modulating hydrolysis, substrate binding, or the conformational transition between the open and closed states, which is critical for enzymatic activity.

ERAP1 in JSL differs from both C1R/KNE and WE-I at positions 127(R), 528(K), and 730(Q). Therefore, the higher activity of ERAP1 from JSL is in agreement with the reported effects of the K528R and Q730E changes on peptide trimming. Yet, despite the significant differences between the B*27:04 peptidomes of C1R04 and WE-I, their ERAP-1 molecules are identical at positions 528(R) and 730(E), indicating that polymorphism at other positions also influences ERAP1 trimming *in vivo*. For instance, WE-I differs from C1R and all other cell lines by the M349V, D575N, and R725Q, which might affect ERAP1 function, as demonstrated for the latter change *in vitro* (10). Whether the observed differences among B*27:04 peptidomes are predominantly due to a single mutation or to their combined effect cannot be determined from our study. The possibility that the effect of a given mutation in ERAP1 might be modulated by concomitant changes at other positions should always be taken into account. The co-occurrence of AS-associated nonsynonymous SNPs in a given ERAP1 variant is very frequent, leading to the identification of AS-associated ERAP1 haplotypes (21, 40, 41). Because of strong linkage disequilibrium, it was difficult to glean from these studies whether association with AS is determined by a single position or by co-occurring polymorphisms in the susceptible haplotypes.

Genetic analyses are consistent with a two-mutation model in which the association of ERAP1 with AS is determined by a primary effect of rs30187 (K528R) and a secondary effect of rs17482078 (R725Q) and/or rs10050860 (Q730E), two polymorphisms in very tight linkage disequilibrium. In combination, the protective alleles at these loci (R528, Q725, E730) confer particularly strong protection from AS (10). Among the cell lines in our study, only WE-I carried these three protective polymorphisms; C1R04 and KNE showed only two (R528, E730), and JSL carried all three susceptibility allotypes (K528, R725, Q730). Thus, without ruling out an additional contribution of other positions, the observed effects of ERAP1 polymorphism on HLA-B27 in our cell lines are fully consistent with current genetic data and support a major effect of residues 528, 725, and 730, which is most prominent with the co-occurrence of either protective or susceptibility amino acid changes at these positions.

ERAP2 expression in WE-I was about 2-fold higher than in C1R04, despite the lower trimming observed in the former cell line. Heterozygocity of KNE, C1R04, and WE-I for the K392N change in ERAP2 also argues against an effect of ERAP2 in the observed differences between the B27-bound peptidomes from these cell lines. Yet, given that JSL was homozygous for N392 and this variant shows a more efficient trimming of certain peptide substrates than the K392 counterpart (42), some contribution of ERAP2 in the high trimming activity observed in this cell line cannot be formally ruled out. In addition, one might consider the possibility that ERAP1 polymorphism might influence the concerted trimming by ERAP1/ERAP2 complexes (43) by altering the interaction between both molecules. Yet the location of most of the natural ERAP1 changes in sites susceptible to directly altered trimming argue against a major influence of this alternative.

The effects of ERAP1 polymorphism described here might influence HLA-B27 biology in various aspects relevant to AS pathogenesis. In the discussion that follows, we comment on the incidence of this study on the current hypotheses concerning the pathogenetic role of HLA-B27. First, on the basis of our results, ERAP1 polymorphism can affect the immunological properties of the HLA-B27 heterodimer at various levels. The differential effects on trimming observed among ERAP1 variants might result in the production (or not) of some B27 ligands. As protection from AS has been linked to ERAP1 mutations leading to decreased enzymatic activity (10), one might speculate that putative disease-associated epitopes specifically produced in the context of the most

active variants might be peptides with flanking and/or P1 residues not highly susceptible to ERAP1 trimming. Moreover, altering the expression level of many B27 ligands is likely to influence T-cell repertoire selection, which is determined by the avidity of TCR/peptide/MHC interactions and, therefore, by individual epitope amounts at the cell surface. Thus, the autoimmune potential of HLA-B27 might be modulated by ERAP1 polymorphism. Finally, HLA-B27 immunogenicity would also be modulated by ERAP1 through its quantitative effect on the peptidome, because T-cell triggering thresholds are dependent on the number of peptide/MHC complexes within individual TCR clusters during T-cell activation (44). Second, although the influence of ERAP-1 on HLA-B27 folding was not examined, the decreased molecular stability of HLA-B27 observed in WE-I indicates that certain ERAP1 variants containing a number of AS-protective polymorphisms generate suboptimal B27 peptidomes. We have shown previously that high thermostability is a feature of three AS-associated subtypes (B*27:02, B*27:04, and B*27:05) expressed on C1R cells that is not shared by the non-AS-associated B*27:06 and B*27:09 subtypes or the AS-associated B*27:07 and B*1403 (30, 35). The thermostability of B*27:04 in WE-I was closer to that of the latter subtypes, indicating that ERAP1 polymorphism protective against AS can approach the molecular stability phenotype of an AS-associated B27 subtype to that shown by non-AS-associated ones. Decreased thermostability by itself does not correlate with AS susceptibility. However, the molecular mechanism leading to decreased stability in B*27:06, B*27:07, B*27:09, and B*1403 is probably different than that operating in B*27:04 from WE-I. Indeed, the four former subtypes have a hydrophobic F pocket and bind almost exclusively peptides with nonpolar C-terminal residues (34, 45, 46). As shown for HLA-B*44 subtypes (47, 48), increased hydrophobicity of the F pocket leads to intrinsic thermodynamic instability of the empty molecule that favors quick loading of hydrophobic peptides to hide nonpolar regions from exposure to water. Presumably, this mechanism might largely bypass tapasin-mediated peptide editing, leading to fast folding, albeit with a suboptimal peptide cargo. Indeed, B*27:06, B*27:07, B*27:09, and B*1403 did not misfold significantly in the ER (30, 35). The lower stability of B*27:04 in WE-I is not obviously due to altered hydrophobicity of its peptide binding site, because the molecule itself is not altered; rather, presumably, it is due to the inability of the ERAP1 variant to generate an optimal peptide repertoire. If so, thermodynamic factors favoring quick peptide binding would not play a differential role in WE-I relative to other B*27:04-positive cell lines, and tapasin might not be bypassed. Rather, if an optimal peptide pool is not available because of ERAP1 impairment, this might result in slower loading kinetics and perhaps increased B*27:04 misfolding in the context of an ERAP1 variant with multiple protective polymorphisms, in contrast with the HLA-B27 misfolding hypothesis for AS pathogenesis. Although this prediction remains to be confirmed for B*27:04 in WE-I, it is consistent with the association of B*27:07 and B*1403 with AS, despite their presumably low misfolding (30, 35).

The expression of HLA-B27 HC homodimers at the cell surface has been proposed to have pathogenetic significance because of their immunomodulatory potential through their recognition by leukocyte receptors (49). These homodimers are formed upon endosomal recycling of HLA-B27 (50) and presumably arise from dissociation of the canonic heterodimer. If, as shown in this study, ERAP1 polymorphism associated with protection from AS can decrease HLA-B27 stability, one might expect that ERAP1 changes associated with AS susceptibility would lead to decreased expression of B27 HC homodimers. In agreement with this prediction, a recent report (51) showed decreased reactivity with HC10, an antibody that recognizes unfolded MHC-I HC, including homodimers, at the surface of monocytes from B*27:05-positive individuals homozygous for Q730 in ERAP1. This change is associated with AS susceptibility and efficient ERAP1 trimming *in vivo* (39). Again, the effects of AS-associated ERAP1 polymorphism seem to affect HLA-B27 in a way opposite that expected from the surface homodimer pathogenetic hypothesis.

Given that the effects of ERAP1 on the B27 peptidome are essentially dependent on the flanking and P1 residues of the HLA-B27 ligands, these effects should presumably be similar for most of the main HLA-B27 subtypes, because they have overlapping peptide repertoires and similar residue usage at P1 (45). An exception is B*27:03, whose special preference for basic P1 residues (52–54), which are relatively resistant to ERAP1, might lead to decreased epitope destruction (relative to that in other subtypes) by ERAP1. More generally, different P1 residue usage by diverse HLA-I molecules might significantly affect the way in which natural ERAP1 polymorphism shapes their peptidomes.

A different issue is the effect of ERAP1 polymorphism on the stability of other HLA-B27 subtypes. Our results suggest that AS-protective polymorphism might decrease the stability of those subtypes that bind highly optimized peptidomes, such as the AS-associated B*27:02 and B*27:05. However, these effects might not be comparable for B*2706, B*2707, B*2709, and B*1403, whose binding of suboptimal peptidomes is thermodynamically determined by the hydrophobicity of their peptide-binding grooves. A smaller influence of ERAP1 polymorphism on the molecular stability of these subtypes might be expected.

In conclusion, our results reveal large effects of natural ERAP1 polymorphism on the HLA-B27 peptidome *in vivo*, as well as their molecular basis. These effects, through their influence on immunological and other features of HLA-B27, define the nature of the functional interaction between both molecules, underline the fundamental role of peptides in the pathogenesis of HLA-B27-associated disease, and suggest

that this role is mainly to alter the immunological specificity of the HLA-B27 heterodimer.

Acknowledgments—We thank the staff of the Proteomics facility at the Centro Nacional de Biotecnología, Madrid, and Ricardo Ramos (Parque Científico de Madrid) for help in MS and DNA analyses, respectively.

* This work was supported by grants SAF2008/00461 and SAF2011/25681 from the Plan Nacional de I+D+i, RD08/0075 (RIER) from the Instituto de Salud Carlos III, and an institutional grant from the Fundación Ramón Areces to the Centro de Biología Molecular *Severo Ochoa.*

S This article contains supplemental material.

¶ Current address: Instituto de Salud Carlos III, 28220 Madrid, Spain.

‖ To whom correspondence should be addressed: E-mail: aldecastro@cbm.uam.es.

§ N. García-Medel and A. Sanz-Bravo contributed equally to this work.

REFERENCES

1. Benjamin, R., and Parham, P. (1990) Guilt by association: HLA-B27 and ankylosing spondylitis. *Immunol. Today* **11,** 137–142
2. Colbert, R. A. (2000) HLA-B27 misfolding: a solution to the spondyloarthropathy conundrum? *Mol. Med. Today* **6,** 224–230
3. Mear, J. P., Schreiber, K. L., Münz, C., Zhu, X., Stevanovic, S., Rammensee, H. G., Rowland-Jones, S. L., and Colbert., R. A. (1999) Misfolding of HLA-B27 as a result of its B pocket suggests a novel mechanism for its role in susceptibility to spondyloarthropathies. *J. Immunol.* **163,** 6665–6670
4. Dangoria, N. S., DeLay, M. L., Kingsbury, D. J., Mear, J. P., Uchanska-Ziegler, B., Ziegler, A., and Colbert, R. A. (2002) HLA-B27 misfolding is associated with aberrant intermolecular disulfide bond formation (dimerization) in the endoplasmic reticulum. *J. Biol. Chem.* **277,** 23459–23468
5. Allen, R. L., O'Callaghan, C. A., McMichael, A. J., and Bowness, P. (1999) Cutting edge: HLA-B27 can form a novel β2-microglobulin-free heavy chain homodimer structure. *J. Immunol.* **162,** 5045–5048
6. Bowness, P. (2002) HLA B27 in health and disease: a double-edged sword? *Rheumatology (Oxford)* **41,** 857–868
7. Kollnberger, S., Bird, L., Sun, M. Y., Retiere, C., Braud, V. M., McMichael, A., and Bowness, P. (2002) Cell-surface expression and immune receptor recognition of HLA-B27 homodimers. *Arthritis Rheum.* **46,** 2972–2982
8. Marcilla, M., and Lopez de Castro, J. A. (2008) Peptides: the cornerstone of HLA-B27 biology and pathogenetic role in spondyloarthritis. *Tissue Antigens* **71,** 495–506
9. WTCC Consortium (2007) Association scan of 14,500 nonsynonymous SNPs in four diseases identifies autoimmunity variants. *Nat. Genet.* **39,** 1329–1337
10. TASK and WTCCC2 Consortia (2011) Interaction between ERAP1 and HLA-B27 in ankylosing spondylitis implicates peptide handling in the mechanism for HLA-B27 in disease susceptibility. *Nat. Genet.* **43,** 761–767
11. Serwold, T., Gaw, S., and Shastri, N. (2001) ER aminopeptidases generate a unique pool of peptides for MHC class I molecules. *Nat. Immunol.* **2,** 644–651
12. Serwold, T., Gonzalez, F., Kim, J., Jacob, R., and Shastri, N. (2002) ERAAP customizes peptides for MHC class I molecules in the endoplasmic reticulum. *Nature* **419,** 480–483
13. York, I. A., Chang, S. C., Saric, T., Keys, J. A., Favreau, J. M., Goldberg, A. L., and Rock, K. L. (2002) The ER aminopeptidase ERAP1 enhances or limits antigen presentation by trimming epitopes to 8–9 residues. *Nat. Immunol.* **3,** 1177–1184
14. Chang, S. C., Momburg, F., Bhutani, N., and Goldberg, A. L. (2005) The ER aminopeptidase, ERAP1, trims precursors to lengths of MHC class I peptides by a "molecular ruler" mechanism. *Proc. Natl. Acad. Sci. U.S.A.* **102,** 17107–17112
15. Birtley, J. R., Saridakis, E., Stratikos, E., and Mavridis, I. M. (2012) The crystal structure of human endoplasmic reticulum aminopeptidase 2 reveals the atomic basis for distinct roles in antigen processing. *Biochemistry* **51,** 286–295
16. Saveanu, L., Carroll, O., Weimershaus, M., Guermonprez, P., Firat, E., Lindo, V., Greer, F., Davoust, J., Kratzer, R., Keller, S. R., Niedermann, G., and van Endert, P. (2009) IRAP identifies an endosomal compartment required for MHC class I cross-presentation. *Science* **325,** 213–217
17. Saveanu, L., and van Endert, P. (2012) The role of insulin-regulated aminopeptidase in MHC class I antigen presentation. *Front. Immunol.* **3,** 57
18. Georgiadou, D., Hearn, A., Evnouchidou, I., Chroni, A., Leondiadis, L., York, I. A., Rock, K. L., and Stratikos, E. (2010) Placental leucine aminopeptidase efficiently generates mature antigenic peptides in vitro but in patterns distinct from endoplasmic reticulum aminopeptidase 1. *J. Immunol.* **185,** 1584–1592
19. Nguyen, T. T., Chang, S. C., Evnouchidou, I., York, I. A., Zikos, C., Rock, K. L., Goldberg, A. L., Stratikos, E., and Stern, L. J. (2011) Structural basis for antigenic peptide precursor processing by the endoplasmic reticulum aminopeptidase ERAP1. *Nat. Struct. Mol. Biol.* **18,** 604–613
20. Kochan, G., Krojer, T., Harvey, D., Fischer, R., Chen, L., Vollmar, M., von Delft, F., Kavanagh, K. L., Brown, M. A., Bowness, P., Wordsworth, P., Kessler, B. M., and Oppermann, U. (2011) Crystal structures of the endoplasmic reticulum aminopeptidase-1 (ERAP1) reveal the molecular basis for N-terminal peptide trimming. *Proc. Natl. Acad. Sci. U.S.A.* **108,** 7745–7750
21. Harvey, D., Pointon, J. J., Evans, D. M., Karaderi, T., Farrar, C., Appleton, L. H., Sturrock, R. D., Stone, M. A., Oppermann, U., Brown, M. A., and Wordsworth, B. P. (2009) Investigating the genetic association between ERAP1 and ankylosing spondylitis. *Hum. Mol. Genet.* **18,** 4204–4212
22. Zemmour, J., Little, A. M., Schendel, D. J., and Parham, P. (1992) The HLA-A,B "negative" mutant cell line C1R expresses a novel HLA-B35 allele, which also has a point mutation in the translation initiation codon. *J. Immunol.* **148,** 1941–1948
23. Garcia, F., Marina, A., and Lopez de Castro, J. A. (1997) Lack of carboxyl-terminal tyrosine distinguishes the B*2706-bound peptide repertoire from those of B*2704 and other HLA-B27 subtypes associated to ankylosing spondylitis. *Tissue Antigens* **49,** 215–221
24. Ellis, S. A., Taylor, C., and McMichael, A. (1982) Recognition of HLA-B27 and related antigens by a monoclonal antibody. *Hum. Immunol.* **5,** 49–59
25. Paradela, A., Garcia-Peydro, M., Vazquez, J., Rognan, D., and Lopez de Castro, J. A. (1998) The same natural ligand is involved in allorecognition of multiple HLA-B27 subtypes by a single T cell clone: role of peptide and the MHC molecule in alloreactivity. *J. Immunol.* **161,** 5481–5490
26. Paradela, A., Alvarez, I., Garcia-Peydro, M., Sesma, L., Ramos, M., Vazquez, J., and Lopez de Castro, J. A. (2000) Limited diversity of peptides related to an alloreactive T cell epitope in the HLA-B27-bound peptide repertoire results from restrictions at multiple steps along the processing-loading pathway. *J. Immunol.* **164,** 329–337
27. Garcia-Medel, N., Sanz-Bravo, A., Barnea, E., Admon, A., and Lopez de Castro, J. A. (2012) The origin of proteasome-inhibitor resistant HLA Class I peptidomes: a study with HLA-A*68:01. *Mol. Cell. Proteomics.* **11,** M111.011486
28. Hearn, A., York, I. A., and Rock, K. L. (2009) The specificity of trimming of MHC class I-presented peptides in the endoplasmic reticulum. *J. Immunol.* **183,** 5526–5536
29. Evnouchidou, I., Momburg, F., Papakyriakou, A., Chroni, A., Leondiadis, L., Chang, S. C., Goldberg, A. L., and Stratikos, E. (2008) The internal sequence of the peptide-substrate determines its N-terminus trimming by ERAP1. *PLoS One* **3,** e3658
30. Merino, E., Galocha, B., Vazquez, M. N., and Lopez de Castro, J. A. (2008) Disparate folding and stability of the ankylosing spondylitis-associated HLA-B*1403 and B*2705 proteins. *Arthritis Rheum.* **58,** 3693–3704
31. Fruci, D., Ferracuti, S., Limongi, M. Z., Cunsolo, V., Giorda, E., Fraioli, R., Sibilio, L., Carroll, O., Hattori, A., Van Endert, P. M., and Giacomini, P. (2006) Expression of endoplasmic reticulum aminopeptidases in EBV-B cell lines from healthy donors and in leukemia/lymphoma, carcinoma, and melanoma cell lines. *J. Immunol.* **176,** 4869–4879
32. Ramos, M., Paradela, A., Vazquez, M., Marina, A., Vazquez, J., and Lopez de Castro, J. A. (2002) Differential association of HLA-B*2705 and B*2709 to ankylosing spondylitis correlates with limited peptide subsets but not with altered cell surface stability. *J. Biol. Chem.* **277,**

28749–28756
33. Sesma, L., Montserrat, V., Lamas, J. R., Marina, A., Vazquez, J., and Lopez de Castro, J. A. (2002) The peptide repertoires of HLA-B27 subtypes differentially associated to spondyloarthropathy (B*2704 and B*2706) differ by specific changes at three anchor positions. *J. Biol. Chem.* **277,** 16744–16749
34. Gomez, P., Montserrat, V., Marcilla, M., Paradela, A., and López de Castro, J. A. (2006) B*2707 differs in peptide specificity from B*2705 and B*2704 as much as from HLA-B27 subtypes not associated to spondyloarthritis. *Eur. J. Immunol.* **36,** 1867–1881
35. Galocha, B., and López de Castro, J. A. (2010) Mutational analysis reveals a complex interplay of peptide binding and multiple biological features of HLA-B27. *J. Biol. Chem.* **285,** 39180–39190
36. Purcell, A. W., Gorman, J. J., Garcia-Peydro, M., Paradela, A., Burrows, S. R., Talbo, G. H., Laham, N., Peh, C. A., Reynolds, E. C., Lopez de Castro, J. A., and McCluskey, J. (2001) Quantitative and qualitative influences of tapasin on the class I peptide repertoire. *J. Immunol.* **166,** 1016–1027
37. Schatz, M. M., Peters, B., Akkad, N., Ullrich, N., Martinez, A. N., Carroll, O., Bulik, S., Rammensee, H. G., van Endert, P., Holzhutter, H. G., Tenzer, S., and Schild, H. (2008) Characterizing the N-terminal processing motif of MHC class I ligands. *J. Immunol.* **180,** 3210–3217
38. Goto, Y., Hattori, A., Ishii, Y., and Tsujimoto, M. (2006) Reduced activity of the hypertension-associated Lys528Arg mutant of human adipocyte-derived leucine aminopeptidase (A-LAP)/ER-aminopeptidase-1. *FEBS Lett.* **580,** 1833–1838
39. Evnouchidou, I., Kamal, R. P., Seregin, S. S., Goto, Y., Tsujimoto, M., Hattori, A., Voulgari, P. V., Drosos, A. A., Amalfitano, A., York, I. A., and Stratikos, E. (2011) Cutting edge: coding single nucleotide polymorphisms of endoplasmic reticulum aminopeptidase 1 can affect antigenic peptide generation in vitro by influencing basic enzymatic properties of the enzyme. *J. Immunol.* **186,** 1909–1913
40. Maksymowych, W. P., Inman, R. D., Gladman, D. D., Reeve, J. P., Pope, A., and Rahman, P. (2009) Association of a specific ERAP1/ARTS1 haplotype with disease susceptibility in ankylosing spondylitis. *Arthritis Rheum.* **60,** 1317–1323
41. Szczypiorska, M., Sanchez, A., Bartolome, N., Arteta, D., Sanz, J., Brito, E., Fernandez, P., Collantes, E., Martinez, A., Tejedor, D., Artieda, M., and Mulero, J. (2011) ERAP1 polymorphisms and haplotypes are associated with ankylosing spondylitis susceptibility and functional severity in a Spanish population. *Rheumatology (Oxford)* **50,** 1969–1975
42. Evnouchidou, I., Birtley, J., Seregin, S., Papakyriakou, A., Zervoudi, E., Samiotaki, M., Panayotou, G., Giastas, P., Petrakis, O., Georgiadis, D., Amalfitano, A., Saridakis, E., Mavridis, I. M., and Stratikos, E. (2012) A common SNP in ER aminopeptidase 2 induces a specificity switch that leads to altered antigen processing. *J. Immunol.* **189,** 2383–2392
43. Saveanu, L., Carroll, O., Lindo, V., Del Val, M., Lopez, D., Lepelletier, Y., Greer, F., Schomburg, L., Fruci, D., Niedermann, G., and Van Endert, P. M. (2005) Concerted peptide trimming by human ERAP1 and ERAP2 aminopeptidase complexes in the endoplasmic reticulum. *Nat. Immunol.* **6,** 689–697
44. Manz, B. N., Jackson, B. L., Petit, R. S., Dustin, M. L., and Groves, J. (2011) T-cell triggering thresholds are modulated by the number of antigen within individual T-cell receptor clusters. *Proc. Natl. Acad. Sci. U.S.A.* **108,** 9089–9094
45. Lopez de Castro, J. A., Alvarez, I., Marcilla, M., Paradela, A., Ramos, M., Sesma, L., and Vazquez, M. (2004) HLA-B27: a registry of constitutive peptide ligands. *Tissue Antigens* **63,** 424–445
46. Merino, E., Montserrat, V., Paradela, A., and Lopez de Castro, J. A. (2005) Two HLA-B14 subtypes (B*1402 and B*1403) differentially associated with ankylosing spondylitis differ substantially in peptide specificity, but have limited peptide and T-cell epitope sharing with HLA-B27. *J. Biol. Chem.* **280,** 35868–35880
47. Williams, A. P., Peh, C. A., Purcell, A. W., McCluskey, J., and Elliott, T. (2002) Optimization of the MHC class I peptide cargo is dependent on tapasin. *Immunity.* **16,** 509–520
48. Zernich, D., Purcell, A. W., Macdonald, W. A., Kjer-Nielsen, L., Ely, L. K., Laham, N., Crockford, T., Mifsud, N. A., Bharadwaj, M., Chang, L., Tait, B. D., Holdsworth, R., Brooks, A. G., Bottomley, S. P., Beddoe, T., Peh, C. A., Rossjohn, J., and McCluskey, J. (2004) Natural HLA class I polymorphism controls the pathway of antigen presentation and susceptibility to viral evasion. *J. Exp. Med.* **200,** 13–24
49. Kollnberger, S., and Bowness, P. (2009) The role of B27 heavy chain dimer immune receptor interactions in spondyloarthritis. *Adv. Exp. Med. Biol.* **649,** 277–285
50. Bird, L. A., Peh, C. A., Kollnberger, S., Elliott, T., McMichael, A. J., and Bowness, P. (2003) Lymphoblastoid cells express HLA-B27 homodimers both intracellularly and at the cell surface following endosomal recycling. *Eur. J. Immunol.* **33,** 748–759
51. Haroon, N., Tsui, F. W., Uchanska-Ziegler, B., Ziegler, A., and Inman, R. D. (2012) Endoplasmic reticulum aminopeptidase 1 (ERAP1) exhibits functionally significant interaction with HLA-B27 and relates to subtype specificity in ankylosing spondylitis. *Ann. Rheum. Dis.* **71,** 589–595
52. Colbert, R. A., Rowland Jones, S. L., McMichael, A. J., and Frelinger, J. A. (1994) Differences in peptide presentation between B27 subtypes: the importance of the P1 side chain in maintaining high affinity peptide binding to B*2703. *Immunity* **1,** 121–130
53. Griffin, T. A., Yuan, J., Friede, T., Stevanovic, S., Ariyoshi, K., Rowland-Jones, S. L., Rammensee, H. G., and Colbert, R. A. (1997) Naturally occurring A pocket polymorphism in HLA-B*2703 increases the dependence on an accessory anchor residue at P1 for optimal binding of nonamer peptides. *J. Immunol.* **159,** 4887–4897
54. Boisgérault, F., Tieng, V., Stolzenberg, M. C., Dulphy, N., Khalil, I., Tamouza, R., Charron, D., and Toubert, A. (1996) Differences in endogenous peptides presented by HLA-B*2705 and B*2703 allelic variants: implications for susceptibility to spondylarthropathies. *J. Clin. Invest.* **98,** 2764–2770
55. Ben Dror, L., Barnea, E., Beer, I., Mann, M., and Admon, A. (2010) The HLA-B*2705 peptidome. *Arthritis Rheum.* **62,** 420–429
56. Brown, M. A. (2008) Breakthroughs in genetic studies of ankylosing spondylitis. *Rheumatology (Oxford)* **47,** 132–137

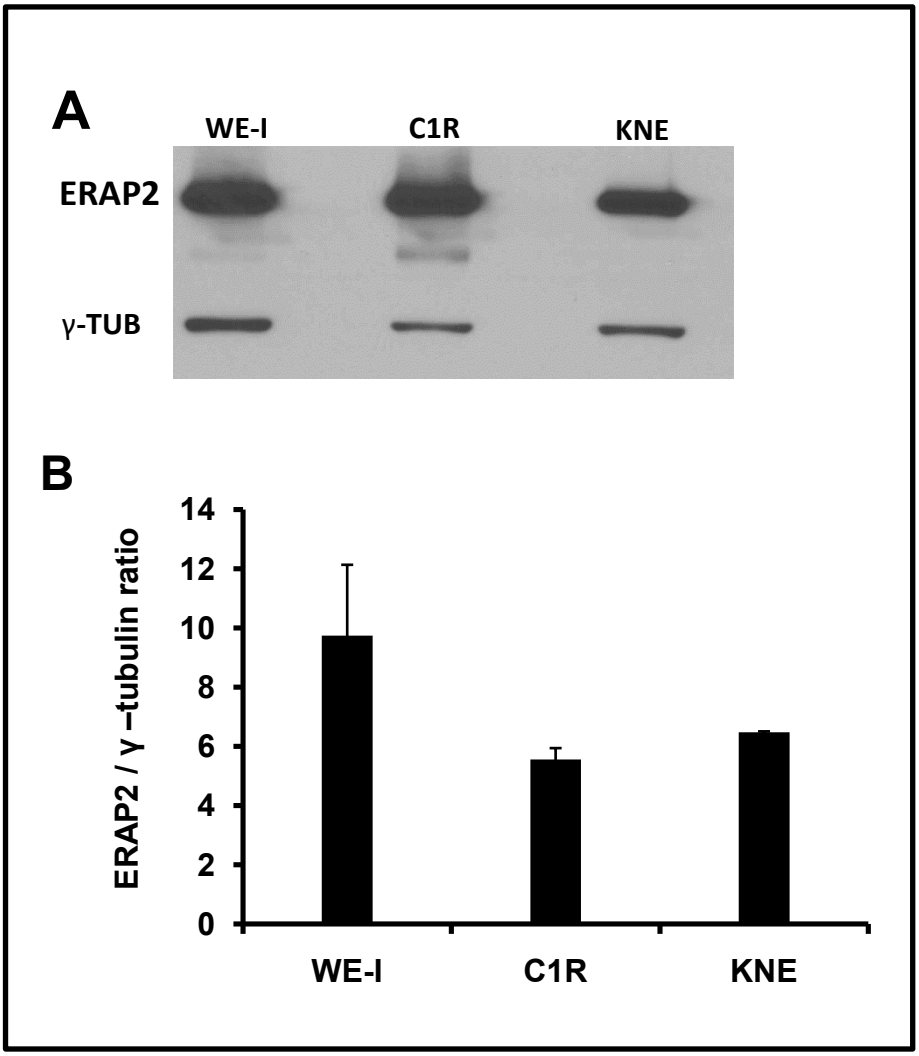
A
WE-I
C1R
KNE
ERAP2
γ-TUB
B
ERAP2 / γ –tubulin ratio
14
12
10
8
6
4
2
0
WE-I
C1R
KNE

Figure S1

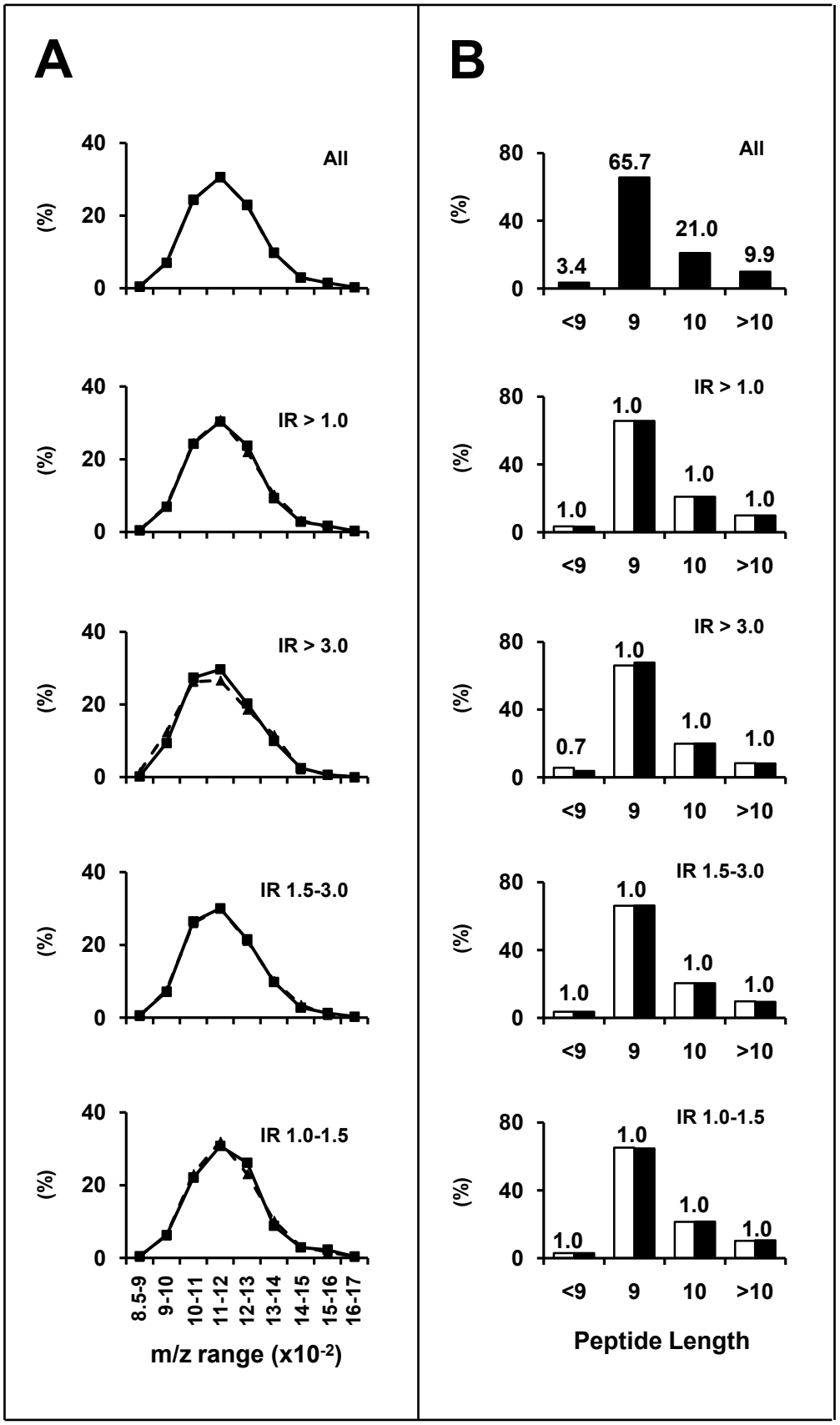
A
B
All
IR > 1.0
IR > 3.0
IR 1.5-3.0
IR 1.0-1.5
(%)
40
20
0
80
40
0
3.4
65.7
21.0
9.9
1.0
1.0
1.0
1.0
0.7
1.0
1.0
1.0
1.0
1.0
1.0
1.0
1.0
1.0
1.0
1.0
<9
9
10
>10
8.5-9
9-10
10-11
11-12
12-13
13-14
14-15
15-16
16-17
m/z range (x10-2)
Peptide Length

Figure S2

Supplementary Figure legends.

Supplementary Fig. S1.ERAP2 expression among cell lines. *(A)* Western blots were performed for the indicated cell lines using the anti-ERAP2 3F5 mAb and the anti-γ-tubulin GTU88 mAb as internal control. A representative experiment is shown. In this figure the exposure was optimized for γ-tubulin. *(B)* ERAP2 protein expression in the indicated cell lines, as established by Western blot. Data are expressed as the ERAP1/γ-tubulin ratio and are means ± S.D. of 3 experiments.

Supplementary Fig. S2. Comparative size and length distribution of B*27:04 ligands from two independent C1R04 peptide pools.*(A)* The upper histogram shows the Mw distribution of 8403 shared ligands. The other 4 histograms compare the Mw distribution of the peptide sets predominant (IR>1.0) in C1R04-I (solid line) or C1R04-II (dotted line) as well the corresponding subsets showing IR>3.0, IR >1.5-3.0 and IR>1.0-1.5 in each peptide pool; *(B)* The upper histogram shows the length distribution in the whole set of shared ligands The percent of peptides with <9, 9, 10, or >10 residues is indicated. The other 4 histograms compare the length distribution of the peptide sets predominant (IR>1.0) in C1R04-I (black bars) or C1R04-II (white bars), and those of the corresponding subsets showing IR>3.0, IR >1.5-3.0 and IR>1.0-1.5 in each peptide pool. The ratio between the percentage of peptides of the same length in both pools is indicated over the corresponding bars. The conversion of peptide size to length was done as in **Fig.5** and is explained in the Results section of the main text.

Table S1. Score systems for amino acid residues

Trimming susceptibility scores for N-terminal flanking and P1 residues[a]		*Internal peptide sequence scores*[b]						
Residue	***Score***	**P3**	**P4**	**P5**	**P6**	**P7**	**P8**	**P9**
P	0	2.5	0	0	4.0	0	0.5	1.0
R	4					2.5		8.5
K	4	4.0	2.5	2.0	2.0	1.0	5.5	
V	5	4.0	2.0	0		0	1.0	6.0
D	5							
W	8							
E	8	1.5	0	0	0.5	0	0	
N	13							
T	19	4.0	0.5		4.0	0	1.0	
G	20	4.0	0	0	4.0	0	1.0	
H	20							
Q	22	5.0	1.5	0	2.5	0	1.0	1.0
S	32							
F	34	2.0	3.5	2.5	7.0	2.5	0.5	6.0
I	47							
C	55							
A	76						1.0	
L	88							
M	91	6.0	1.5	0	8.0		1.5	4.0
Y	100							

[a]Based on data from Hearn et al. (2009), J.Immunol. 183: 5526-5536. [b]Based on data from Evnouchidou et al. (2008), PLoS One 3 (11): e3658. Empty cells mean that the corresponding residues at those positions were not scored.

Table S2. Automated comparison of B*27:04-bound peptidomes expressed in various ERAP1 contexts.

Exp.	Comparison	Ion peaks	Filter[a]					Comparison	
1		Unfiltered	A	B	C	D	E	Shared	Other
	WE-I	14326	12990	12292	9666	9343	5760	3222	2538
	JSL	13507	12230	11750	8885	8541	5072	3222	1850
2	WE-I	54185	49716	17262	15146	14771	8504	5240	3264
	C1R04	57118	51534	18120	16476	15860	9988	5240	4748
3[b]	WE-I	29880	24513	16187	10909	9245	6301	3558	2743
	C1R04	34425	2880	22475	17419	15491	9703	3558	6145
4	C1R04	53612	47760	26236	25492	24773	13597	6974	6223
	KNE	49854	42069	20354	19161	18501	10005	6974	3031
5[c]	C1R04 (I)	25317	25299	22267	21916	21490	11393	6531	4862
	KNE	22031	22017	19098	18633	18206	9625	6531	3094
6[c]	C1R04 (II)	24731	24707	20602	20245	19870	10796	6395	4401
	KNE	22031	22017	19098	18633	18206	9625	6395	3230
7[c]	C1R04 (I)	25317	25299	23931	23482	23027	12145	8403	3742
	C1R04 (II)	24731	24707	22561	22087	21678	11738	8403	3335

[a]Figures indicate the number of ion peaks remaining after applying the following filters: A, Mw cutoff ≤850, >1700; B, intensity cutoff 200 or, for C1R04/KNE , 300; C, removal of ions with decimal m/z value in the ranges 0.0-0.2 and 0.9-0.0; D, removal of matrix-related ion peaks; E, removal of redundancies: among ion peaks with identical (±0.2) m/z eluting in consecutive HPLC fractions only the one showing the maximal intensity was selected. [b]This experiment was carried out with 10^9 cells. Intensity cutoff was set at 100. The removal of matrix-related ion peaks carried out by the automatic filter of the MShandler was supplemented by manual removal of ion peaks in the m/z range 850-900 appearing 10 times or more across the whole chromatography. [c]These experiments were carried out with $5x10^9$ cells.

Table S3. Relative expression and mean Mw of shared B*27:04 ligands in various ERAP1 contexts[a]

Exp.	Comparison	All			IR>1.0[b]		IR >3.0		IR >1.5-3.0		IR>1.0-1.5[b]	
		N (%)	m/z	Intensity	N (%)	m/z	N (%)	m/z	N (%)	m/z	N (%)	m/z
1	WE-I	3222 (100)	1162.0	2028	1726 (54)	1177.8	289 (9)	1197.4	686 (21)	1179.2	751 (23)	1168.9
	JSL	3222 (100)	1162.0	1865	1493 (46)	1144.0	260 (8)	1124.3	554 (17)	1130.0	679 (21)	1163.0
	Δ m/z					**33.8**		**73.1**		**49.2**		**5.9**
2	WE-I	5240 (100)	1154.3	1181	2439 (47)	1170.6	380 (7)	1170.6	888 (17)	1176.7	1171 (22)	1165.8
	C1R04	5240 (100)	1154.3	1246	2790 (53)	1139.9	439 (8)	1112.0	1089 (21)	1138.3	1262 (24)	1151.1
	Δ m/z					30.7		58.6		38.4		14.7
3	WE-I	3558 (100)	1157.2	435	1277 (36)	1173.7	194 (5)	1192.2	426 (12)	1187.0	657 (18)	1159.7
	C1R04	3558 (100)	1157.2	593	2266 (64)	1147.6	541 (15)	1143.8	875 (25)	1143.9	850 (24)	1153.7
	Δ m/z					26.2		48.4		43.1		6.0
2-3	**Mean Δ m/z**					**28.5 ± 3.2**		**53.5 ± 7.2**		**40.8 ± 3.3**		**10.4 ± 6.2**
4	C1R04	6974 (100)	1149.4	2799	4553 (65)	1151.5	1009 (14)	1141.9	1832 (26)	1156.3	1712 (25)	1151.9
	KNE	6974 (100)	1149.4	2083	2412 (35)	1145.3	323 (5)	1133.3	804 (12)	1146.9	1285 (18)	1147.4
	Δ m/z					6.2		8.6		9.4		4.5
5	C1R04 (I)	6351 (100)	1154.4	3451	3604 (57)	1159.5	880 (14)	1160.2	1389 (22)	1158.4	1335 (21)	1160.3
	KNE	6351 (100)	1154.4	3288	2923 (46)	1148.1	533 (8)	1126.7	1079 (17)	1141.5	1311 (21)	1162.2
	Δ m/z					11.4		33.5		16.9		-1.9
6	C1R04 (II)	6395 (100)	1155.6	3361	3511 (55)	1161.7	753 (12)	1157.4	1451 (23)	1160.7	1307 (20)	1165.2
	KNE	6395 (100)	1155.6	3329	2878 (45)	1148.2	551 (9)	1129.8	1134 (18)	1146.5	1193 (19)	1158.2
	Δ m/z					13.5		27.6		14.2		7.0
4-6	**Mean Δ m/z**					**10.4±3.8**		**23.2±13.1**		**13.5±3.7**		**3.2±4.6**
7	C1R04 (I)	8403 (100)	1169	2918	4439 (53)	1169.4	479 (6)	1153.5	1650 (20)	1162.6	2310 (27)	1177.7
	C1R04 (II)	8403 (100)	1169	2771	3959 (47)	1168.4	274 (3)	1144.4	1574 (19)	1163.8	2111 (25)	1174.9
	Δ m/z					**1.0**		**9.1**		**-1.2**		**2.8**

[a] IR: intensity ratio between the corresponding ion peaks in the MS spectra from the cell lines compared; N: number and % of peptides; m/z: mean value in the peptide set. In MALDI-TOF MS this is equivalent to the mean Mw ($M+H^+$). Intensity: Mean intensity of all shared ligands. [b]Ion peaks with IR=1 were not included.

Table S4. Amino acid sequence of 372 B*27:04 ligands.[a]

Flanking Seq.	*Peptide Seq.*	*A. N.*		*Intensity Ratio*		
				C1R04/WE-I	*JSL/WE-I*	*C1R04/KNE*
TW	RRQNKVF	Q5NDL2	7	*	0.3	*
LY	ARFKPVAV	Q8WVK7	8	*	*	0.3
VV	GRYPDPNF	Q92466	8	*	1.9	*
VS	HRRPPIGY	Q9H6H4	8	*	*	2.4
YG	IRKGNLLF	O15205	8	*	*	0.2
NF	KRFHGRAF	Q92598	8	0.3	*	*
NH	KRYHPIYI	P78317	8	*	34.1	0.2
EE	QRYQALKI	O75410	8	*	*	5.2
TL	RRAVPLAL	Q13200	8	*	3.0	*
DD	RRGRPVGF	P61978	8	*	5.9	*
RG	RRLGLALG	Q15293	8	*	1.7	*
EK	RRNEPIKY	Q9UHA3	8	20.5	2.7	1.1
VR	RRVLRPVL	Q9H9V9	8	*	0.5	2.3
LN	RRYLSPKY	P60842	8	*	*	0.1
IF	SRFRPISV	Q9Y4B6	8	*	0.2	*
VG	SRGFPLRL	Q9UI30	8	*	*	8.3
QH	SRIWPLYL	Q9HCS7	8	*	*	5.4
DT	SRVQPIKL	P62857	8	*	3.0	*
AG	ARARFALGL	O95336	9	0.1	*	*
FI	ARFFKQPTF	P17252	9	0.3	1.4	0.5
TD	ARFGHGSDY	Q9NWH9	9	*	*	4.7
FL	ARFKERVGY	Q96AT1	9	0.3	0.2	0.3
LA	ARFLFTTGF	O00507	9	0.1	0.7	0.3
NR	ARFRGRKGY	Q86WW8	9	*	0.1	0.7
EA	ARHEHQVML	Q15233	9	*	*	0.2
RL	ARHGGVKRI	Q99525	9	*	*	1.4
AR	ARIAKGLRL	P47914	9	0.0	0.3	1.8
FE	ARIALLPLL	Q9P0J0	9	1.7	*	*
CT	ARIEIGLHY	O43325	9	0.4	*	0.3
KY	ARILFPVTF	P48169	9	0.4	*	*
EL	ARKERQLHM	Q9NQB0	9	*	0.2	0.2
RG	ARKGRGLVV	P83876	9	*	*	0.0
DF	ARKHFVLLL	Q9BPX3	9	0.1	0.0	1.6
SM	ARKIGARVY	P13796	9	0.4	*	*
AI	ARLKEVLEY	P14324	9	4.1	*	3.9
YK	ARLPLRLFL	O00767	9	0.4	0.5	5.0
M	ARLQTALLV	O00626	9	0.5	1.1	0.7
AR	ARTPRLLLL	Q6PCB8	9	*	*	6.9
QG	ARVPSSLAY	Q9NQS7	9	*	*	7.6

KY	ARVVQKLGF	P20226	9	0.1	*	*
SL	ARYGKSPYL	P50395	9	*	1.0	0.3
EM	ARYKRKLLI	Q14493	9	*	1.1	*
AA	ERLQYVFGY	Q96MG7	9	2.7	*	*
EM	ERTLALLAF	Q9NWU2	9	*	*	5.3
RQ	FRFDPQFAL	P01909	9	*	*	9.2
SY	FRLDTPLYF	Q32P28	9	10.5	*	12.4
SR	FRQQRPLEF	Q15773	9	0.2	0.6	0.5
PT	FRRPKTLRL	P62750	9	3.0	*	*
NS	FRYNGLIHR	P46779	9	2.7	*	*
TL	FRYQGHVGA	P40306	9	2.6	*	*
ML	FRYQGYIGA	Q99436	9	3.1	*	6.3
VC	GRAFIFPSY	Q8TBZ8	9	0.3	0.3	0.5
KR	GRAPQVLVL	Q9NR30	9	0.4	*	1.6
QN	GRDTHMRQI	Q9UM13	9	*	*	3.8
QA	GRFARGLRL	Q13393	9	0.0	*	*
SR	GRFGGVITI	O43315	9	*	1.6	*
ER	GRFHGGNLF	P55789	9	*	*	4.7
AT	GRFKDILAL	Q8N1W1	9	*	*	0.1
AT	GRFKDVLVL	Q92974	9	2.9	*	0.2
LT	GRFSHRIYV	P46977	9	*	*	5.0
ML	GRHGVFLEL	Q13200	9	2.6	0.8	1.2
TQ	GRHSTPLHL	Q9H2K2	9	*	*	0.3
KL	GRHVRALVL	P22314	9	0.3	*	*
RP	GRIDRKIEF	P62195	9	0.6	*	0.1
NW	GRIVTIFAF	Q16548	9	*	0.2	*
NW	GRIVTLISF	Q07820	9	1.1	*	0.9
AL	GRKKNGEEY	Q8WV28	9	*	*	0.1
VF	GRKKTATAV	P62249	9	*	*	0.1
PS	GRLCLLTIV	Q96DB9	9	*	*	0.6
GV	GRLGHILEY	Q8IXQ5	9	4.2	14.5	7.5
TS	GRLKDILAI	Q6ZSZ5	9	*	*	3.9
CP	GRLRGVRAV	P49207	9	0.3	*	0.1
RR	GRLTKHTKF	Q9Y3U8	9	2.2	3.6	0.7
AL	GRNKPHTPF	O00139	9	0.5	*	0.3
SR	GRNRQPLVL	Q9NTI7	9	0.2	*	0.1
KF	GRNSNICHY	Q96CG3	9	18.5	*	18.2
DD	GRRHGFLIL	Q10570	9	45.3	*	*
RY	GRRPYGVGL	P25786	9	*	*	3.6
NS	GRRYGLIGL	Q9UG63	9	*	*	9.1
NL	GRSFHILAI	Q96EE3	9	3.8	*	*
RL	GRSRWQGEL	Q12789	9	*	*	4.3
KM	GRTKIFIRF	O00159	9	*	1.2	*
CY	GRVAPRSGL	P33316	9	*	0.4	*
LD	GRWFGGRQI	O43719	9	*	*	4.4

TY	GRWQYPLIY	Q9BX95	9	*	*	0.3
GC	GRYAGGQGY	O75592	9	*	0.5	*
SQ	GRYEVAVPL	Q07866	9	*	*	3.2
LN	GRYFGGRVV	Q96I25	9	2.3	*	*
RA	GRYGGFLLA	P18858	9	*	1.3	*
AY	GRYNPRRSL	P33993	9	*	0.7	*
QQ	GRYPGVSNY	Q13564	9	2.3	4.5	2.1
ED	GRYRDPTTV	P63151	9	0.4	*	19.1
VS	GRYRGSVHF	Q9C0C9	9	*	*	0.5
LA	GRYSGRKAV	P61353	9	*	1.1	0.3
GI	GRYSRSAMY	Q02878	9	*	8.5	*
VT	GRYTILIKY	P21333	9	6.3	*	*
RG	HRHGKPFVF	O43187	9	3.1	*	*
RA	HRIGQQNEV	P51531	9	*	*	6.2
RA	HRIGQTKTV	O60264	9	*	*	9.9
WA	HRLFPKLQF	Q9BVW5	9	5.1	*	1.9
KD	HRNKAMINL	Q9NZ45	9	*	*	1.7
NI	IRAGLIPKF	P52292	9	0.4	3.3	0.4
NY	IRCIPSQAV	P16260	9	6.8	*	14.5
VT	IRKSKNILF	Q13765	9	1.2	*	2.6
EV	IRNDGVLLL	O60763	9	*	*	12.0
QS	IRSSLLLGF	P42704	9	0.6	1.5	4.4
SF	IRTRLLLQF	Q96K31	9	*	1.2	*
LR	IRYGQTKKM	P49591	9	*	1.5	*
TL	KQYPRKNLF	O60667	9	*	23.5	*
YA	KRASVFVKL	Q8IZP2	9	0.2	*	*
SL	KRFDDKYTL	Q15005	9	*	*	2.5
HL	KRFEHSAKL	Q9UPT9	9	0.1	1.1	0.0
LF	KRFEKQKEV	Q9Y6A5	9	*	*	0.1
EC	KRFGKAYNL	Q86XP3	9	*	*	0.2
DP	KRFPHGIPF	P17050	9	2.2	*	*
PG	KRFRPMDNL	Q14683	9	*	1.4	*
KD	KRFSGTVRL	P62906	9	0.7	*	0.2
CK	KRFSHSGSY	P37275	9	*	*	0.1
DM	KRHRIQFKY	P11388	9	0.2	*	0.1
TH	KRILKFLKL	P54619	9	0.2	*	*
TH	KRILKFLQL	Q9UGJ0	9	0.2	*	*
DA	KRINWRTVL	P54368	9	*	*	4.0
DK	KRKGQVIQF	Q969Q0	9	2.6	7.9	1.3
VF	KRKKPQLRL	Q5EE01	9	0.8	*	*
AF	KRLGASLAF	P78527	9	*	*	0.2
RG	KRLGILVVF	Q6UWH6	9	*	0.4	3.8
EQ	KRLGLLAGF	P55061	9	9.4	*	5.3
EQ	KRLKTVLEL	Q14444	9	*	*	0.3
LS	KRNPRQINW	P83731	9	*	*	3.4

KG	KRRDDGLSA	P84101	9	*	*	6.1
GY	KRRGGVPSL	Q9Y6G1	9	*	*	0.1
QR	KRRKALPTF	Q00653	9	*	0.5	*
DA	KRRQQGSSL	Q14161	9	*	*	0.3
QT	KRSSRNPVF	Q969W3	9	*	*	0.3
AK	KRTNIIPVI	P22087	9	0.1	*	1.1
AK	KRTNIIPVL	A6NHQ2	9	0.1	*	1.1
NI	KRYHIAKVY	P12081	9	0.5	*	*
NS	KRYKEAQKI	O43242	9	*	*	8.1
TE	KRYKSIVKY	P14324	9	2.0	1.0	1.2
DT	KRYQEALHL	O00231	9	*	*	3.5
MA	LRAGLVLGF	P06340	9	*	*	0.2
TC	LRFPGQLNA	Q9BVA1	9	2.2	1.8	1.3
HH	LRHGGRMQY	P49643	9	*	*	13.7
VN	NRFKGVKYF	Q6V1X1	9	*	*	6.1
VC	NRYLVVLYY	Q9Y3B4	9	3.3	*	*
SI	QRFPKILVL	O75604	9	12.4	*	18.3
FY	QRFPLSFGF	P17050	9	*	1.5	*
RG	QRKGAGSVF	P62917	9	*	0.4	*
AD	QRKKAYADF	P09669	9	3.5	*	1.5
FL	QRLDLQIKL	Q8IV50	9	0.3	*	0.5
MA	QRLVRVLQI	Q9NSP4	9	0.2	0.1	*
QI	QRNDYVHAL	Q9NR22	9	2.8	*	4.1
SF	QRNLFILAY	O95573	9	*	*	0.6
QV	QRSRFIVVV	Q9BRQ8	9	*	0.7	*
FS	QRYAKVPLF	Q9BQ52	9	0.5	0.1	*
NG	RRAFIGIGF	Q9NVZ3	9	*	8.9	*
LA	RRAIYQATY	P28074	9	*	0.5	0.4
VR	RRAKGSVSL	Q13115	9	*	*	0.1
LR	RRARGPPAA	Q05923	9	*	*	0.2
M	RRDVRILLL	Q8IXI1	9	14.3	*	*
DV	RRESRLLQL	P82930	9	5.4	*	*
GL	RRFAFPLSL	Q13144	9	*	0.8	*
RE	RRFEKPLEE	Q8NC51	9	*	2.1	*
YL	RRFFKAKKL	P49755	9	0.7	0.4	*
LY	RRFFKSPHF	Q8NEG7	9	0.1	2.5	*
YS	RRFFPYYVY	P20618	9	1.1	2.3	1.0
QL	RRFGDKLNF	Q13794	9	1.1	4.2	0.4
PA	RRFGGPVHH	Q15717	9	*	0.9	0.2
VR	RRFKGQILM	P62910	9	0.3	0.2	1.2
AL	RRFMQTFVL	Q13283	9	*	*	1.4
GF	RRFRASPLF	Q2NL82	9	*	1.6	*
TL	RRFRGDVTL	Q96F44	9	*	*	0.1
EK	RRFRKFLVY	P50395	9	*	*	0.1

RS	RRFRPRSEF	Q14999	9	0.1	0.7	0.2
VK	RRFSDFLGL	Q13596	9	*	4.6	*
VY	RRFTEIYEF	A6NI72	9	*	4.1	1.4
CL	RRFTRPEHL	A6NNY8	9	1.6	0.3	0.6
KA	RRFWGKIVA	P55040	9	*	*	5.5
YS	RRFWQGDTF	Q9BUX1	9	*	*	13.1
RA	RRGLPRLAV	Q96AZ6	9	0.1	0.9	*
PA	RRGPFPLAL	P49755	9	*	2.2	*
HS	RRGPPPRRY	Q01130	9	*	0.5	8.8
PK	RRGRPPSKF	Q9UIF9	9	0.1	*	*
VC	RRHFPPAVI	O43164	9	*	*	0.3
EI	RRHWGGNVL	P62424	9	*	*	1.9
RD	RRISGVDRY	O15239	9	*	*	5.2
HE	RRISQIQQL	O60306	9	*	2.6	*
DR	RRIYLILEY	Q96GD4	9	2.1	*	1.9
SY	RRKDGVFLY	P62829	9	1.4	*	4.5
EG	RRKEQERSF	P37198	9	*	*	4.7
EE	RRKERQEAL	Q13111	9	*	0.5	*
CG	RRKGEQIYY	O95711	9	2.0	0.3	0.2
MD	RRKKALTDY	Q5TA31	9	3.6	*	*
PK	RRKKPPIQY	Q96JP5	9	0.5	1.8	*
EL	RRKQFHVLL	Q6I9Y2	9	0.2	*	*
EE	RRKQLQNYL	Q8TEQ0	9	*	*	0.2
QC	RRLDRSAHF	O15294	9	*	*	0.3
EW	RRLGVQQSL	P33552	9	*	0.9	*
NS	RRLPIFSRL	Q07352	9	0.5	10.6	1.9
AW	RRLPQAFRP	P13598	9	*	*	3.9
NR	RRLSELLRY	P08238	9	0.4	6.6	0.7
DT	RRLSFLVSY	P47897	9	*	3.1	*
VR	RRLSLFLNV	Q99836	9	*	*	0.1
HE	RRNDKIIVF	P19447	9	*	*	3.0
GI	RRNEKIAVH	P62913	9	2.6	*	*
WE	RRNKVLNHF	P35269	9	*	1.0	*
ES	RRNREIAQL	Q7Z4S6	9	*	*	0.3
EL	RRQQEQLRY	Q14151	9	*	*	0.2
PQ	RRRDIQQTL	Q9HAV4	9	*	*	0.2
EE	RRREKAEEL	Q04323	9	*	*	0.1
RV	RRRFKGQIL	P62910	9	2.1	*	*
QL	RRRGKTNHY	Q13291	9	*	0.3	*
TY	RRRLSYNTA	P49207	9	0.3	0.4	8.8
YR	RRRPENPKP	P67809	9	0.2	0.1	3.4
EM	RRRREEEGL	P52294	9	*	*	0.2
EE	RRRRSFQDY	Q9NP64	9	*	*	0.3
GD	RRRSNTLDI	O94915	9	*	*	3.3
CC	RRRSSVAFF	O15297	9	*	0.5	*

HF	RRSGQHPRY	Q9NWZ8	9	4.0	0.6	0.3
HL	RRSPFLQVF	Q15437	9	1.0	1.6	0.5
NS	RRSQPLISL	Q9H967	9	9.2	*	*
HL	RRSSFLQVF	Q15436	9	*	2.1	*
SD	RRSSIPITV	P33992	9	0.3	*	*
QV	RRSSSVAQV	O15205	9	*	3.3	*
LD	RRTGYLKGY	Q9Y5S9	9	6.9	*	*
SL	RRTRLILFV	Q96TA2	9	*	2.2	*
EA	RRVARQAQL	O60239	9	*	7.2	0.0
LC	RRVLVQVSY	Q00266	9	*	*	0.1
AE	RRWEKSSRY	Q9HCG8	9	*	*	0.3
LA	RRYGDVFQI	Q16678	9	*	18.5	0.1
TG	RRYGRRHAY	O43164	9	*	1.0	*
TA	RRYIGIVKQ	P52597	9	0.5	1.1	0.2
LN	RRYLSPKYI	P60842	9	0.6	0.9	0.7
VY	RRYNDFVVF	Q9Y5X2	9	*	4.6	*
PF	RRYNGGVGR	P18621	9	*	1.1	*
HL	RRYNIIPVL	Q9UI12	9	0.3	1.1	0.4
LR	RRYPQIYTT	Q6PL18	9	*	*	3.0
EI	RRYQKSTEL	Q6NXT2	9	0.6	0.4	0.8
RT	RRYVRKFVL	O43633	9	0.1	0.5	0.7
RS	SRAGLQFPV	P0C0S8	9	2.6	0.3	0.2
NV	SRAKAVRAL	Q9H009	9	4.3	*	42.7
VL	SRANSLFAF	P61009	9	4.2	*	*
NS	SRAPVFLQF	Q4ZIN3	9	3.7	4.8	2.1
ST	SRFARLQKL	P04035	9	*	*	6.7
QA	SRFDIPLGL	O94913	9	0.3	*	1.7
NS	SRFGKFIQL	Q96H55	9	12.0	*	*
NS	SRFGKFIQV	B2RTY4	9	0.7	1.4	1.3
NS	SRFGKFIRI	P35749	9	0.5	1.0	1.0
NS	SRFGKFVEI	Q9UM54	9	13.0	*	*
KK	SRFGNAFHL	Q6P2Q9	9	*	*	0.1
RG	SRFIKFQEM	P33993	9	*	*	14.6
KF	SRFPEALRL	Q13200	9	7.7	*	2.3
AF	SRFPSFLKA	Q9BTD8	9	2.9	*	*
DL	SRFRGFLEH	Q9P241	9	*	3.4	*
IF	SRFRPISVF	Q9Y4B6	9	0.1	0.7	0.3
FC	SRHSKALKL	Q92974	9	0.4	*	0.2
RA	SRIRKLFNL	P62753	9	0.5	0.2	1.4
QN	SRLGLPLLL	Q9BSV6	9	0.5	*	*
VT	SRLGSVFPF	Q13217	9	*	5.5	*
EA	SRLKSILKL	Q9BRT6	9	0.1	*	0.5
AG	SRLPRQLFL	Q9BU23	9	3.0	*	5.1
YL	SRLRNQSVF	P37268	9	2.8	0.1	6.0

SL	SRMIRKMKL	Q07020	9	0.1	*	*
YH	SRMQRGGLR	Q9BTL4	9	*	0.8	*
NS	SRNLFVLGF	Q9UHI7	9	0.9	*	4.9
HF	SRNPKVLNP	Q9ULX3	9	3.8	*	*
SS	SRRAGGEHY	Q5T4S7	9	*	*	6.5
ET	SRRKAGHQF	Q96EY7	9	*	*	7.8
NY	SRTGRHLAF	O15213	9	2.8	2.0	0.3
AI	SRTPVLMNF	Q9H3K2	9	*	*	18.2
KS	SRTSVQPTF	Q5T4S7	9	0.3	0.9	0.3
LH	SRVKLILEY	Q7L5N1	9	0.2	0.4	0.2
TT	SRVLKVLSV	P35222	9	10.9	0.1	1.2
SF	SRVPLFPVF	Q9H6F2	9	0.9	2.0	5.1
YR	SRVRPCVVY	O15523	9	0.2	0.2	*
VA	SRYFKGPEL	P68400	9	0.6	*	1.1
RC	SRYLYTLVI	P63173	9	0.1	*	1.6
RR	SRYQDILVF	P19623	9	0.5	*	0.7
VY	SRYRPQYGY	Q8IYM9	9	0.1	0.1	*
LS	SRYSQKQHY	Q8WUB2	9	*	*	3.7
FK	SRYTGINQF	O75417	9	4.1	*	*
LQ	SRYYRAPEI	Q9H2X6	9	26.3	0.1	*
IC	SRYYRAPEL	P49840	9	26.3	0.1	*
NK	TRGRFELAF	O14925	9	0.4	*	0.8
FS	TRLFAVLRF	P46977	9	4.0	0.1	2.2
NL	TRMRHVISY	O14949	9	0.8	*	0.4
FR	TRSAIILHL	P53350	9	*	0.8	0.3
CL	TRTGLFLRF	Q9NX02	9	3.0	*	1.0
AW	TRVDTILEF	O14980	9	*	0.3	*
DA	TRVYLILEY	O14965	9	1.1	0.3	0.6
EY	TRYLFALQL	O94887	9	0.1	0.6	2.4
HR	TRYPTILQL	Q8WW24	9	0.1	*	*
RI	TRYQGVNLY	P11940	9	2.3	*	*
TD	VRAQIRLQF	Q92878	9	*	7.3	0.1
YY	VRAVLHLLL	P13498	9	0.3	*	*
SR	VRFGQQKRY	Q68E01	9	*	*	4.3
SH	VRFLGNLVL	Q7L523	9	*	*	3.5
EV	VRLPYPLQM	Q9NPA0	9	*	*	6.7
MA	WRALHPLLL	O95944	9	*	*	4.9
DE	WRFKPIEQL	Q96DE5	9	*	8.1	*
KD	WRSGKPVRV	Q96T88	9	20.1	*	8.0
YY	YRYPTGESY	Q16875	9	*	*	3.3
SD	ARLQYGLLIF	Q96BI3	10	0.2	*	*
AF	ARNKEIVHTF	Q8NI36	10	*	0.1	*
SL	ARYGKSPYLY	P31150	10	2.3	0.3	8.3
EC	GRAFSRKSLL	Q9BS31	10	0.2	*	*

RG	GRFGRKGVAI	Q14240	10	*	0.5	*
ER	GRFHGGNLFF	P55789	10	0.8	0.9	5.4
VT	GRFNGQFKTY	P63220	10	1.1	*	5.0
ST	GRIAHIPLYF	Q9NRG9	10	0.8	*	*
YT	GRIKAIQLEY	O43242	10	0.7	*	7.0
LF	GRKTGQAPGY	P99999	10	0.3	*	2.9
VR	GRWPGSSLYY	Q14739	10	4.5	*	9.4
TQ	GRWPKKSAEF	P18621	10	*	*	5.7
RY	GRYGGETKVY	Q16629	10	*	0.6	*
RS	GRYGRKGVAI	P38919	10	0.4	*	*
AG	GRYLGKKVQF	P55199	10	0.1	*	*
ML	HRFYGKNSSY	Q13283	10	0.3	0.9	0.6
TG	HRWLKGGVVL	P35613	10	*	*	3.6
SD	HRYGDGGSTF	P31943	10	8.8	2.1	1.3
KP	HRYRPGTVAL	Q6NXT2	10	0.8	1.2	0.5
EA	IQRTPKIQVY	P61769	10	*	0.1	*
II	KRFEQKGFRL	O60361	10	0.1	*	*
RL	KRFGPNVPAL	Q96SB8	10	0.2	*	0.8
TW	KRFSVPVQHF	Q99829	10	0.1	*	1.0
SN	KRHRPIGIGV	P23921	10	0.5	0.2	*
RY	KRNENQLIIF	Q15393	10	0.6	*	*
TD	KRNGVIIAGY	Q9UKF6	10	10.3	*	1.4
FL	KRNPGVKEGY	P22234	10	2.6	*	11.2
AL	KRQGRTLYGF	P62805	10	*	*	3.9
	MRLGSPGLLF	O75144	10	*	*	5.6
TI	RRDAPAGRKV	P62917	10	19.0	*	*
YN	RRFVNVVPTF	P62861	10	0.1	*	*
VL	RRHALIVQGF	Q9Y5Q9	10	*	0.5	*
RD	RRISGVDRYY	O15239	10	1.1	*	*
TA	RRKDAKSVKI	P63173	10	1.2	*	8.3
SY	RRKDGVFLYF	P62829	10	0.7	0.4	10.4
EK	RRKDHSFLGF	O75563	10	*	*	3.1
RL	RRLALFPGVA	P30101	10	1.7	1.7	3.4
ML	RRLGVQPSKY	Q9HAY2	10	0.5	*	1.6
AW	RRLSRDSGGY	Q14761	10	3.0	*	5.1
TL	RRNGLGQLGF	Q9P2F8	10	*	1.3	*
TW	RRNGPLPLKY	P35226	10	1.0	*	14.1
QT	RRRAAKNVSY	O14647	10	*	0.1	*
QE	RRRHYNGEAY	P31689	10	*	0.1	0.3
AL	RRSINQPVAF	Q9GZT3	10	1.2	*	2.2
DN	RRTGNKGLRL	Q14807	10	*	*	5.5
GR	RRYDRKQSGY	Q969Q0	10	1.3	0.5	1.0
IM	RRYGEQPASY	Q53H80	10	*	1.8	*
IM	RRYGTRPTSY	Q9H9L7	10	*	*	0.2

MM	RRYQDAIRVF	Q9Y262	10	0.9	*	4.9
EI	RRYQKSTELL	Q16695	10	2.1	*	6.1
ET	RRYRPTKNYL	O75934	10	0.3	0.1	0.8
SN	SRLEDQVIGV	Q2KHR3	10	*	*	11.0
AK	SRSSRAGLQF	Q6FI13	10	2.8	0.3	4.0
AA	WRRLPQAFRP	P13598	10	4.1	*	*
NR	GRFSSTTGLFY	P51817	11	0.5	0.4	10.8
EL	KRFNADNKLLL	Q9NRZ9	11	0.3	*	*
EK	KRYDREFLLGF	Q04637	11	0.9	0.1	1.7
DS	LRFGPNGGLVF	Q9UHW5	11	6.5	*	6.7
NE	LRVAPEEHPVL	P60709	11	*	0.2	*
KE	RRRTESINSAF	O96004	11	*	*	0.1
WL	RRYLENGKETL	P10319	11	3.4	*	13.8
EI	RRYQKSTELLI	Q71DI3	11	0.7	*	3.1
ET	SRFRQQRPLEF	Q15773	11	0.0	1.1	*
M	SRSVALAVLAL	P61769	11	2.5	*	20.3
RS	GRYGRKGVAINF	P38919	12	0.0	*	3.2
YN	RRFVNVVPTFGK	P62861	12	0.3	*	*
MC	RRKSSGGKGGSY	P01889	12	0.0	0.2	0.2
EI	RRYQKSTELLIR	Q16695	12	*	0.1	23.2
ES	RRFSPIPFPPLSY	Q6P2Q9	13	*	0.3	*
TF	YNELRVAPEEHPVL	P60709	15	*	0.0	*

[a]The amino acid sequence of B*27:04 ligands, their N-terminal flanking sequences, the accession number (A.N.) of the corresponding parental proteins, the peptide length and the intensity ratio in the cell line pairs where they were detected are indicated. Asterisks indicate that the corresponding peptide was not detected in that comparison. In the few cases where two similar peptide sequences involving isobaric residues were compatible with a same MS/MS spectrum, both possibilities were taken into account. All the sequences were determined by MALDI-TOF/TOF MS/MS form $[M+H]^+$ parental ions.

Table S5. Influence of internal sequence positions of B*27:04-bound nonamers on ERAP1-mediated trimming[a]

Subset [b]									
WE-I/JSL	**N[c]**	**Peptide Position**							
IR>3		**P3**	**P4**	**P5**	**P6**	**P7**	**P8**	**P9**	**Mean P3-P9**
WE- I	26	3.2	1.4	1.0	3.5	0.7	1.0	5.1	2.3
JSL	23	2.6	0.6	0.5	5.1	0.7	1.4	6.0	2.4
Ratio		**1.2**	**2.4**	**1.9**	**0.7**	**1.0**	**0.7**	**0.9**	**1.0**
IR>1-3									
WE- I	34	3.3	0.9	0.8	3.6	0.5	1.1	6.0	2.3
JSL	34	2.7	0.9	0.9	5.0	0.4	1.5	5.7	2.4
Ratio		**1.2**	**1.0**	**1.0**	**0.7**	**1.5**	**0.8**	**1.1**	**1.0**
WE-I/C1R04									
IR>3		**P3**	**P4**	**P5**	**P6**	**P7**	**P8**	**P9**	**Mean P3-P9**
WE-I	42	3.4	1.9	1.1	4.1	0.7	2.4	5.4	2.7
C1R04	37	2.6	1.0	0.7	5.0	0.9	1.1	5.6	2.4
Ratio		**1.3**	**2.0**	**1.5**	**0.8**	**0.8**	2.2	1.0	**1.1**
IR>1-3									
WE-I	35	3.2	1.2	0.9	4.2	0.8	1.8	5.9	2.6
C1R04	32	3.0	1.2	0.6	3.9	1.2	1.9	6.3	2.6
Ratio		**1.1**	**1.0**	**1.4**	**1.1**	**0.7**	**0.9**	**0.9**	**1.0**
KNE/C1R04									
IR>3		**P3**	**P4**	**P5**	**P6**	**P7**	**P8**	**P9**	**Mean P3-P9**
KNE	58	2.9	1.0	0.7	3.6	0.5	1.1	5.9	2.2
C1R04	64	2.8	0.7	0.3	3.7	0.9	1.2	5.4	2.1
Ratio		**1.0**	**1.6**	**2.2**	**1.0**	**0.6**	**0.9**	**1.1**	**1.0**
IR>1-3									
KNE	32	3.1	1.6	1.0	3.6	0.3	1.6	6.0	2.5
C1R04	33	3.0	0.7	0.9	5.0	1.2	0.9	6.0	2.5
Ratio		**1.0**	**2.3**	**1.2**	**0.7**	**0.3**	**1.8**	**1.0**	**1.0**

[a]Each residue at a given position was assigned a score related to its effect on ERAP1-mediated trimming (**supplementary Table S1**). The mean score of each position for each peptide subset, as well as the corresponding ratios are given. [b]Peptide subsets whose ion peaks show the indicated intensity ratio (IR) relative to the other cell line. [c]Number of nonamers sequenced.

THE JOURNAL OF BIOLOGICAL CHEMISTRY VOL. 289, NO. 7, pp. 3978–3990, February 14, 2014

Combined Effects of Ankylosing Spondylitis-associated ERAP1 Polymorphisms Outside the Catalytic and Peptide-binding Sites on the Processing of Natural HLA-B27 Ligands*

Received for publication, October 23, 2013, and in revised form, November 28, 2013 Published, JBC Papers in Press, December 18, 2013, DOI 10.1074/jbc.M113.529610

Adrian Martín-Esteban[1,2], **Patricia Gómez-Molina**[2], **Alejandro Sanz-Bravo, and José A. López de Castro**[3]

From the Centro de Biología Molecular Severo Ochoa (Consejo Superior de Investigaciones Científicas and Universidad Autónoma), 28049 Madrid, Spain

Background: The endoplasmic reticulum aminopeptidase (ERAP) 1 is associated with HLA-B27$^+$-ankylosing spondylitis.
Results: ERAP1 polymorphism at residues 528/575 affects the processing of HLA-B27 ligands in variant- and peptide-dependent and mutually dependent ways.
Conclusion: ERAP1 shapes HLA-B27 peptidomes through combined effects of co-occurring polymorphisms.
Significance: ERAP1-induced, peptide-mediated alterations of the immunological/pathogenetic features of HLA-B27 explain the epistasis of both molecules in ankylosing spondylitis.

ERAP1 polymorphism involving residues 528 and 575/725 is associated with ankylosing spondylitis among HLA-B27-positive individuals. We used four recombinant variants to address the combined effects of the K528R and D575N polymorphism on the processing of HLA-B27 ligands. The hydrolysis of a fluorogenic substrate, Arg-528/Asp-575 < Lys-528/Asp-575 < Arg-528/Asn-575 < Lys-528/Asn-575, indicated that the relative activity of variants carrying Arg-528 or Lys-528 depends on residue 575. Asp-575 conferred lower activity than Asn-575, but the difference depended on residue 528. The same hierarchy was observed with synthetic precursors of HLA-B27 ligands, but the effects were peptide-dependent. Sometimes the epitope yields were variant-specific at all times. For other peptides, concomitant generation and destruction led to similar epitope amounts with all the variants at long, but not at short, digestion times. The generation/destruction balance of two related HLA-B27 ligands was analyzed *in vitro* and in live cells. Their relative yields at long digestion times were comparable with those from HLA-B27-positive cells, suggesting that ERAP1 was a major determinant of the abundance of these peptides *in vivo*. The hydrolysis of fluorogenic and peptide substrates by an HLA-B27 ligand or a shorter peptide, respectively, was increasingly inhibited as a function of ERAP1 activity, indicating that residues 528 and 575 affect substrate inhibition of ERAP1 trimming. The significant and complex effects of co-occurring ERAP1 polymorphisms on multiple HLA-B27 ligands, and their potential to alter the immunological and pathogenetic features of HLA-B27 as a function of the ERAP1 context, explain the epistatic association of both molecules in ankylosing spondylitis.

ERAP1 is a multifunctional aminopeptidase of the endoplasmic reticulum involved in the final processing steps of major histocompatibility complex class I (MHC-I) ligands. Its role in this pathway is to trim peptides to the optimal size for MHC-I binding, which is 9–10 amino acid residues (1–3). Various nonsynonymous polymorphisms, involving amino acid changes in the protein (4, 5), are associated with ankylosing spondylitis (AS),[4] a chronic form of arthritis typically affecting the axial skeleton and very strongly associated with HLA-B27 (6, 7). Because of strong linkage disequilibrium between polymorphisms within the same gene, it is often difficult to discern the contribution of each mutation to AS susceptibility or protection. Yet, it has been determined that this association fits a two-mutation model with contributions of both the single nucleotide polymorphisms rs301087 (coding for K528R) and rs10050860/rs17482078 (coding for D575N/R725Q), the two latter changes being indistinguishable due to tight linkage disequilibrium (8). The fact that the association of ERAP1 with AS concerns only the HLA-B27-positive disease (8, 9) strongly suggests that it is based on the functional interaction between ERAP1 and HLA-B27. In a recent study (10), we showed that the AS-associated natural polymorphism of ERAP1 variants altered the expression level of many HLA-B27-bound peptides in live cells. On the basis of that study, we proposed that the mechanism of functional interaction between these two proteins, and presumably the basis for their joint association with AS, is the alteration in the balance between epitope generation and destruction induced by ERAP1 polymorphism on the HLA-B27 peptidome.

Several *in vitro* studies using recombinant ERAP1 mutants and synthetic peptides have shown that the AS-protective changes Arg-528, Gln-725, and Glu-730 result in decreased enzymatic activity, whereas no effect on trimming was reported for R127P or D575N using single-residue mutants (8, 11, 12). In these studies, few peptides were tested. Because ERAP1 activity

* This work was supported by Grant SAF2011/25681 (Plan Nacional de I+D+i) (to J. A. L. C.) and an institutional grant from the Fundación Ramón Areces to the Centro de Biología Molecular Severo Ochoa.
[1] Fellow of the Ministerio de Economía y Competitividad of Spain.
[2] Both authors contributed equally to this work.
[3] To whom correspondence should be addressed: Centro de Biología Molecular Severo Ochoa, Nicolás Cabrera N. 1, Universidad Autónoma, 28049 Madrid, Spain. Tel.: 34-91-196-4554; Fax: 34-91-196-4420; E-mail: aldecastro@cbm.uam.es, aldecastro@cbm.csic.es.

[4] The abbreviations used are: AS, ankylosing spondylitis; L-AMC, Leu-7-amido-4-methylcoumarin.

is influenced by the N-terminal residue of the substrate (13) and its sequence downstream from the N terminus (14), an incomplete and potentially misleading picture of the effect of a mutation might be obtained. In addition, the use of single mutants precluded analyzing possible combined effects among co-occurring mutations. This is particularly relevant because natural ERAP1 variants are complex allotypes that differ among each other by multiple amino acid changes (15–17), whose individual contribution to disease is not always distinguished by genetic analyses and whose concurrent influence on ERAP1 activity needs to be directly tested. Indeed, significant specificity differences, including some mediated by residue 575, were reported among natural ERAP1 variants with diverse combinations of amino acid changes, reflecting complex interactive effects in ERAP1 haplotypes on enzymatic activity (18).

In this study, four recombinant ERAP1 variants and a panel of synthetic peptides were used to analyze the context-dependent contribution of the AS-associated changes K528R and D575N to the processing of natural HLA-B27 ligands. We focused on these two residues for the following reasons: 1) as mentioned above, both K528R and D575N and/or R725Q are critical in the two-mutation model that explains the genetics of ERAP1 association with AS (8); 2) contrary to residue 725, which is known to affect ERAP1 activity (8), there are conflicting reports concerning D575N, although two studies (8, 11) found no effect of this mutation, a recent report (18) found a positive effect; and 3) both residues 528 and 575 are located outside the catalytic and peptide-binding sites of the enzyme and are thought to influence the domain rearrangements associated with the acquisition of an active ERAP1 conformation (19, 20). These three features are not fulfilled for other AS-associated polymorphisms. Two issues were specifically addressed as follows: 1) the influence of each mutation on the generation and destruction of natural HLA-B27 ligands; and 2) how the effect of a given residue in one position on ERAP1 activity and in the generation/destruction balance of HLA-B27 ligands was influenced by the residue at the other position.

EXPERIMENTAL PROCEDURES

ERAP1 Variants—The starting ERAP1 construct (a kind gift of Dr. S. C. Chang, National Taiwan University) was a pFastBac/myc-His-ERAP1 plasmid containing a full-length cDNA coding for an ERAP1 variant that, upon re-sequencing in our laboratory, showed four nonsynonymous substitutions (coding for Asp-346, Arg-514, Arg-528, and Glu-730) relative to the GenBank™ reference sequence NP-057526. Three additional ERAP1 variants (Table 1) were generated from the initial construct, hereby termed wild type, by PCR-mediated site-directed mutagenesis of codons 528 and 575. The primers used were as follows: R528K, 5′-cacttggacactgcagaagggttttcccctaataacc-3′ (sense) and 5′-ggttattaggggaaaaccccttctgcagtgtccaagtg-3′ (antisense); D575N, 5′-gacattcatcaccagcaaatccaacatggtccatcgatttttgc-3′ (sense) and 5′-gcaaaaatcgatggaccatgttggatttgctggtgatgaatgtc-3′ (antisense).

To our knowledge the variants in this study are not identical to any known natural allotypes. However, all the individual amino acid changes encoded in the four constructs are naturally occurring polymorphisms, and it is known from reported natural variants (10, 18) that individual polymorphisms occur in very diverse combinations. Thus, it is likely that the variants analyzed here may correspond to as yet undetected natural ones.

Generation of Recombinant Baculovirus—The correct products were confirmed by sequencing and subsequently used to transform competent DH10Bac *Escherichia coli*. Recombinant bacmids were isolated by standard DNA preparation methods and used to transfect Hi-5 adherent insect cells with Cellfectin II (both from Invitrogen) to produce the recombinant baculoviruses. These were harvested from the cell supernatant after 72 h, and its titer was determined by an immunofluorescence plaque assay with a mouse anti-His antibody (Qiagen, Hilden, Germany) and an Alexa 488 donkey anti-mouse antibody (Invitrogen), at 1:400 and 1:500 dilutions, respectively. Larger amounts of viruses were produced by infecting Hi-5 adherent cell cultures at a high multiplicity of infection and collecting the supernatant after 72 h.

Protein Expression and Purification—Recombinant ERAP1 proteins were produced in nonadherent Hi-5 insect cells grown in Express Five serum-free medium (Invitrogen). After infection with baculovirus carrying the ERAP1 gene construct, the culture medium containing the secreted enzyme was harvested by centrifugation (3000 × *g*, 30 min, 4 °C). The supernatant was concentrated in a Stirred Ultrafiltration Cell (Amicon, Millipore), adjusted to 50 mM phosphate, 300 mM NaCl, 10 mM imidazole, pH 8.0, and loaded onto a Poly-prep chromatography column (Bio-Rad) pre-loaded with nickel-nitrilotriacetic acid-agarose (Qiagen). The column was washed with the same buffer, containing 20 mM imidazole, and the protein was eluted with a 40–150 mM imidazole gradient. Protein elution was checked by SDS-PAGE. Protein-containing fractions were dialyzed in Vivaspin 500 (Sartorius Stedim Biotech, Goettingen, Germany) against 50 mM Tris/HCl buffer, 1 mM DTT, pH 7.4, aliquoted, and stored at −70 °C.

Fluorogenic Substrate Hydrolysis Assay—Three μg of Leu-7-amido-4-methylcoumarin (L-AMC) (Bachem Distribution, Wei an Rhein, Germany) in 50 μl of 1 M Tris/HCl buffer, pH 8.0, was mixed with 100 ng of ERAP1 in an equal volume of 50 mM Tris/HCl, 1 mM DTT, pH 7.4 (E/S ratio, 1:30), and incubated at 37 °C up to 1 h. The substrate hydrolysis was assessed by measuring its fluorescence, at 14-s intervals, at 380 and 460 nm excitation and emission wavelengths, respectively, in a Fluostar Optima Multiwave Plate Reader (BMG Labtec, Ortenberg, Germany).

Synthetic Peptides—A total of 10 peptides, including eight precursors of prominent natural HLA-B27 ligands and two fully processed ones (Table 2), were obtained using standard Fmoc (*N*-(9-fluorenyl)methoxycarbonyl) chemistry and purified by HPLC (purity >80%). The correct molecular weight and sequence of the synthetic peptides were confirmed by MALDI-TOF mass spectrometry (MS) using a 4800 Proteomics Analyzer (Applied Biosystems).

Peptide Trimming Assays—One μg of each peptide was incubated with 100 ng of ERAP1 (E/S ratio 1:10) in 50 μl of 50 mM Tris/HCl buffer, 1 mM DTT, pH 7.4, at 37 °C at various times from for 5 min to 4 h. After incubation, the reaction was stopped with 5 μl of 5% trifluoroacetic acid. The peptides in the

TABLE 1

ERAP1 variants used in this study

Residues associated with increased risk to AS are underlined. Residues in italics are altered relative to the reference sequence (NCBI accession number NP-057526), but have not been reported to influence AS susceptibility. Arg-528/Asp-575 is termed wild type because this was the starting variant from which the other three variants were generated by site-directed mutagenesis. SNP indicates single nucleotide polymorphism.

SNP	Polymorphism[a]	R528/D575 (wild type)	Lys-528/Asp-575	Arg-528/Asn-575	Lys-528/Asn575	C1R[b]	WE-I[b]
rs26653	R127P	Arg	Arg	Arg	Arg	Pro	Pro
rs27895	G346D	*Asp*	*Asp*	*Asp*	*Asp*	Gly	Gly
rs2287987	M349V	Met	Met	Met	Met	Met	Val
rs78649652	G514R	*Arg*	*Arg*	*Arg*	*Arg*	Gly	Gly
rs30187	K528R	Arg	Lys	Arg	Lys	Arg	Arg
rs10050860	D575N	Asp	Asp	Asn	Asn	Asp	Asn
rs17482078	R725Q	Arg	Arg	Arg	Arg	Arg	Gln
rs27044	Q730E	Glu	Glu	Glu	Glu	Glu	Glu

[a] Naturally occurring amino acid changes are relative to the reference sequence.
[b] The sequence of ERAP1 from these cell lines was reported previously (10).

reaction mixtures were purified with OMIX C18 pipette tips (Varian Inc. Palo Alto, CA) following the instructions of the manufacturer. The samples were dried down in a SpeedVac, dissolved in 1 μl of 30% acetonitrile, 15% isopropyl alcohol, and 0.1% trifluoroacetic acid, and sonicated for 3 min. The digestion mixtures were analyzed by MALDI-TOF MS in positive ion reflector mode at 25 kV in the mass-to-charge (m/z) range of 400–2200 as described previously (21). Peptide yields were estimated on the basis of the relative intensity of the respective ion peaks.

MS was used instead of the more conventional HPLC due to the significantly higher sensitivity of the former method and to the difficulties of separating similar and co-eluting peptide species in the relatively complex digestion mixtures generated from the long precursors used in our study. Yet to confirm the reliability of MS-based estimations, we carried out pilot experiments to assess the correspondence between both detection methods. In those experiments, the precursor peptide 7 (LREI.RRYQKSTEL) was digested with Arg-528/Asp-575 or Lys-528/Asn-575 and analyzed at every time point by MS and HPLC.

Identification of HLA-B27 Ligands in Live Cells—This was performed exactly as described previously (10). Briefly, HLA-B27-bound peptides were isolated from C1R-B*27:04 or -B*27:05 transfectant cells and from the B*27:04$^+$ lymphoblastoid cell line Wewak I by immunopurification of HLA-B27 and acid extraction and fractionated by HPLC. Each chromatographic fraction was analyzed by MALDI-TOF MS, and individual peptides were identified by MS/MS sequencing.

RESULTS

Context-dependent Effects of AS-associated ERAP1 Polymorphism on L-AMC Hydrolysis—The relative activity of four ERAP1 variants differing at residue 528 (Lys/Arg), 575 (Asp/Asn), or both (Table 1) was assessed by measuring the hydrolysis of the fluorogenic L-AMC substrate as a function of time (Fig. 1). Substantial differences were observed with the following activity ranking: Lys-528/Asn-575 > Arg-528/Asn-575 > Lys-528/Asp-575 > Arg-528/Asp-575. These results indicate the following: 1) Lys-528 confers higher activity than Arg-528 if residue 575 is the same; 2) Asn-575 confers higher activity than Asp-575 regardless of residue 528; 3) the relative activity of variants differing by the K528R change depends on residue 575: Lys-528/Asn-575 > Arg-528/Asn-575 and Lys-528/Asp-575 > Arg-528/Asp-575, but Arg-528/Asn-575 > Lys-528/Asp-575; and 4) this is due to the fact that the D575N mutation increased ERAP1 activity more than R528K in this system.

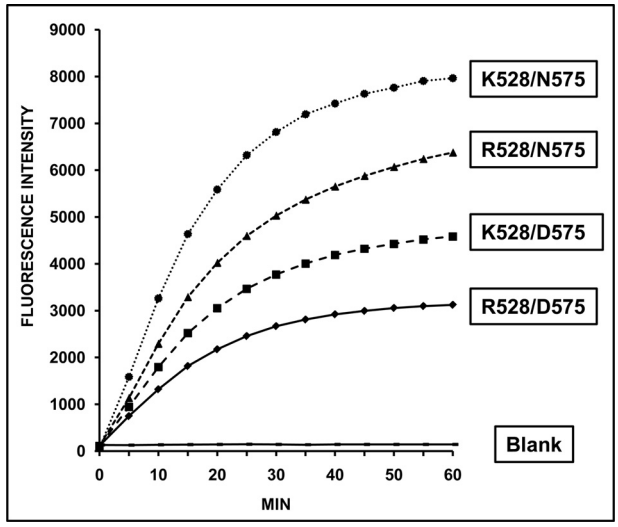

FIGURE 1. **Hydrolytic activity of ERAP1 variants toward L-AMC.** The indicated ERAP1 variants were incubated with the fluorogenic substrate at an E/S ratio of 1:30 (w/w), and the fluorescence intensity of the generated fluorophore was measured as a function of time. The data are means of 10–13 experiments.

ERAP1 Polymorphism at Residues 528 and 575 Influences the Generation and Destruction of HLA-B27 Ligands in a Variant and Peptide-dependent Way—The effect of AS-associated polymorphism at each or both positions on the generation and destruction of natural HLA-B27 ligands was analyzed with 10 peptide substrates (Table 2). Peptides 1–6 were 16-mer precursors of natural ligands, including four nonamers and two decamers. In addition, two natural ligands, a 9-mer and a C-terminally extended 12-mer variant (peptides 9 and 10), as well as their N-terminally extended precursors with four flanking residues (peptides 7 and 8) were used. This panel was chosen to favor diversity of N- and C-terminal residues, as well as internal sequences, to assess peptide-dependent differences in ERAP1 trimming. The flanking and P1 residues were assigned a score of 1 to 4 based on the susceptibility of each residue to ERAP1 (Table 2). The peptides were digested at various times up to 4 h, because longer incubation times usually yielded little further digestion.

In the following analyses (Fig. 2), we computed the combined digestion of all the species longer than the natural ligand

TABLE 2

Digestion of peptide precursors by ERAP1 variants

The data represent the maximal combined digestion (%) of peptide species longer than the natural HLA-B27 ligands (sequences highlighted in boldface) resulting from digestion of the synthetic precursor by the indicated ERAP1 variant. It was calculated as follows: 100 − % combined yield of the corresponding species. The minimal and maximal values observed with the peptides tested with each variant are highlighted in boldface. The fully processed natural ligands RRYQKSTEL (peptide 9) and RRYQKSTELLIR (peptide 10) are not included. The data are means ± S.D. of at least three experiments.

	Peptide	Arg-528/Asp-575, % maximum	Lys-528/Asp-575, % maximum	Arg-528/Asn-575, % maximum	Lys-528/Asn-575, % maximum	Trimming score[a]	
						Mean of F.R.	P1
1	GRHHEAS.**IRLPSQYNF**	15.0 ± 3.0	15.9 ± 2.5	34.7 ± 1.1	79.8 ± 9.2	**1.6**	**2**
2	LGVFRKF.**SRFPEALRL**	**6.8 ± 1.2**	36.5 ± 3.4	76.7 ± 6.9	95.1 ± 6.7	**1.7**	**2**
3	NLKARNS.**FRYNGLIHR**	48.4 ± 5.4	51.3 ± 2.4	63.7 ± 1.8	84.9 ± 1.7	**2.0**	**2**
4	IMYKKRT.**KRLVVFDAR**	29.6 ± 2.5	32.8 ± 0.1	29.9 ± 3.0	77 ± 2.7	**2.0**	**1**
5	DVVYAL.**KRQGRTLYGF**	10.5 ± 0.7	**3.6 ± 0.5**	**24.6 ± 2.1**	**99.9 ± 0.5**	**2.5**	**1**
6	LYSESL.**ARYGKSPYLY**	**79.8 ± 0.3**	**72.8 ± 2.3**	**79.2 ± 4.1**	77.9 ± 2.6	**2.8**	**4**
7	LREI.**RRYQKSTEL**	48 ± 1.2	59.3 ± 3.4	73.7 ± 1.8	**74.5 ± 5.3**	**2.0**	**1**
8	LREI.**RRYQKSTELLIR**	50.9 ± 5.8	61.2 ± 2.1	67.7 ± 0.8	85.5 ± 1.3	**2.0**	**1**
	Mean	**36.1**	**41.7**	**56.3**	**84.3**		

[a] Trimming susceptibility scores for each residue are based on relative cleavage efficiencies as determined in a previous study (13): score 1, 0–25% (T, H, Q, G, N, E, W, D, K, V, R, P); 2, 25–50% (F, I, S); 3, 50–75% (C); 4, 75–100% (A, L, M, Y). For each substrate the mean score of all the flanking residues (mean of F.R.) and the score of the N-terminal residue of the natural ligand (P1) are shown.

excluding the original substrate, designated as epitope precursors, the yield of the ligand, and the yield of shorter species, resulting from destructive cleavages, as a function time. The cumulative digestion of epitope precursors was chosen because the digestion rate of the enzyme is strongly dependent on the N-terminal residue of the substrate, so that the generation of the natural epitope will depend on the combined digestion rate of all the precursor species. The yield of the ligand at each time point is the epitope amount generated minus that destroyed at that time point.

To validate the reliability of the MS-based assessment of yields of digestion products, we performed two comparative experiments in which one of the substrates in Fig. 2 (peptide 7) was digested with Arg-528/Asp-575 or Lys-528/Asn-575 and analyzed by MALDI-TOF MS and HPLC (Fig. 3). The results show that digestion rates and relative yields are similar with both techniques. The small differences observed are due to the higher sensitivity of MS that allows detection of peptide species present in very low amounts that go undetected by HPLC.

Digestion of Epitope Precursors—The four ERAP1 variants showed distinct patterns of digestion that were both peptide- and variant-dependent (Fig. 2*A*). Distinct peptides were digested with very different rates and efficiencies by any given variant. The relative efficiency with which the four variants digested a given substrate also differed widely among peptides. Yet the average values of the maximal digestion of epitope precursors from peptides 1 to 8 increased in the following order: Arg-528/Asp-575 (36.1%) < Lys-528/Asp-575 (41.7%) < Arg-528/Asn-575 (56.3%) < Lys-528/Asn-575 (84.3%). Thus, the relative activity of the four ERAP1 variants toward peptidic substrates is the same as established with L-AMC. Peptide-dependent differences in the digestion of precursors correlated with the susceptibility of the flanking sequences to ERAP1 trimming (Table 2). These differences were much larger with the less active variants Arg-528/Asp-575 and Lys-528/Asp-575 (6.8–79.8 and 3.6–72.8%, respectively) than with the most active variant Lys-528/Asn-575 (74.5–99.9%). Thus, resistance of the flanking sequences to ERAP1 has a larger influence on the digestion of epitope precursors by less active variants. This is clear, for instance, when comparing peptides 1 and 2 with peptide 6 (Fig. 2*A* and Table 2).

Destructive Cleavages—The rate and efficiency of epitope destruction were estimated by measuring the combined yield of species shorter than the natural epitope as a function of time. In general, the patterns of epitope destruction (Fig. 2*C*) paralleled those of precursor digestions (Fig. 2*A*), showing similar variant and peptide-dependent differences. In addition, the mean maximal yield of species shorter than the natural HLA-B27 ligands for peptides 1–8 paralleled that of the digestion of precursors for each ERAP1 variant, revealing the same activity ranking (Table 3) as follows: Arg-528/Asp-575 (22.5%) < Lys-528/Asp-575 (26.8%) < Arg-528/Asn-575 (42.1%) < Lys-528/Asn-575 (75.9%). These results indicate that, in general, there is a concomitant and similar effect on both epitope generation and destruction resulting from the alterations in enzymatic activity induced by ERAP1 polymorphism.

Generation of HLA-B27 Ligands—All the natural ligands were generated with the four ERAP1 variants, albeit with widely different efficiencies (Table 4). Because of the concomitant increase of cleavages leading to generation and destruction of the epitopes as a function of ERAP1 activity, the mean maximal yield of the eight ligands was similar for Arg-528/Asp-575 (14.0%) and Lys-528/Asp-575 (12.5%) and only slightly higher with the most active ones Arg-528/Asn-575 (17.9%) and Lys-528/Asn-575 (19.2%). The average time at which the maximal yield of epitopes was obtained was longest with the less active variant Arg-528/Asp-575 (101.9 min) and shortest with the most active variant Lys-528/Asn-575 (35.6 min). A similar activity ranking was reflected at the mean earliest time at which the natural ligands were detected in the digestion mixtures (Table 4).

Significant peptide-to-peptide and variant-dependent differences were observed in the maximal amount of epitope and, more importantly, in the time at which this was obtained (Fig. 2*B*). Four situations were distinguished. For peptides 1, 3, 5, and 7, the highest epitope yields were obtained with the most active enzyme, Lys-528/Asn-575, at shorter times, and the tendency was reversed at longer times due to more efficient destruction of the epitope by this enzyme. A second pattern was observed with peptides 4 and 8. For these two substrates, the epitope yields were similar with Arg-528/Asp-575, Lys-528/Asp-575, and Arg-528/Asn-575 and were consistently higher with Lys-

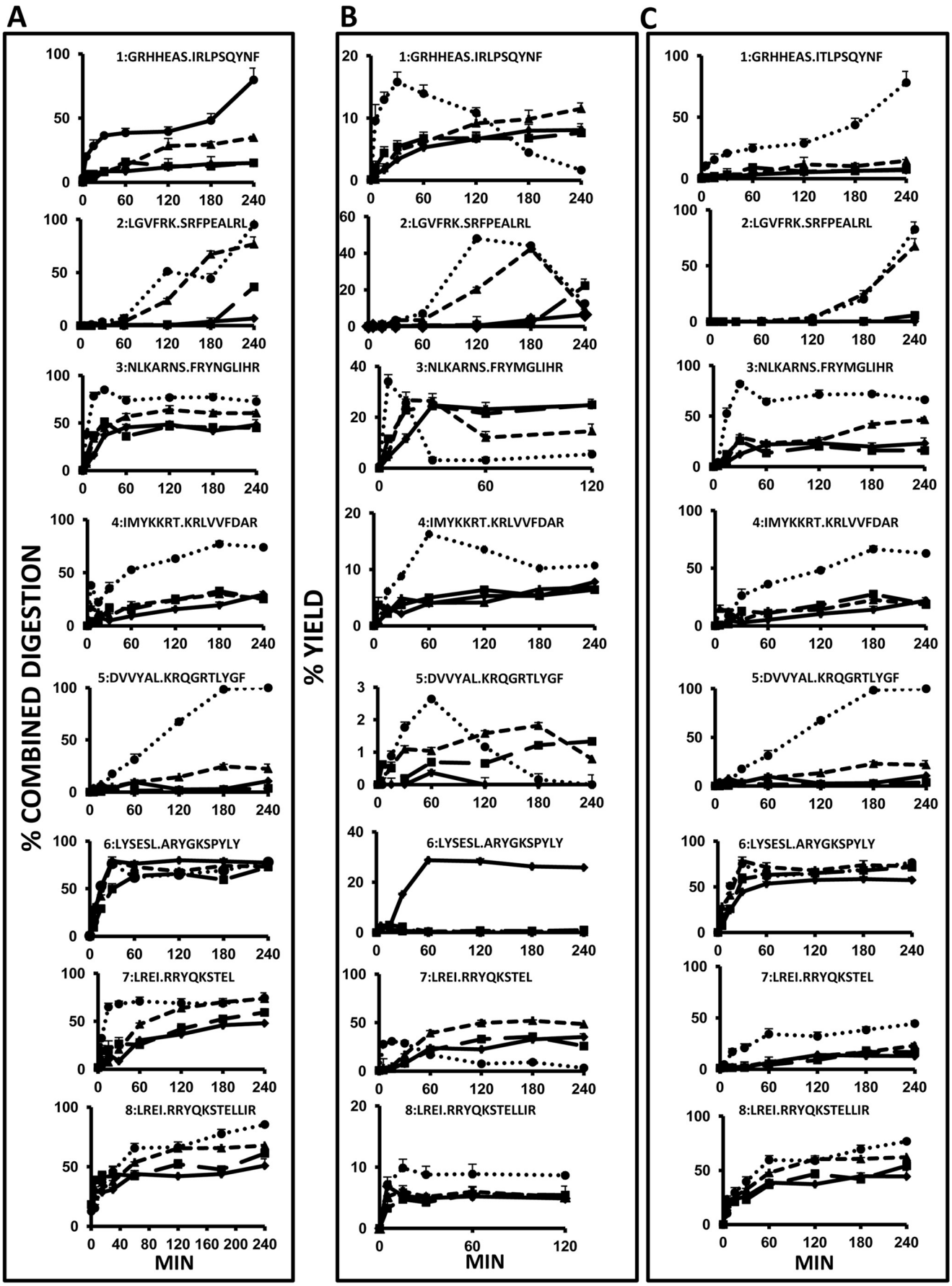

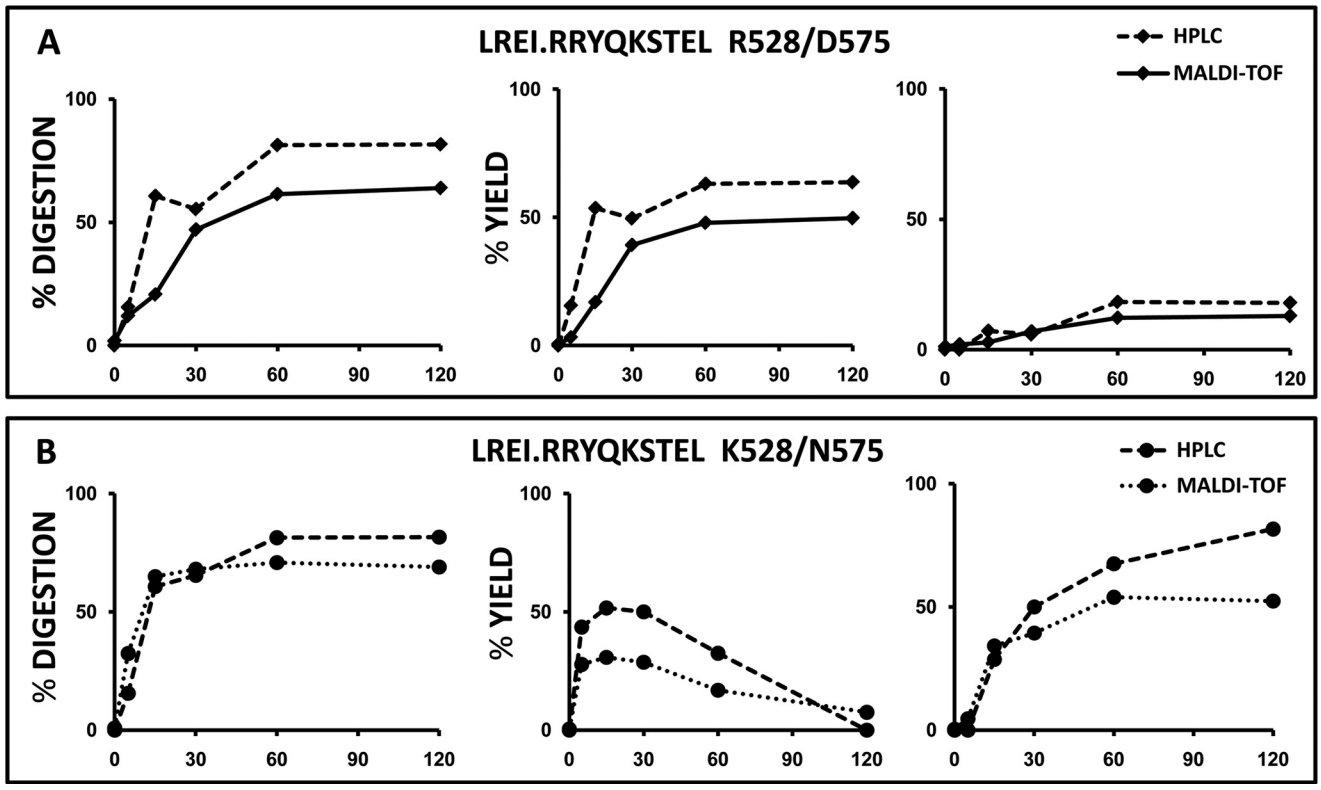

FIGURE 3. **Comparison of the digestion of a synthetic peptide substrate analyzed by MALDI-TOF MS and HPLC.** *A,* peptide 7 was digested with Arg-528/Asp-575 at the indicated times in parallel experiments, and the digestion mixtures were analyzed by MALDI-TOF and HPLC, respectively. Conventions are as in Fig. 2. The *left graph* shows the combined digestion of peptide species longer than the natural ligand, excluding peptide 7 itself. Digestion was calculated as 100% − the combined yield of the corresponding species. The *middle* and *right graphs* show the % yield of the natural ligand and of shorter peptide(s), respectively. *B,* same substrate was digested with Lys-528/Asn-575 and analyzed as in *A*. The data in each panel are from a single experiment, but it was carried out separately for samples to be analyzed by either MS or HPLC.

TABLE 3

HLA-B27 epitope destruction by ERAP1 variants

The data represent the maximal % yield of peptide species shorter than the natural HLA-B27 ligands (sequences highlighted in boldface) by the indicated ERAP1 variant. For each variant, the minimal and maximal (Max)values observed with the peptides tested are highlighted in boldface. Peptides 9 (RRYQKSTEL) and 10 (RRYQKSTELLIR) are not included. The data are means ± S.D. of at least three experiments.

	Peptide	Arg-528/Asp-575, % Max	Lys-528/Asp-575, % Max	Arg-528/Asn-575, % Max	Lys-528/Asn-575, % Max
1	GRHHEAS.**IRLPSQYNF**	6.9 ± 0.4	9.1 ± 0.9	**14.4 ± 1.1**	78.1 ± 9.2
2	LGVFRKF.**SRFPEALRL**	**0.3 ± 0.1**	5.6 ± 1.2	67.5 ± 6.9	82.6 ± 6.7
3	NLKARNS.**FRYNGLIHR**	23.1 ± 2.7	25.7 ± 0.8	46.4 ± 1.8	81.7 ± 1.7
4	IMYKKRT.**KRLVVFDAR**	21.8 ± 2.5	27.5 ± 0.1	22.4 ± 3.0	66.6 ± 2.7
5	DVVYAL.**KRQGRTLYGF**	10.5 ± 0.7	**3.6 ± 0.5**	22.8 ± 2.1	**99.9 ± 0.5**
6	LYSESL.**ARYGKSPYLY**	**58.5 ± 2.6**	**71.5 ± 2.3**	**78.4 ± 4.1**	76.6 ± 2.6
7	LREI.**RRYQKSTEL**	14.1 ± 0.3	17 ± 3.5	23 ± 2.2	**44.5 ± 2.6**
8	LREI.**RRYQKSTELLIR**	44.5 ± 3.1	54.2 ± 2.1	62.2 ± 0.8	76.8 ± 1.3
	Mean	**22.5**	**26.8**	**42.1**	**75.9**

528/Asn-575 at all times. A third pattern concerned substrate 2. Again, the highest epitope yield was obtained at the shortest time with Lys-528/Asn-575, and the rate of production was slower than for all other peptides. Significant epitope amounts were also produced with Arg-528/Asn-575 but at a slower rate. The less active enzymes produced the epitope only at the longest digestion times. Finally, substrate 6 generated significant amounts of epitope only with the less active enzyme, Arg-528/Asp-575. With the three other variants, the epitope was detected in very low amounts and only at short times. This pattern was due to the very efficient digestion of substrate 6 by all four variants. However, although the digestion of the epitope precursors was slightly higher with Arg-528/Asp-575 (Fig. 2*A*), the destruction of the natural ligand by this variant was less efficient (Fig. 2*C*). Thus, the generation/destruction balance favored epitope production by the less active variant in this case. Significantly, peptide 6 had, among those in this study, the flanking and P1 residues most susceptible to ERAP1 trimming

FIGURE 2. **Digestion rate of synthetic peptide precursors of HLA-B27 ligands by ERAP1 variants.** *A,* combined digestion (%) of peptide species longer than the natural ligand, excluding the original substrate. It was calculated as: 100% − the combined yield of the corresponding species; *B,* yield of the natural ligand; *C,* yield of peptides shorter than the natural ligand, resulting from destructive cleavages. ♦, Arg-528/Asp-575; ■, Lys-528/Asp-575; ▲, Arg-528/Asn-575; ●, Lys-528/Asn-575. Yields are relative to the total amount of peptide, which was estimated as the added intensity of the ion peaks corresponding to each peptide species in the MALDI-TOF MS spectrum of the digestion mixture. The data are mean ± S.D. of 3–5 experiments. Note that for any given substrate and time point, the value in *A* is essentially accounted for by the added yield of the corresponding ligand and its digestion product(s) in *B* and *C*, respectively.

TABLE 4

HLA-B27 epitope generation by ERAP1 variants

Detection indicates the time (in min) and % yield where the HLA-B27 ligand was detected at ≥1% of the total digestion mixture with the indicated ERAP1 variant. Because peptide 5 did not reach this value with Arg-528/Asp-575, the longest digestion time was assigned. Maximum indicates the earliest time (in min), and the % yield where the HLA-B27 ligand was detected at ≥80% of the maximal value observed with the indicated ERAP1 variant. The data are means ± S.D. of at least three experiments.

		R528/D575				K528/D575				R528/N575				K528/N575			
		Detection		Maximum		Detection		Maximum		Detection		Maximum		Detection		Maximum	
	Peptide	Min	%	Min	%	Min	%	Min	%	Min	%	Min	%	Min	%	Min	%
1	GRHHEAS.**IRLPSQYNF**	5	1 ± 0.1	120	6.6 ± 1	5	2.1 ± 0.2	60	6.7 ± 0.9	15	2 ± 0.1	120	9.2 ± 1.9	5	9.6 ± 0.3	15	13 ± 1.2
2	LGVFRKF.**SRFPEALRL**	180	3.5 ± 0.2	240	6.4 ± 0.8	180	1.3 ± 0.2	240	22.3 ± 3.5	30	3.3 ± 1	180	42.5 ± 2.4	15	1.3 ± 0.5	120	48 ± 0.6
3	NLKARNS.**FRYNGLIHR**	5	4.4 ± 0.4	30	24.7 ± 3.5	5	11.5 ± 0.2	15	22.8 ± 2.0	5	5.5 ± 2.3	15	26.7 ± 3.1	5	34 ± 2.7	5	34 ± 2.7
4	IMYKKRT.**KRLVVFDAR**	15	3.2 ± 0.2	120	5.3 ± 0.5	5	3.7 ± 0.6	60	5 ± 0.7	15	2.2 ± 0.2	180	6.5 ± 0.1	15	6.1 ± 0.6	60	16.3 ± 0.5
5	DVVYAL.**KRQGRTLYGF**	240	0.4 ± 0.1	60	0.4 ± 0.1	180	1.2 ± 0.1	180	1.2 ± 0.1	30	1.1 ± 0.1	120	1.6 ± 0.1	30	1.8 ± 0.2	60	2.6 ± 0.1
6	LYSESL.**ARYGKSPYLY**	5	2.7 ± 0.3	60	28.7 ± 0.4	5	1.9 ± 0.3	15	3 ± 0.9	5	2 ± 0.1	5	2 ± 0.1	5	2.1 ± 0.2	5	2.1 ± 0.2
7	LREI.**RRYQKSTEL**	5	1 ± 0.1	180	32.7 ± 0.2	5	1.1 ± 0.5	120	33 ± 2.8	5	3.1 ± 0.1	120	49.6 ± 2.8	5	27.8 ± 0.2	5	27.8 ± 0.2
8	LREI.**RRYQKSTELLIR**	5	6.9 ± 0.4	5	6.9 ± 0.4	5	3.3 ± 1	60	5.6 ± 1.2	5	5.2 ± 0.2	5	5.2 ± 0.2	5	7.2 ± 1.2	15	9.9 ± 1.4
	MEAN	55.7	2.9	**101.9**	**14.0**	48.8	3.3	**93.8**	**12.5**	13.8	3.1	**93.1**	**17.9**	10.6	11.2	**35.6**	**19.2**

(Table 2). The earliest times at which the natural ligands were detected and their yields at these times also showed significant peptide-to-peptide and variant-dependent differences and reflected the same activity ranking among the four variants (Table 4).

In summary, these results indicate the following. 1) The four ERAP1 variants differ in their enzymatic activity toward peptide substrates with the same ranking as determined with L-AMC. 2) Globally, both the cleavages leading to generation and to destruction of the natural ligands increase with the enzymatic activity. 3) As a result, the mean maximal yield of the HLA-B27 ligands was rather similar for all four variants. 4) Significant differences were observed in the processing of individual substrates, both in the way (rate and yield) in which the same variant processed different substrates and in the way in which different variants processed the same substrate. 5) With only one exception epitope production was significantly higher at shorter times with the most active enzyme, while at longer times the differential epitope destruction by the different variants tended to decrease or even reverse relative epitope yields. 6) In one out of eight substrates analyzed, the generation/destruction balance favored the preferential production of the natural ligand by the less active ERAP1 variant.

Generation of Peptide Length Variants in Vitro—Related natural ligands differing in length by C-terminal extensions are frequent in the HLA-B27 and other MHC-I peptidomes. An example is RRYQKSTEL, a prominent ligand of B*27:05 and other HLA-B27 subtypes (22), and its C-terminally extended variant RRYQKSTELLIR, found in B*27:04 (10) and B*27:05 (Fig. 4). To examine the influence of ERAP1 polymorphism in the generation of these peptides, we digested their N-terminally extended precursors, peptides 7 and 8, and the natural ligands themselves (peptides 9 and 10) with the four ERAP1 variants.

The cumulative digestion of epitope precursors from substrates 7 and 8 was very efficient with all four variants, especially with Arg-528/Asn-575 and Lys-528/Asn-575 (Fig. 2*A*). However, although for substrate 7 digestion of the natural ligand was very inefficient with all but the most active enzyme, destructive cleavages were more prominent on peptide 8 (Fig. 2*C*), as expected from the larger length of RRYQKSTELLIR. Thus, the yield of the shorter epitope RRYQKSTEL was significantly higher than that of RRYQKSTELLIR with all four enzymes (Fig. 2*B*). With the most active variant, the maximal yield of epitope 7 was obtained at short times and decreased later due to further digestion. With the three other variants, the longer epitope was generated at a faster rate, so that at the shortest times (up to 15 min) the yield of the longer ligand (about 3–7%, depending on time and enzyme variant) was comparable or even higher than the yield of the shorter one (about 1–5%).

The direct digestion of the natural ligands, peptides 9 and 10, showed dramatic differences (Fig. 5). RRYQKSTEL showed a significant resistance to ERAP1. At the longest digestion time only the most active variant fully digested the nonamer, whereas with the three other enzymes, about 35–55% of the peptide remained undigested. At shorter times, such as 60 min, as much as 40 – 88% of the ligand remained undigested with any given variant. In contrast, RRYQKSTELLIR was completely degraded by all four variants at 180 min of digestion. It was already fully digested after 15 min by Lys-528/Asp-575 and Arg-528/Asn-575 and about 85% by Lys-528/Asn-575. Only the less active variant, Arg-528/Asp-575, showed a significantly lower degradation rate with this peptide, which nevertheless was much faster than for RRYQKSTEL.

Generation of Peptide Length Variants in Live Cells—We asked to what extent the more efficient generation of RRYQKSTEL, relative to RRYQKSTELLIR, observed *in vitro* might hold in live cells, where other variables can influence the endogenous processing of these peptides. Thus, we examined their recovery in the HLA-B*27:04 and B*27:05 peptidomes isolated from the lymphoid cell lines Wewak I (B*27:04$^+$), C1R-B*27:04, and C1R-B*27:05. The endogenous ERAP1 variants of these cell lines (10) are not identical to any of those used *in vitro*, but ERAP1 in C1R has Arg-528 + Asp-575 and in Wewak I has Arg-528 + Asn-575 (Table 1). The HLA-B27 peptidome isolated from each cell line was fractionated by HPLC, and each fraction was analyzed by MALDI-TOF MS. Each of the peptides was identified by MS/MS sequencing of the corresponding ion peak in the MALDI-TOF spectrum (Fig. 4). The added intensity of the corresponding ion peak in the consecutive HPLC fractions in which the eluted peptide was detected was taken as an

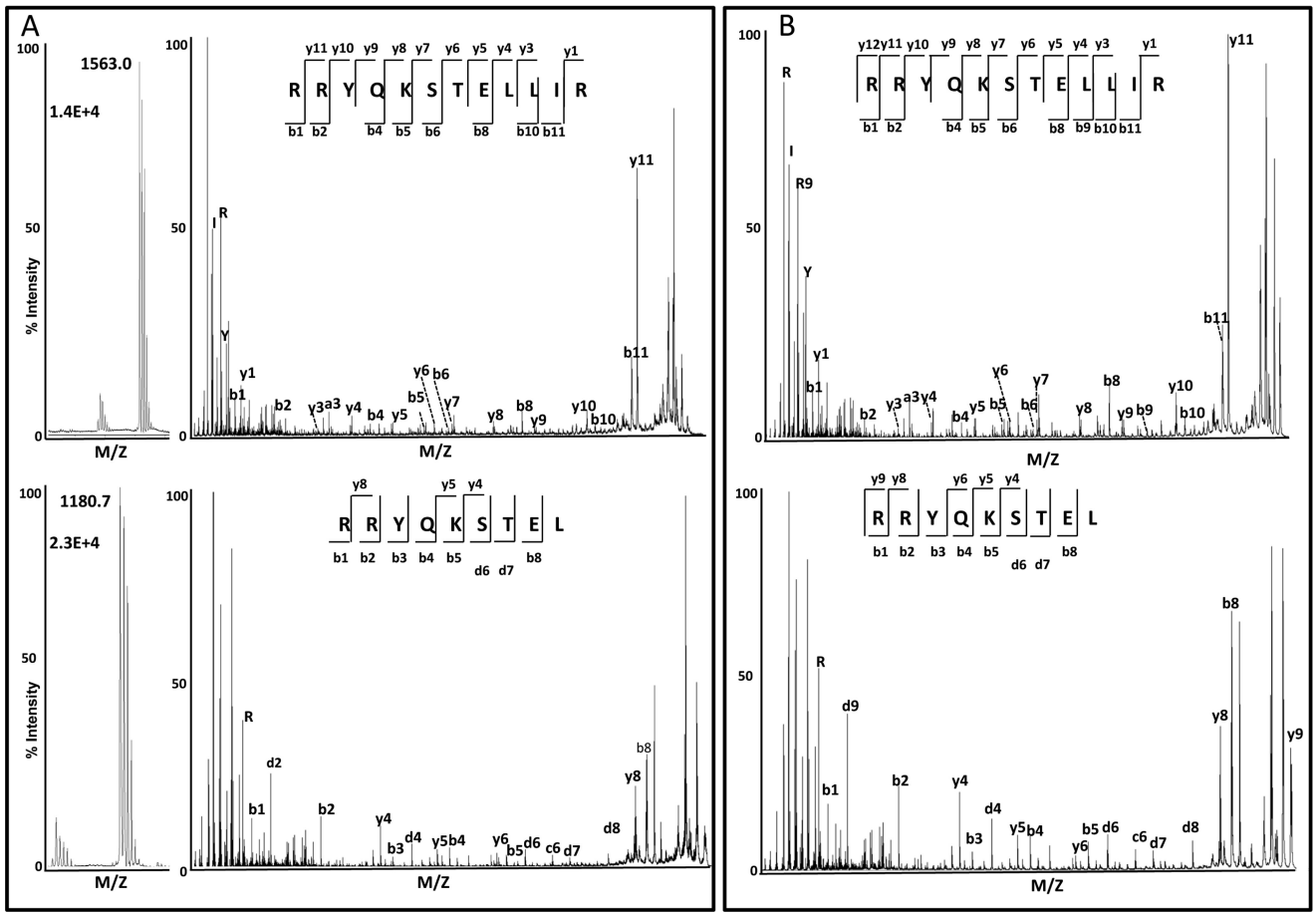

FIGURE 4. **Identification of RRYQKSTELLIR and RRYQKSTEL from C1R-B*27:05 cells.** *A,* MALDI-TOF MS spectra (*left panel*) from the HPLC fractions 150 and 121, respectively, corresponding to the maximum of the elution profile of each peptide during the fractionation of the B*27:05-bound peptide pool. Only the relevant ion peaks are shown. The sequence of both ligands was determined by MALDI-TOF/TOF MS/MS (*right panel*); *B,* MALDI-TOF/TOF MS/MS spectra of the corresponding synthetic peptides.

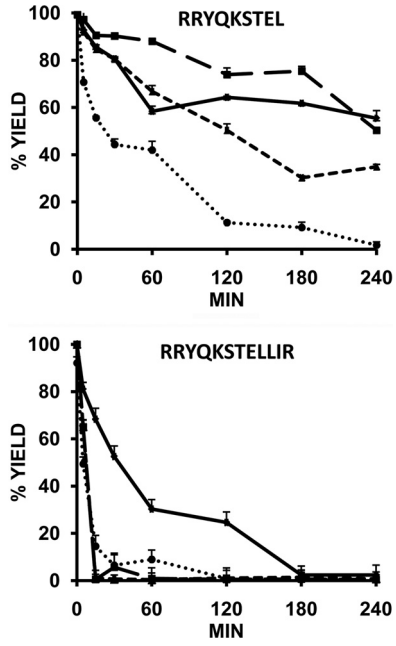

FIGURE 5. **Digestion of two related HLA-B27 ligands of distinct length by ERAP1 variants.** The indicated peptides were digested at an E/S ratio 1:10 (w/w) at various times with the following ERAP1 variants: Arg-528/Asp-575 (◆); Lys-528/Asp-575 (■); Arg-528/Asn-575 (▲); and Lys-528/Asn-575 (●).The data are means ± S.D. of three experiments.

estimation of its abundance. Because of the nonquantitative nature of MALDI-TOF MS, the measurements were carried out in eight independent preparations from C1R-B*27:04, four from Wewak I and three from C1R-B*27:05, and the average intensity of the ion peak corresponding to each of the peptides in all the experiments was calculated for each cell line. The ratio between the average ion peak intensity obtained for the 9- and 12-mer was taken as an estimation of the relative recovery of both peptides in each cell line, and this was compared with the yield of the corresponding peptides upon *in vitro* digestion of their precursors by Arg-528/Asp-575 and Arg-528/Asn-575. The 9-mer was recovered with higher yield than the 12-mer in ratios of about 4–8-fold from the three cell lines. These ratios were very similar to those obtained *in vitro* at 60 min or larger digestion times (Table 5). These results suggest that, despite the many variables that can influence the amount of MHC-I ligands *in vivo*, the generation of RRYQKSTEL and RRYQKSTELLIR by ERAP1 may be a major determinant of their abundance in live cells.

ERAP1 Polymorphism Influences the Competition between Peptidic and Nonpeptidic Substrates—In the following experiments, we examined to what extent the polymorphism at residues 528 and 575 influenced the inhibition of L-AMC hydrolysis by a peptidic substrate. Each ERAP1 variant was incubated

TABLE 5
Generation of length variants of HLA-B27 ligands *in vitro* and in live cells

% Yield from their precursors *in vitro*[a]						
	R528/D575			R528/N575		
Min	RRYQKSTEL	RRYQKSTELLIR	Ratio	RRYQKSTEL	RRYQKSTELLIR	Ratio
5	1.0 ± 0.1	6.9 ± 0.1	0.1	3.1 ± 0.2	5.2 ± 0.1	0.6
15	3.5 ± 0.1	5.3 ± 1.6	0.7	4.8 ± 0.2	6.1 ± 2.1	0.8
30	7.7 ± 1.0	4.9 ± 1.7	1.6	16.9 ± 0.7	5.2 ± 2.0	3.3
60	23.7 ± 0.2	5.2 ± 2.0	**4.5**	39.2 ± 2.3	6.0 ± 1.0	**6.6**
120	22.4 ± 2.1	4.9 ± 1.2	**4.6**	49.6 ± 3.7	5.1 ± 0.5	**9.7**
180	32.7 ± 0.5	6.4 ± 0.8	**5.1**	52.0 ± 0.6	5.1 ± 1.4	**10.2**
240	35.2 ± 3.0	4.8 ± 1.0	**7.3**	48.4 ± 2.2	5.6 ± 1.3	**8.7**

Human cells	Intensity of ion peak[b]		
Cell line	RRYQKSTEL	RRYQKSTELLIR	Ratio
WEWAK I (RN)	31350	4711	**6.7**
C1R-04 (RD)	42867	10258	**4.2**
C1R-05 (RD)	62232	8405	**7.4**

[a] The data are from the digestions of peptides 7 and 8 at the indicated times (Fig. 2*B*) and are means ± S.D. from three (RRYQKSTELLIR) or five (RRYQKSTEL) independent experiments.
[b] The data are means from four (Wewak I), eight (C1R-04), and three (C1R-05) independent preparations, respectively.

with L-AMC in the presence of various concentrations of the natural HLA-B27 ligand RRYQKSTEL (Fig. 6*A*). The peptide inhibited L-AMC hydrolysis with an efficiency that increased with the activity of the variant: the inhibition was lowest for Arg-528/Asp-575, increased for Lys-528/Asp-575, and was highest for Arg-528/Asn-575 and Lys-528/Asn-575. With the latter variant, a decreased inhibition was observed at the highest peptide concentration. Because short peptides that are not further trimmed by ERAP1 allosterically activate the hydrolysis of small nonpeptidic substrates (12, 19, 23), we tested the possibility that the diminished inhibition with Lys-528/Asn-575 was due to an activating effect of the RYQKSTEL octamer, arising from the digestion of the 9-mer. In the presence of 100 μM octamer, L-AMC hydrolysis was particularly activated with this variant (Fig. 6*B*). Accordingly, the highest production of the octamer from 100 μM nonamer in the same conditions as in Fig. 6*A* was obtained with Lys-528/Asn-575 (Fig. 6*C*). These results indicate that, although ERAP1 polymorphism affects the hydrolysis of peptidic and nonpeptidic substrates, peptides compete advantageously in a more active context.

ERAP1 Polymorphism Influences the Inhibition of Peptide Processing by Short Peptides—Because short peptides inhibit the processing of longer substrates (19), we examined whether

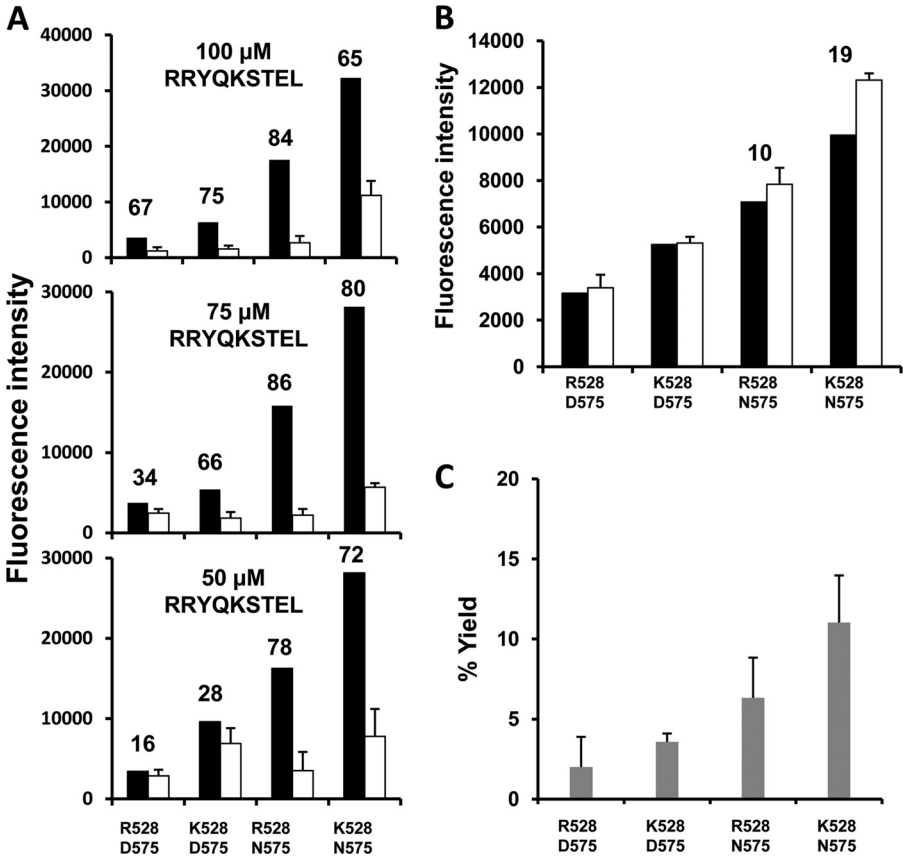

FIGURE 6. **Influence of ERAP1 polymorphism on the inhibition of L-AMC hydrolysis by a natural HLA-B27 ligand.** *A*, L-AMC was incubated at 100 μM concentration, with the indicated ERAP1 variants at an E/S ratio of 1:30 (w/w), in the presence of 100, 75, or 50 μM of RRYQKSTEL for 1 h. The fluorescence intensity of the processed fluorogenic substrate in the absence (*black*) or in the presence of peptide (*white*) is indicated. The figures *above* the histograms indicate the % inhibition of L-AMC hydrolysis. *B*, L-AMC was incubated for 1 h at 100 μM concentration, with the indicated ERAP1 variants, at an E/S ratio of 1:30 (w/w), in the absence (*black*) or in the presence (*white*) of 100 μM of the RYQKSTEL octamer, resulting from the digestion of the nonamer used in *A*. Figures *above* the histogram bars of the most active variants indicate the % activation of L-AMC hydrolysis. *C*, percent yield of RYQKSTEL after incubation of 100 μM RRYQKSTEL with the indicated ERAP1 variants in exactly the same conditions as in *A*. The data are means ± S.D. of three experiments.

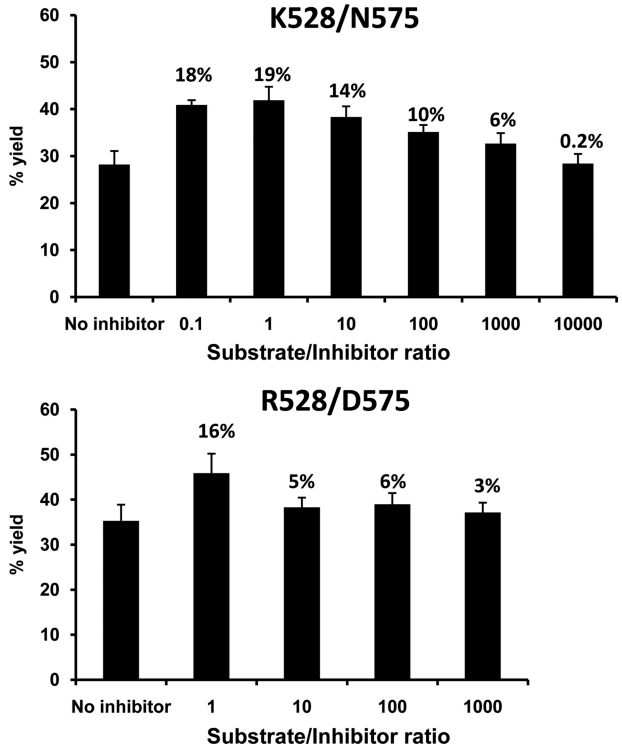

FIGURE 7. **Influence of ERAP1 polymorphism on the inhibition of peptide trimming by a short peptide.** Peptide 6 (LYSELARYGKSPYLY) was incubated with the indicated ERAP1 variants in the presence of various amounts of RYQKSTEL for 4 h at an E/S ratio of 1:10. In each panel, the % yield of the precursor substrate, relative to the total digestion mixture, was plotted for the indicated substrate/inhibitor ratios. The figures *above* the histograms indicate the % inhibition of substrate hydrolysis. The data are means ± S.D. of three experiments.

ERAP1 polymorphism influenced the extent of this inhibition. Peptide 6, a 16-mer that was efficiently processed by all ERAP1 variants (Fig. 2), was tested for the inhibition of its processing in the presence of the RYQKSTEL octamer. The recovery of the precursor substrate after 4 h of digestion by the two ERAP1 variants with the largest activity differences, Arg-528/Asp-575 and Lys-528/Asn-575, was analyzed as a function of the octamer concentration (Fig. 7). At high inhibitor concentration (weight ratio 1:1 or higher), the inhibition was similar (19 and 16%) for both enzymes. However, whereas the inhibition fell almost to background levels (6%), at 10:1 substrate/inhibitor ratio for Arg-528/Asp-575, a 1000:1 ratio was required to reach this level with Lys-528/Asn-575. Thus, as with L-AMC, the octamer inhibited peptide trimming by the most active variant more efficiently than for the less active variant.

DISCUSSION

To assess the contribution of this study to our understanding of the functional ERAP1/B27 interaction in AS, the following three issues must be considered: 1) the influence of ERAP1 polymorphism on the mechanism of peptide trimming; 2) the complexity of natural ERAP1 variants, which usually differ among each other by multiple amino acid residues; and 3) the correspondence of *in vitro* assays with the situation in live cells.

X-ray diffraction studies (19, 20) have virtually confirmed the molecular ruler mechanism of ERAP1 trimming (23), which is dependent on the affinity and length of the substrate and requires a peptide-binding site that is topologically distinct from the catalytic site. A conformational transition, involving global domain movements, is required for optimal enzymatic activity. Thus, ERAP1 polymorphism can influence peptide trimming by affecting the following: 1) the catalytic site or its immediate environment (*i.e.* residue 349); 2) the peptide-binding site and substrate/enzyme interactions (*i.e.* residue 730); and 3) the domain rearrangement. Residue 528 is located at the interdomain II to III region, which is the hinge for the domain rotation taking place during the conformational transition. This probably explains the functional effects of K528R. In contrast, residue 575 is located in a loop of eight residues connecting two β-strands in the middle of domain III, away from interdomain junctions or other functional sites. There are no obvious effects of the D575N mutation on ERAP1 activity that one can infer from just considering its topology. They are not due to changes in the glycosylation pattern, because Asn-575 is not in a consensus glycosylation sequence. Presumably, they are also not due to just an influence on the peptide-binding site, because the mutation also affected the hydrolysis of L-AMC, which binds close to the catalytic site. Thus, it is conceivable that D575N may affect the conformation and/or flexibility of domain III in a way that could alter the conformational transition required for increased activity. This transition induces critical changes in the active site (19, 20), which could explain the observed influence of residue 575 on the hydrolysis of the fluorogenic substrate.

Given the potential of single-residue polymorphisms to alter ERAP1 activity, combined effects among co-occurring mutations in natural variants are very likely. Thus, to understand the role of natural ERAP1 polymorphism *in vivo*, the effect of a mutation must be assessed as a function of its structural context. Only recently has the effect of natural ERAP1 haplotypes on peptide trimming been analyzed in live cells (10, 18, 24). These studies showed that ERAP1 activity depends on the precise combination of amino acid changes in a given variant.

Besides obviating context-dependent effects, previous *in vitro* studies using single mutants (8, 11, 12) cannot be directly generalized to HLA-B27 and to the situation in live cells due to some limitations, which we tried to overcome in our study. Because ERAP1 trimming is strongly dependent on the structure of the substrate (13, 14, 23), extrapolating the effects of ERAP1 polymorphism on other peptides to HLA-B27 ligands is unreliable. Thus, we examined the effect of AS-associated changes on peptide precursors of natural HLA-B27 ligands that were selected for structural diversity, to better assess peptide-dependent effects. Moreover, *in vitro* conditions, using recombinant enzymes and single substrates, differ significantly from those in human cells, where ERAP1 acts in the presence of ERAP2 (25) and of complex peptide pools that may influence ERAP1 activity (12). These considerations do not invalidate *in vitro* approaches but impose a cautious extrapolation and, ideally, a correlation with data from human cells, as done in this study.

The hydrolysis of L-AMC confirmed the lower activity of Arg-528 relative to Lys-528 in a given context, as reported in previous studies (8, 11, 12) and revealed that Asn-575 conferred higher activity compared with Asp-575. Although the magni-

tude of this difference was dependent on residue 528, Asn-575 was more active than Asp-575 in both the Arg-528 and Lys-528 contexts. In contrast, the relative activity of Arg-528 and Lys-528 variants was dependent on residue 575, demonstrating the context-dependent effect of these AS-associated mutations in complex allotypes. The induction of higher activity by D575N in the Arg-528 context was independently observed with natural ERAP1 variants and N-terminally extended precursors of an H-2K^b-restricted epitope (18). D575N is so far unique among the AS-protective mutations in that it enhanced ERAP1 activity, because K528R, R725Q, and Q730E have the opposite effect.

The relative activity of the four ERAP1 variants toward peptide substrates paralleled that with L-AMC when their joint effects over multiple substrates were considered. However, significant peptide-dependent differences were observed, as expected from the strong dependence of ERAP1 on the structure of the substrate.

We previously reported that AS-associated ERAP1 polymorphism induced quantitative differences in the HLA-B27 peptidome from human cells, affecting many peptides expressed in distinct ERAP1 contexts (10). Now we found that epitope amounts, which result from the balance between their generation and destruction, were strongly dependent on both ERAP1 activity and digestion time. Frequently, faster generation of the epitope by the most active variant led to higher yield at shorter times, whereas destructive cleavages tended to equal or decrease epitope yields, relative to less active variants, at long reaction times. This may be relevant to the mechanism of peptide transfer from ERAP1 to the MHC molecule. If ERAP1 would act in close spatial connection with the peptide-loading complex, this could allow a fast transfer of the natural ligand to the MHC, which would protect it from further degradation. This mechanism would be compatible with a protective effect of MHC-I molecules from destructive ERAP-mediated trimming (26), and it would enable the most active variants with an advantage to generate many MHC ligands. Alternatively, if ERAP1 generates a peptide pool in the endoplasmic reticulum that is uncoupled to the peptide-loading mechanism of MHC-I molecules, allowing for a more extensive iteration of substrate trimming, the most active ERAP1 variants would not be necessarily advantageous over less active ones in generating the MHC ligands, as observed in our experiments at long digestion times. This latter alternative explains why a more active ERAP1 variant, with AS-predisposing polymorphisms, reduced the presentation of multiple HLA-B27-restricted ligands, relative to a less active variant expressing multiple AS-protective polymorphisms in a recent study (24). Furthermore, to our knowledge, there is no consistent evidence for any coupling between ERAP1 and the peptide-loading complex of MHC-I that could allow fast peptide transfer to MHC and prevent further epitope degradation.

Given the significant differences between peptide digestion *in vitro* and in live cells, where many different variables may condition the expression level of HLA-B27 ligands, extrapolating our results to the situation *in vivo* must be done with great caution. Yet the close correlation found between the relative yields of RRYQKSTEL and RRYQKSTELLIR, both *in vitro* and in live cells in two distinct ERAP1 contexts, strongly suggests that ERAP1 processing may be a major determinant of the relative amounts of these two ligands *in vivo*. Of note, that this correlation held only at relatively long digestion times further supports that there is no coordinated peptide transfer from ERAP1 to the MHC-I molecule. Instead, ERAP1 presumably generates peptide pools that become available for MHC-I binding in the ER.

That the inhibition of L-AMC hydrolysis by a natural HLA-B27 ligand increased with ERAP1 activity suggests a dominant effect of ERAP1 polymorphism on peptide substrates, relative to small nonpeptidic ones. A likely explanation may be that the conformational transition induced by the peptide substrate to the active state of the enzyme favors peptide hydrolysis over that of a small one. Alternatively, the peptide-induced transition to the closed/active conformation may limit access of L-AMC to the catalytic site to an extent that would depend on the efficiency with which the enzyme is activated upon peptide binding.

It has been suggested that small peptides may unproductively bind in the catalytic site, without inducing the transition to the active state, and block the binding of longer, productive substrates (19). Our study showed that the inhibition of the trimming of a peptide substrate by the octamer product of a natural HLA-B27 ligand depended on the activity of the ERAP1 variant. Thus, ERAP1 polymorphism influences the inhibition of peptide processing by short peptides resulting from the destructive cleavage of natural ligands. Although the competition among peptide substrates, as presumably occurs *in vivo* (12), was not addressed here, our observations show that the influence of ERAP1 polymorphism on peptide trimming has a regulatory component affecting substrate competition, including that mediated by small digestion products.

In conclusion, this study demonstrates that the AS-associated residues 528 and 575 influence ERAP1 function in a mutual context-dependent way, so that the relative activity of variants carrying a given change at one of these positions depends on the polymorphism at the other position. Although for most of the AS-associated polymorphisms the protective alleles (*i.e.* Arg-528, Gln-725, and Glu-730) diminish ERAP1 activity, the protective Asn-575 change had the opposite effect. The various residue combinations at both positions affected the generation and destruction of HLA-B27 ligands in a variant and peptide-dependent way. The resulting effect is both extensive and complex. In some cases, both epitope generation and destruction increased similarly with ERAP1 activity, resulting in little alteration in the final yield of the natural ligand at long digestion times. In these cases the ligand was obtained with highest yield by the most active variant at short digestion times, when generation dominated over destruction. In other cases, relative epitope yields among variants were maintained at all times. Our results support that the mechanism of functional interaction between ERAP1 and HLA-B27 involves a widespread alteration in the balance between generation and destruction of HLA-B27 ligands induced by AS-associated ERAP1 polymorphism. This results in large variant- and peptide-dependent effects on epitope levels and, presumably, in the

generation or not of particular ligands in a given ERAP1 context, consistent with observations in live cells (10).

Thus, the involvement of ERAP1 in the pathogenesis of AS can be envisaged as a far-reaching influence in the shaping of the HLA-B27 peptidome, affecting peptide binding and presentation in quantitative and qualitative ways, depending on the particular combination of polymorphic residues. As shown here and also noted recently (24) some HLA-B27 epitopes are more extensively destroyed by a more active ERAP1 variant, resulting in their higher production in a less active context. However, other epitopes are predominantly generated in a more active one, as shown here (*i.e.* peptides 4 and 8) and in live cells (10).

Besides the obvious effects on antigen presentation, the influence of ERAP1 polymorphism on the peptidome may affect folding and stability of HLA-B27, which also depend on the bound peptides (27). Through its effect on these features, ERAP1 could influence the mechanisms by which HLA-B27 activates the IL23/IL17 axis in spondyloarthropathies, either through misfolding (28) or activation of KIR3DL2$^+$ CD4$^+$ T cells mediated by surface heavy chain homodimers (29), which are generated upon endosomal recycling of HLA-B27 (30). How these features are affected by AS-associated ERAP1 polymorphism is currently a major issue in HLA-B27 research.

Acknowledgments—We thank Dr. Shi-Chung Chang (National Taiwan University) for providing the ERAP1 construct and Sergio Ciordia and Juan P. Albar (Proteomics Facility, Centro Nacional de Biotecnología, Madrid) for help in MS. We also acknowledge our colleagues at the Centro de Biología Molecular Severo, Ochoa Carlos Alvarez-Navarro and Juan J. Cragnolini (currently at Massachusetts Institute of Technology, Cambridge, MA), for help in the generation of recombinant ERAP1 proteins, Noel García-Medel for analytical software, and Jorgina Satrústegui for help in fluorometry.

REFERENCES

1. York, I. A., Chang, S. C., Saric, T., Keys, J. A., Favreau, J. M., Goldberg, A. L., and Rock, K. L. (2002) The ER aminopeptidase ERAP1 enhances or limits antigen presentation by trimming epitopes to 8–9 residues. *Nat. Immunol.* **3,** 1177–1184
2. Saric, T., Chang, S. C., Hattori, A., York, I. A., Markant, S., Rock, K. L., Tsujimoto, M., and Goldberg, A. L. (2002) An IFN-γ-induced aminopeptidase in the ER, ERAP1, trims precursors to MHC class I-presented peptides. *Nat. Immunol.* **3,** 1169–1176
3. Serwold, T., Gonzalez, F., Kim, J., Jacob, R., and Shastri, N. (2002) ERAAP customizes peptides for MHC class I molecules in the endoplasmic reticulum. *Nature* **419,** 480–483
4. Wellcome Trust Case Control Consortium, Australo-Anglo-American Spondylitis Consortium (TASC), Burton, P. R., Clayton, D. G., Cardon, L. R., Craddock, N., Deloukas, P., Duncanson, A., Kwiatkowski, D. P., McCarthy, M. I., Ouwehand, W. H., Samani, N. J., Todd, J. A., Donnelly, P., Barrett, J. C., Davison, D., Easton, D., Evans, D. M., Leung, H. T., Marchini, J. L., Morris, A. P., Spencer, C. C., Tobin, M. D., Attwood, A. P., Boorman, J. P., Cant, B., Everson, U., Hussey, J. M., Jolley, J. D., Knight, A. S., Koch, K., Meech, E., Nutland, S., Prowse, C. V., Stevens, H. E., Taylor, N. C., Walters, G. R., Walker, N. M., Watkins, N. A., Winzer, T., Jones, R. W., McArdle, W. L., Ring, S. M., Strachan, D. P., Pembrey, M., Breen, G., St Clair, D., Caesar, S., Gordon-Smith, K., Jones, L., Fraser, C., Green, E. K., Grozeva, D., Hamshere, M. L., Holmans, P. A., Jones, I. R., Kirov, G., Moskivina, V., Nikolov, I., O'Donovan, M. C., Owen, M. J., Collier, D. A., Elkin, A., Farmer, A., Williamson, R., McGuffin, P., Young, A. H., Ferrier, I. N., Ball, S. G., Balmforth, A. J., Barrett, J. H., Bishop, T. D., Iles, M. M., Maqbool, A., Yuldasheva, N., Hall, A. S., Braund, P. S., Dixon, R. J., Mangino, M., Stevens, S., Thompson, J. R., Bredin, F., Tremelling, M., Parkes, M., Drummond, H., Lees, C. W., Nimmo, E. R., Satsangi, J., Fisher, S. A., Forbes, A., Lewis, C. M., Onnie, C. M., Prescott, N. J., Sanderson, J., Matthew, C. G., Barbour, J., Mohiuddin, M. K., Todhunter, C. E., Mansfield, J. C., Ahmad, T., Cummings, F. R., Jewell, D. P., Webster, J., Brown, M. J., Lathrop, M. G., Connell, J., Dominiczak, A., Marcano, C. A., Burke, B., Dobson, R., Gungadoo, J., Lee, K. L., Munroe, P. B., Newhouse, S. J., Onipinla, A., Wallace, C., Xue, M., Caulfield, M., Farrall, M., Barton, A., Biologics in RA Genetics and Genomics Study Syndicate (BRAGGS) Steering Committee, Bruce, I. N., Donovan, H., Eyre, S., Gilbert, P. D., Hilder, S. L., Hinks, A. M., John, S. L., Potter, C., Silman, A. J., Symmons, D. P., Thomson, W., Worthington, J., Dunger, D. B., Widmer, B., Frayling, T. M., Freathy, R. M., Lango, H., Perry, J. R., Shields, B. M., Weedon, M. N., Hattersley, A. T., Hitman, G. A., Walker, M., Elliott, K. S., Groves, C. J., Lindgren, C. M., Rayner, N. W., Timpson, N. J., Zeggini, E., Newport, M., Sirugo, G., Lyons, E., Vannberg, F., Hill, A. V., Bradbury, L. A., Farrar, C., Pointon, J. J., Wordsworth, P., Brown, M. A., Franklyn, J. A., Heward, J. M., Simmonds, M. J., Gough, S. C., Seal, S.; Breast Cancer Susceptibility Collaboration (UK), Stratton, M. R., Rahman, N., Ban, M., Goris, A., Sawcer, S. J., Compston, A., Conway, D., Jallow, M., Newport, M., Sirugo, G., Rockett, K. A., Bumpstead, S. J., Chaney, A., Downes, K., Ghori, M. J., Gwilliam, R., Hunt, S. E., Inouye, M., Keniry, A., King, E., McGinnis, R., Potter, S., Ravindrarajah, R., Whittaker, P., Widden, C., Withers, D., Cardin, N. J., Davison, D., Ferreira, T., Pereira-Gale, J., Hallgrimsdo'ttir, I. B., Howie, B. N., Su, Z., Teo, Y. Y., Vukcevic, D., Bentley, D., Brown, M. A., Compston, A., Farrall, M., Hall, A. S., Hattersley, A. T., Hill, A. V., Parkes, M., Pembrey, M., Stratton, M. R., Mitchell, S. L., Newby, P. R., Brand, O. J., Carr-Smith, J., Pearce, S. H., McGinnis, R., Keniry, A., Deloukas, P., Reveille, J. D., Zhou, X., Sims, A. M., Dowling, A., Taylor, J., Doan, T., Davis, J. C., Savage, L., Ward, M. M., Learch, T. L., Weisman, M. H., and Brown, M. (2007) Association scan of 14,500 nonsynonymous SNPs in four diseases identifies autoimmunity variants. *Nat. Genet.* **39,** 1329–1337
5. Harvey, D., Pointon, J. J., Evans, D. M., Karaderi, T., Farrar, C., Appleton, L. H., Sturrock, R. D., Stone, M. A., Oppermann, U., Brown, M. A., and Wordsworth, B. P. (2009) Investigating the genetic association between ERAP1 and ankylosing spondylitis. *Hum. Mol. Genet.* **18,** 4204–4212
6. Brewerton, D. A., Hart, F. D., Nicholls, A., Caffrey, M., James, D. C., and Sturrock, R. D. (1973) Ankylosing spondylitis and HL-A 27. *Lancet* **1,** 904–907
7. Schlosstein, L., Terasaki, P. I., Bluestone, R., and Pearson, C. M. (1973) High association of an HL-A antigen, W27, with ankylosing spondylitis. *N. Engl. J. Med.* **288,** 704–706
8. Evans, D. M., Spencer, C. C., Pointon, J. J., Su, Z., Harvey, D., Kochan, G., Oppermann, U., Opperman, U., Dilthey, A., Pirinen, M., Stone, M. A., Appleton, L., Moutsianas, L., Moutsianis, L., Leslie, S., Wordsworth, T., Kenna, T. J., Karaderi, T., Thomas, G. P., Ward, M. M., Weisman, M. H., Farrar, C., Bradbury, L. A., Danoy, P., Inman, R. D., Maksymowych, W., Gladman, D., Rahman, P., Spondyloarthritis Research Consortium of Canada (SPARCC), Morgan, A., Marzo-Ortega, H., Bowness, P., Gaffney, K., Gaston, J. S., Smith, M., Bruges-Armas, J., Couto, A. R., Sorrentino, R., Paladini, F., Ferreira, M. A., Xu, H., Liu, Y., Jiang, L., Lopez-Larrea, C., Díaz-Peña, R., López-Vázquez, A., Zayats, T., Band, G., Bellenguez, C., Blackburn, H., Blackwell, J. M., Bramon, E., Bumpstead, J. S., Casas, J. P., Corvin, A., Craddock, N., Deloukas, P., Dronov, S., Duncanson, A., Edkins, S., Freeman, C., Gillman, M., Gray, E., Gwilliam, R., Hammond, N., Hunt, S. E., Jankowski, J., Jayakumar, A., Langford, C., Liddle, J., Markus, H. S., Mathew, C. G., McCann, O. T., McCarthy, M. I., Palmer, C. N., Peltonen, L., Plomin, R., Potter, S. C., Rautanen, A., Ravindrarajah, R., Ricketts, M., Samani, N., Sawcer, S. J., Strange, A., Trembath, R. C., Viswanathan, A. C., Waller, M., Weston, P., Whittaker, P., Widaa, S., Wood, N. W., McVean, G., Reveille, J. D., Wordsworth, B. P., Brown, M. A., Donnelly, P., Australo-Anglo-American Spondyloarthritis Consortium (TASC), Wellcome Trust Case Control Consortium 2 (WTCCC2) (2011) Interaction between ERAP1 and HLA-B27 in ankylosing spondylitis implicates peptide handling in the mechanism for HLA-B27 in disease susceptibility. *Nat. Genet.* **43,** 761–767

9. Wang, C. M., Ho, H. H., Chang, S. W., Wu, Y. J., Lin, J. C., Chang, P. Y., Wu, J., and Chen, J. Y. (2012) ERAP1 genetic variations associated with HLA-B27 interaction and disease severity of syndesmophytes formation in Taiwanese ankylosing spondylitis. *Arthritis Res. Ther.* **14,** R125
10. García-Medel, N., Sanz-Bravo, A., Van Nguyen, D., Galocha, B., Gómez-Molina, P., Martín-Esteban, A., Alvarez-Navarro, C., and de Castro, J. A. (2012) Functional interaction of the ankylosing spondylitis-associated endoplasmic reticulum aminopeptidase 1 polymorphism and HLA-B27 *in vivo*. *Mol. Cell. Proteomics* **11,** 1416–1429
11. Goto, Y., Hattori, A., Ishii, Y., and Tsujimoto, M. (2006) Reduced activity of the hypertension-associated Lys528Arg mutant of human adipocyte-derived leucine aminopeptidase (A-LAP)/ER-aminopeptidase-1. *FEBS Lett.* **580,** 1833–1838
12. Evnouchidou, I., Kamal, R. P., Seregin, S. S., Goto, Y., Tsujimoto, M., Hattori, A., Voulgari, P. V., Drosos, A. A., Amalfitano, A., York, I. A., and Stratikos, E. (2011) Cutting Edge: Coding single nucleotide polymorphisms of endoplasmic reticulum aminopeptidase 1 can affect antigenic peptide generation in vitro by influencing basic enzymatic properties of the enzyme. *J. Immunol.* **186,** 1909–1913
13. Hearn, A., York, I. A., and Rock, K. L. (2009)) The specificity of trimming of MHC class I-presented peptides in the endoplasmic reticulum. *J. Immunol.* **183,** 5526–5536
14. Evnouchidou, I., Momburg, F., Papakyriakou, A., Chroni, A., Leondiadis, L., Chang, S. C., Goldberg, A. L., and Stratikos, E. (2008.) The internal sequence of the peptide-substrate determines its N-terminus trimming by ERAP1. *PLoS ONE* **3,** e3658
15. Maksymowych, W. P., Inman, R. D., Gladman, D. D., Reeve, J. P., Pope, A., and Rahman, P. (2009)) Association of a specific ERAP1/ARTS1 haplotype with disease susceptibility in ankylosing spondylitis. *Arthritis Rheum.* **60,** 1317–1323
16. Choi, C. B., Kim, T. H., Jun, J. B., Lee, H. S., Shim, S. C., Lee, B., Pope, A., Uddin, M., Rahman, P., and Inman, R. D. (2010)) ARTS1 polymorphisms are associated with ankylosing spondylitis in Koreans. *Ann. Rheum. Dis.* **69,** 582–584
17. Szczypiorska, M., Sánchez, A., Bartolomé, N., Arteta, D., Sanz, J., Brito, E., Fernández, P., Collantes, E., Martínez, A., Tejedor, D., Artieda, M., and Mulero, J. (2011)) ERAP1 polymorphisms and haplotypes are associated with ankylosing spondylitis susceptibility and functional severity in a Spanish population. *Rheumatology* **50,** 1969–1975
18. Reeves, E., Edwards, C. J., Elliott, T., and James, E. (2013) Naturally occurring ERAP1 haplotypes encode functionally distinct alleles with fine substrate specificity. *J. Immunol.* **191,** 35–43
19. Nguyen, T. T., Chang, S. C., Evnouchidou, I., York, I. A., Zikos, C., Rock, K. L., Goldberg, A. L., Stratikos, E., and Stern, L. J. (2011) Structural basis for antigenic peptide precursor processing by the endoplasmic reticulum aminopeptidase ERAP1. *Nat. Struct. Mol. Biol.* **18,** 604–613
20. Kochan, G., Krojer, T., Harvey, D., Fischer, R., Chen, L., Vollmar, M., von Delft, F., Kavanagh, K. L., Brown, M. A., Bowness, P., Wordsworth, P., Kessler, B. M., and Oppermann, U. (2011) Crystal structures of the endoplasmic reticulum aminopeptidase-1 (ERAP1) reveal the molecular basis for N-terminal peptide trimming. *Proc. Natl. Acad. Sci. U.S.A.* **108,** 7745–7750
21. Cragnolini, J. J., García-Medel, N., and Lopez de Castro, J. A. (2009) Endogenous processing and presentation of T-cell epitopes from *Chlamydia trachomatis* with relevance in HLA-B27-associated reactive arthritis. *Mol. Cell. Proteomics* **8,** 1850–1859
22. Lopez de Castro, J. A., Alvarez, I., Marcilla, M., Paradela, A., Ramos, M., Sesma, L., and Vázquez, M. (2004) HLA-B27: a registry of constitutive peptide ligands. *Tissue Antigens* **63,** 424–445
23. Chang, S. C., Momburg, F., Bhutani, N., and Goldberg, A. L. (2005) The ER aminopeptidase, ERAP1, trims precursors to lengths of MHC class I peptides by a "molecular ruler" mechanism. *Proc. Natl. Acad. Sci. U.S.A.* **102,** 17107–17112
24. Seregin, S. S., Rastall, D. P., Evnouchidou, I., Aylsworth, C. F., Quiroga, D., Kamal, R. P., Godbehere-Roosa, S., Blum, C. F., York, I. A., Stratikos, E., and Amalfitano, A. (2013) Endoplasmic reticulum aminopeptidase-1 alleles associated with increased risk of ankylosing spondylitis reduce HLA-B27 mediated presentation of multiple antigens. *Autoimmunity* **46,** 497–508
25. Saveanu, L., Carroll, O., Lindo, V., Del Val, M., Lopez, D., Lepelletier, Y., Greer, F., Schomburg, L., Fruci, D., Niedermann, G., and van Endert, P. M. (2005) Concerted peptide trimming by human ERAP1 and ERAP2 aminopeptidase complexes in the endoplasmic reticulum. *Nat. Immunol.* **6,** 689–697
26. Kanaseki, T., Blanchard, N., Hammer, G. E., Gonzalez, F., and Shastri, N. (2006) ERAAP synergizes with MHC class I molecules to make the final cut in the antigenic peptide precursors in the endoplasmic reticulum. *Immunity* **25,** 795–806
27. Marcilla, M., and López de Castro, J. A. (2008) Peptides: the cornerstone of HLA-B27 biology and pathogenetic role in spondyloarthritis. *Tissue Antigens* **71,** 495–506
28. DeLay, M. L., Turner, M. J., Klenk, E. I., Smith, J. A., Sowders, D. P., and Colbert, R. A. (2009) HLA-B27 misfolding and the unfolded protein response augment interleukin-23 production and are associated with Th17 activation in transgenic rats. *Arthritis Rheum.* **60,** 2633–2643
29. Bowness, P., Ridley, A., Shaw, J., Chan, A. T., Wong-Baeza, I., Fleming, M., Cummings, F., McMichael, A., and Kollnberger, S. (2011) Th17 cells expressing KIR3DL2+ and responsive to HLA-B27 homodimers are increased in ankylosing spondylitis. *J. Immunol.* **186,** 2672–2680
30. Bird, L. A., Peh, C. A., Kollnberger, S., Elliott, T., McMichael, A. J., and Bowness, P. (2003) Lymphoblastoid cells express HLA-B27 homodimers both intracellularly and at the cell surface following endosomal recycling. *Eur. J. Immunol.* **33,** 748–759

ARTHRITIS & RHEUMATOLOGY
Vol. 68, No. 10, October 2016, pp 2466–2475
DOI 10.1002/art.39734

Functional Interaction of the Ankylosing Spondylitis–Associated Endoplasmic Reticulum Aminopeptidase 2 With the HLA–B*27 Peptidome in Human Cells

Adrian Martín-Esteban,[1] Pablo Guasp,[1] Eilon Barnea,[2] Arie Admon,[2] and José A. López de Castro[1]

Objective. **To determine the influence of endoplasmic reticulum aminopeptidase 2 (ERAP-2) expression on the HLA–B*27 peptidome in live cells.**

Methods. **Using immunoaffinity chromatography and acid extraction, HLA–B*27:05–bound peptides were isolated from 2 ERAP-2–negative lymphoblastoid cell lines and 1 ERAP-2–positive lymphoblastoid cell line expressing functionally indistinguishable ERAP-1 variants. More than 2,000–4,000 B*27:05 ligands were identified from each cell line, and their relative abundance was established by quantitative tandem mass spectrometry and MaxQuant-based peptide analyses. Pairwise comparisons were used to determine the structural features of peptides whose relative abundance was dependent on the presence of ERAP-2. Synthetic peptide digestions were performed with recombinant ERAP-1 and ERAP-2. Peptide affinity was estimated with standard algorithms.**

Results. **The B*27:05 peptidome from ERAP-2–positive cells showed 3–4% fewer peptides with N-terminal basic residues than did the peptidome from ERAP-2–negative cells. Among the shared peptides, those most abundant in the presence of ERAP-2 included more nonamers, fewer decamers, and fewer N-terminal basic residues than the peptides predominant in ERAP-2–negative cells. These ERAP-2–dependent changes did not alter the global affinity of the B*27:05 peptidome.**

Conclusion. **ERAP-2 significantly influences the B*27:05-bound peptidome by destroying some ligands and decreasing the abundance of many more ligands with N-terminal basic residues, while increasing the abundance of nonamers. The former effects are best explained by direct ERAP-2 trimming. The effects on peptide length might be attributed to ERAP-2–induced activation of ERAP-1 trimming. These data support the notion of a peptide-mediated mechanism as the basis for the association of ERAP-2 with ankylosing spondylitis. Analogous effects on other major histocompatibility complex class I peptidomes might explain the involvement of ERAP-2 in HLA–B27–negative spondyloarthritis.**

The final steps of the antigen-processing pathway of major histocompatibility complex (MHC) class I molecules take place in the endoplasmic reticulum (ER). The peptides reaching this compartment are often longer than those optimal for MHC class I binding (1). In humans, the final cut of MHC class I ligands is carried out by 2 related ER aminopeptidases (ERAPs), ERAP-1 and ERAP-2 (2–5), which differ in N-terminal trimming specificity and substrate handling. Another enzyme from the same family, insulin-regulated aminopeptidase, is involved in antigen cross-presentation in dendritic cells (6,7). ERAP-1 cleaves virtually all N-terminal residues, except Pro, with preference for those that are hydrophobic (8). ERAP-2 preferentially cleaves basic residues (3,5,9,10). Moreover, ERAP-1 is essentially unable to digest peptides shorter than nonamers

Supported by the Binational Science Foundation (grant 2009393 to Dr. Admon), the Plan Nacional de I+D+i (grant SAF2014/51931-R to Dr. López de Castro), and an institutional grant from the Fundación Ramón Areces to the Centro de Biología Molecular Severo Ochoa. Mr. Martín-Esteban and Mr. Guasp are fellows of the Spanish Government (grants BES-2012-052113 and BES-2015-072729, respectively).

[1]Adrian Martín-Esteban, MSc, Pablo Guasp, MSc, José A. López de Castro, PhD: Centro de Biología Molecular Severo Ochoa (Consejo Superior de Investigaciones Científicas and Universidad Autónoma), Madrid, Spain; [2]Eilon Barnea, PhD, Arie Admon, PhD: Technion-Israel Institute of Technology, Haifa, Israel.

Address correspondence to José A. López de Castro, PhD, Centro de Biología Molecular Severo Ochoa, Nicolás Cabrera, N. 1, Universidad Autónoma, 28049 Madrid, Spain. E-mail: aldecastro@cbm.csic.es.

Submitted for publication November 24, 2015; accepted in revised form April 21, 2016.

(11). In contrast, ERAP-2 optimally cleaves peptides of 7–8 residues, quickly becoming less efficient with larger substrates (12). Finally, although the peptide sequence downstream of the N-terminus seems to influence substrate binding and the trimming rate for both enzymes, this influence is better characterized and apparently higher for ERAP-1 (12,13).

The formation of ERAP-1/ERAP-2 heterodimers in the ER allows these enzymes to process substrates in a concerted manner, at rates higher than the rates of additive trimming by each enzyme separately (5). In vitro studies suggest that the physical interaction of both enzymes induces allosteric changes in ERAP-1 that increase its enzymatic activity and substrate-binding affinity (14). Thus, the role of ERAP-2 on MHC class I–bound peptidomes might go beyond its particular residue specificity to improve ERAP-1–mediated processing.

A frequent polymorphism in the coding region, N392K, defined by the single-nucleotide polymorphism (SNP) rs2549782, affects ERAP-2 activity and specificity (15). The allele coding for N392 is in tight linkage disequilibrium with a mutation, defined by the SNP rs2248374, that impairs ERAP-2 expression in most individuals carrying this allele (16).

ERAP-1 is the main non-MHC susceptibility gene for ankylosing spondylitis (AS) and shows epistasis with HLA–B*27 (17,18), suggesting that peptides are involved in this disease. Although the association of ERAP-2 with AS was revealed in genome-wide association and family studies (19), linkage disequilibrium impaired its unequivocal distinction from ERAP-1 in HLA–B*27–positive individuals. Recent studies, which were controlled for the association of ERAP-1, determined that ERAP-2 is associated with AS both in HLA–B*27–positive and in HLA–B*27–negative disease. Specifically, polymorphisms leading to loss of protein expression were protective (20,21).

In spite of multiple studies on ERAP-2, its actual contribution to shaping MHC class I–bound peptidomes has not been directly examined. Indirect analyses have produced contradictory findings, to some extent. For instance, in one study (16), absence of ERAP-2 was found to result in reduced MHC class I surface expression, suggesting that ERAP-2 makes a substantial contribution to the generation of an optimal peptidome. In contrast, the similar expression of HLA–B*27 in cells from ERAAP$^{-/-}$ mice, which lack an ERAP-2 ortholog, and in ERAP-1–knockout human cells was taken as evidence for a minor role of ERAP-2 (22).

In this study, we used comparative peptidome analyses to determine the effect of ERAP-2 on the HLA–B*27:05 peptidome. To our knowledge, the current results are the first to show the nature and extent of the influence of ERAP-2 expression on the peptidome of a human MHC class I molecule in living cells, providing a basis for the association of ERAP-2 with AS.

MATERIALS AND METHODS

Cell lines. The human lymphoblastoid cell lines (LCLs) 10151 (HLA–A*02, *31; B*27:05, *15; C*02, *03), 15510 (HLA–A*01, 11; B*27:05, *37; C*01, *06), and 6370 (HLA–A*02, *68; B*27:05, *44; C*02, *07) were kindly provided by Dr. Maxime Breban (Paris, France). These cell lines were established from patients with AS and have been used in a previous study (23). All 3 donors were homozygous for the ERAP-1 rs17482078/rs10050860/rs30187 haplotype associated with increased susceptibility to AS. Two of the donors (LCLs 10151 and 15510) were homozygous for the AS-protective ERAP-2 haplotype rs2549782/rs2248374, whereas the other donor (LCL 6370) was heterozygous for these polymorphisms. The cells were cultured in RPMI 1640 medium, 10% fetal bovine serum (Biowest), 25 m*M* HEPES buffer, 2 m*M* L-glutamine, penicillin, and streptomycin.

Western blotting and genotyping. Expression of ERAP-1 and ERAP-2 was assessed by Western blotting with 6H9 and 3F5 monoclonal antibodies (mAb) (R&D Systems), respectively, and γ-tubulin expression was assessed using GTU mAb (Sigma-Aldrich), as described previously (24). The immunoblots were scanned and quantified using TINA 2.09e software (Raystet Isotopenmessgeräte).

Full genomic sequencing of the ERAP-1 variants was carried out in the following manner. Use of the Custom GeneReadPanel CNGHS-00361X GeneGlobe (Qiagen) provided a complete coverage of target sequences. Libraries were prepared using polymerase chain reaction (PCR) amplification followed by addition of Illumina adapters and sample tags, as indicated by the manufacturer. The libraries were pooled, purified, and titrated by quantitative PCR, followed by paired-end sequencing in an Illumina MiSeq instrument and data analysis using Illumina BaseSpace-integrated software. In addition, the exons, including the nonsynonymous AS-associated SNP in ERAP-1 and ERAP-2 (Table 1), were sequenced as described previously (24).

Recombinant ERAP-1 variants and in vitro digestions. The recombinant ERAP-1 protein expressed in LCLs 10151 and 6370 (UniProtKB accession no. Q9NZ08) was obtained from JSL cells, another LCL that also expresses this variant (24,25). The recombinant ERAP-1 mutant R127P and the ERAP-2 variant identical to that in LCL 6370 were obtained from the corresponding baculoviruses (generously provided by Dr. E. Stratikos) generated at the Protein Chemistry Facility of the Greek National Center for Scientific Research Demokritos (Athens, Greece). Peptide digestions involving only ERAP-1 variants were performed as described previously (25). Those involving ERAP-1 in the presence or absence of ERAP-2 were performed in a similar way, except that the enzymes were kept, and digestions were performed, in 50 m*M* HEPES buffer, 100 m*M* NaCl, pH 7.0. The enzyme-to-substrate ratio was 1:10 for both ERAP-1 and ERAP-2. The ERAP-1–to–ERAP-2 ratio used was 1:1.

Table 1. ERAP-1 and ERAP-2 variants in HLA–B*27:05–positive cell lines*

Enzyme, nucleotide/ amino acid position	SNP	Exon number	Change in coding strand		
			LCL 10151	LCL 15510	LCL 6370
ERAP-1					
380/127	rs26653	2	g/R	c/P	g/R
828/276	rs26618	5	a/I	a/I	a/I
1037/346	rs27895	6	g/G	g/G	g/G
1045/349	rs2287987	6	a/M	a/M	a/M
1583/528	rs30187	11	a/K	a/K	a/K
1723/575	rs10050860	12	g/D	g/D	g/D
2174/725	rs17482078	15	g/R	g/R	g/R
2188/730	rs27044	15	c/Q	c/Q	c/Q
ERAP-2			ERAP-2 (−)	ERAP-2 (−)	ERAP-2 (+)
1176/392	rs2549782	7	t/N	t/N	tg/NK

* Nucleotide/amino acid residue numbering is from human endoplasmic reticulum aminopeptidase 1 (ERAP-1) isoform 2 (UniProt/Swiss-Prot database accession no. Q9NZ08-2) and ERAP-2 isoform 1 (UniProt/Swiss-Prot database accession no. Q6P179-1). All polymorphic positions were determined by genomic sequencing. Other positions were identical in all 3 variants, except for a T12I amino acid change (nucleotide change C35T) in the ERAP-1 variant from lymphoblastoid cell line (LCL) 15510. The single-letter code for amino acids is used. SNP = single-nucleotide polymorphism.

Isolation of HLA–B*27–bound peptidomes. HLA–B*27–bound peptidomes were isolated from 2×10^9 cells in a manner essentially as described previously (25). Briefly, the cells were lysed in 150 m*M* NaCl, 20 m*M* Tris HCl, pH 7.5, 1% Igepal CA-630 (Sigma-Aldrich), and a mixture of protease inhibitors (Roche). B*27–peptide complexes were immunopurified with ME1 mAb (26). The peptides were eluted with 1% trifluoroacetic acid (Sigma-Aldrich) and filtered through a Vivaspin-2 concentrator (with a cutoff value of 5,000 daltons; Sartoriuos Stedim Biotech), and LCL 15510 was subjected to reverse-phase high-performance liquid chromatography (HPLC) (27). For each cell line, 3 preparations were independently obtained from the same cell amounts and analyzed separately.

Mass spectrometry (MS) and data analysis. MS analyses were carried out as previously described (25). Briefly, the samples were analyzed in a Q-Exactive Plus mass spectrometer fitted with an UltiMate 3000 Rapid Separation Liquid Chromatography nanocapillary ultrafast HPLC system (Thermo Fisher Scientific). The peptides were resolved using a 7–40% acetonitrile gradient with 0.1% formic acid for 180 minutes at a flow rate of 0.15 μl/minute. The dynamic exclusion was set to 20 seconds. The selected masses were fragmented from the survey scan, with a mass-to-charge (m/z) ratio of 300–1,800 at a resolution of 70,000. Tandem MS (MS/MS) spectra were acquired starting at an m/z ratio of 200 with a resolution of 17,500. The target value was set to 1×10^5 and the isolation window to 1.8 m/z. The maximum injection time was set to 100 msec, and the normalized collision energy was set to 25 eV. Peptide sequences were assigned using MaxQuant software (version 1.4.1.2) (28) with the Andromeda search engine (29) and the human UniProt/Swiss-Prot database (release 2014_02, with 20,270 entries) under the following parameters: precursor ion mass and fragment mass tolerance of 20 parts per million, false discovery rate (FDR) of 0.01, and peptide-spectrum matching FDR of 0.05. Met oxidation was included as a variable modification. Identifications derived from the reverse database and known contaminants were eliminated.

Binding affinity of B*27:05 ligands. The binding affinity of the B*27:05 ligands was calculated using a Net MHCcons 1.1 Server (available at http://www.cbs.dtu.dk/services/NetMHCcons/). This system integrates 3 different algorithms, as described elsewhere (30).

Statistical analysis. Differences in peptide or residue frequencies were analyzed by chi-square test with Bonferroni correction, when applicable, and MHC binding affinity was compared by Mann-Whitney U test. Data from other experiments were analyzed with Student's *t*-test. *P* values less than 0.05 were considered significant.

RESULTS

ERAP-1 and ERAP-2 variants in B*27:05-positive cells. LCLs 15510, 10151, and 6370 expressed similar levels of ERAP-1, but only LCL 6370 expressed ERAP-2 (Figures 1A and B). The other 2 cell lines had the ERAP-2 allotype with N392, which explains the absence of this protein. Expression of ERAP-2 by LCL 6370 can be attributed to heterozygosity at position 392, corresponding to the K392 variant.

The ERAP-1 variant in LCL 15510 differed from that in the other 2 cell lines in that it contained T12I and R127P mutations (Table 1). The presence of these mutations did not affect ERAP-1 activity, as has been observed previously (31) and as was indicated by the in vitro digestion of 3 synthetic B*27:05 ligands by ERAP-1 variants (see Supplementary Figure 1, available on the *Arthritis & Rheumatology* web site at http://onlinelibrary.wiley.com/doi/10.1002/art.39734/abstract).

Decreased percentages of B*27:05 ligands with N-terminal basic residues in the presence of ERAP-2. The pools of B*27:05-bound peptides isolated from each cell line were subjected to MS/MS analysis in biologic triplicate experiments. The peptides identified as

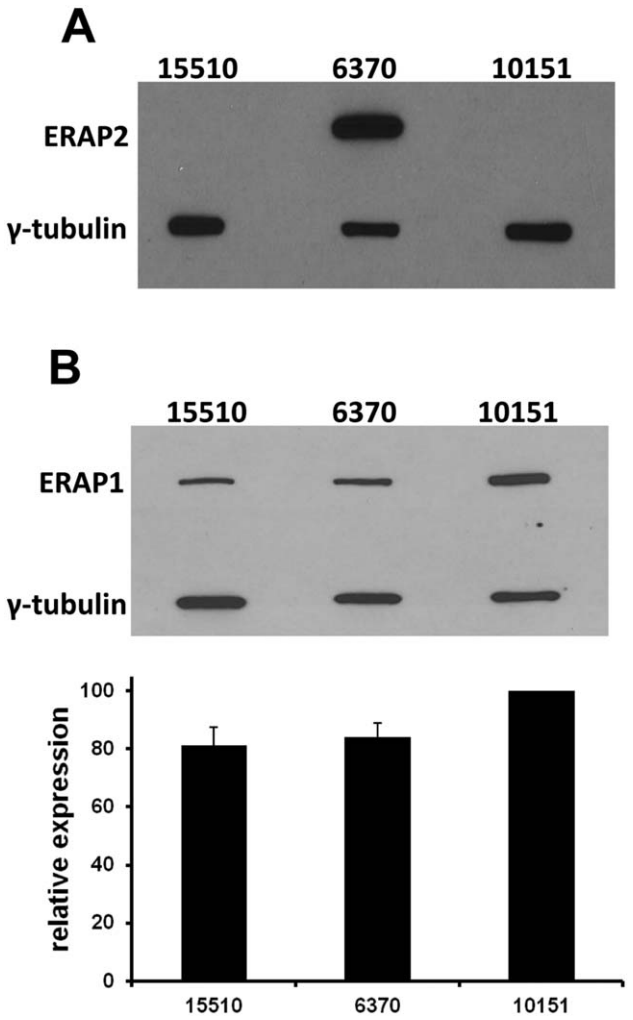

Figure 1. Western blot analysis of endoplasmic reticulum aminopeptidase 1 (ERAP-1) and ERAP-2 protein expression. **A** and **B** (top), Expression of ERAP-2 proteins **(A)** and ERAP-1 proteins **(B)** was assessed by Western blotting in human lymphoblastoid cell lines (LCLs) 15510, 6370, and 10151, with γ-tubulin used as the loading control. Representative results are shown. **B** (bottom), The amount of ERAP-1 was determined relative to the LCL with the highest expression of the enzyme. Results are the mean ± SD of 3 independent analyses. Differences between the cell lines were not statistically significant.

having 8–14 residues and the Arg_2/Gln_2 motif of HLA–B*27 were selected for further analyses. A total of 4,771 peptides, 3,379 peptides, and 2,623 peptides with these features were identified in LCLs 10151, 15510, and 6370, respectively (the complete table of peptides is available upon request from the corresponding author). The molecular weight (MW) distribution of the total peptides showed no differences among the 3 cell lines (see Supplementary Figure 2A, available on the *Arthritis & Rheumatology* web site at http://onlinelibrary.wiley.com/doi/10.1002/art.39734/abstract).

The higher percentage of nonamers in LCL 6370, relative to LCL 10151, was comparable to that among the ERAP-2–negative LCLs 10151 and 15510 (see Supplementary Figure 2B) and could not be attributed to the presence of ERAP-2. In contrast, the percentage of peptides with N-terminal Arg or Lys was lower in LCL 6370 than in LCLs 10151 and 15510, whereas the difference in the percentages of these peptides between the 2 ERAP-2–negative cell lines was not statistically significant (Figure 2). This finding indicates that cell-to-cell differences unrelated to the presence of ERAP-2 do not account for the variation in the percentages of N-terminal Arg and Lys observed in the ERAP-2–positive cell line when compared to the 2 unrelated ERAP-2–negative cell lines. Thus, our results strongly suggest that ERAP-2 destroys ~3–4% of the B*27:05 ligands with N-terminal basic residues expressed in ERAP-2–negative cells.

Decreases in the MW and length of B*27:05 ligands with quantitative expression differences in the presence of ERAP-2. To address the influence of ERAP-2 on the relative amounts of B*27:05 ligands expressed both in the presence and in the absence of the enzyme, we carried out the following pairwise comparisons of the B*27:05 peptidomes: LCL 10151 versus LCL 15510, LCL 10151 versus LCL 6370, and LCL 15510 versus LCL 6370. The first pairwise comparison allowed us to assess ERAP-2–independent cell-to-cell variability on a functionally equivalent ERAP-1 background in the absence of ERAP-2, while the latter 2 pairwise

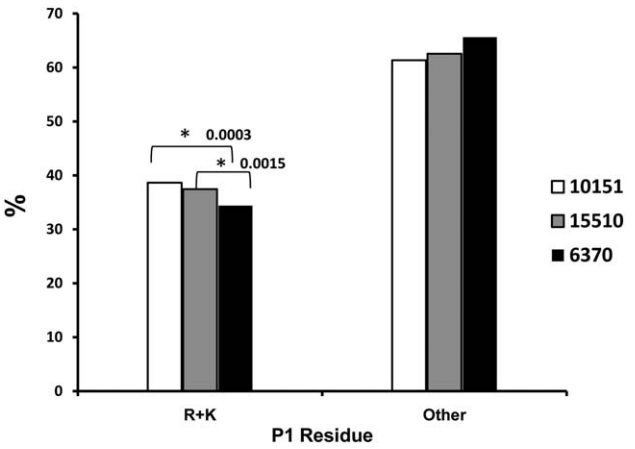

Figure 2. Percentage of peptides with N-terminal basic residues (R + K) or other residues in lymphoblastoid cell lines (LCLs) 10151, 15510, and 6370. **Asterisks** with *P* values indicate the significance of differences between the LCLs, by chi-square test. The total number of peptides from LCLs 10151, 15510, and 6370 was 4,471, 3,379, and 2,623, respectively.

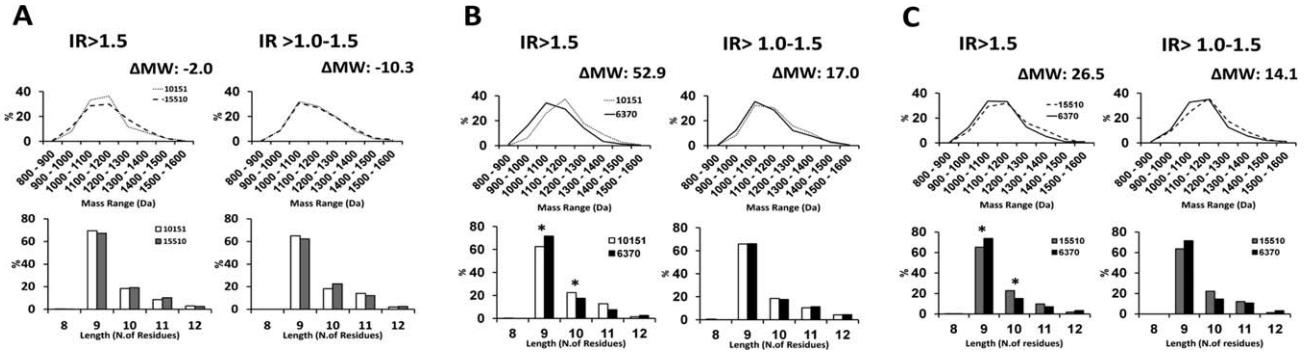

Figure 3. Molecular weight (MW) (upper panels) and length (lower panels) of shared B*27:05 ligands from ERAP-2–negative LCLs (10151 and 15510) and an ERAP-2–positive LCL (6370). The predominant peptides from each cell line were subdivided on the basis of their ion peak intensity relative to the other cell line and grouped as those with an intensity ratio (IR) of >1.5 or those with an IR of >1.0–1.5. The equivalent IR subsets were compared. The intensity assigned to each peptide in a cell line was normalized by dividing its mean intensity by the total intensity of all shared peptides from that cell line in the corresponding pairwise comparison. **A,** In the comparison of LCLs 10151 and 15510, of 2,462 shared peptides, the number of peptides with an IR of >1.5 was 991 and 809, respectively, and the number with an IR of >1.0–1.5 was 383 and 279, respectively. The differences in the mean MW (ΔMW) of the peptides in each subset from both cell lines are indicated. **B,** In the comparison of LCLs 10151 and 6370, of 2,297 shared peptides, the number with an IR of >1.5 was 764 and 817, respectively, and the number with an IR of >1.0–1.5 was 355 and 361, respectively. * = $P = 3.7 \times 10^{-4}$ and $P = 3.0 \times 10^{-3}$ for 9-mers and 10-mers, respectively, by chi-square test. **C,** In the comparison of LCLs 15510 and 6370, of 1,870 shared peptides, the number with an IR of >1.5 was 390 and 590, respectively, and the number with an IR of >1.0–1.5 was 390 and 458, respectively. * = $P = 0.041$ and $P = 0.019$ for 9-mers and 10-mers, respectively. See Figure 1 for other definitions.

comparisons allowed us to assess the effect of ERAP-2 expression relative to that in cells lacking ERAP-2.

The shared peptides were classified on the basis of their relative intensity in each paired set of cell lines compared (details available upon request from the corresponding author). Peptides predominant in a cell line, that is, with a normalized intensity ratio (IR) of >1.0 relative to the other cell line, were subdivided into 2 subsets: IR >1.0–1.5 and IR >1.5. The relationship between this division and the statistical significance of IR values was previously reported (32). Those peptides with an IR of >1.0–1.5 and those with an IR of >1.5 in one cell line were compared to the peptides in the IR >1.0–1.5 and IR >1.5 subsets, respectively, in the other cell line. These analyses revealed the differential features of the peptides showing the same level of increased abundance in one cell line relative to the other. The rationale of this approach is that changes specifically related to the presence or absence of ERAP-2 should be best reflected among peptides showing the largest differences in abundance between the relevant cell lines, whereas peptides unaffected by the enzyme would tend to show unaltered expression levels between the cell lines compared. Cell-to-cell differences in relative abundance due to ERAP-2–unrelated factors would be expected to be revealed in the comparison between ERAP-2–negative cells or to show patterns inconsistent with the known enzymatic features of ERAP-2 or to be inconsistent in the comparison between the ERAP-2–positive LCL and the 2 ERAP-2–negative LCLs.

In the pairwise comparison of LCLs 10151 and 15510, the predominant peptides from each cell line showed no differences in MW or length (Figure 3A). In contrast, in the comparisons of LCLs 10151 and 6370 and LCLs 15510 and 6370, a shift toward lower MW values, a statistically significant increase in the percentage of nonamers, and a decrease in the percentage of decamers were observed among all of the peptides with IR >1.0 from LCL 6370, relative to those with IR >1.0 in LCLs 10151 or 15510 (see Supplementary Figure 3, available on the *Arthritis & Rheumatology* web site at http://onlinelibrary.wiley.com/doi/10.1002/art.39734/abstract). These differences were detected among the subsets of peptides with IR >1.5, but not among peptides with more similar abundance, having an IR of >1.0–1.5 (Figures 3B and C).

Alteration of the B*27:05 peptidome by selective trimming of N-terminal basic residues by ERAP-2. We next compared the frequencies of N-terminal (P1) residues among B*27:05 ligands predominant in either the presence or the absence of ERAP-2. In the pairwise comparison of LCLs 10151 and 15510, no statistically significant differences in the frequency of P1 residues were observed (Figure 4A), indicating that cell-to-cell differences unrelated to ERAP-2 had a minimal impact. In the comparison of LCLs 10151 and 6370, a statistically significant decrease in the frequencies of

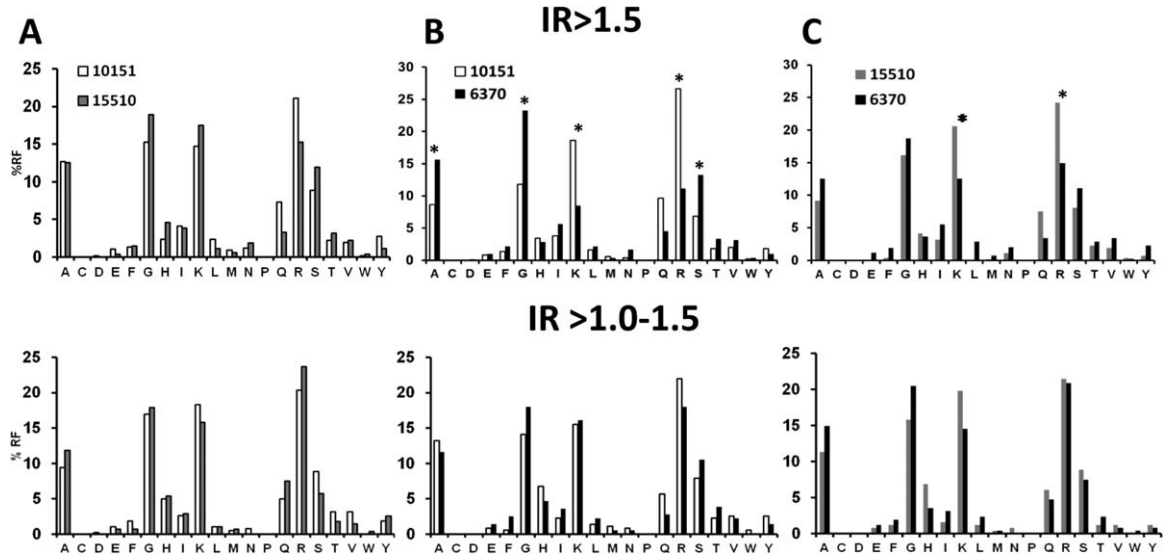

Figure 4. Residue frequencies (RF) (expressed as a percentage) at the N-terminal position among shared B*2705 ligands in lymphoblastoid cell lines (LCLs) 10151, 15510, and 6370. The predominant peptides from each cell line were subdivided into 2 subsets, those having an intensity ratio (IR) of >1.5 (upper panels) and those having an IR of >1.0–1.5 (lower panels), and the equivalent subsets from each paired set of cell lines were compared. Pairwise comparisons were of LCLs 10151 and 15510 **(A)**, LCLs 10151 and 6370 **(B)**, and LCLs 15510 and 6370 **(C)**. In **B,** $* = P = 1.2 \times 10^{-3}$ (for Ala), $P = 2.0 \times 10^{-7}$ (for Gly), $P = 4.2 \times 10^{-8}$ (for Lys), $P = 7.3 \times 10^{-15}$ (for Arg), and $P = 0.016$ (for Ser). In **C,** $* = P = 2.1 \times 10^{-3}$ (for Lys) and $P = 6.0 \times 10^{-4}$ (for Arg). All P values were calculated by chi-square test with Bonferroni correction. Only the differences among residues with >10% RF in at least 1 LCL were taken into account.

Arg_1 and Lys_1 was observed in the IR >1.5 subset of peptides from LCL 6370, with a concomitant increase in the frequencies of Gly_1, Ala_1, and Ser_1 (Figure 4B). No differences in the frequencies of P1 residues were detected in the subset of peptides with IR >1.0–1.5. A pattern similar to these findings was observed when comparing LCLs 15510 and 6370 (Figure 4C), although only the decrease in frequency of the 2 basic P1 residues in LCL 6370 reached statistical significance. No ERAP-2–dependent differences were found in the N-terminal flanking (P-1) residues of B*27:05 ligands (see Supplementary Figure 4, available on the *Arthritis & Rheumatology* web site at http://onlinelibrary.wiley.com/doi/10.1002/art.39734/abstract).

Since basic P1 residues are very frequent, a significant fraction of the B*27:05 peptidome was quantitatively altered. Indeed, the frequency of the B*27:05 ligands with IR >1.0 (i.e., both the IR >1.0–1.5 subset and the IR >1.5 subset) and the frequency of basic P1 residues were each decreased in LCL 6370, by 20% ($P = 5.0 \times 10^{-22}$) and 9.3% ($P = 3.7 \times 10^{-10}$), respectively, relative to LCLs 10151 and 15510, whereas the percentages of peptides with basic P1 residues in the IR >1.0 subset from the latter 2 cell lines were almost identical, at 38.1% and 37.1%, respectively (see details in Supplementary Figure 3).

Increased degradation of B*27:05 ligands with N-terminal basic residues by ERAP-2. To further support the concept that the specifically decreased abundance of B*27:05 ligands with N-terminal basic residues was due to the presence of ERAP-2, 4 synthetic substrates (QL.RRFGDKLNF, LA.RRYGDVFQI, AS.IRLPSQYNF, and NS.FRYNGLIHR), including the sequences of natural B*27:05 ligands as well as the 2 N-terminal flanking residues in their parental proteins, were digested with the ERAP-1 variant expressed in LCL 6370, both in the presence and in the absence of ERAP-2 (details available upon request from the corresponding author). The 2 B*27:05 ligands with N-terminal Arg used in these experiments were recovered with ~4-fold and ~3-fold higher yield in the absence of ERAP-2 than in the presence of ERAP-2. In contrast, the yield of B*27 ligands with nonbasic N-terminal residues was only affected slightly or not affected at all by this enzyme.

MW differences among HLA–B*27 ligands are mainly attributable to distinct P1 residue usage. In order to discern whether the MW differences among shared HLA–B*27 ligands from ERAP-2–positive and ERAP-2–negative LCLs (Figures 3B and C) could be attributed to peptide length, to residue usage, or to both, comparisons were performed with only the nonamers from the IR >1.5 subset of peptides. A shift

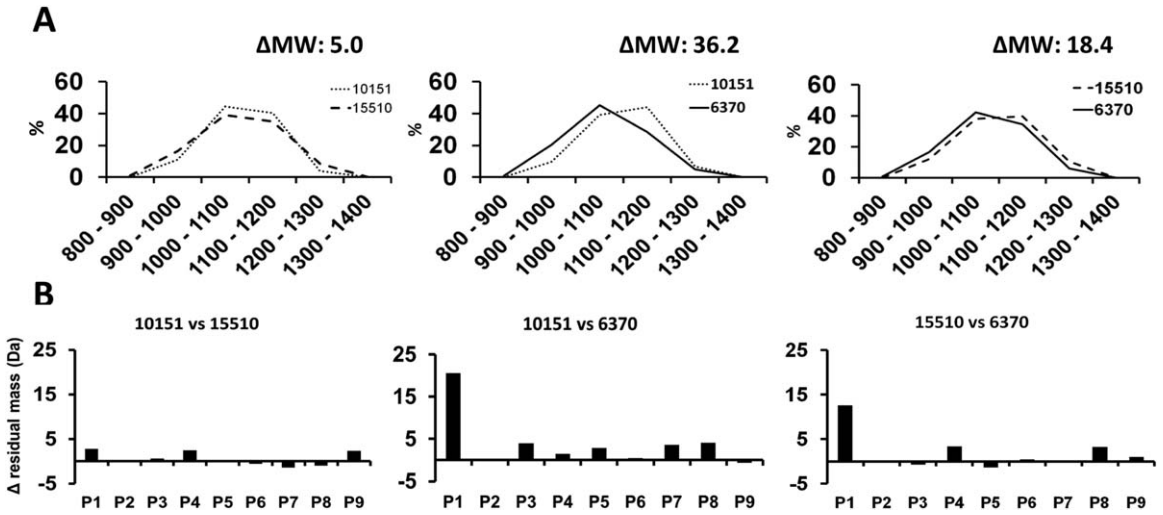

Figure 5. Molecular weight (MW) and residue mass distribution among shared B*27:05 nonamers from the IR >1.5 subsets of peptides in pairwise cell line comparisons. **A,** MW distribution of the nonamers in the IR >1.5 subsets from LCL 10151 (688 peptides) versus LCL 15510 (544 peptides), LCL 10151 (499 peptides) versus LCL 6370 (602 peptides), and LCL 15510 (358 peptides) versus LCL 6370 (577 peptides). The differences in the mean MW (ΔMW) of the nonamers in each IR subset are indicated. **B,** Mean residual mass differences at individual peptide positions among the shared B*27:05 nonamers from the IR >1.5 subsets in the pairwise LCL comparisons (same as those indicated in **A**). See Figure 4 for other definitions.

toward lower MW was observed on LCL 6370 relative to LCLs 10151 and 15510, but not when these latter 2 LCLs were compared (Figure 5A). The changes in MW (ΔMW) of the nonamers in the pairwise comparisons of LCLs 10151 and 6370 and LCLs 15510 and 6370 (73.0% for LCL 10151 versus LCL 6370, and 69.8% for LCL 15510 versus LCL 6370) were slightly lower than the ΔMW of peptides of all lengths in the IR >1.5 subset (Figures 3B and C), indicating that length-independent effects on the peptide sequence are the major influence of ERAP-2 on the MW of HLA–B*27 ligands.

We then addressed whether these effects could be attributed to P1 only or to additional positions downstream, as has been described for ERAP-1 (13,32,33). The differences in the mean residual mass (ΔW) at each peptide position among the nonamers from the IR >1.5 subset in all pairwise comparisons were calculated (Figure 5B). No differences were found between LCL 10151 and LCL 15510 (ΔW <3 daltons). For the comparisons of LCLs 10151 and 6370 and LCLs 15510 and 6370, differences in the mean residual mass of P1 (ΔW 20.6 daltons and 12.6 daltons, respectively) accounted for 56.9% of the ΔMW and 68.5% of the ΔMW, respectively, between the corresponding nonamers (Figure 5A), whereas the ΔW values were no larger than 4 daltons at any other position.

Accordingly, very few differences in residue usage were found among the nonamers from these subsets in the 3 pairwise comparisons (results available upon request from the corresponding author). Among the peptides predominant in the presence of ERAP-2, only the lower frequency of His_5 could be attributed to the presence of ERAP-2, since the difference reached statistical significance in the comparisons of LCLs 10151 and 6370 and LCLs 15510 and 6370 ($P < 0.048$ and $P < 0.006$, respectively), but not in the comparison of LCLs 10151 and 15510. Thus, the length-independent effects of ERAP-2 on the HLA–B*27 peptidome occur mainly on the P1 residue.

Minimal effect of ERAP-2 on the affinity of the B*27:05 peptidome. When the theoretical affinity of the shared peptides from the IR >1.5 subset was compared, no differences were observed between LCL 6370 and LCL 15510. However, differences in peptide affinity were found in LCL 6370 compared to LCL 10151, and also in LCL 10151 compared to LCL 15510. The difference between the latter 2 cell lines is a reflection of ERAP-2–independent cell-to-cell differences. Thus, the lower affinity of B*27:05 ligands predominant in LCL 6370 relative to LCL 10151 cannot be attributed to the presence of ERAP-2. Nevertheless, this enzyme did not increase the global affinity of the B*27:05 peptidome.

DISCUSSION

The identification of ERAP-2 as a risk factor for AS (20,21) highlights the importance of determining the role of this enzyme in shaping the B*27:05 peptidome.

The specificity differences between ERAP-1 and ERAP-2 suggest that the latter enzyme should have a distinct influence on MHC class I–bound peptidomes. Due to the concerted trimming by ERAP-1/ERAP-2 heterodimers (5,14), the alterations induced by ERAP-2 on the HLA–B*27 peptidome may reflect both the preference of this enzyme for basic N-terminal residues and the allosteric activation of ERAP-1. An additional mechanism by which ERAP-2 could increase ERAP-1 trimming is by degrading short peptides. The octameric digestion products, which are not further cleaved by ERAP-1, inhibit its trimming of longer substrates (34,35). The destruction of octamers with appropriate P1 residues by ERAP-2 might prevent the inhibitory effect of these peptides on ERAP-1.

Thus, a question arises about the actual impact of the potentially complex effects of ERAP-2 on the B*27:05 peptidome. Our estimation that ERAP-2 destroys ~3–4% of the peptides with N-terminal basic residues expressed in the absence of this enzyme is probably a minimal one, because other ligands might be lost by the induced activation of ERAP-1. The identification of individual ligands specifically presented in the presence or absence of ERAP-2 was not further addressed, because absence of a given ligand cannot be formally established when it is not detected by MS. Instead, we focused on the relative abundance of shared peptides in LCLs either expressing or not expressing ERAP-2 in a functionally indistinguishable ERAP-1 context. The rationale is that much of the effect of ERAP-2 is on determining the amounts of peptides rather than their generation or total destruction. Moreover, the same mechanisms underlying the quantitative differences will determine, in the extreme situation, the selective presentation of some ligands.

Since our comparisons involved 3 unrelated cell lines that may differ in the expression of many proteins, 2 criteria were adopted for establishing the validity of ERAP-2–related effects. First, the observation that 2 LCLs lacking ERAP-2 and expressing functionally indistinguishable ERAP-1 variants did not show any statistically significant differences in peptide length or N-terminal residue usage indicates that cell-to-cell differences unrelated to ERAP-2 are not responsible for the effects observed. In particular, we note that the limited structural differences between the ERAP-1 variants in LCL 10151 and LCL 15510 (T12I and R127P mutations) did not induce any detectable alterations in the B*27:05 peptidomes from these cell lines. Second, in the 2 pairwise comparisons involving ERAP-2–negative and ERAP-2–positive LCLs, only those changes consistently observed in both comparisons were attributed to ERAP-2, in order to rule out differences among individual cell lines unrelated to ERAP-2. Taken together, these 2 criteria strongly argue against the formal possibility that biochemical disparity among cell lines may account for the specific effects observed, which, in addition, were highly consistent with the known biochemical properties of ERAP-2. Nevertheless, experiments with isogenic cell lines involving differences in only ERAP-2 should be done to formally rule out the possibility of unforeseen ERAP-2–unrelated effects.

The influence of ERAP-2 on the B*27:05-bound peptidome was mainly observed at 2 levels: effects on peptide length, and effects on P1 residue usage. In the presence of ERAP-2, the percentage of the most abundant 9-mer and 10-mer peptides was higher and lower, respectively, than among peptides predominant in the absence of this enzyme. The magnitude was comparable to that on B*27:04 ligands (24) and A*29:02 ligands (32) in distinct ERAP-1 contexts. We cannot rule out the possibility that ERAP-2 directly affects peptide length. Nevertheless, since this enzyme is relatively inefficient with decamers (12), length optimization of B*27:05 ligands might result mainly from the activation of ERAP-1 trimming by ERAP-2.

In contrast, the specific decrease in the percentage of Arg or Lys at P1 among the peptides predominant in the presence of ERAP-2 is most easily explained by a direct effect on destroying the corresponding B*27:05 ligands, as was observed in vitro in this study. ERAP-2 is more efficient than ERAP-1 with substrates of lower length, such as nonamers (12). Moreover, although increased trimming of basic residues may occur upon ERAP-2–induced activation of ERAP-1, this would result in even higher cleavage of ERAP-1–susceptible residues, actually leading to an increased percentage of the basic residues, as was previously observed with highly active ERAP-1 variants (33). Our results show the opposite situation, implying a direct and selective trimming of basic P1 residues by ERAP-2.

A previous report claimed that, due to the resistance of dibasic N-terminal sequences to most aminopeptidases, the preference for peptides with this feature allows HLA–B*27 to present epitopes generated in relatively low amounts, since they would survive the strongly degrading cytosolic conditions better (36). The significant trimming of basic P1 residues by ERAP-2 partially limits this feature of HLA–B*27 in ERAP-2–positive individuals.

Unlike ERAP-1 (33), we observed only a minor influence of ERAP-2 on the sequences of B*27:05 ligands downstream of the N-terminus, consisting of a decreased usage of His_5. In recent crystallographic

studies (12), some His side chains of the substrate established π-stacking interactions in the peptide-binding site of ERAP-2. Thus, peptides with internal His residues might bind and be trimmed better by ERAP-2, thereby explaining their lower abundance in the presence of this enzyme. Findings in that same study (12) suggested that the influence of internal substrate residues upon ERAP-2 trimming is smaller than that with ERAP-1, a finding that is consistent with our observations.

Our results suggested some possible mechanisms by which ERAP-2 increases the risk of AS in HLA–B*27–positive individuals (21). Peptide presentation by HLA–B*27 may be altered in various ways. For instance, the destruction of peptides with basic P1 residues may render HLA–B*27 unable to present certain epitopes, which might upset the immune homeostasis of the gut (37). More generally, quantitative changes on many B*27:05 ligands may alter the immunogenic/tolerogenic potential of HLA–B*27, since T cell triggering depends on T cell receptor avidity and epitope density (38). In addition to the direct effects of ERAP-2, those that result in activation of ERAP-1 may also be associated with disease susceptibility, since high ERAP-1 activity is associated with the risk of AS (17).

Again, in contrast to ERAP-1 (39), ERAP-2 did not show a clear influence on the global affinity of the B*27:05 peptidome. This is consistent with previously reported findings in which ERAP-2 did not affect the expression of free MHC class I heavy chains at the cell surface (40), although another report claimed that absence of ERAP-2 correlated with increased surface expression of these MHC class I forms (41). Since N-terminal Arg residues make a positive contribution to B*27:05 binding (42), we cannot rule out the possibility of a limited effect of ERAP-2 on lowering affinity below the detection limits of our analysis.

In conclusion, our results suggest that the AS-promoting activity of ERAP-2 could be attributed to both its direct degradation of peptides with basic P1 residues and its indirect favoring of ERAP-1–mediated trimming. Although these effects are globally significant and critical on some particular peptides, the influence of ERAP-2 on the B*27:05 peptidome seems smaller than that of ERAP-1, at least with regard to peptide features and binding affinity.

ACKNOWLEDGMENTS

We thank Dr. Maxime Breban (Université de Versailles Saint-Quentin-en-Yvelines, INSERM U1016, Paris, France) and Irini Evnouchidou and Peter van Endert (Hôpital Necker, INSERM U1151, Paris, France) for providing the LCLs 10151, 15510, and 6370, and Dr. Efstratios Stratikos and the Protein Chemistry Facility of the Greek National Center for Scientific Research Demokritos (Athens, Greece) (infrastructure associated with the National Research Infrastructure in Structural Biology, Instruct-EL) for providing the recombinant baculoviruses. We also thank Sergio Ciordia and María del Carmen Mena (Proteomics Unit, Centro Nacional de Biotecnología, Madrid, Spain) for providing technical assistance with the MS analyses.

AUTHOR CONTRIBUTIONS

All authors were involved in drafting the article or revising it critically for important intellectual content, and all authors approved the final version to be published. Dr. López de Castro had full access to all of the data in the study and takes responsibility for the integrity of the data and the accuracy of the data analysis.

Study conception and design. Martín-Esteban, López de Castro.
Acquisition of data. Martín-Esteban, Guasp, Barnea, Admon.
Analysis and interpretation of data. Martín-Esteban, Admon, López de Castro.

REFERENCES

1. Cascio P, Hilton C, Kisselev AF, Rock KL, Goldberg AL. 26S proteasomes and immunoproteasomes produce mainly N-extended versions of an antigenic peptide. EMBO J 2001;20:2357–66.
2. Saric T, Chang SC, Hattori A, York IA, Markant S, Rock KL, et al. An IFN-gamma-induced aminopeptidase in the ER, ERAP1, trims precursors to MHC class I-presented peptides. Nat Immunol 2002;3:1169–76.
3. Tanioka T, Hattori A, Masuda S, Nomura Y, Nakayama H, Mizutani S, et al. Human leukocyte-derived arginine aminopeptidase: the third member of the oxytocinase subfamily of aminopeptidases. J Biol Chem 2003;278:32275–83.
4. Tsujimoto M, Hattori A. The oxytocinase subfamily of M1 aminopeptidases. Biochim Biophys Acta 2005;1751:9–18.
5. Saveanu L, Carroll O, Lindo V, Del Val M, Lopez D, Lepelletier Y, et al. Concerted peptide trimming by human ERAP1 and ERAP2 aminopeptidase complexes in the endoplasmic reticulum. Nat Immunol 2005;6:689–97.
6. Saveanu L, Carroll O, Weimershaus M, Guermonprez P, Firat E, Lindo V, et al. IRAP identifies an endosomal compartment required for MHC class I cross-presentation. Science 2009;325:213–7.
7. Saveanu L, van Endert P. The role of insulin-regulated aminopeptidase in MHC class I antigen presentation. Front Immunol 2012;3:57.
8. Hearn A, York IA, Rock KL. The specificity of trimming of MHC class I-presented peptides in the endoplasmic reticulum. J Immunol 2009;183:5526–36.
9. Zervoudi E, Papakyriakou A, Georgiadou D, Evnouchidou I, Gajda A, Poreba M, et al. Probing the S1 specificity pocket of the aminopeptidases that generate antigenic peptides. Biochem J 2011;435:411–20.
10. Birtley JR, Saridakis E, Stratikos E, Mavridis IM. The crystal structure of human endoplasmic reticulum aminopeptidase 2 reveals the atomic basis for distinct roles in antigen processing. Biochemistry 2012;51:286–95.
11. Chang SC, Momburg F, Bhutani N, Goldberg AL. The ER aminopeptidase, ERAP1, trims precursors to lengths of MHC class I peptides by a "molecular ruler" mechanism. Proc Natl Acad Sci U S A 2005;102:17107–12.
12. Mpakali A, Giastas P, Mathioudakis N, Mavridis IM, Saridakis E, Stratikos E. Structural basis for antigenic peptide recognition and processing by ER aminopeptidase 2. J Biol Chem 2015;290:26021–32.

13. Evnouchidou I, Momburg F, Papakyriakou A, Chroni A, Leondiadis L, Chang SC, et al. The internal sequence of the peptide-substrate determines its N-terminus trimming by ERAP1. PLoS One 2008;3:e3658.
14. Evnouchidou I, Weimershaus M, Saveanu L, van Endert P. ERAP1-ERAP2 dimerization increases peptide-trimming efficiency. J Immunol 2014;193:901–8.
15. Evnouchidou I, Birtley J, Seregin S, Papakyriakou A, Zervoudi E, Samiotaki M, et al. A common SNP in ER aminopeptidase 2 induces a specificity switch that leads to altered antigen processing. J Immunol 2012;189:2383–92.
16. Andres AM, Dennis MY, Kretzschmar WW, Cannons JL, Lee-Lin SQ, Hurle B, et al. Balancing selection maintains a form of ERAP2 that undergoes nonsense-mediated decay and affects antigen presentation. PLoS Genet 2010;6:e1001157.
17. The TASK and WTCCC2 Consortia. Interaction between ERAP1 and HLA-B27 in ankylosing spondylitis implicates peptide handling in the mechanism for HLA-B27 in disease susceptibility. Nat Genet 2011;43:761–7.
18. WTCC Consortium. Association scan of 14,500 nonsynonymous SNPs in four diseases identifies autoimmunity variants. Nat Genet 2007;39:1329–37.
19. Tsui FW, Haroon N, Reveille JD, Rahman P, Chiu B, Tsui HW, et al. Association of an ERAP1 ERAP2 haplotype with familial ankylosing spondylitis. Ann Rheum Dis 2010;69:733–6.
20. Cortes A, Hadler J, Pointon JP, Robinson PC, Karaderi T, Leo P, et al. Identification of multiple risk variants for ankylosing spondylitis through high-density genotyping of immune-related loci. Nat Genet 2013;45:730–8.
21. Robinson PC, Costello ME, Leo P, Bradbury LA, Hollis K, Cortes A, et al. ERAP2 is associated with ankylosing spondylitis in HLA-B27-positive and HLA-B27-negative patients. Ann Rheum Dis 2015;74:1627–9.
22. Reeves E, Colebatch-Bourn A, Elliott T, Edwards CJ, James E. Functionally distinct ERAP1 allotype combinations distinguish individuals with ankylosing spondylitis. Proc Natl Acad Sci U S A 2014;111:17594–9.
23. Costantino F, Talpin A, Evnouchidou I, Kadi A, Leboime A, Said-Nahal R, et al. ERAP1 gene expression is influenced by nonsynonymous polymorphisms associated with predisposition to spondyloarthritis. Arthritis Rheumatol 2015;67:1525–34.
24. Garcia-Medel N, Sanz-Bravo A, Van Nguyen D, Galocha B, Gomez-Molina P, Martin-Esteban A, et al. Functional interaction of the ankylosing spondylitis-associated endoplasmic reticulum aminopeptidase 1 polymorphism and HLA-B27 in vivo. Mol Cell Proteomics 2012;11:1416–29.
25. Guasp P, Alvarez-Navarro C, Gomez-Molina P, Martin-Esteban A, Marcilla M, Barnea E, et al. The peptidome of the Behcet's disease-associated HLA-B*51:01 includes two sub-peptidomes differentially shaped by ERAP1. Arthritis Rheumatol 2016;68:505–15.
26. Ellis SA, Taylor C, McMichael A. Recognition of HLA-B27 and related antigens by a monoclonal antibody. Hum Immunol 1982; 5:49–59.
27. Paradela A, Alvarez I, Garcia-Peydro M, Sesma L, Ramos M, Vazquez J, et al. Limited diversity of peptides related to an alloreactive T cell epitope in the HLA-B27-bound peptide repertoire results from restrictions at multiple steps along the processing-loading pathway. J Immunol 2000;164:329–37.
28. Cox J, Mann M. MaxQuant enables high peptide identification rates, individualized p.p.b.-range mass accuracies and proteome-wide protein quantification. Nat Biotechnol 2008;26:1367–72.
29. Cox J, Neuhauser N, Michalski A, Scheltema RA, Olsen JV, Mann M. Andromeda: a peptide search engine integrated into the MaxQuant environment. J Proteome Res 2011;10:1794–805.
30. Karosiene E, Lundegaard C, Lund O, Nielsen M. NetMHCcons: a consensus method for the major histocompatibility complex class I predictions. Immunogenetics 2012;64:177–86.
31. Goto Y, Hattori A, Ishii Y, Tsujimoto M. Reduced activity of the hypertension-associated Lys528Arg mutant of human adipocyte-derived leucine aminopeptidase (A-LAP)/ER-aminopeptidase-1. FEBS Lett 2006;580:1833–8.
32. Alvarez-Navarro C, Martin-Esteban A, Barnea E, Admon A, Lopez de Castro JA. ERAP1 polymorphism relevant to inflammatory disease shapes the peptidome of the birdshot chorioretinopathy-associated HLA-A*29:02 antigen. Mol Cell Proteomics 2015;14:1770–80.
33. Sanz-Bravo A, Campos J, Mazariegos MS, Lopez de Castro JA. Dominant role of the ERAP1 polymorphism R528K in shaping the HLA–B27 peptidome through differential processing determined by multiple peptide residues. Arthritis Rheumatol 2015; 67:692–701.
34. Evnouchidou I, Kamal RP, Seregin SS, Goto Y, Tsujimoto M, Hattori A, et al. Cutting edge: coding single nucleotide polymorphisms of endoplasmic reticulum aminopeptidase 1 can affect antigenic peptide generation in vitro by influencing basic enzymatic properties of the enzyme. J Immunol 2011;186: 1909–13.
35. Martin-Esteban A, Gomez-Molina P, Sanz-Bravo A, Lopez de Castro JA. Combined effects of ankylosing spondylitis-associated ERAP1 polymorphisms outside the catalytic and peptide-binding sites on the processing of natural HLA-B27 ligands. J Biol Chem 2014;289:3978–90.
36. Herberts CA, Neijssen JJ, de Haan J, Janssen L, Drijfhout JW, Reits EA, et al. Cutting edge: HLA-B27 acquires many N-terminal dibasic peptides. Coupling cytosolic peptide stability to antigen presentation. J Immunol 2006;176:2697–701.
37. Kenna TJ, Brown MA. Immunopathogenesis of ankylosing spondylitis. Int J Clin Rheumatol 2013;8:265–74.
38. Manz BN, Jackson BL, Petit RS, Dustin ML, Groves J. T-cell triggering thresholds are modulated by the number of antigen within individual T-cell receptor clusters. Proc Natl Acad Sci U S A 2011;108:9089–94.
39. Sanz-Bravo A. Mecanismo molecular implicado en la configuración del peptidoma de HLA-B*27 por variantes naturales de ERAP1 asociadas a la espondilitis anquilosante. PhD Thesis. Universidad Autónoma de Madrid; 2015.
40. Robinson PC, Lau E, Keith P, Lau MC, Thomas GP, Bradbury LA, et al. ERAP2 functional knockout in humans does not alter surface heavy chains or HLA-B27, inflammatory cytokines or endoplasmic reticulum stress markers. Ann Rheum Dis 2015;74: 2092–5.
41. Zhang Z, Ciccia F, Yee K, Guggino G, Abdullah H, Alessandro R, et al. Functional implications of the endoplasmic reticulum aminopeptidase 2 (ERAP2) association with ankylosing spondylitis and Crohn's disease: impact on the unfolded protein response [abstract]. Arthritis Rheum 2014;66 Suppl:S268.
42. Lamas JR, Paradela A, Roncal F, Lopez de Castro JA. Modulation at multiple anchor positions of the peptide specificity of HLA–B27 subtypes differentially associated with ankylosing spondylitis. Arthritis Rheum 1999;42:1975–85.

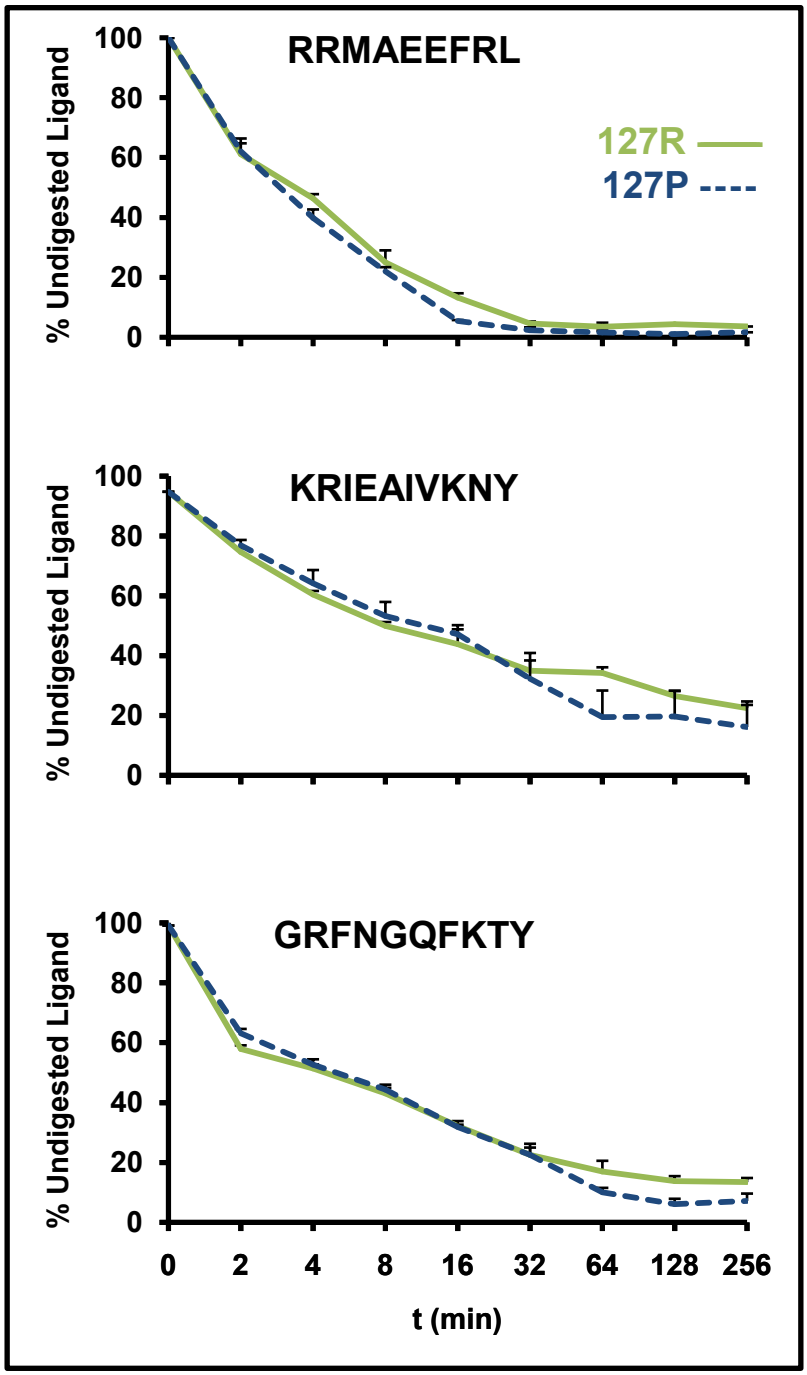
RRMAEEFRL
127R
127P
% Undigested Ligand
100
80
60
40
20
0
KRIEAIVKNY
% Undigested Ligand
GRFNGQFKTY
% Undigested Ligand
0
2
4
8
16
32
64
128
256
t (min)

Fig. S1

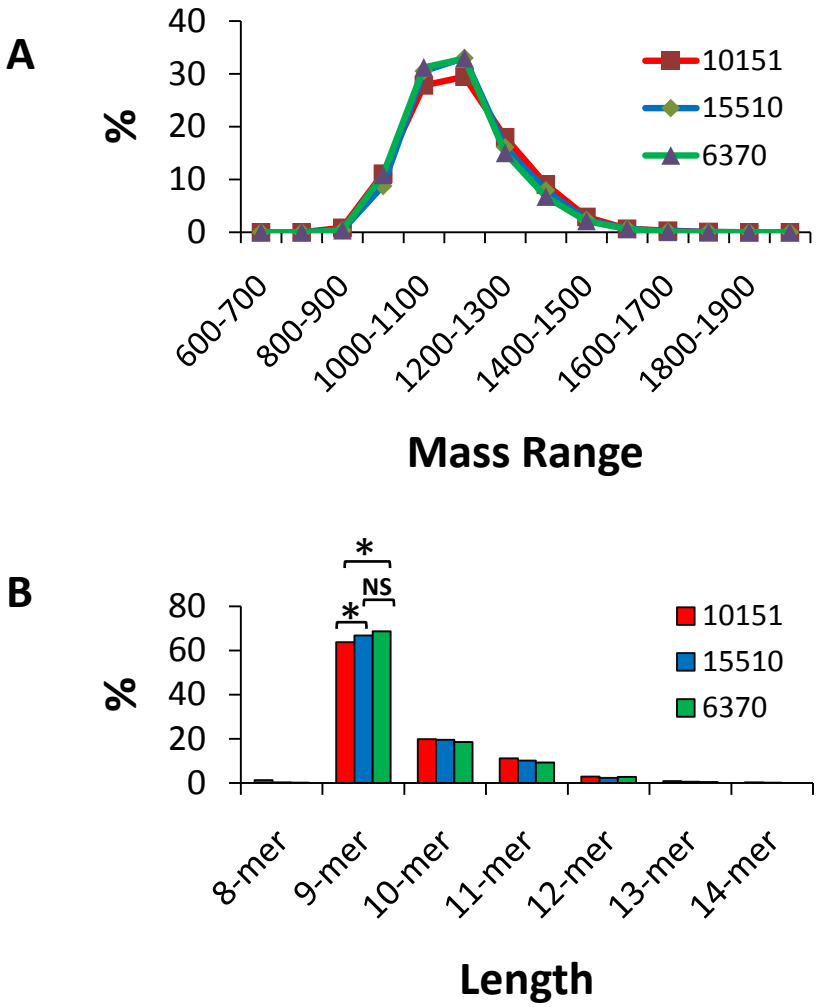
A
40
30
20
10
0
%
10151
15510
6370
600-700
800-900
1000-1100
1200-1300
1400-1500
1600-1700
1800-1900
Mass Range
B
80
60
40
20
0
%
*
NS
*
10151
15510
6370
8-mer
9-mer
10-mer
11-mer
12-mer
13-mer
14-mer
Length

Fig. S2

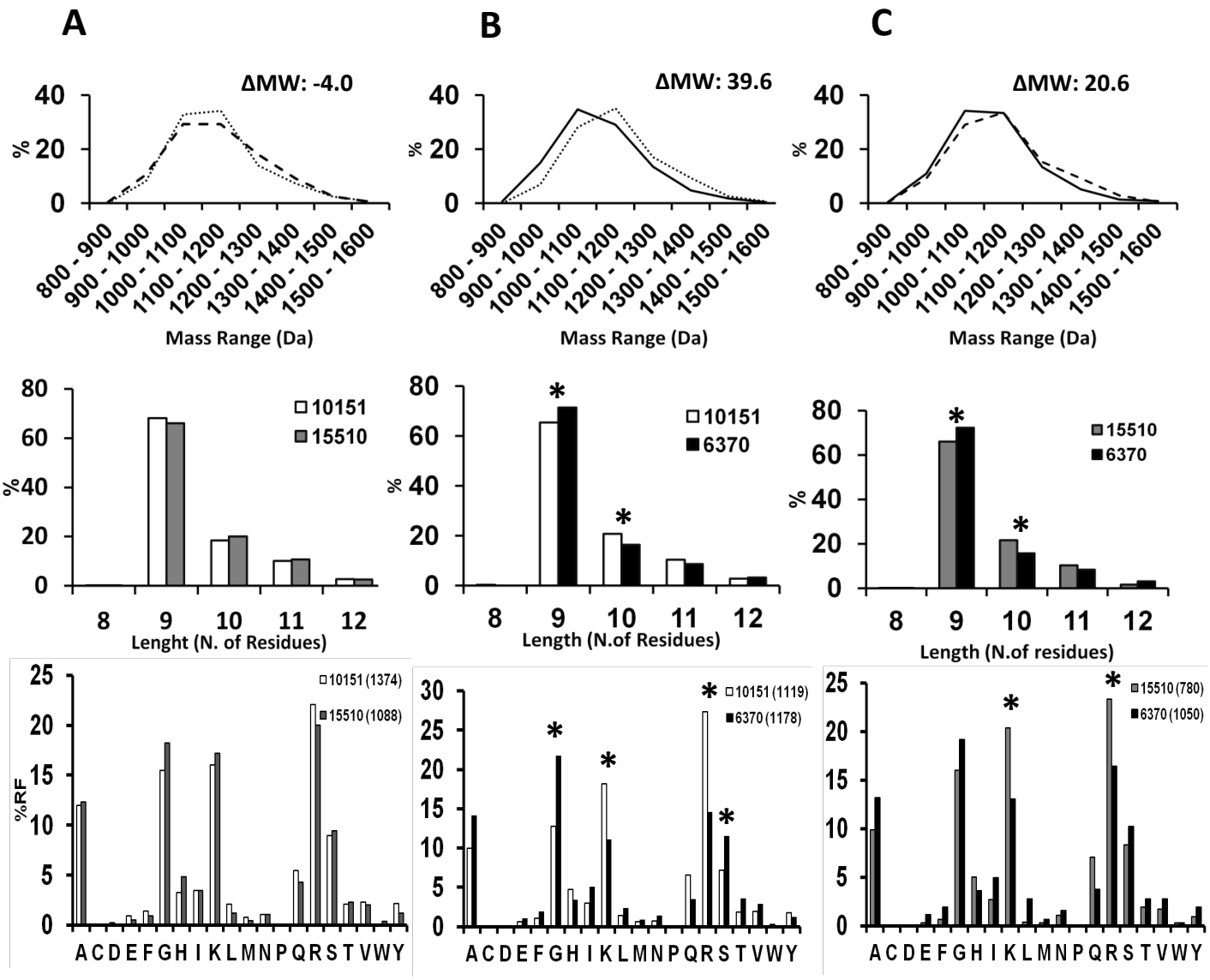
A
B
C
ΔMW: -4.0
ΔMW: 39.6
ΔMW: 20.6
%
Mass Range (Da)
800 - 900
900 - 1000
1000 - 1100
1100 - 1200
1200 - 1300
1300 - 1400
1400 - 1500
1500 - 1600
10151
15510
6370
Lenght (N. of Residues)
Length (N.of Residues)
Length (N.of residues)
%RF
10151 (1374)
15510 (1088)
10151 (1119)
6370 (1178)
15510 (780)
6370 (1050)
A C D E F G H I K L M N P Q R S T V W Y

Figure S3

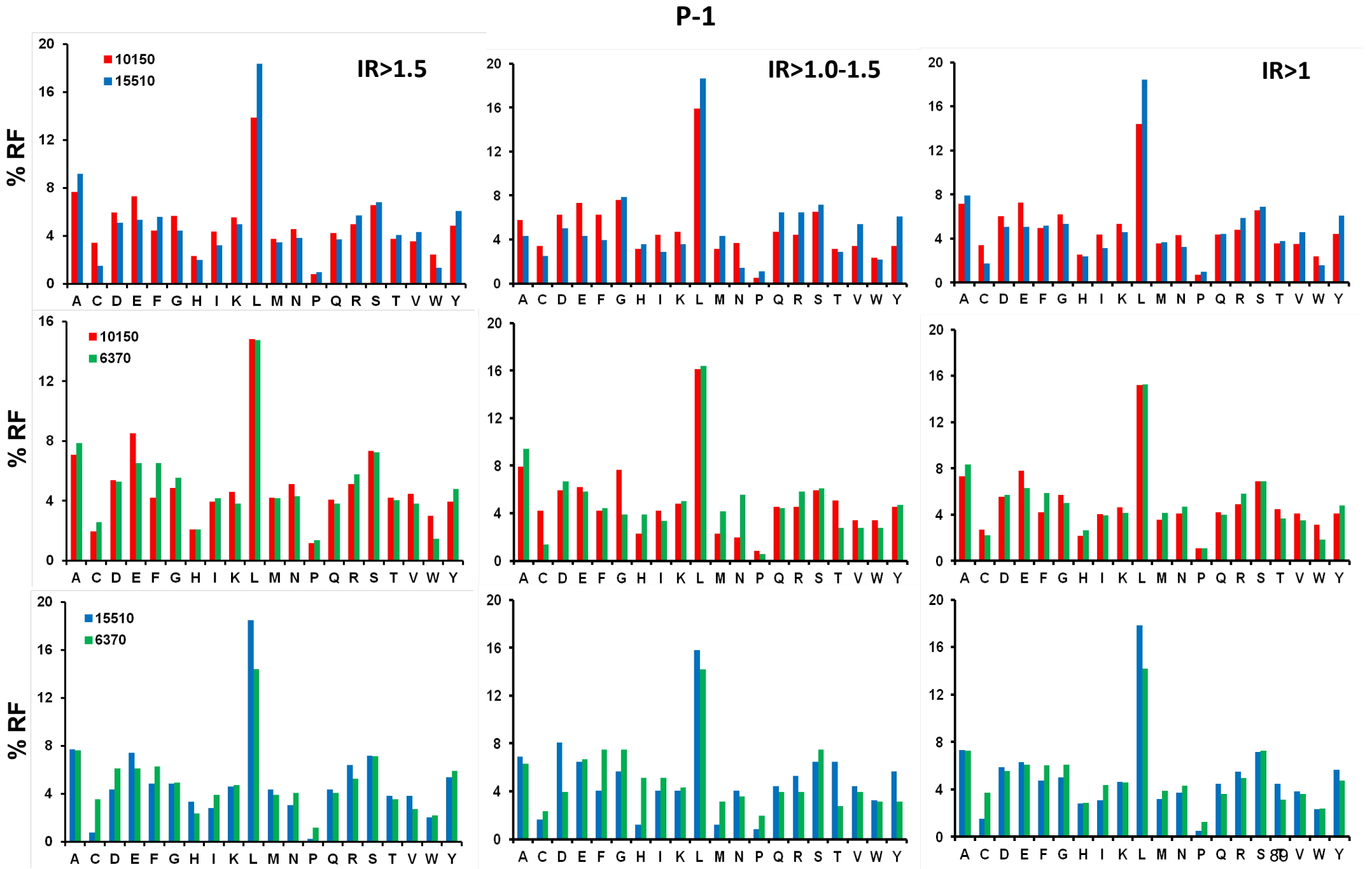
P-1
IR>1.5
IR>1.0-1.5
IR>1
10150
15510
6370
% RF
A C D E F G H I K L M N P Q R S T V W Y

Fig. S4

Supplementary Figure legends

Supplementary Figure 1. In vitro digestion of synthetic B*27:05 ligands by ERAP-1 variants. The indicated peptides, with the sequence of natural B*27:05 ligands, were digested at various times with the recombinant wild-type variant (Q9NZ08), identical to that from LCL 10151 and 6370 (127R), and the R127P variant (127P) at an enzyme:substrate ratio of 1:10. The results are expressed as the percentage of undigested substrate as a function of time. Values are the mean ± standard deviation of 3 independent experiments. No statistically significant differences were found, except at two unrelated time points: upper panel, time point 16 min (p:007) and lower panel, time point 128 min (0.035).

Supplementary Figure 2. Molecular weight (MW) and length of the B*27:05 ligands from lymphoblastoid cell lines 10151 (N: 4771), 15510 (N: 3379) and 6370 (N: 2623). (A) MW distribution; (B) length distribution: the differences in the percentage of 9-mers between lymphoblastoid cell line 10151/15510 (p: $4.8x10^{-3}$) or 10151/6370 (p: $2.5x10^{-5}$) were statistically significant (*), but those between lymphoblastoid cell line 15510/6370 were not (NS). The χ^2 test was used.

Supplementary Figure 3. MW (upper panels), length distribution (middle panels) and N-terminal residue frequencies (RF) of shared B*27:05 ligands from ERAP2-negative (lymphoblastoid cell lines 10151 and 15510) or -positive (lymphoblastoid cell line 6370) cells. All the peptides from each cell line with IR >1 relative to the oher cell line in each pairwaise comparison were taken into account and the IR >1 subsets from each two cell lines were compared. **(A),** 10151/15510: 1374 and 1088 peptides, respectively, were compared. The differences in the mean MW of the peptides in each subset from both cell lines (ΔMW) are indicated; **(B),** 10151/6370: 1119 and 1178 peptides, respectively, were compared. Asterisks (*) in the middle panel indicate statistically significant differences, as assessed by the χ^2 test. P-values were 0.004 and 0.009 for 9-mers and 10-mers, respectively; Asterisks in the lower panel indicate statistically significant differences, as assed by the χ^2 test with Bonferroni correction. P-values were $1.7x10^{-7}$, $0.3x10^{-3}$ and $1.7x10^{-11}$ and 0.01 for G, K, R, and S, respectively. Only the

differences among residues with >10% RF in at least one lymphoblastoid cell line were taken into account; **(C),** 15510/6370: 780 and 1050 peptides, respectively, were compared. Conventions are as above. P values were $3.9x10^{-3}$ and $1.5x10^{-3}$ for 9-mers and 10-mers, respectively (middle panel) and $0.6\ x10^{-3}$ and $4.9\ x10^{-3}$, for K and R, respectively.

Supplementary Figure 4. Percent residue frequencies (RF) at the N-terminal flanking (P-1) position among shared B*2705 ligands expressed in the ERAP-2-negative lymphoblastoid cell lines 10151 and 15510 and the ERAP-2-positive lymphoblastoid cell line 6370. The predominant peptides from each cell line in the indicated pairwise comparisons were subdivided in two subsets on the basis of the intensity of the corresponding ion peaks relative to the other cell line: those with intensity ratio (IR) >1.5, and those with IR >1.0-1.5. The equivalent subsets from both cell lines were compared. The 10151/151510, 10151/6370, and 15510/6370 comparisons are shown in the upper, central and lower panels, respectively.

Title:

Separate effects of the ankylosing spondylitis associated ERAP1 and ERAP2 aminopeptidases determine the influence of their combined phenotype on the HLA-B*27 peptidome

Authors: Adrian Martín-Esteban*[1], Alejandro Sanz-Bravo*[1], Pablo Guasp[1], EilonBarnea[2], ArieAdmon[2], and José A. López de Castro[1].

*Equal contribution to this work.

Affiliation: [1]Centro de Biología Molecular Severo Ochoa (Consejo Superior de Investigaciones Científicas and Universidad Autónoma), Madrid, Spain. [2]Faculty of Biology, Technion - Israel Institute of Technology, Haifa, Israel.

Corresponding author: Dr. José A. López de Castro. Centro de Biología Molecular Severo Ochoa, Nicolás Cabrera, N. 1, Universidad Autónoma, 28049 Madrid, Spain. **Phone**: 34-91-1964554; **Fax**: 34-91-1964420; **Email**: aldecastro@cbm.csic.es

ABSTRACT

Ankylosing spondylitis (AS) is an inflammatory disease strongly associated with the Major Histocompatibility Complex class I (MHC-I) allotype HLA-B*27. The endoplasmic reticulum aminopeptidases (ERAP)1 and 2, which trim peptides to their optimal length for MHC-I binding, are also susceptibility factors for this disease. Both highly active ERAP1 variants and ERAP2 expression favor AS, whereas loss-of-function ERAP1 and loss-of-expression ERAP2 variants are protective. Yet, only ERAP1 is in epistasis with HLA-B*27. We addressed two issues concerning the functional interaction of ERAP1 and ERAP2 with the HLA-B*27 peptidome in human cells: 1) distinguishing the effects of ERAP1 from those of ERAP2, and 2) determining the influence of ERAP2 in distinct ERAP1 contexts. Quantitative comparisons of the HLA-B*27:05 peptidomes from cells with various ERAP1/ERAP2 phenotypes were carried out. When cells expressing ERAP2 and either high or low activity ERAP1 variants were compared, increased amounts of nonamers, relative to longer ligands, and decreased amounts of peptides with Ala1, were observed in the more active ERAP1 context. When cells expressing ERAP2 in a low activity ERAP1 context or lacking ERAP2 but expressing a highly active ERAP1 variant were compared, the same effects on peptide length and Ala1, but also significantly lower amounts of peptides with N-terminal basic residues and lower affinity of the peptidome, were observed in the ERAP2-positive context. Thus, ERAP1 and ERAP2 have significant and distinct effects on the HLA-B*27 peptidome, suggesting that both enzymes largely act as separate entities *in viv*o. This may explain their different patterns of association with AS.

KEYWORDS: Ankylosing spondylitis, ERAP1, ERAP2, HLA-B*27

1. Introduction

Major Histocompatibility Complex Class I (MHC-I) molecules constitutively bind large peptide repertoires, which are essential for proper folding and stability of the molecule, and present them at the cell surface where they can be recognized by T-cell antigen and Natural Killer receptors. MHC-I-bound peptides arise from endogenous protein degradation, largely in the cytosol, and are transported into the lumen of the endoplasmic reticulum (ER), where they are trimmed to a suitable length for MHC-I binding by the ER aminopeptidases (ERAP)1 and 2 [1,2]. These enzymes are members of the oxytocinase subfamily of M1 zinc metallopeptidases [3], also including insulin-regulated aminopeptidase, which is involved in antigen cross-presentation [4].

In spite of significant similarity in the sequence [5] and three-dimensional structure [6,7], ERAP2 shows fundamental differences with ERAP1 in enzymatic specificity and substrate handling (reviewed in [8]). For instance, ERAP2 has preference for N-terminal basic residues, although it can also cleave a few others. In contrast, ERAP1 preferentially cleaves hydrophobic residues and shows much lower efficiency with basic ones [6,9,10]. In addition, ERAP1 efficiently cleaves relatively long peptides, is less efficient with nonamers and virtually inactive with shorter substrates, a feature known as the molecular ruler mechanism [11]. ERAP2 is most efficient with nonamers and shorter peptides and its activity quickly decreases with larger substrates [7].

The majority of ERAP1 and ERAP2 molecules seem to be in monomeric form in the ER, although ERAP1/ERAP2 heterodimers account for 10-30% of the enzyme pool [2]. These heterodimers increase the trimming rate of substrates and allosterically activate ERAP1 *in vitro* [12], but their relevance *in vivo* is unknown.

Both enzymes also differ in their expression patterns in human populations. ERAP1 shows extensive polymorphism, which affects its enzymatic activity, resulting in the expression of a relatively large spectrum of functional variants differing among each other by multiple amino acid changes, and referred to as ERAP1 haplotypes,. The most common ones are designated as Hap1 to Hap10 [13]. ERAP2 shows a much more limited polymorphism. Two

functional variants, differing by the Asn392Lys mutation have been identified, which show distinct enzymatic specificity [10]. However, due to another mutation that impairs ERAP2 expression and is in strong linkage disequilibrium with the 392Asn variant, this is usually not expressed at the protein level [14]. As a result, most individuals differ by either expressing the 392Lys allotype (≈75%) or being ERAP2-negative (≈25%). An exception to this pattern was reported in the Chilean population [15].

Besides their significance in antigen processing, ERAP1 and ERAP2 have attracted much recent attention due to their genetic association with a variety of inflammatory diseases [8], including ankylosing spondylitis (AS), a chronic arthritis strongly linked to HLA-B*27 [16], and other MHC-I associated disorders. The associations of both enzymes with AS are somewhat different. ERAP1 is in epistasis with the susceptibility alleles HLA-B*27 [17] and B*40:01[18]. ERAP2 is associated with AS both among HLA-B*27-positive and negative individuals [19,20]. This might suggest that the mechanism by which each enzyme predisposes to AS is at least partially independent from each other.

The association of ERAP1 with AS fits a two-mutation model where the 528Arg and the 575Asn/725Gln polymorphisms, both decreasing the enzymatic activity [21,22], are protective [17]. Likewise, the loss-of-expression allele of ERAP2 is protective from AS [23]. Thus, it appears that optimal functionality of ERAP1 and ERAP2 is a risk factor for this disease.

Due to the distinct specificity and disease association patterns of both enzymes it is important to dissect their respective roles in shaping the HLA-B*27 peptidome. Two studies addressed the effect of natural ERAP1 variants on the HLA-B*27 peptidome in live cells [24,25], demonstrating an effect of distinct ERAP1 backgrounds on peptide length and N-terminal residue frequencies. In the first of these studies there was a difference also in ERAP2 expression between some of the cell lines used, so that the effects of ERAP1 and ERAP2 could not always be distinguished. We have now examined cells of the same ERAP1 backgrounds similarly to that study but expressing ERAP2, which allowed us to distinguish the effects of each enzyme on the HLA-B*27 peptidome.

Furthermore, we recently characterized the influence of ERAP2 expression on the HLA-B*27 peptidome in cells expressing ERAP1 variants of high activity [26]. In that study ERAP2 had a moderate influence on peptide length, presumably through modulating ERAP1 activity, and a much larger one on decreasing the abundance of peptides with N-terminal basic residues, which was most consistent with a direct effect of ERAP2. Yet, since both ERAP1 and ERAP2 contribute to processing MHC-I ligands in the ER, the question remains concerning the relevance of ERAP2 in distinct ERAP1 contexts. Thus, in the present study we analyzed the effects of ERAP2 expression in a low activity, AS-protective, ERAP1 context, relative to cells expressing highly active, AS-predisposing, ERAP1 variants, but not ERAP2.

2. Materials and methods

2.1. Cell lines

The four B*27:05-positive lymphoblastoid cell lines (LCL) used in this study, P50, 6370, 10151 and 15510 and their ERAP1 and ERAP2 phenotypes were previously described. P50 [25] and LCL 6370 [26] express the same ERAP2 variant (392Lys), but differ in ERAP1. P50 expresses the low activity ERAP1 haplotype Hap10, associated with AS protection, whereas LCL 6370 expresses the high activity haplotype Hap2, associated with AS risk. LCL 10151 and 15510 [26] are ERAP2-negative cells expressing very similar and highly active ERAP1 variants, Hap2 and Hap1 respectively, associated with AS risk (**Table 1**).

2.2. Western blotting

ERAP1, ERAP2 and ɣ-tubulin expression was assessed by Western blots using the 6H9 (a generous gift of Dr. Peter van Endert, Paris), 3F5 (R&D Systems, Minneapolis, MN) and GTU (Sigma Aldrich, St. Louis, Mo) monoclonal antibodies (mAb), respectively, as previously described [24]. The immunoblots were scanned and quantified using the TINA 2.09e software (Raystet Isotopenmessgeräte, Straubenhardt, Germany).

*2.3. Isolation of HLA-B*27-bound peptides*

This was done from $2x10^9$ cells by immunopurification of HLA-B*27/peptide complexes from cell lysates with the ME1 mAb [27] and acid extraction as described elsewhere

[28]. For each LCL, three preparations were independently obtained from the same cell amounts.

2.4. Mass spectrometry and data analysis

Aliquots of each sample (about $2x10^8$ to $1x10^9$) were analyzed in a Q-Exactive-Plus mass spectrometer fitted with Ultimate 3000 RSLC nanocapillary UHPLC (Thermo Fisher Waltham, MA, USA). The peptides were resolved using a 7-40% acetonitrile gradient with 0.1% formic acid for 180 min and 0.15 μL/min. The dynamic exclusion was set to 20s. The selected masses were fragmented from the survey scan of mass-to-charge ratio (m/z) 300-1,800 AMU at resolution 70,000. MS/MS spectra were acquired starting at m/z 200 with a resolution of 17,500. The target value was set to $1x10^5$ and the isolation window to 1.8 m/z. The maximum injection time was set to 100 ms and normalized collision energy to 25 eV. Peptide sequences were assigned using the MaxQuant software (version 1.5.0.25) [29] with the Andromeda search engine [30] and the human UniProt/Swiss-Prot database (release 2014_02, 20,270 entries) under the following parameters: precursor ion mass and fragment mass tolerance 20 ppm, false discovery rate (FDR) 0.01 and peptide-spectrum matching FDR 0.05. N-terminal acetylation, Cys carbamidodimethylation, Gln-to-Pyroglutamic cyclation and Met oxidation were included as variable modifications. Identifications derived from the reverse database and known contaminants were eliminated.

2.5. Binding affinity

Theoretical binding affinities of HLA-B*27 ligands were calculated using the NetMHCcons 1.1 Server (http://www.cbs.dtu.dk/services/NetMHCcons/), which integrates three different algorithms, as described elsewhere [31].

2.6. Statistical analysis

Differences in peptide length or residue frequencies and MHC binding affinity were analyzed by the χ^2 test with Bonferroni correction, when applicable, and the Mann-Whitney U test, respectively. $P<0.05$ was considered as statistically significant.

2.7. Peptide digestions in vitro

Recombinant ERAP1 and ERAP2 proteins were obtained and synthetic peptide digestions were carried out as previously described [26]. The ERAP2 construct (392Lys variant) was generated at the Protein Chemistry Facility of the Greek National Center for Scientific Research Demokritos (Athens) and generously provided by Dr. E. Stratikos.

3. Results

*3.1. ERAP1 and ERAP2 expression in HLA-B*27:05-positive LCL*

ERAP1 protein expression was rather similar in all four LCL **(Fig. 1)**. P50 showed the lowest value (73±5%), relative to the cell line with maximal ERAP1 expression, LCL 10151. The ERAP2-positive cells, P50 and 6370, also expressed similar levels of this enzyme.

*3.2. Influence of ERAP1 and ERAP2 on the HLA-B*27 peptidome in live cells: strategy*

Two issues were addressed in this study: 1) the influence of two ERAP1 variants associated with AS risk (Hap2) or protection (Hap10) on the HLA-B*27 peptidome in the presence of ERAP2, and 2) the influence of ERAP2 expression together with a low activity, AS-protective, ERAP1 variant (Hap10), relative to its absence in high activity, AS-promoting, ERAP1 contexts. The main strategy focused on the changes in the abundance of HLA-B*27 ligands observed with distinct ERAP1/ERAP2 combinations. For this purpose, quantitative comparisons of the shared ligands identified in various cell line pairs were carried out as follows. HLA-B*27 peptide pools from any 2 cell lines to be compared were isolated in 3 independent preparations and identified by Tandem MS and MaxQuant-based assignments. The peptides identified in both cell lines that had 8 to 14 amino acid residues, and the HLA-B*27 binding motif of Arg or Gln at peptide position (P)2 were selected. The intensity of the ion peaks corresponding to each peptide in each cell line was normalized to the total intensity of the ion peaks corresponding to all the shared peptides in that cell line. The normalized intensity ratio (IR) of any given peptide in the two cell lines was taken as an indication of the relative expression levels of that peptide in both cell lines. Peptides found in only one cell line were not included in these analyses.

The shared peptides in each pairwise comparison were classified on the basis of their relative abundance as follows (**Fig. S1**). The peptides that were more abundant in one cell line, with IR>1.0, were classified in two subsets: those with IR>1.0 to 1.5 (hereafter abbreviated as IR>1-1.5) and those with IR>1.5. The first subset included those peptides with slightly increased levels in one cell line relative to the other. The second subset included those peptides showing higher expression differences in each cell line compared to the other. The relationship of this classification to the statistical significance of the quantitative differences among MHC-I ligands in pairwise comparisons was previously reported [32].

To determine the influence of ERAP1/ERAP2 on the B*27:05 peptidome we looked for differential features between the peptide subsets showing the largest differences in relative abundance. Thus, we compared the peptides with IR>1.5 in cell line A relative to cell line B with those showing IR>1.5 in cell line B relative to cell line A. These comparisons were based on the assumption that any effect of ERAP1/ERAP2 should be most clearly observed among peptides showing larger differences in relative amounts between the two cell lines compared. As an internal control, analogous comparisons were carried out between the peptide subsets with IR>1-1.5 from each cell line, assuming that any differences due to ERAP1/ERAP2 should be attenuated or absent altogether among the peptides with similar abundance in the two cell lines. As an external control, a comparison was carried out between LCL 10151 and 15510, both lacking ERAP2 and expressing highly similar ERAP1 variants (**Table 1**), to account for cell-to-cell differences in the HLA-B*27 peptidome unrelated to ERAP1/ERAP2. Using this strategy, the following comparisons were carried out:

1) LCL 6370 *vs.* P50 (Hap2/ERAP2^{+} *vs*. Hap10/ERAP2^{+}). This comparison allowed us to assess the influence of two functionally distinct ERAP1 variants differentially associated with AS, in the presence of ERAP2.

2) LCL 10151 *vs.* P50 (Hap2/ERAP2^{-} *vs.* Hap10/ERAP2^{+}) and LCL 15510 *vs.* P50 (Hap1/ERAP2^{-} *vs.* Hap10/ERAP2^{+}). These two comparisons allowed us to assess the influence of ERAP2 expressed together with the low activity ERAP1 variant Hap10, relative to high activity ERAP1 contexts (Hap2, Hap1) without ERAP2. Together with a previous analysis

[26], these comparisons allowed us to establish the effects of ERAP2 expression in distinct ERAP1 contexts on the HLA-B*27 peptidome.

3) LCL 10151 *vs.* 15510 (Hap2/ERAP2$^-$ *vs*. Hap1/ERAP2$^-$). This comparison is similar to that in our previous study [26], but was independently performed here in parallelel and identical conditions with the other cell pairs, as a control for ERAP1/2-unrelated cell-to-cell differences.

*3.3. Influence of differentially AS-associated ERAP1 polymorphism on the B*27:05 peptidome in an ERAP2-positive context*

This analysis involved the comparison of the peptidomes from LCL 6370 and P50. A total of 1712 and 2366 HLA- B*27 ligands, respectively, were identified from each cell line, of which 1470 peptides were found in both LCL. Among these, 825 and 645 peptides showed IR>1 in LCL 6370 and P50, respectively (**Table S1)**.

A comparison of the peptides with IR>1 revealed that those from LCL 6370 had a globally smaller MW (ΔMW: 31.4 Da), relative to P50, which was reflected in a uniform shift of the Gaussian distribution of MW towards lower values. This difference was increased between the IR>1.5 subsets (ΔMW: 40.8 Da) and was substantially smaller between the IR>1-1.5 subsets (**Fig. 2A**). Distinct MW between peptide subsets can be due to differences in length, sequence or both. Therefore, in this and subsequent comparisons, we focused on changes in peptide length, frequency of P1 residues, and mean residue size at each peptide position.

Significant differences in peptide length distribution were observed between both the IR>1 and IR>1.5 subsets, consisting in an increased frequency of nonamers and a corresponding decrease of longer peptides in LCL 6370 relative to P50. These differences were very attenuated and non-significant between the IR>1-1.5 subsets (**Fig. 2B**).

A comparison of the P1 residue frequencies between either the IR>1 or IR>1.5 subsets revealed that the only statistically significant difference concerned the lower frequency of Ala1 in LCL 6370, relative to P50. No differences were observed between the IR>1-1.5 subsets (**Fig. 2C**). Thus, in the presence of ERAP2, the more active ERAP1 context of LCL 6370 results in a selective decrease in the abundance of peptides with Ala1, and much smaller effect on other

peptides. Of the five most frequent P1 residues among HLA-B*27 ligands (Ala, Gly, Lys, Arg, Ser) Ala is the one most susceptible to ERAP1 trimming. Only minor differences in the mean residue size at positions other than P1 were detected when the 9-mers of the IR>1.5 subsets were compared (**Fig. S2**).

The predicted affinity of the predominant B*27:05 ligands from both LCL (**Fig. 3A**) showed no significant differences, even when the comparison was restricted to the peptides showing the highest disparity in relative abundance (IR>3). Thus, in spite of the influence on peptide length, the Hap2/Hap10 ERAP1 mismatch in these cell lines did not induce global affinity changes. Accordingly, when the affinity of HLA-B*27 ligands was calculated as a function of peptide length, no differences were observed between 9-mers and 10-mers, which account for the large majority of the peptidome, with 11-mers, but not longer peptides, showing lower affinity (F**ig. 3B**).

*3.4. ERAP2 levels out the differential yield of HLA-B*27 ligands with N-terminal basic residues by ERAP1 variants*

In order to explain the similar abundance of peptides with basic P1 residues in the context of ERAP1 variants with distinct activity, Hap2 (LCL 6370) and Hap10 (LCL P50), in the presence of ERAP2, we determined the generation of six such ligands *in vitro* from synthetic precursors with two N-terminal extensions (**Fig. 4 A-B**). Recombinant ERAP1 Hap2 and Hap10 proteins were used in the presence or absence of ERAP2. Both the epitope yields with each ERAP1 variant and the effect of ERAP2 differed widely among individual peptides. Yet, whereas the mean yield of the six ligands was 1.8-fold higher with Hap2, relative to Hap10 (43.2% and 23.7%, respectively) in the absence of ERAP2, in presence of this enzyme it was 1.3-fold higher with Hap10 (27.7% *vs.* 20.7%). The effect of ERAP2 was particularly noticeable in the Hap2 context, where the mean yield of the ligands was 2.1-fold higher in the absence than in the presence of ERAP2, compared with 0.85-fold in the case of Hap10. These results indicate that ERAP2 diminishes the differences in the yields of HLA-B*27 ligands with basic P1 residues due to the differential activity of ERAP1 variants, leading to similar yields of these peptides, as observed in live cells.

A similar experiment concerning a B*27:05 ligand with N-terminal Ala, reproduced the pattern observed in LCL, whereby the yield of the ligand was higher in the less active ERAP1 context, both in the absence and presence of ERAP2 (**Fig. 4C**).

*3.5. Influence of ERAP2 expression in low activity ERAP1 contexts on the HLA-B*27 peptidome*

To determine the effects of ERAP2 in a low activity ERAP1 context (Hap10), relative to high activity ERAP1 variants in the absence of ERAP2, peptidome comparisons were carried out between LCL P50 (Hap10, ERAP2^{+}) and either LCL 10151 (Hap2, ERAP2^{-}) or 15510 (Hap1, ERAP2^{-}). As a control for ERAP-independent cell-to-cell differences, a contextual peptidome comparison was carried out between LCL 10150 and 15510. For each cell line pair the IR>1 (**Fig. S3)**, IR>1.5 (**Fig. 5**), and IR>1-1.5 (**Fig. S4**) subsets were compared.

3.5.1. LCL 10151/15510

These two cell lines express similar levels of the closely related, functionally undistinguishable [26], and high activity ERAP1 variants Hap2 and Hap1, respectively, and do not express ERAP2 **(Fig. 1**). A total of 3514 and 3002 HLA-B*27 ligands were identified from LCL 10150 and 15510, respectively, of which 2579 were found in both cell lines (**Table S2)**. A comparison of the IR>1.0 and the IR>1.5 peptide subsets from both cell lines revealed some differences in the MW distribution (ΔMW: 24.7 and 30.6 Da, respectively), which correlated with small, but statistically significant, differences in peptide length towards shorter peptides in LCL 15510, not observed in the IR>1-1.5 subsets. These differences were not previously detected [26], presumably due to their small magnitude or to the non-identical peptide sets identified in both analyses. Without ruling out a small influence of ERAP1 due to the Arg127Pro mismatch between the Hap2 and Hap1 variants, or to slightly different expression levels of the enzyme in both cell lines, our observation is also compatible with a moderate ERAP-independent effect on the length of HLA-B*27 ligands. No differences were found in the frequency of P1 residues between both cell lines, regardless of the IR subsets compared.

3.5.2. LCL 10151/P50

A total of 3459 and 2599 HLA-B*27 ligands were identified, of which 1922 were found in both cell lines (**Table S3)**. The MW distribution of the shared peptides showed only minimal

differences (ΔMW<8 Da) regardless of the IR subsets compared in both cell lines. However, marked differences in the distribution of peptide lengths were observed when either the IR>1.0 or IR>1.5 subsets of both cell lines were compared, consisting in an increased frequency of nonamers in LCL 10151 and a correspondingly lower frequency of longer peptides. These differences were absent in the comparison of the IR>1-1.5 groups from both cell lines.

The P1 residue frequencies among the peptides from the IR>1 and IR>1.5 subsets also showed highly significant differences, consisting n an increased frequency of Ala1 and Ser1 and lower frequency of basic P1 residues (Arg1, Lys1) in the Hap10/ERAP2^{+} context of LCL P50. These differences account for the similar mean MW of the peptides from these subsets: although the peptides from LCL P50 were longer they showed more small residues (Ala, Ser) and less bulky ones (Arg, Lys). No differences in P1 residue usage were observed in the comparison of the IR>1-1.5 subsets.

3.5.3. LCL 15510/P50

A very similar pattern was found in the peptidome comparisons involving these two cell lines. Of 2553 and 2488 HLA-B*27 ligands, 1731 were found in both LCL (**Table S4**). The comparisons involving all 3 peptide subsets with IR>1.0, IR>1.5 and IR>1.0-1.5 from both cell lines showed a moderate shift towards lower MW values in P50 (ΔMW: 19.2, 20.8 and 14.7 Da, respectively). This was not due to peptide length differences. Indeed, in the IR>1 and IR>1.5 subsets, 9-mers were more abundant in LCL 15510 and longer peptides prevailed in P50, with no differences in the IR>1-1.5 subsets. This pattern was like that in the 10151/P50 comparison.

Also like in 10151/P50, the P1 residues in the IR>1 and IR>1.5 subsets of LCL 15510 and P50 showed an increased frequency of Ala1 and Ser1 and decreased frequency of Arg1 and Lys1 in the latter cell line. In addition, a statistically significant increase in Gly1 was observed in the IR>1.5 subset of LCL P50. No differences were seen in the IR>1-1.5 subsets.

Small differences in the mean residue size at positions other than P1 were detected in the various pairwise comparisons (**Fig. S2**) that, together with the differential P1 usage, largely account for the MW differences observed. However, no consistent or specific pattern could be defined at these positions.

Both the increased length and higher frequency of Ala1 residues among the most abundant HLA-B*27 ligands from P50, relative to the ERAP2-negative LCL 10151 and 15510 were also observed when P50 was compared with the ERAP2^{+} LCL 6370, expressing the same ERAP1 variant as LCL 10151 (**Fig. 2**), indicating that both features are determined by ERAP1. However, the selective decrease of basic P1 residues was only observed across differences in ERAP2 expression and can be assigned to ERAP2. Thus, our results allowed us to distinguish the effects of ERAP1 and ERAP2, at least in this particular combination of ERAP1 variants, on the HLA-B*27 peptidome.

*3.6. ERAP2 expression decreases the affinity of the HLA-B*27 peptidome*

The theoretical affinity of the IR>1 peptide subsets for B*27:05 in the P50/10151, P50/15510 and 10151/15510 comparisons was determined (**Fig. 6A**). Small differences (p: 0.006) were observed between the ERAP2^{-} cells 10151/15510 that are, therefore, ERAP2-independent. The global affinity of the peptides in the IR>1 subsets from P50 relative to both 10151 and 15510 was lower and the differences in both cases were larger ($P<0.0001$) than in the 10151/15510 comparison. When the same analysis was carried out among the peptide subsets showing the highest differences in peptide abundance (IR>3), lower affinity was clearly observed in P50 relative to either 10151 or 15510, with no difference between the two latter LCL. The lower affinity of HLA-B*27 ligands predominant in the presence of ERAP2 is explained by the lower frequency of peptides with N-terminal basic residues in this context, since the affinity of peptides with either Arg1 or Lys1 was significantly higher than those with other P1 residues (**Fig. 6B**).

Thus, ERAP2 expression results in a lower affinity of the HLA-B*27:05 peptidome, which is mainly due to the effects of the enzyme on decreasing the abundance of peptides with N-terminal basic residues.

*3.7. Selective destruction of HLA-B*27 ligands with N-terminal Arg by ERAP2*

We previously showed that about 3-4% of the peptides with N-terminal basic residues from ERAP2^{-} cells expressing high activity ERAP1 variants were destroyed by ERAP2 [26]. We now compared the P1 residue frequencies of the total peptides identified from LCL P50,

6370, 10151 and 15510 (**Fig. 7**). There were no differences in the percentage of peptides with N-terminal basic residues (Arg+Lys) between either the two ERAP2^{+} or the ERAP2^{-} cells, but a statistically significant decrease between any ERAP2^{+} and any ERAP2^{-} LCL, ranging 6.6 to 10.2%, was observed (**Fig. 7A**). In a more detailed analysis (**Fig. 7B**), Arg was the only P1 residue that reproduced this pattern, showing 5.6 to 7.5% decrease in ERAP2^{+}, relative to ERAP2^{-} cells. These results strongly suggest that ERAP2 expressed in either high or low activity ERAP1 contexts destroys a significant amount of the peptides with Arg1 presented in the absence of this enzyme.

4. Discussion

The mechanism by which ERAP1 and ERAP2 jointly shape MHC-I peptidomes *in vivo* is still undefined. Their complementary substrate length and N-terminal residue specificities suggest a superior efficiency of their cooperative trimming. About 10-30% of the intracellular enzyme pools consist of ERAP1/ERAP2 heterodimers [2]. These are more efficient than the uncoupled enzymes in substrate processing, leading to faster rates and to the allosteric activation of ERAP1 [12], and may be able to process long peptides bound to MHC-I molecules [33]. Yet, the relevance of these heterodimers *in vivo* is not known and the predominance of monomeric enzymes in the ER suggests that ERAP1 and ERAP2 may trim peptides largely as separate enzymes.

The present study aimed at distinguishing the effects of ERAP1 and ERAP2 on shaping the HLA-B*27:05 peptidome in human cells. To this end we performed peptidome comparisons from cell lines with two distinct patterns of ERAP1/ERAP2 expression. A comparison involving two ERAP2-positive cell lines expressing either an AS-promoting ERAP1 variant with high activity (Hap2) or an AS-protective one (Hap10) with low activity, allowed us to assess the differential effects of these two variants when ERAP2 is also present. In a previous analysis of the B*27:04 peptidomes expressed in the context of these same ERAP1 haplotypes [24] the cell line expressing the most active variant did not express ERAP2, so that the effects of both enzymes could not be separated. Our results now allow us to distinguish the effects due to

ERAP1 polymorphism from those due to ERAP2 expression on the B*27:05 peptidome. Whereas a high activity ERAP1 context resulted in higher abundance of nonamers and increased over-trimming of peptides with Ala1, a residue that is highly susceptible to ERAP1 [9], the abundance of peptides with N-terminal basic residues was not affected. Thus, the differential usage of N-terminal basic residues among B*27:04 ligands found across the Hap2/Hap10 mismatch in our previous study was likely due to differences in ERAP2 expression. The lack of effect of this ERAP1 mismatch on the affinity of B*27:05 ligands is explained by the fact that nonamers and decamers, which account for the overwhelming majority of the peptidome, have similar affinity for B*27:05. This pattern, also observed in B*51:01 [28], is in contrast to MHC-I molecules, such as HLA-A*29:02, where 9-mers showed higher affinity than longer peptides [32]. HLA-B*27 ligands with Ala1 also showed no significant differences in affinity relative to most other peptides.

The increased abundance of nonamers in the Hap2 context, relative to Hap10, was also observed among B*27:04 ligands [24], and is presumably due to the Gln730Glu mismatch between these ERAP1 variants, because this difference determines distinct substrate length preferences, making the 730Gln variant more efficient with peptides longer than nonamers [34]. Length differences among B*27:05 ligands were not observed in peptidome comparisons involving ERAP1 variants with identity at residue 730 [25].

The second issue addressed in the present study is to what extent the effects of ERAP2 are dependent on the ERAP1 context. We previously reported that ERAP2 expression together with a high activity ERAP1 variant resulted in a moderate increase in the abundance of nonamers, which we attributed to an indirect effect of ERAP2 on ERAP1, and a very substantial decrease of peptides with N-terminal basic residues, which we ascribed directly to ERAP2 [26]. Now we extended these studies to determine the effects of ERAP2 when this enzyme is expressed in a low activity ERAP1 context.

The optimization of peptide length and decreased abundance of ligands with Ala1 observed in LCL 10151 and 15510, relative to P50, are explained by the highly active ERAP1 variants in the two former LCL (Hap2 and Hap1, respectively), which lack ERAP2, because an

identical pattern was observed when comparing the ERAP2^{+} cells with the same ERAP1 mismatch, LCL 6370 (Hap2) and P50 (Hap10).

The large decrease in the amounts of peptides with N-terminal basic residues in a low activity ERAP1/ERAP2^{+}, relative to a high activity ERAP1/ERAP2^{-} context, reproduced almost exactly the differences observed when the peptidomes from ERAP2^{-} and ERAP2^{+} cells expressing high activity ERAP1 variants were compared [26]. Thus, the major influence of ERAP2 on the B*27:05 peptidome is on the expression of peptide ligands with N-terminal basic residues and this effect is similar in either high or low activity ERAP1 contexts, compared to a high activity ERAP1/ERAP2^{-} context. On the basis of the *in vitro* digestions, ERAP2-mediated trimming may by more relevant in an active ERAP1 context, where peptides with N-terminal basic residues are generated by ERAP1 in higher amounts than with low activity variants. Since basic P1 residues favor B*27:05 binding [35,36] this explains the higher affinity of peptides with these residues and that, in the presence of ERAP2, the global affinity of the B*27:05 peptidome was lower.

These conclusions have significant implications to understand both the trimming of MHC-I ligands in the ER and the different patterns of ERAP1 and ERAP2 association with AS. Although the presence of ERAP2 may indirectly enhance ERAP1 trimming, the major effect on basic P1 residues regardless of the ERAP1 context strongly suggests that ERAP2 acts largely uncoupled from ERAP1 *in vivo*. Our results do not exclude a role of ERAP1/ERAP2 heterodimers, but these are not needed to explain the observed pattern of P1 residue usage. The preference of ERAP2 for short substrates makes this enzyme particularly relevant in epitope destruction, especially of peptides with basic P1 residues, which are relatively resistant to ERAP1. Thus, whereas highly active variants may favor over-trimming of B*27:05 ligands, especially those with susceptible residues, such as Ala, the presence of ERAP2 will induce over-trimming of those peptides that are more resistant to ERAP1.

These effects of ERAP2 should presumably be similar on other MHC-I peptidomes, depending on their P1 frequencies. For instance, HLA-B*40, which also shows some association with AS, binds a similar percentage of ligands with basic P1 residues, compared to

HLA-B*27 [37]. These effects imply significant alterations in the peptidome and argue towards a major role of ERAP2 in MHC-I epitope processing, rather than just an accessory function to that of ERAP1.

The associations of ERAP1 and ERAP2 with AS show some analogies, but also significant differences between each other. A major difference is that ERAP1 is associated with AS only among HLA-B*27 and HLA-B*40 positive individuals [17,18], whereas ERAP2 is a risk factor for both HLA-B*27 positive and negative AS [20]. The largely uncoupled nature of ERAP1 and ERAP2 trimming and the general effects of ERAP2 on destruction of epitopes with basic P1 residues may explain the distinct genetic association patterns.

A significant analogy concerning the involvement of ERAP1 and ERAP2 in AS is that both highly active ERAP1 variants and ERAP2 expression are risk factors, whereas loss-of-function ERAP1 variants or loss-of expression ERAP2 alleles are protective (reviewed in [23]). Thus, AS risk correlates with increased trimming by both enzymes, which is compatible with the idea that either epitope destruction or the optimal generation of particular epitope(s) in a highly active ERAP1/ERAP2 context, may favor disease.

In contrast, the disease association patterns of ERAP1 and ERAP2 are related to affinity and basic P1 residue usage in a more complex way**,** suggesting that these features of the HLA-B*27 peptidome are determined in each individual by his particular ERAP1/ERAP2 phenotype (**Table 2)**. For instance, a risk ERAP2 phenotype ($ERAP2^{+}$) leads to lower abundance of peptides with basic P1 residues and lower affinity, independently of the ERAP1 context, compared to a risk ERAP1(Hap1, Hap2)/$ERAP2^{-}$ phenotype. When protective (Hap10) and risk (Hap2, Hap3) ERAP1 variants are compared in the presence of ERAP2 the effects seem to depend on the specific ERAP1 haplotype.

Taken together, our results on the interactions of ERAP1 and ERAP2 with HLA-B*27 support a central role of peptides in AS pathogenesis, either through the generation or destruction of particular epitopes, affecting the role of HLA-B*27 in host defense and immune

homeostasis, or through alterations in the stability of the HLA-B*27 molecule, in turn affecting folding and/or cell surface dissociation, due to a modulation of peptide affinity by distinct ERAP1/ERAP2 phenotypes.

ACKNOWLEDGEMENTS

Supported by grants SAF2014/51931-R (Plan Nacional de I+D+i) to JALC, Binational Science Foundation Grant 2009393 to AA, and an institutional grant of the Fundación Ramón Areces to the Centro de Biología Molecular *Severo Ochoa.* AME and PG are fellows of the Spanish Government (BES-2012-052113 and BES-2015-072729, respectively). We thank Dr. Maxime Breban (Université de Versailles Saint-Quentin-en-Yvelines, INSERM U1016), Irini Evnouchidou and Peter van Endert (Hôpital Necker, INSERM U1151, Paris) for the LCL 10151, 15510 and 6370, and Dr. Efstratios Stratikos for recombinant baculoviruses. We also thank Sergio Ciordia and María del Carmen Mena (Proteomics Unit, Centro Nacional de Biotecnología, Madrid) for technical assistance in MS.

Table 1. ERAP1 and ERAP2 expression in the cell lines used in this study[a].

LCL	ERAP2	ERAP1[b]	12	56	127	276	346	349	528	575	725	730
P50	+	Hap10	T	E	P	I	G	V	R	N	Q	E
6370	+	**Hap2**	T	E	**R**	I	G	**M**	**K**	**D**	**R**	**Q**
10151	-	**Hap2**	T	E	**R**	I	G	**M**	**K**	**D**	**R**	**Q**
15510	-	**Hap1**	**I**	E	P	I	G	**M**	**K**	**D**	**R**	**Q**

[a]This table is a summary of previously published data [25,26], which are shown here only for clarity. [b]The ERAP1 haplotype (Hap) nomenclature proposed for the most common ERAP1 variants in HapMap populations [13] has been adopted. The corresponding polymorphic positions are shown. ERAP1 haplotypes and amino acid residues associated with increased risk of AS are shown in boldface.

Table 2. ERAP1/ERAP2 phenotypes in LCL and their effects on HLA-B*27 ligands with basic P1 residues and affinity.

LCL compared	ERAP1 (ERAP2) phenotype	AS association of ERAP1 and ERAP2[a]	Abundance of peptides with basic P1 residues	Effect on affinity	Reference
6370/10151	Hap2 (+)/Hap2 (-)	RR/RP	Decreased	ND[b]	[26]
6370/15510	Hap2 (+)/Hap1 (-)	RR/RP	Decreased	ND[b]	[26]
10151/15510	Hap2 (-)/Hap1 (-)	RP/RP	Unchanged	None	This study
P50/6370	Hap10 (+)/Hap2 (+)	PR/RR	Unchanged	None	This study
P50/LG2	Hap10 (+)/Hap3 (+)	PR/RR	Decreased	Decreased	[25,38]
P50/10151	Hap10 (+)/Hap2 (-)	PR/RP	Decreased	Decreased	This study
P50/15510	Hap10 (+)/Hap1 (-)	PR/RP	Decreased	Decreased	This study
WEI/JSL[c]	Hap10 (+)/Hap2 (-)	PR/RP	Decreased	Decreased	[24,38]

[a]R: risk variant; P: protective variant. Only comparisons involving risk (Hap1-Hap3) o protective (Hap10) ERAP1 variants are included. [b] ND: not determined.. [c]B*27:04$^+$ cell lines.

Figure legends.

Figure 1. ERAP1 and ERAP2 protein expression on HLA-B*2705-positive LCL. Western blots showing the expression of (A) ERAP1 and (B) ERAP2 in the indicated LCL. In each case the upper panel shows a representative experiment. The lower panels show the expression levels of ERAP1or ERAP2, relative to the LCL showing maximal values. These results are the mean ± standard deviation of triplicate experiments. ERAP1 and ERAP2 expression in LCL 10151, 15510 and 6370 [26] and those of P50 [25] were previously reported. The immunoblots were jointly repeated here to directly compare the relative expression levels in the four LCL.

Figure 2. Quantitative comparison of shared B*27:05 ligands from LCL 6370 and P50. Of a total of 1470 ligands found in both cell lines, 825 and 645 showed IR>1 in LCL 6370 and P50, respectively. These were subdivided in two subsets: IR>1.5 (629 and 426 peptides, respectively) and IR>1 to 1.5 (196 and 219 peptides, respectively). **(A)** MW distribution of the peptides from the indicated IR subsets from both LCL. (B) Length distribution of the peptides from the indicated IR subsets. (C) Percent frequency of peptides in the indicated IR subsets from each cell line with the N-terminal residues shown in the x-axis. Statistically significant differences were estimated by the χ^2 test with Bonferroni correction. They are labeled with asterisks (*) and their p-values are indicated.

Figure 3. Theoretical affinity of shared B*27:05 ligands from LCL 6370 and P50. (A) Comparison of the binding affinity of the predominant peptides in both cell lines. The IR subsets compared are indicated. The affinity distribution in each peptide subset is indicated by its median. (B) Binding affinity of the shared B*27:05 ligands from both cell lines as a function of their length. Statistical comparisons were carried out by the Mann-Whitney test. NS: not significant; (*): $p<0.01$; (**): $p<0.001$; (***): $p<0.0001$.

Figure 4. Effect of ERAP2 on the generation of B*27:05 ligands *in vitro*. (A) Percent yields of six B*27:05 ligands with N-terminal basic residues, from synthetic precursors with two N-terminal extensions, by the recombinant ERAP1 variants Hap2 and Hap10 in the absence or presence of ERAP2. Horizontal bars indicate the mean of each series. Yields were measured at the longest reaction time, 64 min, and are means of three experiments. (B) Percent yield of two

B*27:05 ligands with N-terminal basic residues (RRYGDVFQI and KRQGRTLYGF), out of the six in panel A, from the indicated synthetic precursors, as a function of time, with the ERAP1 variants Hap2 and Hap10 in the absence (solid lines) or presence (dotted lines) of ERAP2. (C) Percent yield of a B*27:05 ligand with N-terminal Ala (ARYGKSPYLY) from the indicated synthetic precursor, as described in panel B. The data in panes B and C are means ± standard deviation of three independent experiments.

Figure 5. Quantitative comparison of shared B*27:05 ligands between LCL pairs: IR>1.5 subsets.. (**A**) MW and (**B**) length distribution of the peptides from the indicated LCL. (**C**) Percentage of peptides with the N-terminal residues shown in the x-axis from the indicated cell lines (code as in panel B). Statistically significant differences are labeled with asterisks (*) and their p-values are indicated. The number of peptides from the IR>1.5 subsets in each comparison were as follows. LCL 10151/15510: 929 and 731; LCL 10151/P50: 787 and 657; LCL 15510/P50: 663 and 622.

Figure 6. Theoretical affinity of shared B*27:05 ligands from ERAP2-negative and -positive cells. (**A**) Comparison of the binding affinity of the predominant peptide subsets from the indicated cell lines and IR subsets. The affinity distribution in each peptide subset is indicated by its median. (**B**) Predicted affinity of B*27:05 ligands according to the nature of their N-terminal residues: Arg1 (R), Lys1 (K), or other. All the 4945 peptides identified in this study from the 4 cell lines were included in this analysis. Statistical comparisons were carried out by the Mann-Whitney test. NS: not significant; (*): $p<0.01$; (**): $p<0.001$; (***): $p<0.0001$.

Figure 7. N-terminal residue usage among B*27:05 ligands from ERAP2-negative and -positive cells. (A) Percent of HLA-B*27:05 ligands identified from LCL 10151 (N: 3756), 15510 (N: 3275), 6370 (N: 1712) and P50 (N: 3098) with N-terminal basic (R+K) or other residues. Statistically significant differences were estimated by the χ^2 test. They are labeled with asterisks (*) and their p-values are indicated. NS: not significant. (B) Percent frequencies of the N-terminal residues shown in the x-axis among the B*27:05 ligands of the indicated cell lines. Arg1 usage was statistically different between ERAP2-positive and negative cell lines (labeled with *: p values ranging 2.5E-04 to 6.8E-9).

Reference List

[1] T. Saric, S.C. Chang, A. Hattori, I.A. York, S. Markant, K.L. Rock, M. Tsujimoto, A.L. Goldberg, An IFN-gamma-induced aminopeptidase in the ER, ERAP1, trims precursors to MHC class I-presented peptides, Nat.Immunol. 3 (2002) 1169-1176.

[2] L. Saveanu, O. Carroll, V. Lindo, M. Del Val, D. Lopez, Y. Lepelletier, F. Greer, L. Schomburg, D. Fruci, G. Niedermann, P.M. Van Endert, Concerted peptide trimming by human ERAP1 and ERAP2 aminopeptidase complexes in the endoplasmic reticulum, Nat.Immunol. 6 (2005) 689-697.

[3] M. Tsujimoto,A. Hattori, The oxytocinase subfamily of M1 aminopeptidases, Biochim.Biophys.Acta 1751 (2005) 9-18.

[4] L. Saveanu,P. van Endert, The role of insulin-regulated aminopeptidase in MHC class I antigen presentation, Front Immunol. 3 (2012) 57.

[5] T. Tanioka, A. Hattori, S. Masuda, Y. Nomura, H. Nakayama, S. Mizutani, M. Tsujimoto, Human leukocyte-derived arginine aminopeptidase. The third member of the oxytocinase subfamily of aminopeptidases, J.Biol.Chem. 278 (2003) 32275-32283.

[6] J.R. Birtley, E. Saridakis, E. Stratikos, I.M. Mavridis, The crystal structure of human endoplasmic reticulum aminopeptidase 2 reveals the atomic basis for distinct roles in antigen processing, Biochemistry 51 (2012) 286-295.

[7] A. Mpakali, P. Giastas, N. Mathioudakis, I.M. Mavridis, E. Saridakis, E. Stratikos, Structural basis for antigenic peptide recognition and processing by ER aminopeptidase 2, J.Biol.Chem. 290 (2015) 26021-26032.

[8] J.A. Lopez de Castro, C. Alvarez-Navarro, A. Brito, P. Guasp, A. Martin-Esteban, A. Sanz-Bravo, Molecular and pathogenic effects of endoplasmic reticulum aminopeptidases ERAP1 and ERAP2 in MHC-I-associated inflammatory disorders: Towards a unifying view, Mol.Immunol. 77 (2016) 193-204.

[9] A. Hearn, I.A. York, K.L. Rock, The specificity of trimming of MHC class I-presented peptides in the endoplasmic reticulum, J.Immunol. 183 (2009) 5526-5536.

[10] I. Evnouchidou, J. Birtley, S. Seregin, A. Papakyriakou, E. Zervoudi, M. Samiotaki, G. Panayotou, P. Giastas, O. Petrakis, D. Georgiadis, A. Amalfitano, E. Saridakis, I.M. Mavridis, E. Stratikos, A common SNP in ER aminopeptidase 2 induces a specificity switch that leads to altered antigen processing, J.Immunol. 189 (2012) 2383-2392.

[11] S.C. Chang, F. Momburg, N. Bhutani, A.L. Goldberg, The ER aminopeptidase, ERAP1, trims precursors to lengths of MHC class I peptides by a "molecular ruler" mechanism, Proc.Natl.Acad.Sci.U.S.A 102 (2005) 17107-17112.

[12] I. Evnouchidou, M. Weimershaus, L. Saveanu, P. van Endert, ERAP1-ERAP2 Dimerization Increases Peptide-Trimming Efficiency, J.Immunol. 193 (2014) 901-908.

[13] M.J. Ombrello, D.L. Kastner, E.F. Remmers, Endoplasmic reticulum-associated amino-peptidase 1 and rheumatic disease: genetics, Curr.Opin.Rheumatol. 27 (2015) 349-356.

[14] A.M. Andres, M.Y. Dennis, W.W. Kretzschmar, J.L. Cannons, S.Q. Lee-Lin, B. Hurle, P.L. Schwartzberg, S.H. Williamson, C.D. Bustamante, R. Nielsen, A.G. Clark, E.D.

Green, Balancing selection maintains a form of ERAP2 that undergoes nonsense-mediated decay and affects antigen presentation, PLoS.Genet. 6 (2010) e1001157.

[15] D.L. Vanhille, L.D. Hill, D.D. Hilliard, E.D. Lee, M.E. Teves, S. Srinivas, J.P. Kusanovic, R. Gomez, E. Stratikos, M.A. Elovitz, R. Romero, J.F. Strauss, III, A Novel Haplotype Structure in a Chilean Population: Implications for ERAP2 Protein Expression and Preeclampsia Risk, Mol.Genet.Genomic.Med. 1 (2013) 98-107.

[16] D.A. Brewerton, F.D. Hart, A. Nicholls, M. Caffrey, D.C. James, R.D. Sturrock, Ankylosing spondylitis and HL-A 27, Lancet 1 (1973) 904-907.

[17] The TASK and WTCCC2 Consortia, Interaction between ERAP1 and HLA-B27 in ankylosing spondylitis implicates peptide handling in the mechanism for HLA-B27 in disease susceptibility, Nat.Genet. 43 (2011) 761-767.

[18] A. Cortes, S.L. Pulit, P.J. Leo, J.J. Pointon, P.C. Robinson, M.H. Weisman, M. Ward, L.S. Gensler, X. Zhou, H.J. Garchon, G. Chiocchia, J. Nossent, B.A. Lie, O. Forre, J. Tuomilehto, K. Laiho, L.A. Bradbury, D. Elewaut, R. Burgos-Vargas, S. Stebbings, L. Appleton, C. Farrah, J. Lau, N. Haroon, J. Mulero, F.J. Blanco, M.A. Gonzalez-Gay, C. Lopez-Larrea, P. Bowness, K. Gaffney, H. Gaston, D.D. Gladman, P. Rahman, W.P. Maksymowych, J.B. Crusius, van der Horst-Bruinsma IE, R. Valle-Onate, C. Romero-Sanchez, I.M. Hansen, F.M. Pimentel-Santos, R.D. Inman, J. Martin, M. Breban, B.P. Wordsworth, J.D. Reveille, D.M. Evans, P.I. de Bakker, M.A. Brown, Major histocompatibility complex associations of ankylosing spondylitis are complex and involve further epistasis with ERAP1, Nat.Commun. 6 (2015) 7146.

[19] A. Cortes, J. Hadler, J.P. Pointon, P.C. Robinson, T. Karaderi, P. Leo, K. Cremin, K. Pryce, J. Harris, S. Lee, K.B. Joo, S.C. Shim, M. Weisman, M. Ward, X. Zhou, H.J. Garchon, G. Chiocchia, J. Nossent, B.A. Lie, O. Forre, J. Tuomilehto, K. Laiho, L. Jiang, Y. Liu, X. Wu, L.A. Bradbury, D. Elewaut, R. Burgos-Vargas, S. Stebbings, L. Appleton, C. Farrah, J. Lau, T.J. Kenna, N. Haroon, M.A. Ferreira, J. Yang, J. Mulero, J.L. Fernandez-Sueiro, M.A. Gonzalez-Gay, C. Lopez-Larrea, P. Deloukas, P. Donnelly, P. Bowness, K. Gafney, H. Gaston, D.D. Gladman, P. Rahman, W.P. Maksymowych, H. Xu, J.B. Crusius, van der Horst-Bruinsma IE, C.T. Chou, R. Valle-Onate, C. Romero-Sanchez, I.M. Hansen, F.M. Pimentel-Santos, R.D. Inman, V. Videm, J. Martin, M. Breban, J.D. Reveille, D.M. Evans, T.H. Kim, B.P. Wordsworth, M.A. Brown, Identification of multiple risk variants for ankylosing spondylitis through high-density genotyping of immune-related loci, Nat.Genet. 45 (2013) 730-738.

[20] P.C. Robinson, M.E. Costello, P. Leo, L.A. Bradbury, K. Hollis, A. Cortes, S. Lee, K.B. Joo, S.C. Shim, M. Weisman, M. Ward, X. Zhou, H.J. Garchon, G. Chiocchia, J. Nossent, B.A. Lie, O. Forre, J. Tuomilehto, K. Laiho, L. Jiang, Y. Liu, X. Wu, D. Elewaut, R. Burgos-Vargas, L.S. Gensler, S. Stebbings, N. Haroon, J. Mulero, J.L. Fernandez-Sueiro, M.A. Gonzalez-Gay, C. Lopez-Larrea, P. Bowness, K. Gafney, J.S. Gaston, D.D. Gladman, P. Rahman, W.P. Maksymowych, H. Xu, van der Horst-Bruinsma IE, C.T. Chou, R. Valle-Onate, M.C. Romero-Sanchez, I.M. Hansen, F.M. Pimentel-Santos, R.D. Inman, J. Martin, M. Breban, D. Evans, J.D. Reveille, T.H. Kim, B.P. Wordsworth, M.A. Brown, ERAP2 is associated with ankylosing spondylitis in HLA-B27-positive and HLA-B27-negative patients, Ann.Rheum.Dis. 74 (2015) 1627-1629.

[21] Y. Goto, A. Hattori, Y. Ishii, M. Tsujimoto, Reduced activity of the hypertension-associated Lys528Arg mutant of human adipocyte-derived leucine aminopeptidase (A-LAP)/ER-aminopeptidase-1, FEBS Lett. 580 (2006) 1833-1838.

[22] E. Reeves, C.J. Edwards, T. Elliott, E. James, Naturally Occurring ERAP1 Haplotypes Encode Functionally Distinct Alleles with Fine Substrate Specificity, J.Immunol. 191 (2013) 35-43.

[23] P.C. Robinson,M.A. Brown, Genetics of ankylosing spondylitis, Mol.Immunol. 57 (2014) 2-11.

[24] N. Garcia-Medel, A. Sanz-Bravo, D. Van Nguyen, B. Galocha, P. Gomez-Molina, A. Martin-Esteban, C. Alvarez-Navarro, J.A. López de Castro, Functional Interaction of the Ankylosing Spondylitis-associated Endoplasmic Reticulum Aminopeptidase 1 Polymorphism and HLA-B27 in Vivo, Mol.Cell Proteomics. 11 (2012) 1416-1429.

[25] A. Sanz-Bravo, J. Campos, M.S. Mazariegos, J.A. Lopez de Castro, Dominant Role of the ERAP1 Polymorphism R528K in Shaping the HLA-B27 Peptidome Through Differential Processing Determined by Multiple Peptide Residues, Arthritis Rheumatol. 67 (2015) 692-701.

[26] A. Martin-Esteban, P. Guasp, E. Barnea, A. Admon, J.A. Lopez de Castro, Functional Interaction of the Ankylosing Spondylitis Associated Endoplasmic Reticulum Aminopeptidase 2 with the HLA-B*27 Peptidome in Human Cells, Arthritis Rheumatol. 68 (2016) 2466-2475.

[27] S.A. Ellis, C. Taylor, A. McMichael, Recognition of HLA-B27 and related antigens by a monoclonal antibody, Hum.Immunol. 5 (1982) 49-59.

[28] P. Guasp, C. Alvarez-Navarro, P. Gomez-Molina, A. Martin-Esteban, M. Marcilla, E. Barnea, A. Admon, J.A. López de Castro, The peptidome of the Behcet's disease-associated HLA-B*51:01 includes two sub-peptidomes differentially shaped by ERAP1, Arthritis Rheumatol. 68 (2016) 505-515.

[29] J. Cox,M. Mann, MaxQuant enables high peptide identification rates, individualized p.p.b.-range mass accuracies and proteome-wide protein quantification, Nat.Biotechnol. 26 (2008) 1367-1372.

[30] J. Cox, N. Neuhauser, A. Michalski, R.A. Scheltema, J.V. Olsen, M. Mann, Andromeda: a peptide search engine integrated into the MaxQuant environment, J.Proteome.Res. 10 (2011) 1794-1805.

[31] E. Karosiene, C. Lundegaard, O. Lund, M. Nielsen, NetMHCcons: a consensus method for the major histocompatibility complex class I predictions, Immunogenetics 64 (2012) 177-186.

[32] C. Alvarez-Navarro, A. Martin-Esteban, E. Barnea, A. Admon, J.A. Lopez de Castro, ERAP1 polymorphism relevant to inflammatory disease shapes the peptidome of the birdshot chorioretinopathy-associated HLA-A*29:02 antigen, Mol.Cell Proteomics 14 (2015) 1770-1780.

[33] H. Chen, L. Li, M. Weimershaus, I. Evnouchidou, P. van Endert, M. Bouvier, ERAP1-ERAP2 dimers trim MHC I-bound precursor peptides; implications for understanding peptide editing, Sci.Rep. 6 (2016) 28902.

[34] A. Stamogiannos, D. Koumantou, A. Papakyriakou, E. Stratikos, Effects of polymorphic variation on the mechanism of Endoplasmic Reticulum Aminopeptidase 1, Mol.Immunol. 67 (2015) 426-435.

[35] J.R. Lamas, A. Paradela, F. Roncal, J.A. Lopez de Castro, Modulation at multiple anchor positions of the peptide specificity of HLA-B27 subtypes differentially associated with ankylosing spondylitis, Arthritis Rheum. 42 (1999) 1975-1985.

[36] R.C. Hillig, M. Huelsmeyer, W. Saenger, K. Welfle, R. Misselwitz, H. Welfle, C. Kozerski, A. Volz, B. Uchanska-Ziegler, A. Ziegler, Thermodynamic and structural analysis of peptide-and allele-dependent properties of two HLA-B27 subtypes exhibiting differential disease association, J.Biol.Chem. 279 (2004) 652-663.

[37] N. Hillen, G. Mester, C. Lemmel, A.O. Weinzierl, M. Muller, D. Wernet, J. Hennenlotter, A. Stenzl, H.G. Rammensee, S. Stevanovic, Essential differences in ligand presentation and T cell epitope recognition among HLA molecules of the HLA-B44 supertype, Eur.J.Immunol. 38 (2008) 2993-3003.

[38] A. Sanz-Bravo, Mecanismo molecular implicado en la configuración del peptidoma de HLA-B*27 por variantes naturales de ERAP1 asociadas a la espondilitis anquilosante, PhD Thesis, Universidad Autónoma de Madrid (2015).

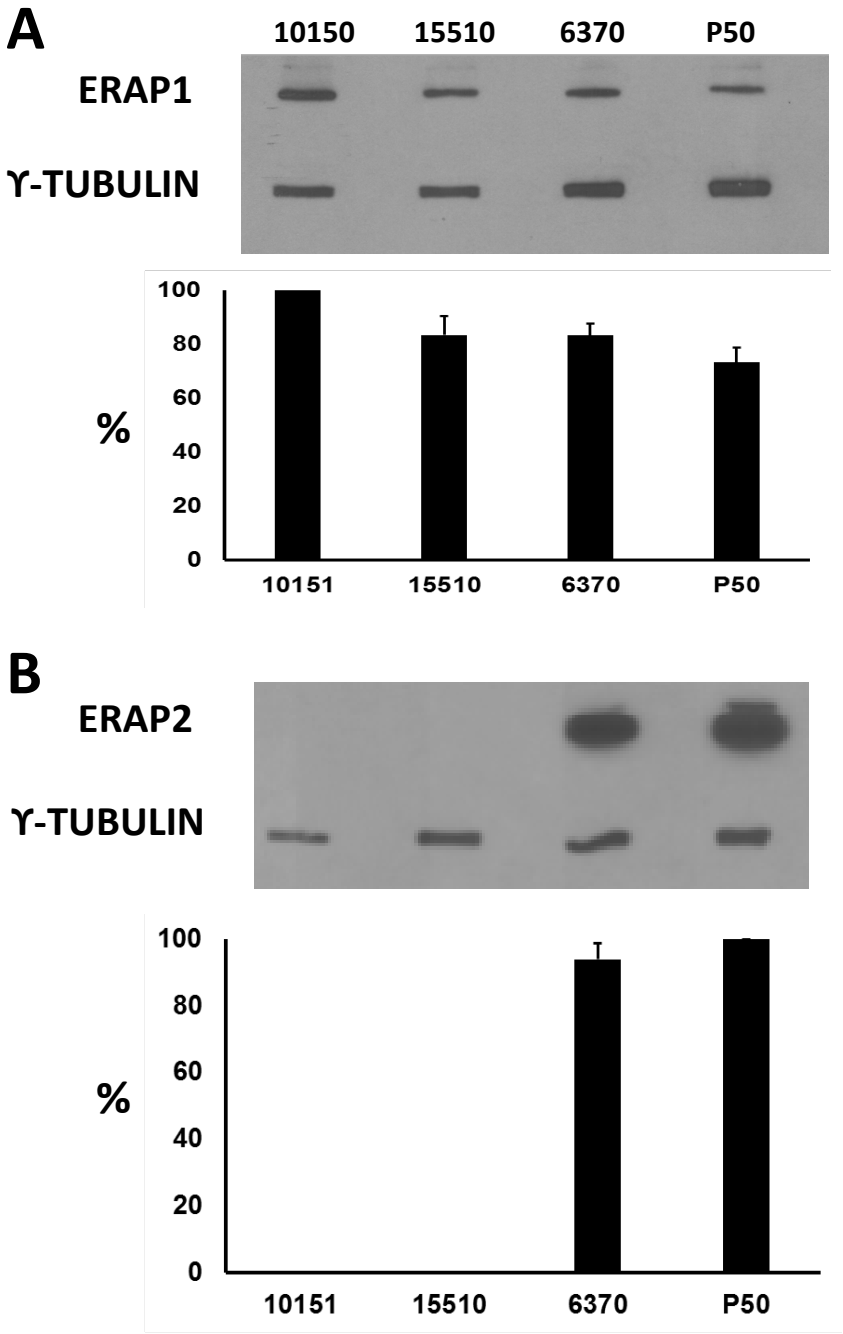
A
10150
15510
6370
P50
ERAP1
ϒ-TUBULIN
%
100
80
60
40
20
0
10151
15510
6370
P50
B
ERAP2
ϒ-TUBULIN
%
100
80
60
40
20
0
10151
15510
6370
P50

Figure 1

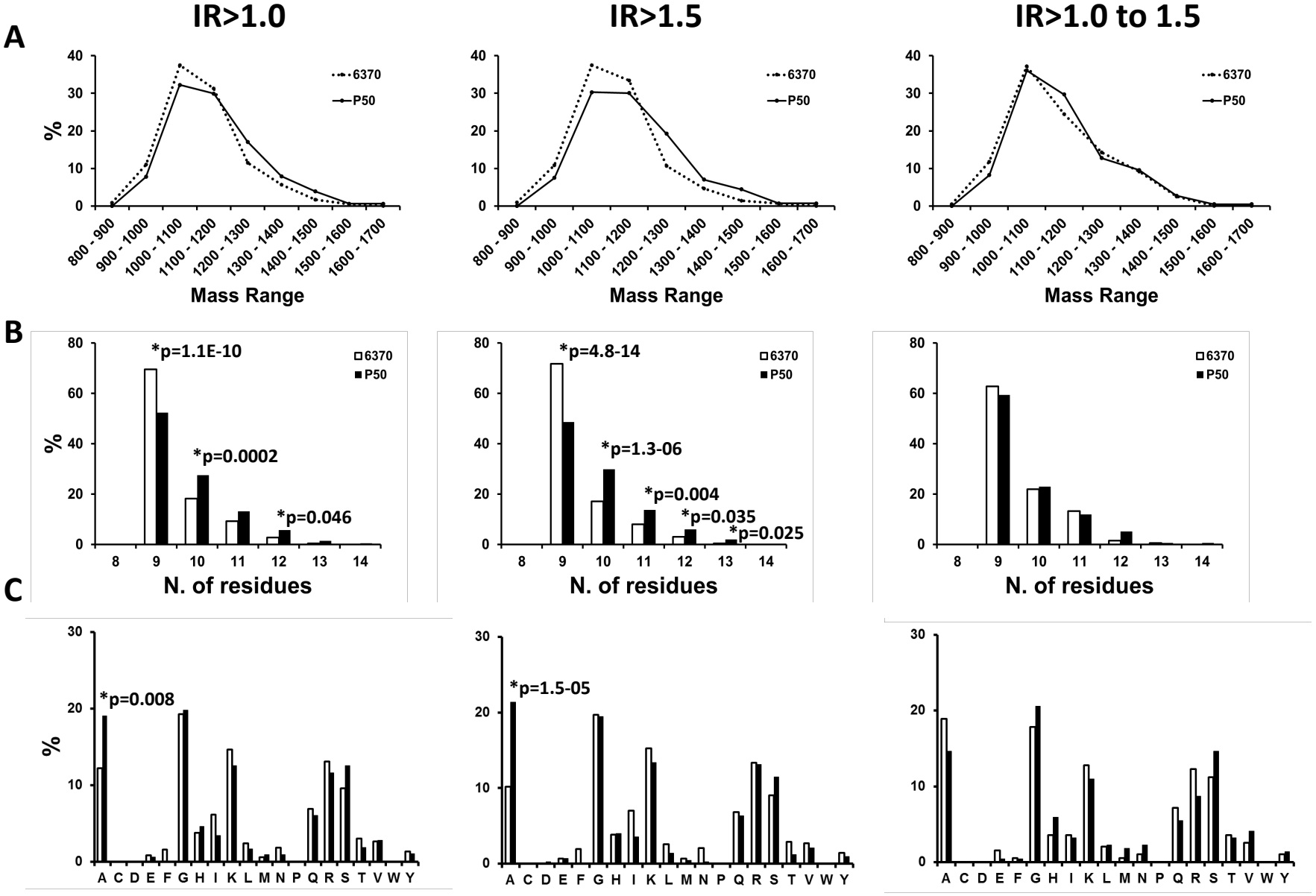
A
IR>1.0
IR>1.5
IR>1.0 to 1.5
%
6370
P50
800 - 900
900 - 1000
1000 - 1100
1100 - 1200
1200 - 1300
1300 - 1400
1400 - 1500
1500 - 1600
1600 - 1700
Mass Range
B
*p=1.1E-10
*p=0.0002
*p=0.046
*p=4.8-14
*p=1.3-06
*p=0.004
*p=0.035
*p=0.025
N. of residues
C
*p=0.008
*p=1.5-05
A C D E F G H I K L M N P Q R S T V W Y

Figure 2

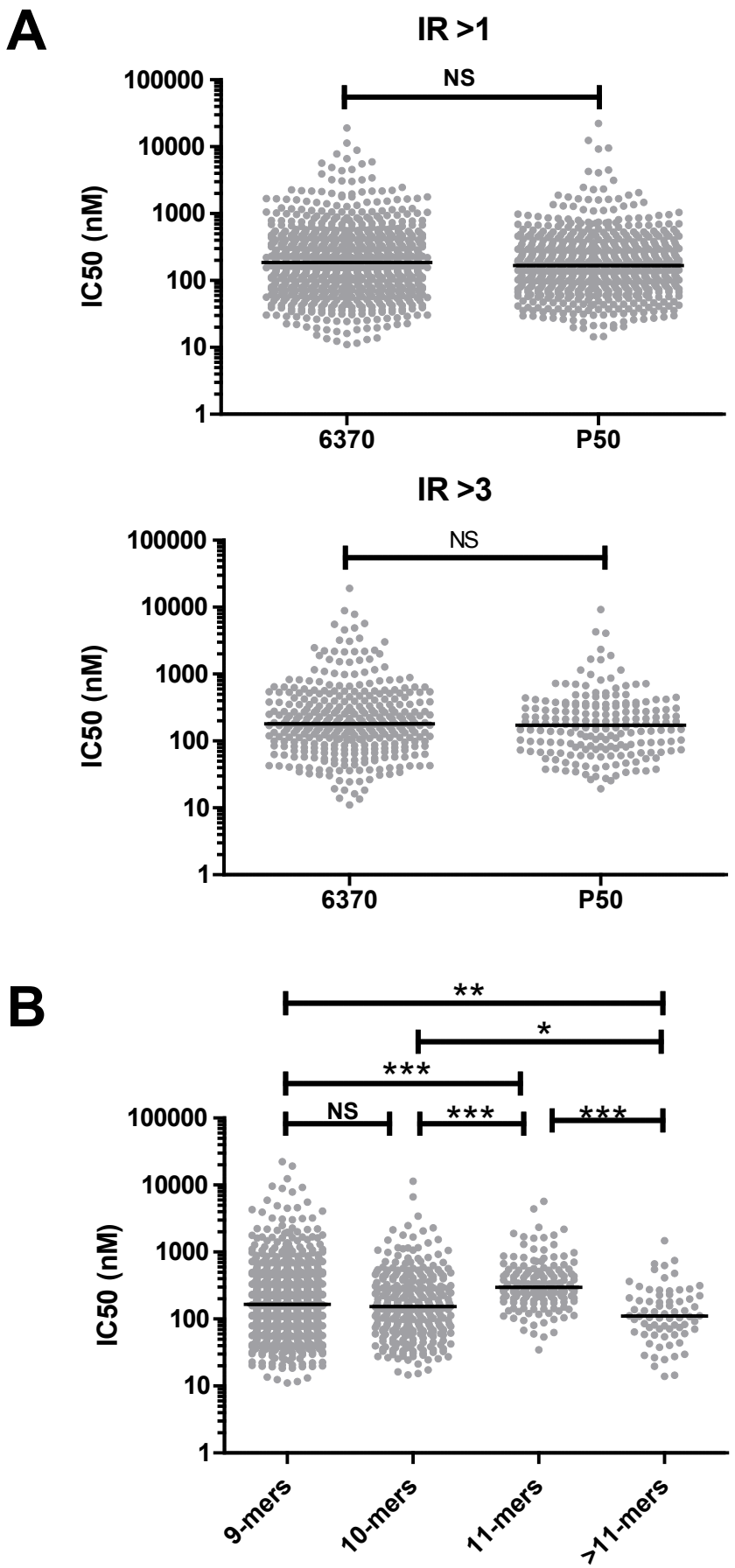
A
IR >1
NS
100000
10000
1000
100
10
1
IC50 (nM)
6370
P50
IR >3
NS
100000
10000
1000
100
10
1
IC50 (nM)
6370
P50
B
**
*
***
NS
***
***
100000
10000
1000
100
10
1
IC50 (nM)
9-mers
10-mers
11-mers
>11-mers

Figure 3

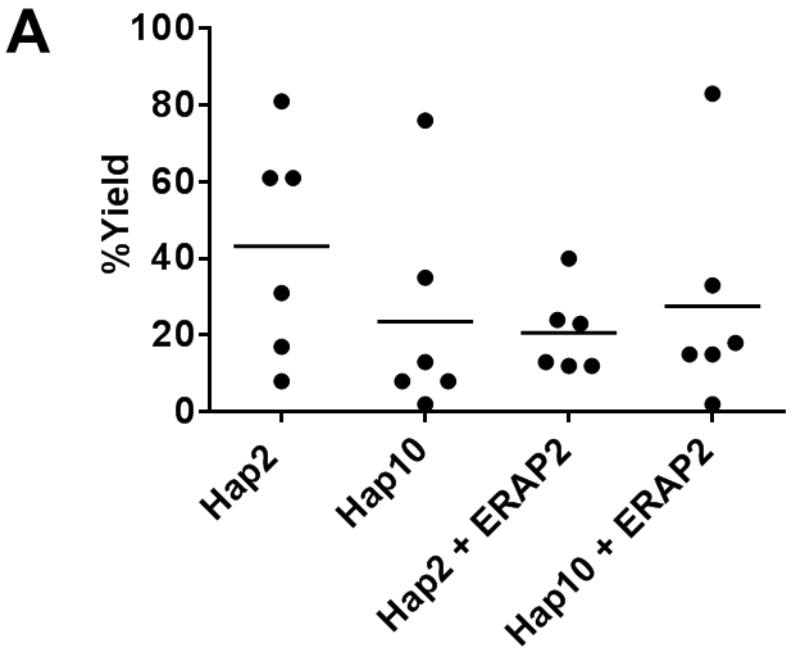
A
100
80
60
40
20
0
%Yield
Hap2
Hap10
Hap2 + ERAP2
Hap10 + ERAP2

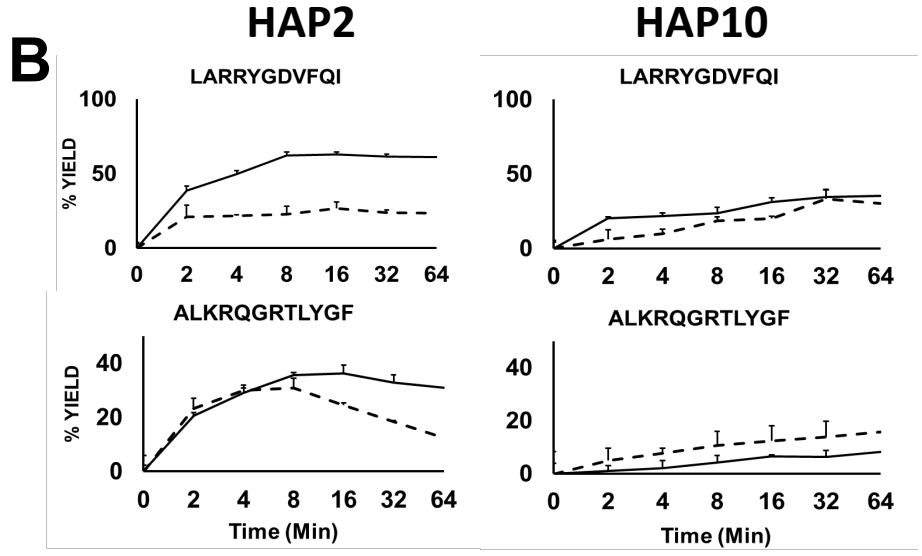
B
HAP2
HAP10
LARRYGDVFQI
% YIELD
100
50
0
0 2 4 8 16 32 64
ALKRQGRTLYGF
40
20
Time (Min)

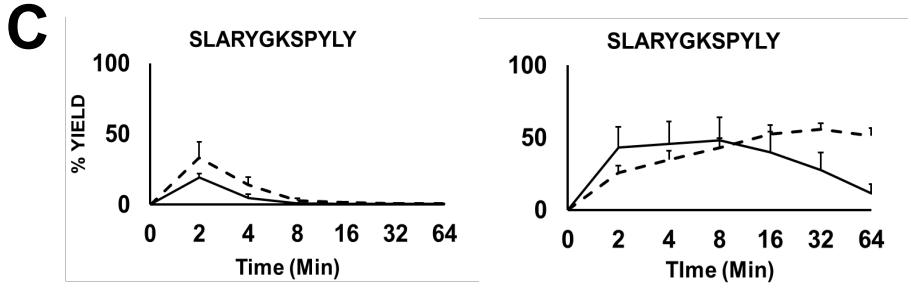
C
SLARYGKSPYLY
% YIELD
100
50
0
0 2 4 8 16 32 64
Time (Min)
TIme (Min)

Figure 4

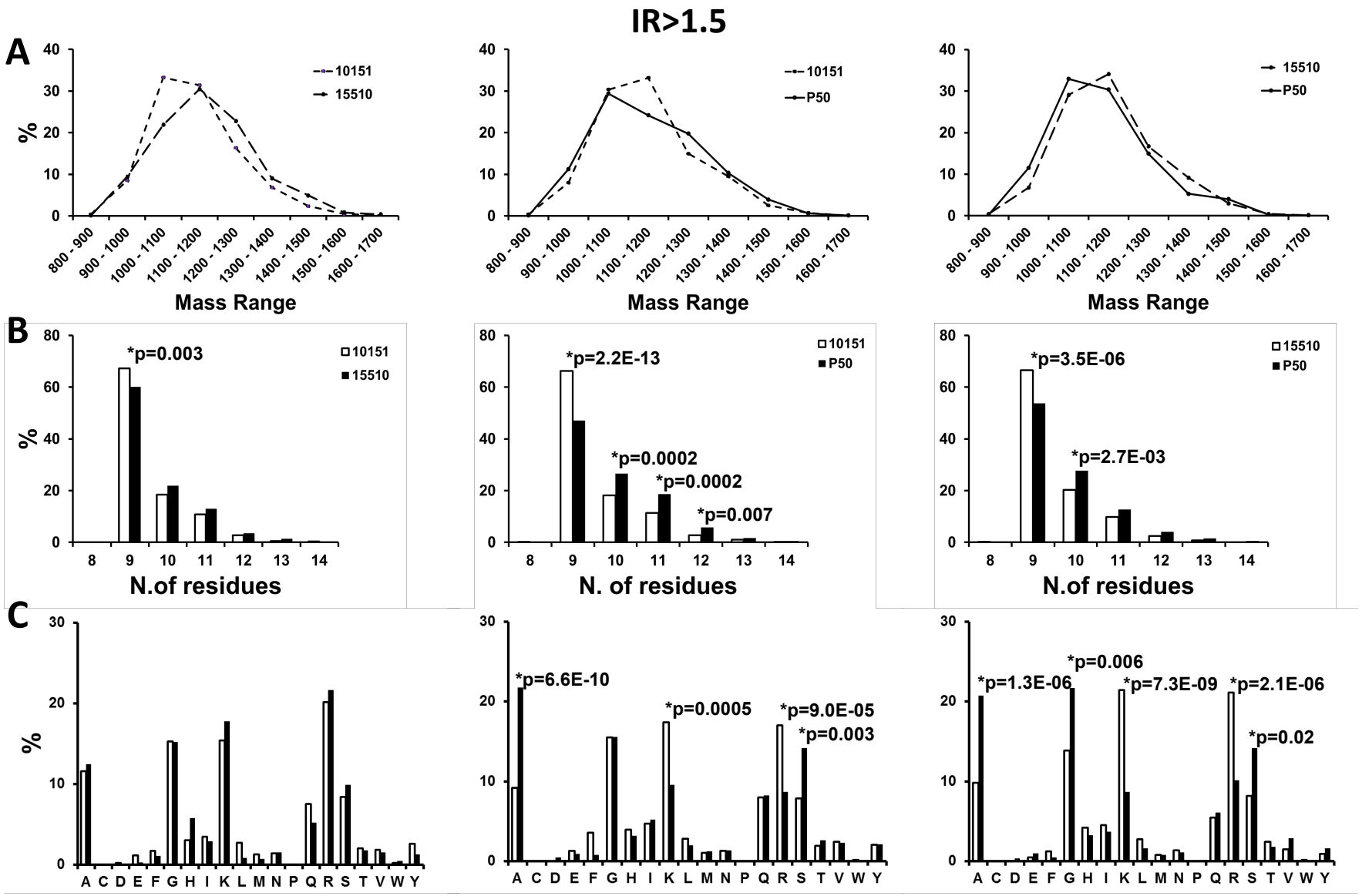
IR>1.5
A
%
10151
15510
P50
Mass Range
800 - 900
900 - 1000
1000 - 1100
1100 - 1200
1200 - 1300
1300 - 1400
1400 - 1500
1500 - 1600
1600 - 1700
B
N.of residues
N. of residues
*p=0.003
*p=2.2E-13
*p=0.0002
*p=0.0002
*p=0.007
*p=3.5E-06
*p=2.7E-03
C
*p=6.6E-10
*p=0.0005
*p=9.0E-05
*p=0.003
*p=0.006
*p=1.3E-06
*p=7.3E-09
*p=2.1E-06
*p=0.02
A C D E F G H I K L M N P Q R S T V W Y

Figure 5

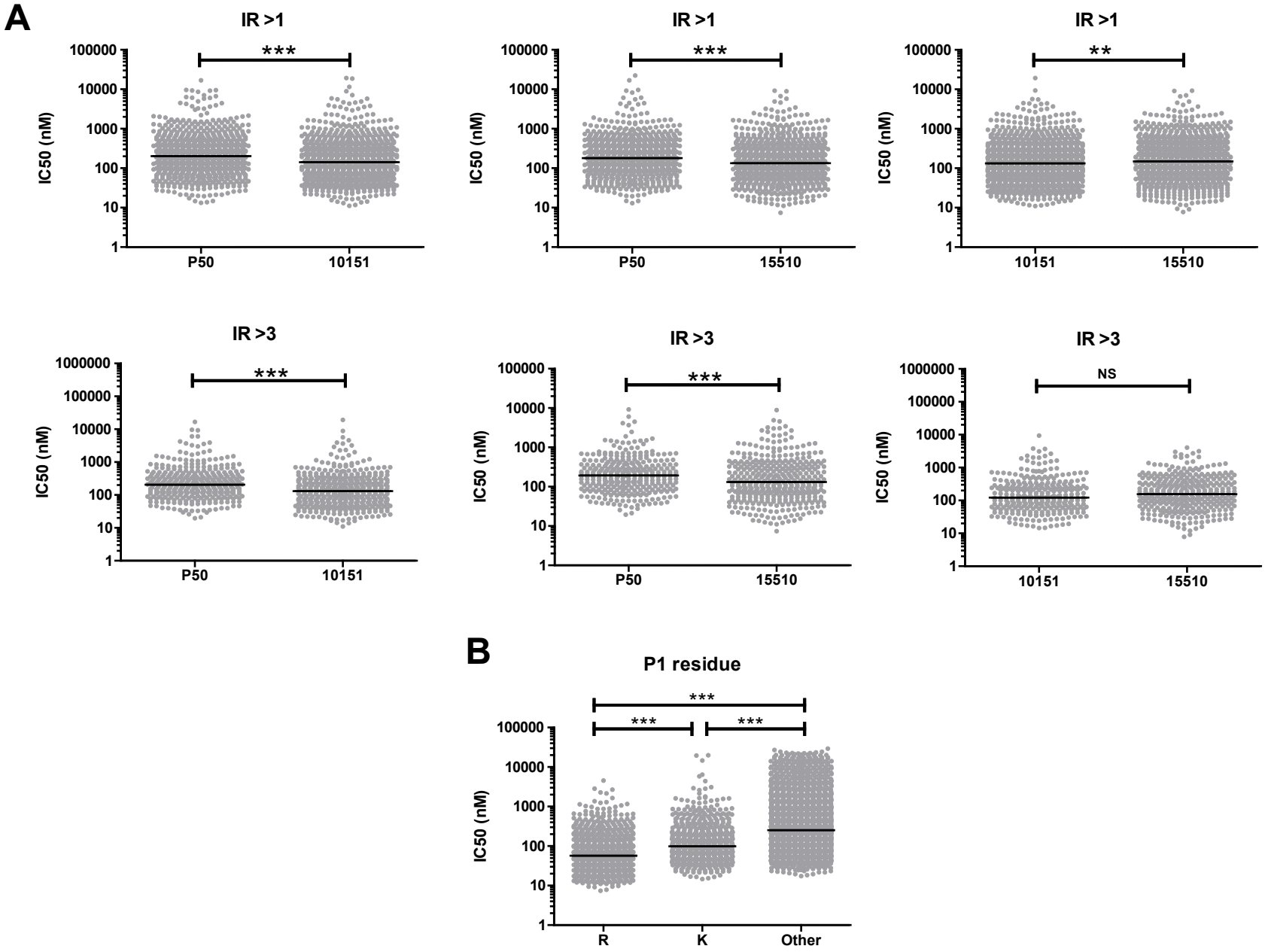
A
IR >1
***
IC50 (nM)
100000
10000
1000
100
10
1
P50
10151
IR >1
***
P50
15510
IR >1
**
10151
15510
IR >3
***
1000000
P50
10151
IR >3
***
P50
15510
IR >3
NS
10151
15510
B
P1 residue
***
***
***
R
K
Other

Figure 6

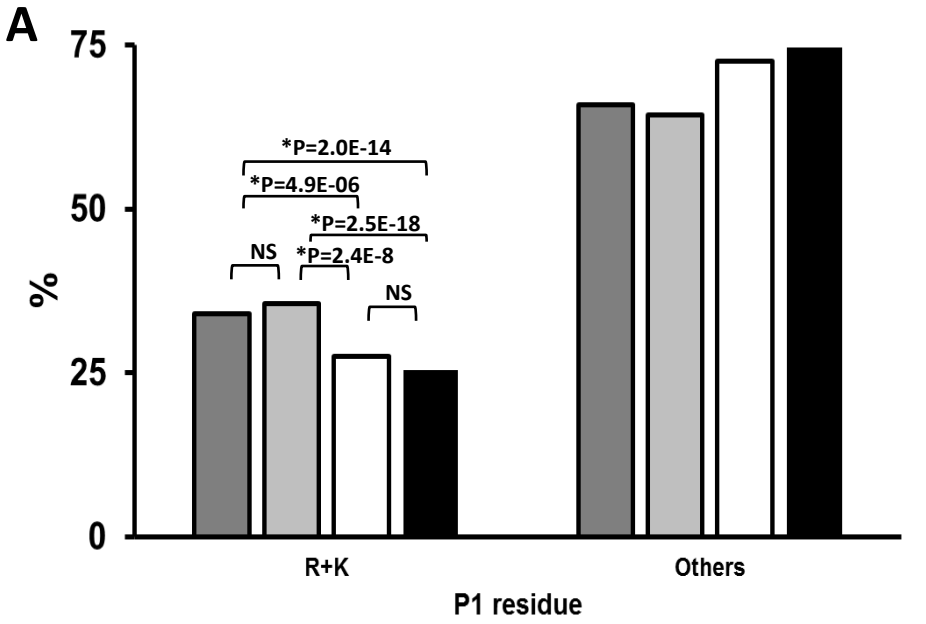
A
75
50
25
0
%
*P=2.0E-14
*P=4.9E-06
*P=2.5E-18
NS
*P=2.4E-8
NS
R+K
Others
P1 residue

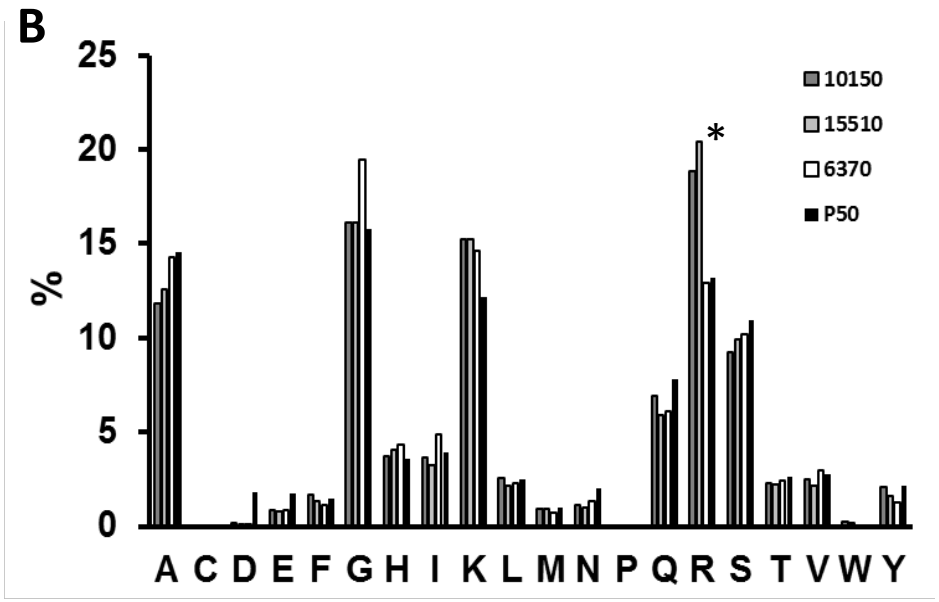
B
25
20
15
10
5
0
%
10150
15510
6370
P50
*
A C D E F G H I K L M N P Q R S T V W Y

Figure 7

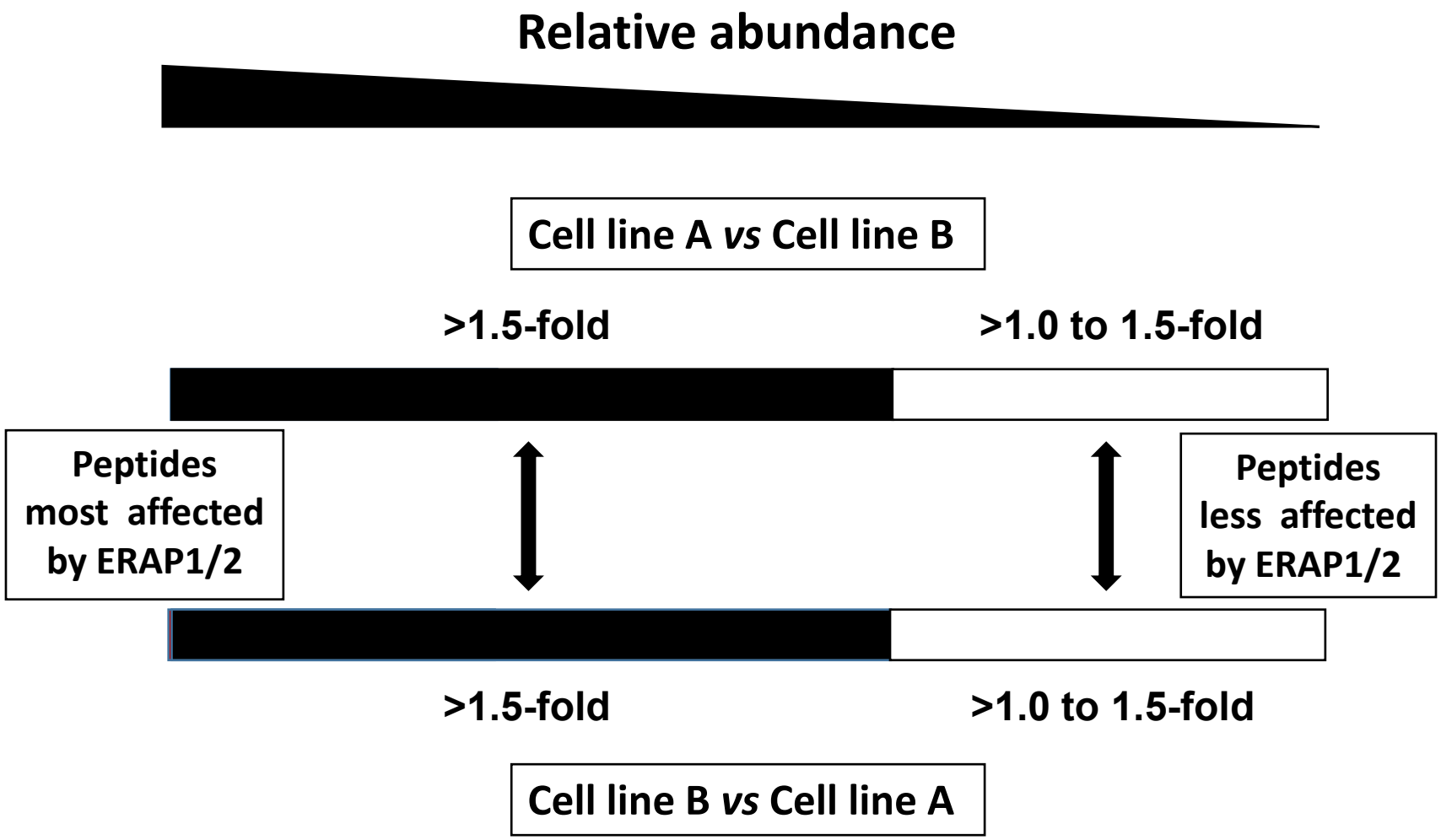
Relative abundance
Cell line A *vs* Cell line B
>1.5-fold
>1.0 to 1.5-fold
Peptides most affected by ERAP1/2
Peptides less affected by ERAP1/2
>1.5-fold
>1.0 to 1.5-fold
Cell line B *vs* Cell line A

Figure S1

IR>1.5

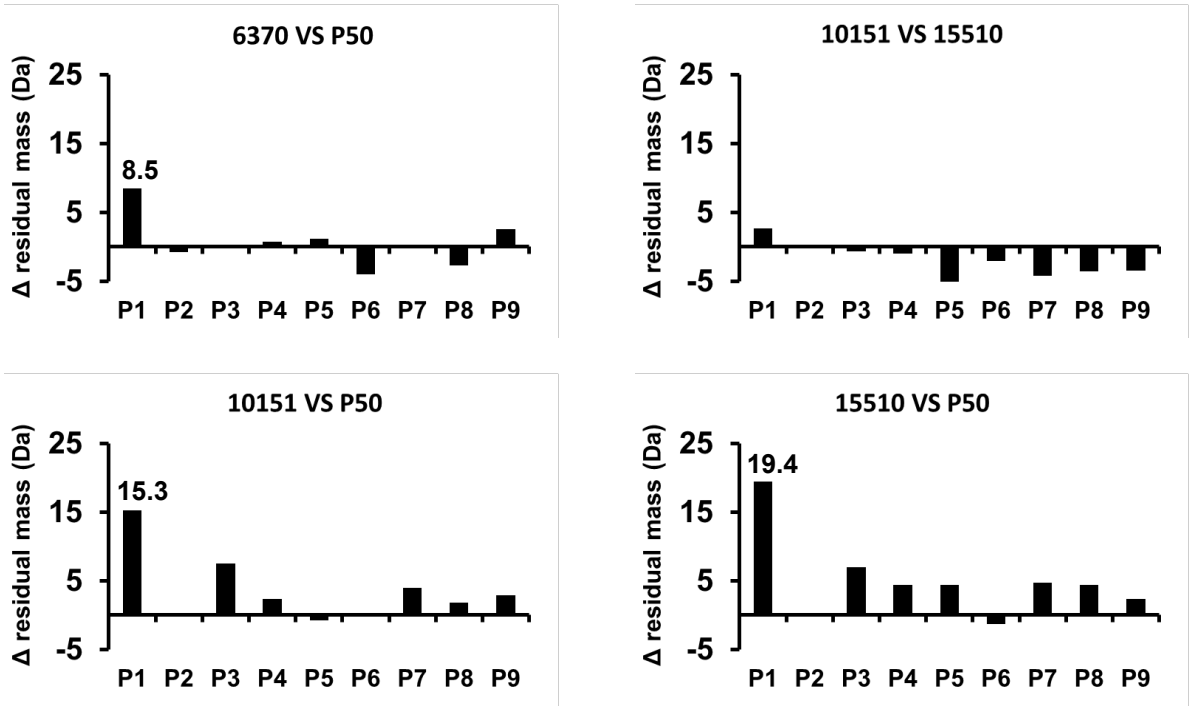

Figure S2

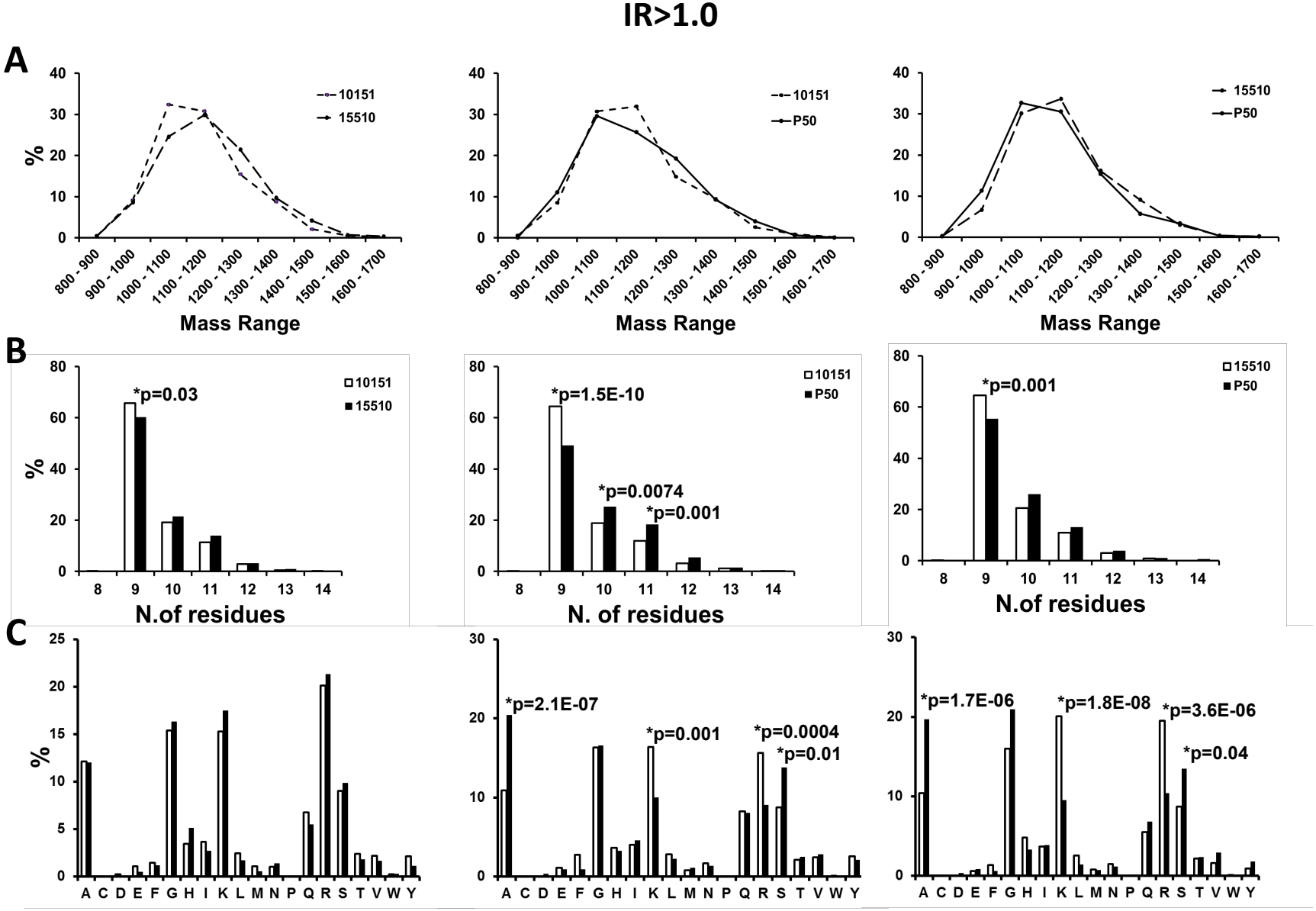
IR>1.0
A
%
Mass Range
10151
15510
P50
B
N.of residues
*p=0.03
*p=1.5E-10
*p=0.0074
*p=0.001
C
*p=2.1E-07
*p=0.001
*p=0.0004
*p=0.01
*p=1.7E-06
*p=1.8E-08
*p=3.6E-06
*p=0.04

Figure S3

IR>1.0 to 1.5

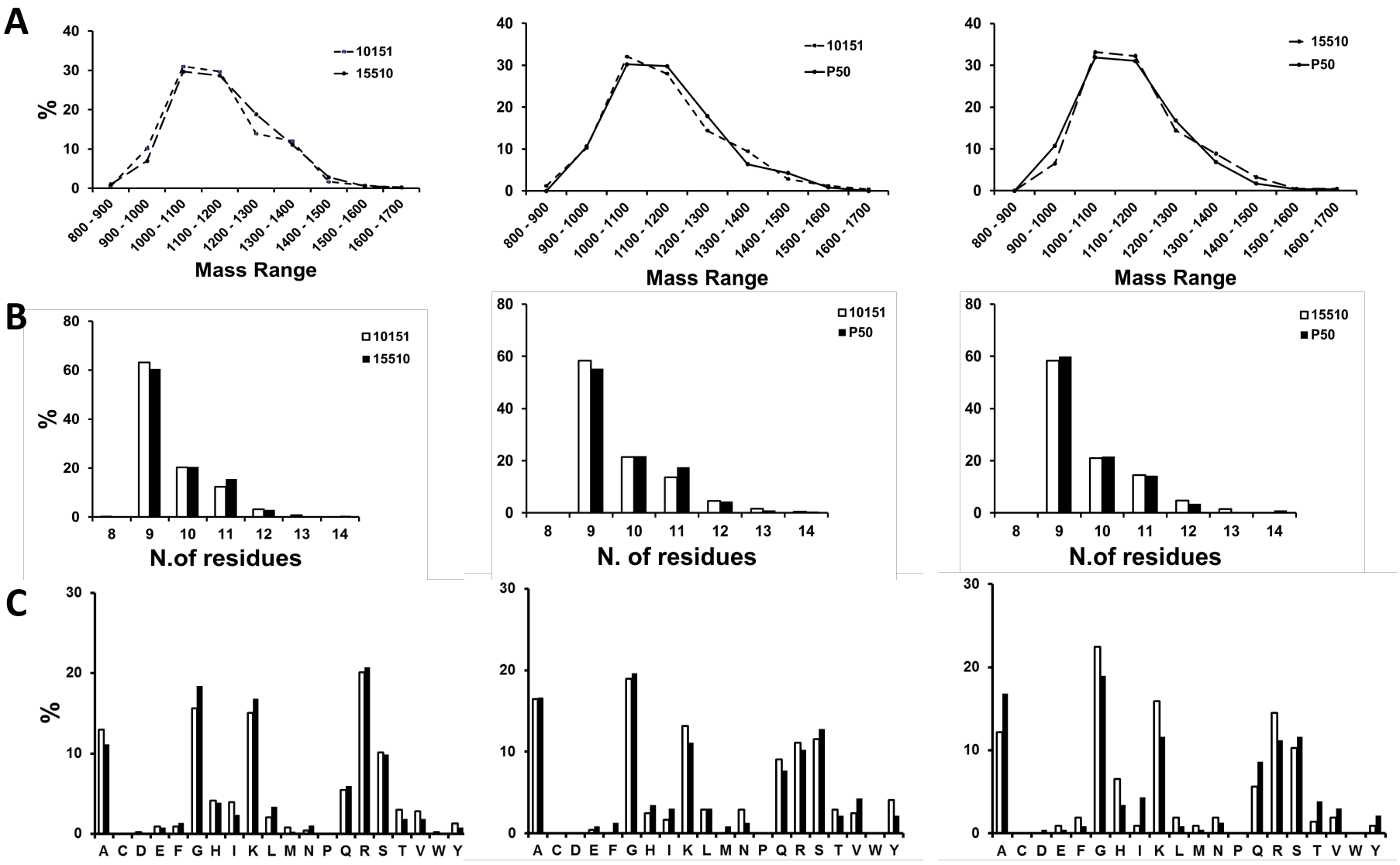

Figure S4

Supplementary Figure Legends

Figure S1. Strategy for the quantitative comparison of HLA-B*27 peptidomes. Schematic diagram showing the strategy for the comparison of HLA-B*27-bound peptidomes from distinct cell line pairs**.** The shared peptides between any given cell line pair were grouped based on their abundance in one cell line relative to the other. The peptide sets from each cell line showing a comparable degree of relative abundance were then compared.

Figure S2. Differences in the mean residue mass at individual positions between the nonamers in the IR>1.5 subsets from the indicated cell line pairs. This analysis was restricted to nonamers because it requires peptide length uniformity. The mean MW differences (ΔMW) between the peptides compared were the following: 6370/P50, 5.7 Da; 10151/15510, -18.8 Da; 10151/P50, 33.1 Da; 15510/P50, 45.1 Da.

Figure S3. Quantitative comparison of shared B*27:05 ligands between LCL pairs: IR>1.0 subsets. (A) MW and (B) length distribution of the peptides from the indicated LCL. (C) Percentage of peptides with the N-terminal residues shown in the x-axis from the indicated cell lines (code as in panel B). Statistically significant differences are labeled with asterisks (*) and their p-values are indicated. The number of peptides from the IR>1.0 subsets in each comparison was as follows. LCL 10151/15510: 1461 and 1118; LCL 10151/P50: 1030 and 892; LCL 15510/P50: 877 and 854.

Figure S4. Quantitative comparison of shared B*27:05 ligands between LCL pairs: IR>1.0 to 1.5 subsets. (A) MW and (B) length distribution of the peptides from the indicated LCL. (C) Percentage of peptides with the N-terminal residues shown in the x-axis from the indicated cell lines (code as in panel B). Statistically significant differences are labeled with asterisks (*) and their p-values are indicated. The number of peptides from the IR>1.0 to 1.5 subsets in each comparison was as follows. LCL 10151/15510: 532 and 387; LCL 10151/P50: 243 and 235; LCL 15510/P50: 214 and 232.

DISCUSIÓN

Discusión

Esta Tesis se ha centrado en describir el efecto de las aminopeptidasas del retículo endoplásmico ERAP1 y ERAP2 sobre el peptidoma constitutivo de HLA-B*27. Nuestro trabajo se fundamenta en la asociación conjunta de las tres moléculas con EA, en que la asociación de ERAP1, pero no de ERAP2, está en epistasis con HLA-B*27 y en que ambas aminopeptidasas participan en el procesamiento de ligandos de MHC-I. Por tanto, existe una base genética y bioquímica para suponer que el peptidoma de HLA-B*27 es, directa o indirectamente, central en la patogenia de la EA. Por otra parte, la distinta naturaleza de la asociación de ERAP1 y ERAP2 con EA y el desconocimiento, previo a esta Tesis, sobre el papel real de ERAP2 *in vivo* ponen de manifiesto la necesidad de diseccionar el papel de cada una de las dos aminopeptidasas en el procesamiento de los ligandos de MHC-I y, en particular, de HLA-B*27.

Las principales aportaciones de esta Tesis son la descripción, por primera vez, del papel de ERAP1 y ERAP2 en la configuración del peptidoma de HLA-B27 en células vivas, la distinción de los papeles respectivos de ambas enzimas y una propuesta sobre la naturaleza de su interacción funcional. Nuestros resultados han permitido definir el papel de ERAP2 en el procesamiento antigénico *in vivo* y proporcionan una base molecular para explicar la asociación de ERAP1 y ERAP2 con EA, basada en la alteración del peptidoma y, a través de éste, de las propiedades biológicas de HLA-B*27.

Consideraciones metodológicas respecto a la comparación de peptidomas.

La estrategia experimental utilizada para analizar los efectos de estas enzimas sobre el peptidoma de HLA-B*27 fue la comparación de dichos peptidomas expresados en líneas celulares con diferentes contextos de ERAP1 y ERAP2. El análisis se centró fundamentalmente en las diferencias cuantitativas globales y no en la identificación de péptidos específicos, ya que por espectrometría de masas es difícil establecer la ausencia de un determinado ligando cuando éste no se detecta en una línea celular concreta.

El análisis comparativo de peptidomas se basó en la suposición de que los cambios cuantitativos en la expresión de péptidos, inducidos por el polimorfismo de ERAP1 o la expresión de ERAP2, deberían ser más fácilmente detectables al comparar los conjuntos de péptidos que mostrasen mayores diferencias en su nivel de expresión entre dos células dadas, mientras que los péptidos cuya abundancia en esas mismas células es similar,

reflejarían en mucha mayor medida los ligandos cuya presentación no está afectada por diferencias en el fenotipo de ERAP1/ERAP2. Por esta razón, las comparaciones se hicieron entre pares de células. Los péptidos identificados en las dos células de cada par se clasificaron en base a su expresión relativa en ambas células y las comparaciones se hicieron entre subconjuntos peptídicos con un nivel de expresión relativa análogo en cada célula. El acierto de nuestra suposición de partida quedó confirmado por el hecho de que las diferencias en el peptidoma se revelaron de manera consistente y más acusada cuando se compararon los conjuntos peptídicos con mayores diferencias en su nivel de expresión entre dos células dadas, que cuando se compararon los conjuntos peptídicos con expresión similar.

Obviamente, las líneas celulares empleadas en nuestras comparaciones pueden presentar diferencias en su proteoma y, en particular, en sus proteasas y peptidasas, que podrían dificultar la interpretación de nuestros resultados. Sin embargo, es improbable que esta disparidad se refleje en cambios específicos que reproducen de manera fehaciente lo que se esperaría de la especificidad enzimática de ERAP1 y ERAP2 caracterizada por ensayos *in vitro*. Por otra parte, dichas diferencias emergerían en comparaciones entre líneas celulares con identidad, o alta similitud, en sus fenotipos de ERAP1 y ERAP2, razón por la cual se incluyeron comparaciones de tales pares de células como control: C1R/KNE (artículo I) y LCL 10151/15510 (artículos III y IV). Estos controles demostraron que, sin disparidad en ERAP1/ERAP2, las posibles diferencias en el peptidoma de HLA-B*27 independientes de estas enzimas son esencialmente indetectables, o muy pequeñas, en nuestro sistema experimental.

ERAP1 y el repertorio peptídico de HLA-B*27

Se abordaron tres aspectos relativos al papel del polimorfismo de ERAP1 en la configuración del peptidoma de HLA-B*27: 1) cómo el efecto de polimorfismos de ERAP1 en posiciones individuales se ve afectado por la presencia de polimorfismos concurrentes en otras posiciones de la molécula, 2) cómo influyen distintas variantes de ERAP1 en el balance generación/destrucción de ligandos naturales de HLA-B27 *in vitro*, y 3) qué alteraciones induce el polimorfismo natural de ERAP1 en el peptidoma constitutivo de HLA-B*27 en células vivas que expresan distintas variantes de esta enzima.

El primer aspecto se analizó centrándonos en los polimorfismos de las posiciones 528 y 575, puesto que ambos determinan la asociación de ERAP1 con EA. Estas posiciones están fuera de los sitios catalítico y de unión del sustrato, por lo que sus efectos se ejercen, muy probablemente, alterando la dinámica de la transición conformacional asociada a la adquisición de la actividad enzimática (Kochan et al. 2011, Nguyen et al. 2011). Como ya se había descrito (Goto et al. 2006, Evnouchidou et al. 2011, Reeves et al. 2013) la mutación Lys528Arg , asociada a protección frente a EA, induce una disminución de la actividad, sin embargo la mutación Asp575Asn, también protectora, la aumentaba, siendo este el primer caso descrito de un polimorfismo de ERAP1 asociado a protección frente a EA que aumenta la actividad de ERAP1. No obstante, Asn575 se encuentra casi siempre asociada a Gln725 y esta combinación sí resulta en una actividad de ERAP1 disminuida (Reeves et al. 2013). En nuestro estudio, las variantes con Arg528 eran menos activas que con Lys528 solo a igualdad de estructura en la posición 575. Sin embargo, el hecho de que la variante Arg528Asn575 era más activa que la combinación Lys528Asp575 indica que la actividad enzimática de ERAP1 es el resultado de su estructura global y que el efecto de una mutación sobre la actividad enzimática depende del contexto estructural en el que ocurre y, en particular, de los polimorfismos en otras posiciones. Este hallazgo fue corroborado con variantes naturales de ERAP1 casi simultáneamente por otro grupo (Reeves et al. 2013).

El segundo aspecto se abordó analizando proteínas recombinantes de diferente actividad enzimática y precursores de epítopos naturales de HLA-B*27. Se observó que el rendimiento de los ligandos *in vitro* variaba dependiendo de la naturaleza de la secuencia flanqueante N-terminal y del residuo P1. La cantidad de cada ligando, resultante del balance generación/destrucción, depende de la actividad enzimática de ERAP1, del tiempo de digestión y del propio ligando.

Generalmente se producía mayor cantidad de ligando a tiempo cortos por una variante más activa que por una menos activa, revirtiéndose este efecto a tiempos largos debido a una mayor destrucción del ligando por la variante de mayor actividad. Con secuencias flanqueantes muy susceptibles a ERAP1 es la enzima menos activa la que genera más cantidad de ligando debido a que la más activa lo destruye. Con secuencias flanqueantes más resistentes a ERAP1 solo la enzima más activa puede generar el epítopo, mientras que una menos activa es incapaz de hacerlo.

Cuando se comparó el peptidoma de diferentes líneas celulares en varios contextos de ERAP1, las variantes más activas, asociadas a riesgo de EA, generaban péptidos más cortos. Además, se observó un aumento de residuos P1 susceptibles a ERAP1 en células con un haplotipo de ERAP1 menos activo, Hap 10 (We-I, P50), en comparación con líneas celulares que tenía haplotipos más activos (JSL, C1R y 6370). Esto se explica porque variantes de mayor actividad inducen una mayor destrucción de estos péptidos, como se observa *in vitro*.

En conclusión, las variantes naturales de ERAP1 tienen una influencia significativa sobre la longitud y abundancia de los ligandos de HLA-B27. La alteración en el balance entre generación y destrucción de ligandos dependiente de la variante enzimática constituye un mecanismo por el que los polimorfismos de ERAP1 configuran los diferentes peptidomas de HLA- B27.

También se observó un descenso de la termoestabilidad de HLA-B*27 expresado en un contexto de ERAP1 de baja actividad, Hap10, en comparación con variantes más activas. Aunque esta observación se realizó en una sola línea celular, es consistente con estudios que demuestran una estabilidad disminuida de HLA-B*27 y otros antígenos MHC-I, cuando se inhibe o impide la expresión de ERAP1, o de su homólogo murino (Hammer et al. 2007, Chen et al. 2014).

ERAP2 y el repertorio peptídico de HLA-B*27.

Aunque la especificidad enzimática y las características bioquímicas de ERAP2 están relativamente bien caracterizadas (Birtley et al. 2012, Mpakali et al. 2015), su efecto real sobre los peptidomas de MHC-I *in vivo* se desconocían. Por otra parte, en contraste con ERAP1, en donde la expresión de la enzima no está comprometida en diferentes individuos y la asociación con EA afecta a variantes con diferente actividad enzimática, en ERAP2 la predisposición a enfermedad está determinada por la expresión de la enzima, mientras que los alelos que no se expresan a nivel de proteína son protectores. Por tanto, la cuestión relevante, tanto desde el punto de vista de la caracterización funcional de ERAP2 como en relación a su asociación con EA, es establecer las diferencias en el peptidoma de MHC-I y, en particular, de HLA-B*27 determinadas por la presencia o ausencia de esta enzima.

Este problema se abordó inicialmente comparando los peptidomas de HLA-B*27 expresados en células con variantes de ERAP1 idénticas o altamente similares en presencia o ausencia de ERAP2. El análisis se centró en analizar los efectos de ERAP2 sobre la longitud de los ligandos y sobre el uso de residuos N-terminales, dos parámetros críticos en la acción de ambas aminopeptidasas. La presencia de ERAP2 reveló un aumento de la abundancia de nonámeros, relativo a péptidos más largos y una disminución altamente significativa en la abundancia de péptidos con residuos N-terminales básicos. Los efectos sobre la longitud son difícilmente explicables por una acción específica y directa de la enzima, debido a que ERAP2 es relativamente ineficiente con sustratos mayores de 9 residuos. Este efecto, sugiere por tanto una acción indirecta sobre la actividad de ERAP1, que podría llevarse a cabo por varios mecanismos, que se discutirán en detalle en el siguiente apartado.

En cambio, la acción específica sobre la destrucción de ligandos con residuos N-terminales básicos, se ajusta perfectamente a lo que conocemos de la preferencia de ERAP2 por este tipo de residuos (Saveanu et al. 2005, Zervoudi et al. 2011, Evnouchidou et al. 2012). En efecto, aunque ERAP2 puede hidrolizar con cierta eficiencia otros residuos N-terminales, tales como la Ala o Gln (Lopez de Castro et al. 2016), estos residuos son generalmente hidrolizados más eficientemente por ERAP1 (Hearn et al. 2009) por lo que esta actividad sería menos relevante en ERAP2. Sin embargo, los residuos básicos son mucho mejor cortados por esta enzima, más aún en sustratos cortos, como nonámeros. Por tanto, la disminución de ligandos de HLA-B*27 con residuos N-terminales básicos puede ser asignada a una acción directa de ERAP2.

Puesto que Arg1 y Lys1 son frecuentes entre los ligandos de HLA-B*27, nuestra observación demuestra que ERAP2 tiene un papel significativo en el repertorio peptídico de HLA-B*27, que va mucho más allá de una acción subsidiaria complementaria a la acción de ERAP1.

En un trabajo previo (Herberts et al. 2006) se hizo notar la resistencia de los péptidos con secuencias N-terminales dibásicas (tales como Arg1-Arg2 o Lys1-Arg2) a muchas aminopeptidasas y se sugirió que la preferencia de HLA-B*27 por este tipo de péptidos confería a esta molécula la capacidad inusual de presentar antígenos generados a muy bajo nivel pero que, debido a su resistencia a la degradación, llegarían en suficiente

cantidad al RE para unirse a un antígeno MHC-I apropiado. Se especulaba asimismo en ese estudio que el papel patogénico de HLA-B*27 podría estar relacionado de alguna manera con esta preferencia inusual por péptidos con secuencias N-terminales dibásicas. Sin embargo, el hecho de que la presencia de ERAP2, una enzima que destruye este tipo de péptidos, predispone a EA, argumenta más bien en contra de dicha proposición.

Interacción funcional de ERAP1 y ERAP2 en el repertorio peptídico de HLA-B*27.

El mecanismo de concertación de ERAP1 y ERAP2 en la configuración de los repertorios peptídicos de MHC-I y el grado en el cual estas enzimas operan conjunta o separadamente *in vivo* no está definido. Como se ha mencionado, estas enzimas parecen encontrarse en forma mayoritariamente monomérica en el interior celular, pero un 10-30% de las mismas se encuentra formando heterodímeros ERAP1/ERAP2 (Saveanu et al. 2005). La actividad de éstos ha sido estudiada *in vitro* utilizando construcciones que intentan reproducir las especies intracelulares. Los heterodímeros así construidos muestran una activación alostérica de ERAP1 y una eficiencia hidrolítica considerablemente superior a la mezcla de las enzimas monoméricas (Evnouchidou et al. 2014). En un estudio reciente, estos heterodímeros fueron capaces de digerir sustratos peptídicos largos unidos a MHC-I, sugiriendo un posible modelo de acción *in vivo* en el que MHC-I podría proteger a los ligandos de ulterior degradación (Chen et al. 2016), un mecanismo reminiscente de observaciones previas en ratón (Kanaseki et al. 2006).

Sin descartar la significación de estos hallazgos en el procesamiento de antígenos *in vivo*, el grado en que la actividad de los heterodímeros ERAP1/ERAP2 influyen en la configuración de los peptidomas de MHC-I puede ser razonablemente cuestionado, al menos por dos motivos. El primero es el bajo porcentaje de dichos heterodímeros en el pool intracelular de ambas enzimas. El segundo es que el efecto principal de ERAP2 sobre el peptidoma de HLA-B*27 en células vivas, o sea, la disminución de péptidos con residuos N-terminales básicos discutido en el apartado anterior, no requiere una acción concertada mediada por heterodímeros ERAP1/ERAP2.

Por tanto, en esta Tesis se abordó la cuestión de la influencia del contexto de ERAP1 en el efecto de ERAP2 sobre el peptidoma de HLA-B*27 para intentar definir los límites de la acción concertada de ambas enzimas y diseccionar en lo posible la acción de cada una de ellas.

Los peptidomas de HLA-B*27 expresados en células ERAP2-positivas, pero con variantes de ERAP1 de distinta actividad, Hap2 y Hap10 respectivamente, demostraron una mayor abundancia de nonámeros, relativa a péptidos mayores, y una disminución de ligandos con Ala1, un residuo muy susceptible a ERAP1, en el contexto de mayor actividad (Hap2), sin cambios en la abundancia de péptidos con residuos N-terminales básicos. Cuando esta comparación se llevó a cabo en células con la misma disparidad de ERAP1, pero difiriendo además en la expresión de ERAP2 (Hap2/ERAP2^{-} vs. Hap10/ERAP2^{+}) se observó el mismo efecto sobre la longitud de los ligandos de HLA-B*27 y la abundancia de péptidos con Ala1 en el contexto de ERAP1 de alta actividad (Hap2), pero carente de ERAP2, lo que indica que este efecto es atribuible a ERAP1. Además, se observó una disminución en la abundancia de péptidos con residuos N-terminales básicos en la línea Hap10/ERAP2^{+}. Esta disminución era muy similar a la observada cuando se compararon peptidomas expresados en células con la misma variante de ERAP1 de alta actividad, pero difiriendo en su expresión de ERAP2, discutidas en el párrafo anterior. En su conjunto, estas observaciones permiten concluir que: 1) los efectos de ERAP1 y ERAP2 son en gran medida independientes y diferenciables, siendo el efecto sobre la longitud peptídica dependiente esencialmente de ERAP1 y el efecto sobre los péptidos con residuos N-terminales básicos dependiente de ERAP2, 2) El efecto de ERAP2, relativo a un contexto de ERAP1 de alta actividad y ausencia de ERAP2, es independiente del contexto de ERAP1. Esto es debido probablemente a que el mayor rendimiento de ligandos de estas características producidos por variantes más activas de ERAP1 es compensado por la destrucción de los mismos debida a ERAP2, 3) estas observaciones sugieren que ERAP1 y ERAP2 actúan esencialmente como entidades separadas *in vivo*.

Con todo, esta diferenciación funcional no excluye una interdependencia en la acción de ambas enzimas en el RE, que podría tener lugar por varios mecanismos no excluyentes entre sí. Por ejemplo, la activación alostérica de ERAP1 por su interacción con ERAP2, descrita para los heterodímeros *in vitro* (Evnouchidou et al. 2014) podría explicar los efectos sobre el incremento de nonámeros detectados en células vivas en presencia de esta enzima. Por otra parte, podría producirse una modulación recíproca de la actividad de ambas enzimas basada en las preferencias complementarias de ERAP1 y ERAP2 por sustratos de diferente longitud (Figura D1). Por ejemplo, los octámeros que

pueden ser generados, entre otros mecanismos, por ERAP2 a partir de nonámeros con residuos N-terminales básicos, podrían inhibir la actividad de ERAP1 (Artículo II, figura 7). Sin embargo, como ERAP2 es capaz de digerir ulteriormente estos octámeros si a su vez presentan residuos N-terminales básicos, como es el caso de los péptidos que derivan de ligandos de HLA-B*27, esta ulterior digestión tendría un efecto activador de ERAP1. Recíprocamente, los sustratos largos, preferidos por ERAP1, podrían unirse también a ERAP2 pero serían digeridos con muy baja eficiencia y actuarían *de facto* inhibiendo competitivamente la actividad de esta enzima. La digestión de estos sustratos por ERAP1, facilitaría a su vez la actividad de ERAP2. Esta interdependencia de ambas enzimas estaría influenciada por la actividad de las variantes de ERAP1, por la presencia o ausencia de ERAP2, por la naturaleza del pool peptídico en el RE y por la topología precisa de la interacción enzima/sustrato. Por tanto, la dimensión real de estos mecanismos *in vivo* está por determinar.

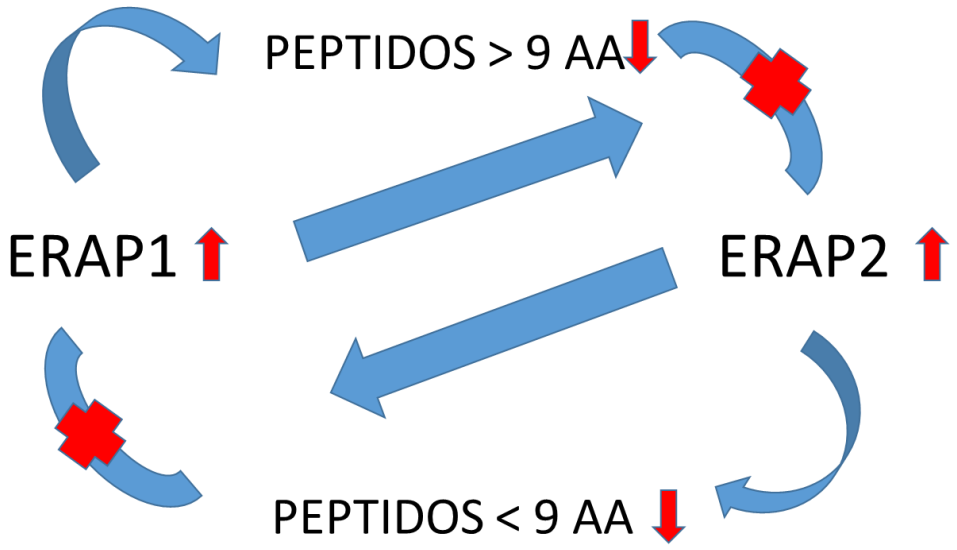

Figura D1: Modelo de posible interdependencia entre ERAP1 y ERAP2 en su actividad enzimática debido a sus preferencias complementarias por sustratos de diferente longitud

Implicaciones para la patogenia de la EA.

Para evaluar las implicaciones de nuestro estudio en el esclarecimiento del papel patogénico de HLA-B*27 en EA es preciso considerar dos aspectos: 1) la naturaleza de la asociación genética de ERAP1 y ERAP2 con esta enfermedad y 2) las posibles consecuencias de las alteraciones en el peptidoma de HLA-B*27 caracterizadas en esta Tesis sobre las propiedades biológicas de la molécula.

Como se ha mencionado, la asociación de ERAP1 y ERAP2 con EA muestra algunas analogías, pero también diferencias significativas entre las dos enzimas.

Las principales diferencias son las siguientes: 1) La asociación de ERAP1 con EA es en epistasis con HLA-B*27 o HLA-B*40, es decir solo se observa en individuos portadores de estos alelos (Evans et al. 2011, Cortes et al. 2015), mientras que ERAP2 está asociado a EA en todos los casos (Robinson et al. 2015), 2) la asociación de ERAP1 con EA reside en el efecto de las diferentes variantes funcionales, mientras que la asociación de ERAP2 está relacionada con la expresión o no de la enzima.

La principal analogía en la asociación de ambas enzimas con EA consiste en que las variantes más activas de ERAP1 y la expresión de ERAP2 son factores de riesgo para la EA, mientras que una variante de poca actividad de ERAP1 y la ausencia de expresión de ERAP 2 son protectores (Robinson et al. 2014).

Las similitudes y diferencias en la asociación de ambas enzimas con EA encuentran cierta correspondencia con la naturaleza de sus efectos sobre el peptidoma de HLA-B*27. En ambos casos estos efectos poseen una magnitud significativa, aunque inciden en características parcialmente diferentes que pueden afectar a distintos tipos de péptidos y tienen consecuencias dispares sobre la molécula y también distintas implicaciones patogénicas. Las características que ERAP1 y ERAP2 pueden alterar en HLA-B*27 se discuten a continuación.

1) Presentación antigénica. La alta actividad de las variantes de riesgo de ERAP1 y la presencia de ERAP2, conllevan una mayor eficiencia en la presentación de determinados ligandos, y con toda probabilidad también la presentación de otros nuevos, como se deduce del aumento en la abundancia de nonámeros. Sin embargo, los fenotipos de riesgo de ambas enzimas también implican una mayor destrucción de ligandos tanto

cualitativa como cuantitativamente. Por estas razones, la presentación específica de antígenos por HLA-B*27 y su potencial tolerógenico, que depende en parte de la densidad de los epítopos, se verán alterados en función del fenotipo ERAP1/ERAP2 en diferentes individuos. Tanto la capacidad de presentar un epítopo artritogénico (Benjamin et al. 1990) como la incapacidad de presentar un epítopo protector que, por ejemplo, ayudara a controlar la homeostasis intestinal (Kenna et al. 2015), podrían verse afectados por fenotipos de riesgo de ERAP1 y/o ERAP2. En este sentido podría ser relevante la reciente observación de que individuos sanos HLA-B27+ presentan un perfil bacteriano intestinal que solapa parcialmente con el perfil de pacientes de EA que muestran disbiosis (Costello et al. 2016).

2) Plegamiento. El plegamiento lento y la tendencia a la acumulación de proteína mal plegada en el RE es una característica de HLA-B*27 (Mear et al. 1999) a la que se le atribuye un papel patogénico, debido a la exacerbación de su potencial pro-inflamatorio mediado por la sobreexpresión de IL23 (Colbert 2000, Colbert et al. 2014). El plegamiento de la molécula de HLA-B*27 depende de la unión de péptidos y su cinética puede verse afectada de maneras contrapuestas por la afinidad de los ligandos disponibles. Por ejemplo, la generación de un repertorio peptídico de mayor afinidad por una variante de ERAP1 de alta actividad (Hap3), observado en un estudio anterior (Sanz-Bravo et al. 2015) podría favorecer un plegamiento lento mediado por la acción editora de la tapasina para unir preferentemente ligandos de alta afinidad generados en dicho contexto. En nuestro estudio (Artículos III y IV) hemos observado que las diferencias entre un alelo de riesgo (Hap2) y uno de protección (Hap10) de ERAP1 no inducen cambios en la afinidad del peptidoma si ERAP2 está presente, pero la presencia de ERAP2 conlleva una disminución de la afinidad global, en relación a la ausencia de esta enzima, debido a la disminución de ligandos con residuos N-terminales básicos (Artículo IV), ya que estos, particularmente Arg1, contribuyen positivamente a la unión de péptidos a HLA-B*27 (Lamas et al. 1999, Hillig et al. 2004). La menor disponibilidad de ligandos de alta afinidad, debido a su destrucción por ERAP2, también podría limitar la acción optimizadora de la tapasina y enlentecer de esta manera el plegamiento de HLA-B27. En conjunto, el fenotipo ERAP1/ERAP2 de cada individuo determinaría la producción de ligandos de HLA-B*27 de afinidad variable, modulando a través de este mecanismo el plegamiento y el mal plegamiento de la molécula. Presumiblemente, estos efectos no son

suficientes para alterar en profundidad las características de plegamiento intrínsecas de HLA-B*27 y serían por tanto compatibles con una asociación más débil de ambas enzimas a enfermedad que la propia molécula de HLA-B*27.

3) Formación de homodímeros de cadena pesada en la superficie celular. Las moléculas de HLA-B*27 que alcanzan la superficie celular dan lugar a una pequeña proporción de homodímeros de cadena pesada (Allen et al. 1999). Estos homodímeros se originan, presumiblemente, tras la disociación de los complejos HLA-B*27/péptido y su formación es dependiente del reciclamiento de dichos complejos entre la membrana celular y el endosoma (Bird et al. 2003) La importancia de los homodímeros y su posible significación patogénica radica en que pueden ser reconocidos por el receptor leucocitario KIR3DL2 (Kollnberger et al. 2007) y estimular una subpoblación de linfocitos Th17 que expresan dicho receptor y que se encuentra aumentada en pacientes con EA (Bowness et al. 2011). Lógicamente, la afinidad del peptidoma por HLA-B*27 debe influir en la capacidad de disociación de dichos heterodímeros. Sin embargo, una vez más, la relación entre la estabilidad molecular de los complejos MHC/péptido y la formación de homodímeros es ambigua. Por ejemplo, complejos HLA-B*27/péptido más estables tendrían una mayor vida media en la superficie celular y por tanto un reciclamiento endosomal mas reiterado, pudiendo incrementar la formación de homodímeros. Por otra parte, complejos de menor afinidad, tales como los favorecidos en presencia de ERAP2, se disociarían más fácilmente en las condiciones ácidas del endosoma, lo que también podría promover la formación de homodímeros. Esta ambigüedad, y la complejidad subyacente, se refleja en una literatura especialmente controvertida. Por ejemplo, en condiciones de inhibición de la expresión de ERAP1, se ha definido una disminución (Chen et al. 2016) o un aumento (Tran et al. 2016) de la expresión de cadena pesada libre de HLA-B*27 en la superficie celular. Esto sugiere que los efectos de ERAP1 sobre dicha expresión pueden depender de múltiples variables, tales como el tipo celular, los niveles de expresión de MHC-I y de ERAP1, etc. Asimismo, parece que la expresión de ERAP2 influye en la expresión de cadena pesada libre en superficie, aunque hay un solo estudio que ha abordado este problema hasta el momento (Zhang Z 2014). Por tanto, aunque no es fácil predecir un efecto concreto, la influencia del fenotipo ERAP1/ERAP2 en cada individuo probablemente influye en los niveles de expresión de estos homodímeros y puede modular, por este mecanismo, el potencial pro-inflamatorio de HLA-B*27.

En conclusión, la asociación de ERAP1 y ERAP2 con EA y el papel significativo y diferenciable de ambas enzimas sobre el peptidoma de HLA-B*27 sugieren que el peptidoma juega un papel central en la capacidad patogénica de HLA-B27. La magnitud y naturaleza de los cambios es tal que éstos podrían alterar la patogenicidad de HLA-B*27 a múltiples niveles, sea modulando su capacidad presentadora de antígeno, su potencial tolerogénico o, directamente, su capacidad pro-inflamatoria. ERAP1 y ERAP2 parecen funcionar en gran medida como entidades separadas in vivo, aunque con un grado indeterminado de interdependencia. Esta diferenciación funcional y los diferentes efectos sobre el peptidoma podrían estar relacionados con el diferente patrón genético de asociación de ambas enzimas con EA.

CONCLUSIONES

1. Los estudios que se aportan en esta Tesis constituyen la primera descripción del papel de ERAP1 (Artículo I) y ERAP2 (Artículo III) en la configuración del peptidoma de HLA-B*27 y, en el caso de ERAP2, de una molécula de MHC-I en células vivas.

2. La actividad de cada variante de ERAP1 es el resultado de la concurrencia de múltiples polimorfismos y no de uno concreto.

3. Las variantes naturales de ERAP1 influyen significativamente en la longitud y abundancia de los ligandos de HLA-B*27.

4. El polimorfismo de ERAP1 altera el balance generación/destrucción de los ligandos de HLA-B*27 de una manera dependiente de cada péptido y de la actividad enzimática de cada variante. Estos efectos son de gran magnitud y diversidad.

5. La presencia de ERAP2, asociada a riesgo de EA, genera peptidomas más cortos, disminuye la abundancia de ligandos con residuos básicos en P1, destruye alrededor de un 5% de estos péptidos y hace disminuir la afinidad global del peptidoma de HLA-B*27.

6. Los efectos de ERAP2 sobre la afinidad son debidos principalmente a la destrucción por esta enzima de ligandos con Arg1.

7. Los efectos de ERAP1 y ERAP2 sobre el peptidoma de HLA-B*27 son en gran medida diferenciables, siendo el efecto sobre la longitud peptídica dependiente esencialmente de ERAP1 y el efecto sobre los péptidos con residuos N-terminales básicos dependiente de ERAP2.

8. Por tanto ambas enzimas parecen actuar separadamente *in vivo*, sin excluir por ello una interdependencia en su actividad funcional.

9. La magnitud de los efectos descritos puede alterar al potencial antigénico y/o pro-inflamatorio de HLA-B*27. Ello constituye una explicación plausible para la asociación de ERAP1 y ERAP2 con EA y subraya el papel central de los péptidos en la patogenia de esta enfermedad.

BIBLIOGRAFÍA

Abbas, A. K. and A. H. Lichtman (2007). Inmunología celular y molecular, ElSevier España.
Alvarez-Navarro, C. and J. A. Lopez de Castro (2014). "ERAP1 structure, function and pathogenetic role in ankylosing spondylitis and other MHC-associated diseases." Mol Immunol **57**(1): 12-21.

Alvarez, I., M. Marti, J. Vazquez, E. Camafeita, S. Ogueta and J. A. Lopez de Castro (2001). "The Cys-67 residue of HLA-B27 influences cell surface stability, peptide specificity, and T-cell antigen presentation." J Biol Chem **276**(52): 48740-48747.

Allen, R. L., P. Bowness and A. McMichael (1999). "The role of HLA-B27 in spondyloarthritis." Immunogenetics **50**(3-4): 220-227.

Allen, R. L., T. Raine, A. Haude, J. Trowsdale and M. J. Wilson (2001). "Leukocyte receptor complex-encoded immunomodulatory receptors show differing specificity for alternative HLA-B27 structures." J Immunol **167**(10): 5543-5547.

Andres, A. M., M. Y. Dennis, W. W. Kretzschmar, J. L. Cannons, S. Q. Lee-Lin, B. Hurle, N. C. S. Program, P. L. Schwartzberg, S. H. Williamson, C. D. Bustamante, R. Nielsen, A. G. Clark and E. D. Green (2010). "Balancing selection maintains a form of ERAP2 that undergoes nonsense-mediated decay and affects antigen presentation." PLoS Genet **6**(10): e1001157.

Arendt, C. S. and M. Hochstrasser (1997). "Identification of the yeast 20S proteasome catalytic centers and subunit interactions required for active-site formation." Proc Natl Acad Sci U S A **94**(14): 7156-7161.

Benjamin, R. and P. Parham (1990). "Guilt by association: HLA-B27 and ankylosing spondylitis." Immunol Today **11**(4): 137-142.

Bird, L. A., C. A. Peh, S. Kollnberger, T. Elliott, A. J. McMichael and P. Bowness (2003). "Lymphoblastoid cells express HLA-B27 homodimers both intracellularly and at the cell surface following endosomal recycling." Eur J Immunol **33**(3): 748-759.

Birtley, J. R., E. Saridakis, E. Stratikos and I. M. Mavridis (2012). "The crystal structure of human endoplasmic reticulum aminopeptidase 2 reveals the atomic basis for distinct roles in antigen processing." Biochemistry **51**(1): 286-295.

Bjorkman, P. J., M. A. Saper, B. Samraoui, W. S. Bennett, J. L. Strominger and D. C. Wiley (1987). "The foreign antigen binding site and T cell recognition regions of class I histocompatibility antigens." Nature **329**(6139): 512-518.

Bjorkman, P. J., M. A. Saper, B. Samraoui, W. S. Bennett, J. L. Strominger and D. C. Wiley (1987). "Structure of the human class I histocompatibility antigen, HLA-A2." Nature **329**(6139): 506-512.

Blum, J. S., P. A. Wearsch and P. Cresswell (2013). "Pathways of antigen processing." Annu Rev Immunol **31**: 443-473.

Bourdetsky, D., C. E. Schmelzer and A. Admon (2014). "The nature and extent of contributions by defective ribosome products to the HLA peptidome." Proc Natl Acad Sci U S A **111**(16): E1591-1599.

Bouvier, M. and D. C. Wiley (1994). "Importance of peptide amino and carboxyl termini to the stability of MHC class I molecules." Science **265**(5170): 398-402.

Bowness, P., A. Ridley, J. Shaw, A. T. Chan, I. Wong-Baeza, M. Fleming, F. Cummings, A. McMichael and S. Kollnberger (2011). "Th17 cells expressing KIR3DL2+ and responsive to HLA-B27 homodimers are increased in ankylosing spondylitis." J Immunol **186**(4): 2672-2680.

Breban, M., J. L. Fernandez-Sueiro, J. A. Richardson, R. R. Hadavand, S. D. Maika, R. E. Hammer and J. D. Taurog (1996). "T cells, but not thymic exposure to HLA-B27, are required for the inflammatory disease of HLA-B27 transgenic rats." J Immunol **156**(2): 794-803.

Brewerton, D. A., M. Caffrey, A. Nicholls, D. Walters, J. K. Oates and D. C. James (1973). "Reiter's disease and HL-A 27." Lancet **302**(7836): 996-998.

Brown, M. A. (2008). "Breakthroughs in genetic studies of ankylosing spondylitis." Rheumatology (Oxford) **47**(2): 132-137.

Cascio, P. (2014). "PA28alphabeta: the enigmatic magic ring of the proteasome?" Biomolecules **4**(2): 566-584.

Ciccia, F., A. Accardo-Palumbo, A. Rizzo, G. Guggino, S. Raimondo, A. Giardina, A. Cannizzaro, R. A. Colbert, R. Alessandro and G. Triolo (2014). "Evidence that autophagy, but not the unfolded protein response, regulates the expression of IL-23 in the gut of patients with ankylosing spondylitis and subclinical gut inflammation." Ann Rheum Dis **73**(8): 1566-1574.

Colbert, R. A. (2000). "HLA-B27 misfolding: a solution to the spondyloarthropathy conundrum?" Mol Med Today **6**(6): 224-230.

Colbert, R. A., T. M. Tran and G. Layh-Schmitt (2014). "HLA-B27 misfolding and ankylosing spondylitis." Mol Immunol **57**(1): 44-51.

Cortes, A., S. L. Pulit, P. J. Leo, J. J. Pointon, P. C. Robinson, M. H. Weisman, M. Ward, L. S. Gensler, X. Zhou, H. J. Garchon, G. Chiocchia, J. Nossent, B. A. Lie, O. Forre, J. Tuomilehto, K. Laiho, L. A. Bradbury, D. Elewaut, R. Burgos-Vargas, S. Stebbings, L. Appleton, C. Farrah, J. Lau, N. Haroon, J. Mulero, F. J. Blanco, M. A. Gonzalez-Gay, C. Lopez-Larrea, P. Bowness, K. Gaffney, H. Gaston, D. D. Gladman, P. Rahman, W. P. Maksymowych, J. B. Crusius, I. E. van der Horst-Bruinsma, R. Valle-Onate, C. Romero-Sanchez, I. M. Hansen, F. M. Pimentel-Santos, R. D. Inman, J. Martin, M. Breban, B. P. Wordsworth, J. D. Reveille, D. M. Evans, P. I. de Bakker and M. A. Brown (2015). "Major histocompatibility complex associations of ankylosing spondylitis are complex and involve further epistasis with ERAP1." Nat Commun **6**: 7146.

Costello, M. E., M. Asquith, K. A. Le Cao, S. Diamond, T. Martin, J. T. Rosenbaum and M. A. Brown (2016). HLA-B27 has major effects on the intestinal microbiome. Tenth International Congress on Spondyloarthritides. Gent, Belgium. **34:** 732.

Costello, M. E., F. Ciccia, D. Willner, N. Warrington, P. C. Robinson, B. Gardiner, M. Marshall, T. J. Kenna, G. Triolo and M. A. Brown (2014). "Intestinal dysbiosis in ankylosing spondylitis." Arthritis Rheumatol **67**: 686-691.

Craiu, A., T. Akopian, A. Goldberg and K. L. Rock (1997). "Two distinct proteolytic processes in the generation of a major histocompatibility complex class I-presented peptide." Proc Natl Acad Sci U S A **94**(20): 10850-10855.

Chang, S. C., F. Momburg, N. Bhutani and A. L. Goldberg (2005). "The ER aminopeptidase, ERAP1, trims precursors to lengths of MHC class I peptides by a "molecular ruler" mechanism." Proc Natl Acad Sci U S A **102**(47): 17107-17112.

Chapiro, J., S. Claverol, F. Piette, W. Ma, V. Stroobant, B. Guillaume, J. E. Gairin, S. Morel, O. Burlet-Schiltz, B. Monsarrat, T. Boon and B. J. Van den Eynde (2006). "Destructive cleavage of antigenic peptides either by the immunoproteasome or by the standard proteasome results in differential antigen presentation." J Immunol **176**(2): 1053-1061.

Chen, H., L. Li, M. Weimershaus, I. Evnouchidou, P. van Endert and M. Bouvier (2016). "ERAP1-ERAP2 dimers trim MHC I-bound precursor peptides; implications for understanding peptide editing." Sci Rep **6**: 28902.

Chen, L., R. Fischer, Y. Peng, E. Reeves, K. McHugh, N. Ternette, T. Hanke, T. Dong, T. Elliott, N. Shastri, S. Kollnberger, E. James, B. Kessler and P. Bowness (2014). "Critical role of endoplasmic reticulum aminopeptidase 1 in determining the length and sequence of peptides bound and presented by HLA-B27." Arthritis Rheumatol **66**(2): 284-294.

Choi, C. B., T. H. Kim, J. B. Jun, H. S. Lee, S. C. Shim, B. Lee, A. Pope, M. Uddin, P. Rahman and R. D. Inman (2010). "ARTS1 polymorphisms are associated with ankylosing spondylitis in Koreans." Ann Rheum Dis **69**(3): 582-584.

D'Amato, M., M. T. Fiorillo, C. Carcassi, A. Mathieu, A. Zuccarelli, P. P. Bitti, R. Tosi and R. Sorrentino (1995). "Relevance of residue 116 of HLA-B27 in determining susceptibility to ankylosing spondylitis." Eur J Immunol **25**(11): 3199-3201.

Eggers, M., B. Boes-Fabian, T. Ruppert, P. M. Kloetzel and U. H. Koszinowski (1995). "The cleavage preference of the proteasome governs the yield of antigenic peptides." J Exp Med **182**(6): 1865-1870.

Evans, D. M., C. C. Spencer, J. J. Pointon, Z. Su, D. Harvey, G. Kochan, U. Oppermann, A. Dilthey, M. Pirinen, M. A. Stone, L. Appleton, L. Moutsianas, S. Leslie, T. Wordsworth, T. J. Kenna, T. Karaderi, G. P. Thomas, M. M. Ward, M. H. Weisman, C. Farrar, L. A. Bradbury, P. Danoy, R. D. Inman, W. Maksymowych, D. Gladman, P. Rahman, C. Spondyloarthritis Research Consortium of, A. Morgan, H. Marzo-Ortega, P. Bowness, K. Gaffney, J. S. Gaston, M. Smith, J. Bruges-Armas, A. R. Couto, R. Sorrentino, F. Paladini, M. A. Ferreira, H. Xu, Y. Liu, L. Jiang, C. Lopez-Larrea, R. Diaz-Pena, A. Lopez-Vazquez, T. Zayats, G. Band, C. Bellenguez, H. Blackburn, J. M. Blackwell, E. Bramon, S. J. Bumpstead, J. P. Casas, A. Corvin, N. Craddock, P. Deloukas, S. Dronov, A. Duncanson, S. Edkins, C. Freeman, M. Gillman, E. Gray, R. Gwilliam, N. Hammond, S. E. Hunt, J. Jankowski, A. Jayakumar, C. Langford, J. Liddle, H. S. Markus, C. G. Mathew, O. T. McCann, M. I. McCarthy, C. N. Palmer, L. Peltonen, R. Plomin, S. C. Potter, A. Rautanen, R. Ravindrarajah, M. Ricketts, N. Samani, S. J. Sawcer, A. Strange, R. C. Trembath, A. C. Viswanathan, M. Waller, P. Weston, P. Whittaker, S. Widaa, N. W. Wood, G. McVean, J. D. Reveille, B. P. Wordsworth, M. A. Brown, P. Donnelly, C. Australo-Anglo-American Spondyloarthritis and C. Wellcome Trust Case Control (2011). "Interaction between ERAP1 and HLA-B27 in ankylosing spondylitis implicates

peptide handling in the mechanism for HLA-B27 in disease susceptibility." Nat Genet **43**(8): 761-767.

Evnouchidou, I., M. J. Berardi and E. Stratikos (2009). "A continuous fluorigenic assay for the measurement of the activity of endoplasmic reticulum aminopeptidase 1: competition kinetics as a tool for enzyme specificity investigation." Anal Biochem **395**(1): 33-40.

Evnouchidou, I., J. Birtley, S. Seregin, A. Papakyriakou, E. Zervoudi, M. Samiotaki, G. Panayotou, P. Giastas, O. Petrakis, D. Georgiadis, A. Amalfitano, E. Saridakis, I. M. Mavridis and E. Stratikos (2012). "A common single nucleotide polymorphism in endoplasmic reticulum aminopeptidase 2 induces a specificity switch that leads to altered antigen processing." J Immunol **189**(5): 2383-2392.

Evnouchidou, I., R. P. Kamal, S. S. Seregin, Y. Goto, M. Tsujimoto, A. Hattori, P. V. Voulgari, A. A. Drosos, A. Amalfitano, I. A. York and E. Stratikos (2011). "Cutting Edge: Coding single nucleotide polymorphisms of endoplasmic reticulum aminopeptidase 1 can affect antigenic peptide generation in vitro by influencing basic enzymatic properties of the enzyme." J Immunol **186**(4): 1909-1913.

Evnouchidou, I., F. Momburg, A. Papakyriakou, A. Chroni, L. Leondiadis, S. C. Chang, A. L. Goldberg and E. Stratikos (2008). "The internal sequence of the peptide-substrate determines its N-terminus trimming by ERAP1." PLoS One **3**(11): e3658.

Evnouchidou, I., M. Weimershaus, L. Saveanu and P. van Endert (2014). "ERAP1-ERAP2 dimerization increases peptide-trimming efficiency." J Immunol **193**(2): 901-908.

Galocha, B. and J. A. de Castro (2008). "Folding of HLA-B27 subtypes is determined by the global effect of polymorphic residues and shows incomplete correspondence to ankylosing spondylitis." Arthritis Rheum **58**(2): 401-412.

Galocha, B. and J. A. Lopez de Castro (2010). "Mutational analysis reveals a complex interplay of peptide binding and multiple biological features of HLA-B27." J Biol Chem **285**(50): 39180-39190.

Gao, G. F., J. Tormo, U. C. Gerth, J. R. Wyer, A. J. McMichael, D. I. Stuart, J. I. Bell, E. Y. Jones and B. K. Jakobsen (1997). "Crystal structure of the complex between human CD8alpha(alpha) and HLA-A2." Nature **387**(6633): 630-634.

Garcia-Medel, N., A. Sanz-Bravo, C. Alvarez-Navarro, P. Gomez-Molina, E. Barnea, M. Marcilla, A. Admon and J. A. de Castro (2014). "Peptide handling by HLA-B27 subtypes influences their biological behavior, association with ankylosing spondylitis and susceptibility to endoplasmic reticulum aminopeptidase 1 (ERAP1)." Mol Cell Proteomics **13**(12): 3367-3380.

Garrett, T. P., M. A. Saper, P. J. Bjorkman, J. L. Strominger and D. C. Wiley (1989). "Specificity pockets for the side chains of peptide antigens in HLA-Aw68." Nature **342**(6250): 692-696.
Goto, Y., A. Hattori, Y. Ishii and M. Tsujimoto (2006). "Reduced activity of the hypertension-associated Lys528Arg mutant of human adipocyte-derived leucine aminopeptidase (A-LAP)/ER-aminopeptidase-1." FEBS Lett **580**(7): 1833-1838.

Goto, Y., H. Tanji, A. Hattori and M. Tsujimoto (2008). "Glutamine-181 is crucial in the enzymatic activity and substrate specificity of human endoplasmic-reticulum aminopeptidase-1." Biochem J **416**(1): 109-116.

Griffin, T. A., D. Nandi, M. Cruz, H. J. Fehling, L. V. Kaer, J. J. Monaco and R. A. Colbert (1998). "Immunoproteasome assembly: cooperative incorporation of interferon gamma (IFN-gamma)-inducible subunits." J Exp Med **187**(1): 97-104.

Groettrup, M., A. Soza, U. Kuckelkorn and P. M. Kloetzel (1996). "Peptide antigen production by the proteasome: complexity provides efficiency." Immunol Today **17**(9): 429-435.

Groll, M., L. Ditzel, J. Lowe, D. Stock, M. Bochtler, H. D. Bartunik and R. Huber (1997). "Structure of 20S proteasome from yeast at 2.4 A resolution." Nature **386**(6624): 463-471.

Gudjonsson, J. E., A. Karason, E. H. Runarsdottir, A. A. Antonsdottir, V. B. Hauksson, H. H. Jonsson, J. Gulcher, K. Stefansson and H. Valdimarsson (2006). "Distinct clinical differences between HLA-Cw*0602 positive and negative psoriasis patients--an analysis of 1019 HLA-C- and HLA-B-typed patients." J Invest Dermatol **126**(4): 740-745.

Hammer, G. E., F. Gonzalez, E. James, H. Nolla and N. Shastri (2007). "In the absence of aminopeptidase ERAAP, MHC class I molecules present many unstable and highly immunogenic peptides." Nat Immunol **8**(1): 101-108.

Harvey, D., J. J. Pointon, D. M. Evans, T. Karaderi, C. Farrar, L. H. Appleton, R. D. Sturrock, M. A. Stone, U. Oppermann, M. A. Brown and B. P. Wordsworth (2009). "Investigating the genetic association between ERAP1 and ankylosing spondylitis." Hum Mol Genet **18**(21): 4204-4212.

Hattori, A., H. Matsumoto, S. Mizutani and M. Tsujimoto (1999). "Molecular cloning of adipocyte-derived leucine aminopeptidase highly related to placental leucine aminopeptidase/oxytocinase." J Biochem **125**(5): 931-938.

Hearn, A., I. A. York and K. L. Rock (2009). "The specificity of trimming of MHC class I-presented peptides in the endoplasmic reticulum." J Immunol **183**(9): 5526-5536.

Heinemeyer, W., M. Fischer, T. Krimmer, U. Stachon and D. H. Wolf (1997). "The active sites of the eukaryotic 20 S proteasome and their involvement in subunit precursor processing." J Biol Chem **272**(40): 25200-25209.

Henseler, T. and E. Christophers (1985). "Psoriasis of early and late onset: characterization of two types of psoriasis vulgaris." J Am Acad Dermatol **13**(3): 450-456.

Herberts, C. A., J. J. Neijssen, J. de Haan, L. Janssen, J. W. Drijfhout, E. A. Reits and J. J. Neefjes (2006). "Cutting edge: HLA-B27 acquires many N-terminal dibasic peptides: coupling cytosolic peptide stability to antigen presentation." J Immunol **176**(5): 2697-2701.

Hillig, R. C., M. Hulsmeyer, W. Saenger, K. Welfle, R. Misselwitz, H. Welfle, C. Kozerski, A. Volz, B. Uchanska-Ziegler and A. Ziegler (2004). "Thermodynamic and structural analysis of peptide- and allele-dependent properties of two HLA-B27 subtypes exhibiting differential disease association." J Biol Chem **279**(1): 652-663.

Hooper, N. M. (1994). "Families of zinc metalloproteases." FEBS Lett **354**(1): 1-6.

Howard, J. C. (1995). "Supply and transport of peptides presented by class I MHC molecules." Curr Opin Immunol **7**(1): 69-76.

International Genetics of Ankylosing Spondylitis, C., A. Cortes, J. Hadler, J. P. Pointon, P. C. Robinson, T. Karaderi, P. Leo, K. Cremin, K. Pryce, J. Harris, S. Lee, K. B. Joo, S. C. Shim, M. Weisman, M. Ward, X. Zhou, H. J. Garchon, G. Chiocchia, J. Nossent, B. A. Lie, O. Forre, J. Tuomilehto, K. Laiho, L. Jiang, Y. Liu, X. Wu, L. A. Bradbury, D. Elewaut, R. Burgos-Vargas, S. Stebbings, L. Appleton, C. Farrah, J. Lau, T. J. Kenna, N. Haroon, M. A. Ferreira, J. Yang, J. Mulero, J. L. Fernandez-Sueiro, M. A. Gonzalez-Gay, C. Lopez-Larrea, P. Deloukas, P. Donnelly, C. Australo-Anglo-American Spondyloarthritis, S. Groupe Francaise d'Etude Genetique des, S. Nord-Trondelag Health, C. Spondyloarthritis Research Consortium of, C. Wellcome Trust Case Control, P. Bowness, K. Gafney, H. Gaston, D. D. Gladman, P. Rahman, W. P. Maksymowych, H. Xu, J. B. Crusius, I. E. van der Horst-Bruinsma, C. T. Chou, R. Valle-Onate, C. Romero-Sanchez, I. M. Hansen, F. M. Pimentel-Santos, R. D. Inman, V. Videm, J. Martin, M. Breban, J. D. Reveille, D. M. Evans, T. H. Kim, B. P. Wordsworth and M. A. Brown (2013). "Identification of multiple risk variants for ankylosing spondylitis through high-density genotyping of immune-related loci." Nat Genet **45**(7): 730-738.

Kanaseki, T., N. Blanchard, G. E. Hammer, F. Gonzalez and N. Shastri (2006). "ERAAP synergizes with MHC class I molecules to make the final cut in the antigenic peptide precursors in the endoplasmic reticulum." Immunity **25**(5): 795-806.

Kenna, T. J., M. C. Lau, P. Keith, F. Ciccia, M. E. Costello, L. Bradbury, P. L. Low, N. Agrawal, G. Triolo, R. Alessandro, P. C. Robinson, G. P. Thomas and M. A. Brown (2015). "Disease-associated polymorphisms in ERAP1 do not alter endoplasmic reticulum stress in patients with ankylosing spondylitis." Genes Immun **16**(1): 35-42.

Kenna, T. J. B., M.A (2013). "Immunopathogenesis of ankylosing spondylitis." Int. J. Clin. Rheumatology **8**: 265-274.

Kochan, G., T. Krojer, D. Harvey, R. Fischer, L. Chen, M. Vollmar, F. von Delft, K. L. Kavanagh, M. A. Brown, P. Bowness, P. Wordsworth, B. M. Kessler and U. Oppermann (2011). "Crystal structures of the endoplasmic reticulum aminopeptidase-1 (ERAP1) reveal the molecular basis for N-terminal peptide trimming." Proc Natl Acad Sci U S A **108**(19): 7745-7750.

Kollnberger, S., A. Chan, M. Y. Sun, L. Y. Chen, C. Wright, K. di Gleria, A. McMichael and P. Bowness (2007). "Interaction of HLA-B27 homodimers with KIR3DL1 and KIR3DL2, unlike HLA-B27 heterotrimers, is independent of the sequence of bound peptide." Eur J Immunol **37**(5): 1313-1322.

Koopmann, J. O., M. Post, J. J. Neefjes, G. J. Hammerling and F. Momburg (1996). "Translocation of long peptides by transporters associated with antigen processing (TAP)." Eur J Immunol **26**(8): 1720-1728.

Lamas, J. R., A. Paradela, F. Roncal and J. A. Lopez de Castro (1999). "Modulation at multiple anchor positions of the peptide specificity of HLA-B27 subtypes differentially associated with ankylosing spondylitis." Arthritis Rheum **42**(9): 1975-1985.

Li, C., Z. Lin, Y. Xie, Z. Guo, J. Huang, Q. Wei, Q. X. Li, X. Wang, S. Cao, Z. Liao, M. Xu, Y. Shen and J. Gu (2011). "ERAP1 is associated with ankylosing spondylitis in Han Chinese." J Rheumatol **38**(2): 317-321.

Lopez-Larrea, C., K. Sujirachato, N. K. Mehra, P. Chiewsilp, D. Isarangkura, U. Kanga, O. Dominguez, E. Coto, M. Pena, F. Setien and et al. (1995). "HLA-B27 subtypes in Asian patients with ankylosing spondylitis. Evidence for new associations." Tissue Antigens **45**(3): 169-176.
Lopez de Castro, J. A., C. Alvarez-Navarro, A. Brito, P. Guasp, A. Martin-Esteban and A. Sanz-Bravo (2016). "Molecular and pathogenic effects of endoplasmic reticulum aminopeptidases ERAP1 and ERAP2 in MHC-I-associated inflammatory disorders: Towards a unifying view." Mol Immunol **77**: 193-204.

Lorente, E., A. Barriga, C. Johnstone, C. Mir, M. Jimenez and D. Lopez (2013). "Concerted in vitro trimming of viral HLA-B27-restricted ligands by human ERAP1 and ERAP2 aminopeptidases." PLoS One **8**(11): e79596.

Madden, D. R. (1995). "The three-dimensional structure of peptide-MHC complexes." Annu Rev Immunol **13**: 587-622.

Madden, D. R., J. C. Gorga, J. L. Strominger and D. C. Wiley (1992). "The three-dimensional structure of HLA-B27 at 2.1 A resolution suggests a general mechanism for tight peptide binding to MHC." Cell **70**(6): 1035-1048.

Martin-Esteban, A., P. Gomez-Molina, A. Sanz-Bravo and J. A. Lopez de Castro (2014). "Combined effects of ankylosing spondylitis-associated ERAP1 polymorphisms outside the catalytic and peptide-binding sites on the processing of natural HLA-B27 ligands." J Biol Chem **289**(7): 3978-3990.

May, E., M. L. Dorris, N. Satumtira, I. Iqbal, M. I. Rehman, E. Lightfoot and J. D. Taurog (2003). "CD8 alpha beta T cells are not essential to the pathogenesis of arthritis or colitis in HLA-B27 transgenic rats." J Immunol **170**(2): 1099-1105.

Mear, J. P., K. L. Schreiber, C. Munz, X. Zhu, S. Stevanovic, H. G. Rammensee, S. L. Rowland-Jones and R. A. Colbert (1999). "Misfolding of HLA-B27 as a result of its B pocket suggests a novel mechanism for its role in susceptibility to spondyloarthropathies." J Immunol **163**(12): 6665-6670.

Mpakali, A., P. Giastas, N. Mathioudakis, I. M. Mavridis, E. Saridakis and E. Stratikos (2015). "Structural Basis for Antigenic Peptide Recognition and Processing by Endoplasmic Reticulum (ER) Aminopeptidase 2." J Biol Chem **290**(43): 26021-26032.

Nguyen, T. T., S. C. Chang, I. Evnouchidou, I. A. York, C. Zikos, K. L. Rock, A. L. Goldberg, E. Stratikos and L. J. Stern (2011). "Structural basis for antigenic peptide precursor processing by the endoplasmic reticulum aminopeptidase ERAP1." Nat Struct Mol Biol **18**(5): 604-613.

Ombrello, M. J., D. L. Kastner and E. F. Remmers (2015). "Endoplasmic reticulum-associated amino-peptidase 1 and rheumatic disease: genetics." Curr Opin Rheumatol **27**(4): 349-356.

Orr, H. T., J. A. Lopez de Castro, D. Lancet and J. L. Strominger (1979). "Complete amino acid sequence of a papain-solubilized human histocompatibility antigen, HLA-B7. 2. Sequence determination and search for homologies." Biochemistry **18**(25): 5711-5720.

Pimentel-Santos, F. M., D. Ligeiro, M. Matos, A. F. Mourao, E. Sousa, P. Pinto, A. Ribeiro, M. Sousa, A. Barcelos, F. Godinho, M. Cruz, J. E. Fonseca, H. Guedes-Pinto, H. Trindade, D. M. Evans, M. A. Brown and J. C. Branco (2009). "Association of IL23R and ERAP1 genes with ankylosing spondylitis in a Portuguese population." Clin Exp Rheumatol **27**(5): 800-806.

Princiotta, M. F., D. Finzi, S. B. Qian, J. Gibbs, S. Schuchmann, F. Buttgereit, J. R. Bennink and J. W. Yewdell (2003). "Quantitating protein synthesis, degradation, and endogenous antigen processing." Immunity **18**(3): 343-354.

Reeves, E., A. Colebatch-Bourn, T. Elliott, C. J. Edwards and E. James (2014). "Functionally distinct ERAP1 allotype combinations distinguish individuals with Ankylosing Spondylitis." Proc Natl Acad Sci U S A **111**(49): 17594-17599.

Reeves, E., C. J. Edwards, T. Elliott and E. James (2013). "Naturally occurring ERAP1 haplotypes encode functionally distinct alleles with fine substrate specificity." J Immunol **191**(1): 35-43.

Reits, E. A., J. C. Vos, M. Gromme and J. Neefjes (2000). "The major substrates for TAP in vivo are derived from newly synthesized proteins." Nature **404**(6779): 774-778.

Reveille, J. D. and M. A. Brown (2010). "Epidemiology of ankylosing spondylitis: IGAS 2009." J Rheumatol **37**(12): 2624-2625.

Robinson, P. C. and M. A. Brown (2014). "Genetics of ankylosing spondylitis." Mol Immunol **57**(1): 2-11.

Robinson, P. C., M. E. Costello, P. Leo, L. A. Bradbury, K. Hollis, A. Cortes, S. Lee, K. B. Joo, S. C. Shim, M. Weisman, M. Ward, X. Zhou, H. J. Garchon, G. Chiocchia, J. Nossent, B. A. Lie, O. Forre, J. Tuomilehto, K. Laiho, L. Jiang, Y. Liu, X. Wu, D. Elewaut, R. Burgos-Vargas, L. S. Gensler, S. Stebbings, N. Haroon, J. Mulero, J. L. Fernandez-Sueiro, M. A. Gonzalez-Gay, C. Lopez-Larrea, P. Bowness, K. Gafney, J. S. Gaston, D. D. Gladman, P. Rahman, W. P. Maksymowych, H. Xu, I. E. van der Horst-Bruinsma, C. T. Chou, R. Valle-Onate, M. C. Romero-Sanchez, I. M. Hansen, F. M. Pimentel-Santos, R. D. Inman, J. Martin, M. Breban, D. Evans, J. D. Reveille, T. H. Kim, B. P. Wordsworth and M. A. Brown (2015). "ERAP2 is associated with ankylosing spondylitis in HLA-B27-positive and HLA-B27-negative patients." Ann Rheum Dis **74**(8): 1627-1629.

Rock, K. L. and A. L. Goldberg (1999). "Degradation of cell proteins and the generation of MHC class I-presented peptides." Annu Rev Immunol **17**: 739-779.

Sadasivan, B., P. J. Lehner, B. Ortmann, T. Spies and P. Cresswell (1996). "Roles for calreticulin and a novel glycoprotein, tapasin, in the interaction of MHC class I molecules with TAP." Immunity **5**(2): 103-114.

Sakane, T., M. Takeno, N. Suzuki and G. Inaba (1999). "Behcet's disease." N Engl J Med **341**(17): 1284-1291.

Sanz-Bravo, A., J. Campos, M. S. Mazariegos and J. A. Lopez de Castro (2015). "Dominant role of the ERAP1 polymorphism R528K in shaping the HLA-B27 Peptidome through differential processing determined by multiple peptide residues." Arthritis Rheumatol **67**(3): 692-701.

Saper, M. A., P. J. Bjorkman and D. C. Wiley (1991). "Refined structure of the human histocompatibility antigen HLA-A2 at 2.6 A resolution." J Mol Biol **219**(2): 277-319.

Saric, T., J. Beninga, C. I. Graef, T. N. Akopian, K. L. Rock and A. L. Goldberg (2001). "Major histocompatibility complex class I-presented antigenic peptides are degraded in cytosolic extracts primarily by thimet oligopeptidase." J Biol Chem **276**(39): 36474-36481.

Saric, T., S. C. Chang, A. Hattori, I. A. York, S. Markant, K. L. Rock, M. Tsujimoto and A. L. Goldberg (2002). "An IFN-gamma-induced aminopeptidase in the ER, ERAP1, trims precursors to MHC class I-presented peptides." Nat Immunol **3**(12): 1169-1176.

Saric, T., C. I. Graef and A. L. Goldberg (2004). "Pathway for degradation of peptides generated by proteasomes: a key role for thimet oligopeptidase and other metallopeptidases." J Biol Chem **279**(45): 46723-46732.

Saveanu, L., O. Carroll, V. Lindo, M. Del Val, D. Lopez, Y. Lepelletier, F. Greer, L. Schomburg, D. Fruci, G. Niedermann and P. M. van Endert (2005). "Concerted peptide trimming by human ERAP1 and ERAP2 aminopeptidase complexes in the endoplasmic reticulum." Nat Immunol **6**(7): 689-697.

Schittenhelm, R. B., T. C. Sian, P. G. Wilmann, N. L. Dudek and A. W. Purcell (2015). "Revisiting the arthritogenic peptide theory: quantitative not qualitative changes in the peptide repertoire of HLA-B27 allotypes." Arthritis Rheumatol **67**(3): 702-713.

Serwold, T., S. Gaw and N. Shastri (2001). "ER aminopeptidases generate a unique pool of peptides for MHC class I molecules." Nat Immunol **2**(7): 644-651.

Serwold, T., F. Gonzalez, J. Kim, R. Jacob and N. Shastri (2002). "ERAAP customizes peptides for MHC class I molecules in the endoplasmic reticulum." Nature **419**(6906): 480-483.

Serwold, T. and N. Shastri (1999). "Specific proteolytic cleavages limit the diversity of the pool of peptides available to MHC class I molecules in living cells." J Immunol **162**(8): 4712-4719.

Shah, K. H., R. D. Levinson, F. Yu, R. Goldhardt, L. K. Gordon, C. R. Gonzales, J. R. Heckenlively, P. J. Kappel and G. N. Holland (2005). "Birdshot chorioretinopathy." Surv Ophthalmol **50**(6): 519-541.

Shaw, J., H. Hatano and S. Kollnberger (2014). "The biochemistry and immunology of non-canonical forms of HLA-B27." Mol Immunol **57**(1): 52-58.

Stamogiannos, A., D. Koumantou, A. Papakyriakou and E. Stratikos (2015). "Effects of polymorphic variation on the mechanism of Endoplasmic Reticulum Aminopeptidase 1." Mol Immunol **67**(2 Pt B): 426-435.

Tanioka, T., A. Hattori, S. Masuda, Y. Nomura, H. Nakayama, S. Mizutani and M. Tsujimoto (2003). "Human leukocyte-derived arginine aminopeptidase. The third member of the oxytocinase subfamily of aminopeptidases." J Biol Chem **278**(34): 32275-32283.

Tran, T. M., S. Hong, J. H. Edwan and R. A. Colbert (2016). "ERAP1 reduces accumulation of aberrant and disulfide-linked forms of HLA-B27 on the cell surface." Mol Immunol **74**: 10-17.

Turner, M. J., M. L. Delay, S. Bai, E. Klenk and R. A. Colbert (2007). "HLA-B27 up-regulation causes accumulation of misfolded heavy chains and correlates with the magnitude of the unfolded protein response in transgenic rats: Implications for the pathogenesis of spondylarthritis-like disease." Arthritis Rheum **56**(1): 215-223.

Turner, M. J., D. P. Sowders, M. L. DeLay, R. Mohapatra, S. Bai, J. A. Smith, J. R. Brandewie, J. D. Taurog and R. A. Colbert (2005). "HLA-B27 misfolding in transgenic rats is associated with activation of the unfolded protein response." J Immunol **175**(4): 2438-2448.

van Endert, P. M., R. Tampe, T. H. Meyer, R. Tisch, J. F. Bach and H. O. McDevitt (1994). "A sequential model for peptide binding and transport by the transporters associated with antigen processing." Immunity **1**(6): 491-500.

Vanhille, D. L., L. D. Hill, D. D. Hilliard, E. D. Lee, M. E. Teves, S. Srinivas, J. P. Kusanovic, R. Gomez, E. Stratikos, M. A. Elovitz, R. Romero and J. F. Strauss, 3rd (2013). "A Novel ERAP2 Haplotype Structure in a Chilean Population: Implications for ERAP2 Protein Expression and Preeclampsia Risk." Mol Genet Genomic Med **1**(2): 98-107.

Wellcome Trust Case Control, C., C. Australo-Anglo-American Spondylitis, P. R. Burton, D. G. Clayton, L. R. Cardon, N. Craddock, P. Deloukas, A. Duncanson, D. P. Kwiatkowski, M. I. McCarthy, W. H. Ouwehand, N. J. Samani, J. A. Todd, P. Donnelly, J. C. Barrett, D. Davison, D. Easton, D. M. Evans, H. T. Leung, J. L. Marchini, A. P. Morris, C. C. Spencer, M. D. Tobin, A. P. Attwood, J. P. Boorman, B. Cant, U. Everson, J. M. Hussey, J. D. Jolley, A. S. Knight, K. Koch, E. Meech, S. Nutland, C. V. Prowse, H. E. Stevens, N. C. Taylor, G. R. Walters, N. M. Walker, N. A. Watkins, T. Winzer, R. W. Jones, W. L. McArdle, S. M. Ring, D. P. Strachan, M. Pembrey, G. Breen, D. St Clair, S. Caesar, K. Gordon-Smith, L. Jones, C. Fraser, E. K. Green, D. Grozeva, M. L. Hamshere, P. A. Holmans, I. R. Jones, G. Kirov, V. Moskivina, I. Nikolov, M. C. O'Donovan, M. J. Owen, D. A. Collier, A. Elkin, A. Farmer, R. Williamson, P. McGuffin, A. H. Young, I. N. Ferrier, S. G. Ball, A. J. Balmforth, J. H. Barrett, T. D. Bishop, M. M. Iles, A. Maqbool, N. Yuldasheva, A. S. Hall, P. S. Braund, R. J. Dixon, M. Mangino, S. Stevens, J. R. Thompson, F. Bredin, M. Tremelling, M. Parkes, H. Drummond, C. W. Lees, E. R. Nimmo, J. Satsangi, S. A. Fisher, A. Forbes, C. M. Lewis, C. M. Onnie, N. J. Prescott, J. Sanderson, C. G. Matthew, J. Barbour, M. K. Mohiuddin, C. E. Todhunter, J. C. Mansfield, T. Ahmad, F. R. Cummings, D. P. Jewell, J. Webster, M. J. Brown, M. G. Lathrop, J. Connell, A. Dominiczak, C. A. Marcano, B. Burke, R. Dobson, J. Gungadoo, K. L. Lee, P. B. Munroe, S. J. Newhouse, A. Onipinla, C. Wallace, M. Xue, M. Caulfield, M. Farrall, A. Barton, R. A. G. Biologics in, C. Genomics Study Syndicate Steering, I. N. Bruce, H. Donovan, S. Eyre, P. D. Gilbert, S. L. Hilder, A. M. Hinks, S. L. John, C. Potter, A. J. Silman, D. P. Symmons, W. Thomson, J. Worthington, D. B. Dunger, B. Widmer, T. M. Frayling, R. M. Freathy, H. Lango, J. R. Perry, B. M. Shields, M. N. Weedon, A. T. Hattersley, G. A. Hitman, M. Walker, K. S. Elliott, C. J. Groves, C. M. Lindgren, N. W. Rayner, N. J. Timpson, E. Zeggini, M. Newport, G. Sirugo, E. Lyons, F. Vannberg, A. V. Hill, L. A. Bradbury, C. Farrar, J. J. Pointon, P. Wordsworth, M. A. Brown, J. A. Franklyn, J. M. Heward, M. J. Simmonds, S. C. Gough, S. Seal, C. Breast Cancer Susceptibility, M. R. Stratton, N. Rahman, M. Ban, A. Goris, S. J. Sawcer, A. Compston, D. Conway, M. Jallow, M. Newport, G.

Sirugo, K. A. Rockett, S. J. Bumpstead, A. Chaney, K. Downes, M. J. Ghori, R. Gwilliam, S. E. Hunt, M. Inouye, A. Keniry, E. King, R. McGinnis, S. Potter, R. Ravindrarajah, P. Whittaker, C. Widden, D. Withers, N. J. Cardin, D. Davison, T. Ferreira, J. Pereira-Gale, I. B. Hallgrimsdo'ttir, B. N. Howie, Z. Su, Y. Y. Teo, D. Vukcevic, D. Bentley, M. A. Brown, A. Compston, M. Farrall, A. S. Hall, A. T. Hattersley, A. V. Hill, M. Parkes, M. Pembrey, M. R. Stratton, S. L. Mitchell, P. R. Newby, O. J. Brand, J. Carr-Smith, S. H. Pearce, R. McGinnis, A. Keniry, P. Deloukas, J. D. Reveille, X. Zhou, A. M. Sims, A. Dowling, J. Taylor, T. Doan, J. C. Davis, L. Savage, M. M. Ward, T. L. Learch, M. H. Weisman and M. Brown (2007). "Association scan of 14,500 nonsynonymous SNPs in four diseases identifies autoimmunity variants." Nat Genet **39**(11): 1329-1337.

Yewdell, J. W., L. C. Anton and J. R. Bennink (1996). "Defective ribosomal products (DRiPs): a major source of antigenic peptides for MHC class I molecules?" J Immunol **157**(5): 1823-1826.

York, I. A., N. Bhutani, S. Zendzian, A. L. Goldberg and K. L. Rock (2006). "Tripeptidyl peptidase II is the major peptidase needed to trim long antigenic precursors, but is not required for most MHC class I antigen presentation." J Immunol **177**(3): 1434-1443.

York, I. A., S. C. Chang, T. Saric, J. A. Keys, J. M. Favreau, A. L. Goldberg and K. L. Rock (2002). "The ER aminopeptidase ERAP1 enhances or limits antigen presentation by trimming epitopes to 8-9 residues." Nat Immunol **3**(12): 1177-1184.

Zervoudi, E., A. Papakyriakou, D. Georgiadou, I. Evnouchidou, A. Gajda, M. Poreba, G. S. Salvesen, M. Drag, A. Hattori, L. Swevers, D. Vourloumis and E. Stratikos (2011). "Probing the S1 specificity pocket of the aminopeptidases that generate antigenic peptides." Biochem J **435**(2): 411-420.

Zhang Z, C. F., Yee K, Guggino G, Abdullah H, Alessandro R, et al (2014). "Functional implications of the endoplasmatic reticulum aminopeptidase 2 (ERAP2) association with ankylosing spondylitis and Crohn disease: impact on the unfolden protein respond." Arthritis Rheum **66**: S268.